THE UNIVERSITY
of EDINBURGH

Phage-mediated adaptation of *Staphylococcus aureus* to the avian innate immune response

Emily Parr

Thesis presented for the degree of Doctor of Philosophy

The University of Edinburgh

2019

Declaration

I declare that this thesis has been composed solely by myself and that it has not been submitted, in whole or in part, in any previous application for a degree. Except where states otherwise by reference or acknowledgment, the work presented is entirely my own.

Emily Parr March 2020

Abstract

Staphylococcus aureus is an important human and livestock pathogen. An *S. aureus* prophage (Avβ) inserted into the chromosome at the β-toxin gene (β-converting phage) is present in approximately 90% of human strains and is known to contribute to human-specific innate immune evasion. Comparative genomic analysis of *S. aureus* isolates from infected poultry has recently revealed an avian-specific subfamily of β-converting phages. Population analysis revealed that 80% of avian isolates tested carry prophage Avβ and that the genes encoded on its putative immune evasion cluster are conserved, suggesting a role in avian host-adaptation. A φAvβ-deficient avian *S. aureus* strain was used to investigate the role of prophage Avβ in avian host-pathogen interactions. Compared to the wild type, the φAvβ-deficient strain has increased susceptibility to chicken bone-marrow derived macrophage killing. Further investigation using GFP-expressing bacteria has revealed that the φAvβ-deficient strain exhibits reduced phagocytosis compared to the wild type and is associated with decreased killing of macrophages. PCR analysis revealed that prophage Avβ is capable of excision from the chromosome, leading to restoration of β-toxin expression and therefore an intact β-toxin could influence *S. aureus*-macrophage interactions. To further dissect whether prophage Avβ mediates immune evasion, deletion mutants of three candidate phage effector genes were constructed. No difference in bacterial survival or phagocytosis was observed by single gene deletion mutants compared to the wild type. Finally, RNA-seq analysis was used to decipher the general response of chicken bone-marrow derived macrophages to *S. aureus*. Toll-like receptor signalling pathways, NF-κB and the type I interferon response are the main drivers of the early chicken macrophage response to *S. aureus*. Importantly, the transcriptomic analysis of infected macrophages revealed that the presence of prophage Avβ (or β-toxin due to prophage Avβ excision), is associated with an inhibition of avian antimicrobial peptide gene expression. Overall, these data provide new insights into innate immune evasion of avian *S. aureus* and mechanisms of bacterial host-adaptation.

Lay summary

Staphylococcus aureus is a major human and livestock microscopic organism called a bacterium. Understanding how *S. aureus* can infect and adapt to different animals is essential for prevention and treatment of the diseases it causes. When *S. aureus* infects an animal, it comes into contact with the innate immune system, which allows the animal to fight back against the infection. However, *S. aureus* can also fight back against these defences and in this study, we aimed to investigate how *S. aureus* can evade the innate immune response of chickens. Recent work has identified that a host-jump from humans into chickens was associated with the gain of mobile genetic elements, which are a type of genetic material that can move around the genome or be transferred from one species to another. This study focused on a bacteriophage found in avian *S. aureus* called prophage Avβ, whose genetic material is inserted and integrated in the *S. aureus* genome at the β-toxin gene. A similar bacteriophage found in human isolates of *S. aureus* encodes for genes associated with human-specific innate immune evasion. We therefore hypothesised that genes encoded on prophage Avβ would be responsible for avoiding the chicken innate immunity. We discovered that prophage Avβ is found in most chicken strains of *S. aureus* tested. To investigate its role in innate immune evasion, we deleted prophage Avβ from the *S. aureus* genome and investigated the bacterium's fate within innate immune cells. Macrophages are important immune cells key that can uptake *S. aureus* and kill it. In absence of prophage Avβ, *S. aureus* was less capable of surviving chicken macrophage killing. We discovered that this could be due to either genes encoded on prophage Avβ or to the restoration of a functional β-toxin when prophage Avβ exits the chromosome. To investigate the role of prophage Avβ in immune evasion, we deleted three genes encoded by prophage Avβ but found no difference compared to the wild type. Importantly, further analysis of genes transcribed by chicken macrophages after infection with *S. aureus* identified that the expression of small molecules involved in *S. aureus* killing, called avian antimicrobial peptides, is inhibited by the presence of prophage Avβ or restoration of the β-toxin. Overall, this study has provided new insights into how *S. aureus* can evade the chicken immune response, which could help to treat *S. aureus* chicken infections in the future.

Acknowledgements

I would like to thank my supervisors Professor Ross Fitzgerald and Professor David Hume for their guidance and support. Particularly I would like to thank Ross for his critical analysis of my work. I would also like to thank Professor Lonneke Vervelde for her expertise in avian immunology and her constructive feedback on my experiments. I am also grateful to my thesis committee for their guidance throughout my PhD.

I am also very grateful to members of LBEP, past and present, who have been an invaluable support system during my PhD. A special thanks to Joana Alves, Amy Pickering and Manouk Vrieling for being a wonderful supportive postdoc team and for providing guidance and feedback throughout my PhD. I am also very grateful to Bryan Wee and Gonzalo Yebra for helping me with my bioinformatics analysis. Thank you to Chriselle and Rodrigo for their help and support at the beginning of my PhD. I would also like to thank members of the Gally, Stevens and Morrison group for all the coffee and karaoke nights we have had and for reminding me to have fun every now and then.

Thank you to all my friends in Scotland for making my time so memorable. A special thanks to my fellow PhD students for keeping me sane including Rebecca, Sally, Flo, Ben, Fiona, Hanne and Amany.

Finally, I would like to thank my family for their endless love and support. Thank you to Tristan for being by my side and my cheerleader every step of the way. Thank you to Mum, Dad and Fiona for always believing in me and helping me through the finish line.

Table of Contents

List of figures

Chapter 1

Chapter 3

Chapter 4

Chapter 5

Chapter 6

List of tables

List of commonly used abbreviations

Abbreviation	Full description
α	Alpha
aa	Amino acid
agr	Accessory gene regulator
Amp	ampicillin
AMP	Antimicrobial peptide
ATc	Anhydrotetracycline
β	Beta
BCO	Bacterial chondronecrosis with osteomyelitis
BLAST	Basic alignment search tool
bp	Base pair
BHI	Brain heart infusion
chBMM	Chicken bone-marrow derived macrophage
°C	Degree
CA-MRSA	Community-associated methicillin resistant *Staphylococcus aureus*
CC	Clonal complex
CFU	Colony forming units
CO_2	Carbon dioxide
Cm	Chloramphenicol
CSF-1	Colony stimulating factor 1
C_t	Cycle threshold
d	Days
DNA	Deoxyribonucleic acid
DEG	Differentially expressed gene
dNTP	Deoxyribonucleotide triphosphate
EDTA	Ethylene-diamine-tetra acetic acid
FACS	Fluorescence-activated cell sorting

Abbreviation	Full description
FBS	Foetal bovine serum
FDR	False discovery rate
x g	Force of gravity
γ	Gamma
g	grams
gDNA	Genomic DNA
h	H
H_2O	Water
H_2O_2	Hydrogen peroxide
HBSS	Hanks balanced salt solution
HCl	Hydrochloric acid
HGT	Horizontal gene transfer
IEC	Immune evasion cluster
IFN	Interferon
IL	Interleukin
IRF	Interferon-regulatory factor
kDa	Kilo-Dalton
KEGG	Kyoto Encyclopedia of Genes and Genomes
kV	Kilo-volts
L	Litres
LB	Luria-Broth
LPS	Lipopolysaccharide
LTA	Lipotechoic acid
Luk	Leukocidin
kb	Kilo-base
MGE	Mobile genetic element
MHC	Major histocompatibility complex
min	Minutes
MSCRAMM	Microbial surface components recognising adhesive matrix molecules

Abbreviation	Full description
µg	Micro-grams
µl	Micro-litre
ml	Milli-litres
MPO	Myeloperoxidase
MRSA	Methicillin-resistant *Staphylococcus aureus*
NaCl	Sodium Chloride
NCBI	National Centre for Biotechnology information
ng	Nano-grams
nm	Nano-metre
nM	Nano-molar
NLR	NOD-like receptor
NO	Nitric oxide
NS	Not significant
NTC	No template control
OCD	Ornithine cylodeaminase
OD	Optical density
PAMP	Pathogen-associated molecular pattern
PBMC	Peripheral blood mononuclear cells
PBS	Phosphate buffered saline
PCR	Polymerase chain reaction
PFA	Paraformaldehyde
PMN	Polymorphonuclear leukocytes
PRR	Pathogen recognition receptor
PVL	Panton-valentine leucocidin
qRT-PCR	Quantitative reverse transcriptase-polymerase chain reaction
RBC	Red blood cells
RFU	Relative fluorescence units
RNA	Ribonucleic acid

Abbreviation	Full description
RNA-seq	RNA sequencing
RPMI	Roswell Park Memorial Institute medium
RT	Reverse transcriptase
s	Second
SAg	Superantigen
SaPI	Staphylococcal pathogenicity island
SCC	Staphylococcal cassette chromosome
sGFP	Superfolder green fluorescent protein
SNP	Single nucleotide polymorphism
SSL	Staphylococcal superantigen-like
ST	Sequence type
STING	Stimulator of interferon genes
TAE	Tris-acetate ethylene diamine-tetra-acetic acid
TCS	Two component system
TLR	Toll-like receptor
TNF	Tumor necrosis factor
TSA	Tryptone soy agar
TSB	Tryptone soy broth
TSST-1	Toxic shock syndrome toxin-1
RLR	RIG-I-like receptor
ROS	Reactive oxygen species
V	Volts
vWbp	Von Willebrand binding protein
v/v	Volume for volume
v/w	Volume for weight
WTA	Wall techoic acid
w/v	Weight for volume
w/w	Weight for weight

Chapter 1. Introduction

1.1. *Staphylococcus aureus*: microbiology and disease

1.1.1. Microbiology

Staphylococcus aureus is a facultative anaerobic Gram positive bacterium and is generally found as a commensal in the nasopharynx (Lowy, 1998). Colonisation can be transient or persistent, with colonisation rates of 25 to 30% in healthy humans (Gorwitz *et al.*, 2008). However, it is also a highly successful opportunistic pathogen that invades tissues and leads to local and systemic diseases such as osteomyelitis, necrotizing pneumonia, sepsis and toxic shock syndrome (Lowy, 1998). *S. aureus* infections are also a major problem in economically important livestock, causing diseases including mastitis in cows, sheep and goats (Bradley *et al.*, 2007; Peton & Le Loir, 2014) and dermatitis in poultry and rabbits (Viana *et al.*, 2015).

1.1.2. Disease in poultry

The expansion of the poultry industry and increase in the number of poultry flocks has increased the opportunity for staphylococcal infections and zoonosis (Murray *et al.*, 2017). *S. aureus* is found as a commensal on the skin and upper respiratory tract of poultry (Zhu, Ching & Hester, 1998; Nagase *et al.*, 2002). It is also found in the house dust and animal feed (Rodgers *et al.*, 2003). Other staphylococcal species found in poultry include coagulase negative species such as *S. epidermidis, S. hyicus* and *S. gallinarum* (Peton & Le Loir, 2014).

S. aureus infections of poultry occur from accidental or intentional wounds, damage to the umbilicus during hatching or trauma causing disruption to the skin barrier (McNamee & Smyth, 2000). Clinical signs of *S. aureus* infection include swollen feet, high mortality in baby chicks and gangrenous dermatitis. Skin wounds can also lead to localized abscesses or systemic dispersal, leading to diseases such as septic arthritis, osteomyelitis and endocarditis (Bystroń *et al.*, 2010; Peton & Le Loir, 2014).

Since the 1990s, *S. aureus* has been identified as the leading cause of bacterial chondronecrosis and osteomyelitis (BCO) in broilers (McNamee & Smyth, 2000). The most affected bones and joints are the femur and tibiofemoral joint (Nair &

Watson, 1972). Lameness is the main clinical presentation, due to affected bones undergoing necrosis and the presence of puss in joint lesions (Bystroń *et al.*, 2010; Peton & Le Loir, 2014). Lameness in broilers can lead to important economic losses, due to the birds being unable to access food or water, leading to decreased weight gain, decreased egg production, death and condemnation at slaughter (McNamee & Smyth, 2000). In addition, septicaemia in broilers can cause green livers or liver granulomas, leading to liver condemnation (Peton & Le Noir, 2014). *S. aureus* has also been isolated from raw broiler meat but the significance to human health is incompletely understood (Bystroń *et al.*, 2005).

1.1.3. Antimicrobial drug resistance

S. aureus infections are treatable with the use of antibiotics, but acquisition of antibiotic resistance emerged soon after introduction of antibiotics (Kirby, 1944; Jevons, 1961). Methicillin resistance is mediated by the staphylococcal cassette chromosome *mec* (SCC*mec*) element, which contains the gene *mecA* encoding penicillin binding protein 2, providing resistance to all β-lactam antibiotics (Shore & Coleman, 2013). Methicillin-resistant *S. aureus* (MRSA) is a global threat to public health, and is observed in hospitals (HA-MRSA), in communities (CA-MRSA) and in livestock species (LA-MRSA) (Cuny *et al.*, 2010; Stryjewski & Corey, 2014). In humans, the rise of a major epidemic of CA-MRSA in the USA, associated with the USA300 clone, and increase in infections in Europe of CA-MRSA, underlines the fact that *S. aureus* is an important challenge to worldwide human health (DeLeo & Chambers, 2009; Otter & French, 2010). In poultry, antimicrobial drug resistance has been identified in isolates from both healthy and diseased chickens, from poultry farms across the world (Nemeghaire *et al.*, 2013; Wendlandt *et al.*, 2013; Mkize, Zishiri & Mukaratirwa, 2017; Kim *et al.*, 2018). The presence of MRSA on raw poultry meat also presents an important risk for the spread of antimicrobial drug resistance (Ribeiro *et al.*, 2018).

1.2. *S. aureus* evolution

1.2.1. Genome organisation

Reduction in the cost of whole genome sequencing has led to a wealth of sequences that have informed the genomic landscape of *S. aureus* (Fitzgerald & Holden, 2016). To differentiate *S. aureus* strains, isolates are assigned to a sequence type (ST) based on the allelic variation of seven housekeeping genes found in all strains of the same species. STs that share alleles at ≥5 loci are then grouped into the same clonal complex (CC) (Fitzgerald & Holden, 2016). Population studies have revealed that the *S. aureus* population is clonal, with at least 10 major dominant clonal complexes (Lindsay, 2014).

The *S. aureus* genome can be divided into the core, core-variable and accessory genome. The core genome makes up approximately 75% of the genome and contains genes essential for growth, survival and virulence (Lindsay & Holden, 2006). There is a high level of similarity in the core genome between different strains and the sequence diversity is mainly due to single nucleotide polymorphisms (SNPs), some of which are non-synonymous mutations, which result in a change of the encoded amino acid (Lindsay & Holden, 2006).

The core-variable genome proposed by Lindsay *et al.* is composed of up to 15% of the whole genome and has been shown to vary between isolates but is stable within lineages. Accordingly, many of the genes encoded in the core-variable genome are lineage-specific and encode surface proteins, secreted virulence factors and their regulators, suggesting they are associated with niche adaptation (McCarthy & Lindsay, 2013). For example, genomic islands vSaα and vSaβ are found in the core-variable genome, present in most *S. aureus* isolates exhibiting highly variable gene content (Moon *et al.*, 2015). In addition, these genomic islands are not found in the genomes of less-pathogenic species such as *Staphylococcus epidermis* and *Staphylococcus haemolyticus* (Gill *et al.*, 2005; Takeuchi *et al.*, 2005). Another example of a core-variable element is the immune evasion cluster 2 (IEC2), defined by Jongerius *et al.*, which has been acquired by horizontal gene transfer and contains allelic variants that are distributed in a lineage-specific way (Jongerius *et al.*, 2007).

In contrast to the core genome, the accessory genome contains genes that vary from strain to strain including non-essential genes linked to virulence and drug resistance (Lindsay & Holden, 2004, 2006). It is composed of mobile genetic elements (MGEs), including bacteriophages, staphylococcal pathogenicity islands (SaPIs), staphylococcal cassette chromosomes (SCC), plasmids, transposons and insertion sequences (Kuroda *et al.*, 2001; Alibayov *et al.*, 2014). Some MGEs are distributed across *S. aureus* lineages in different host-species whilst others are associated with host-specific clonal complexes (Lindsay *et al.* 2010). MGEs are exchanged between strains by horizontal gene transfer (HGT) and play an essential role in the adaptive evolution of *S. aureus* (Malachowa & DeLeo, 2010).

1.2.2. *S. aureus* host-adaptation

The ability of *S. aureus* to adapt to different ecological niches including host species is an important feature of its evolutionary history. *S. aureus* has colonised different animal species following host-switching events and subsequent adaptation by multiple genetic mechanisms, which are discussed below.

1.2.2.1. Genetic basis of host-adaptation

MGEs are key players of *S. aureus* adaptation to new ecological niches. For example, *S. aureus* adaptation to ruminants is largely mediated by MGEs (Herron-Olson *et al.*, 2007a; Guinane *et al.*, 2010). Genome analysis of both S. *aureus* strains ED133 and RF122 revealed the presence host-specific SaPIs (SaPIov1 and SaPIbov1) that encode host-specific variants of superantigens TSST-1, SEC and SElL (Fitzgerald *et al.*, 2001; Herron-Olson *et al.*, 2007b; Guinane *et al.*, 2010). Furthermore, other SaPIs found in ruminant and equine isolates (SaPIov2, SaPIov4, SaPIov5, SaPIeq1) encode a variant of the chromosomal von Willebrand factor binding protein (vWbp), which is capable of coagulating host-specific plasma, unlike the chromosomal copy (Guinane *et al.*, 2010; Viana *et al.*, 2010). Similarly, the bovine-to-human host jump of *S. aureus* CC8 was associated with the loss of the human-specific β-converting prophage Sa3 and gain of a new SCC cassette, encoding a novel cell wall-anchored surface protein (Resch *et al.*, 2013). Further

examples include a livestock to human host-jump in CC97, which was associated with the gain of MGEs involved in human-specific immune evasion and antimicrobial resistance (Spoor *et al.*, 2013), and host-switching from humans into pigs which was associated with the acquisition of a putative novel plasmid linked to SCC*mec* that is associated with resistance to heavy metal ions (Richardson *et al.*, 2018). A recent species-wide population-genomic analysis has revealed that combinations of MGEs are linked to specific host species, suggesting that host-specific accessory gene pools allow *S. aureus* to adapt to new ecological niches (Richardson *et al.*, 2018).

In addition to the known importance of lateral gene transfer in *S. aureus* host-adaptation, there is a growing body of work suggesting the core genome plays an important role in host-adaptation. For example, a human-to-rabbit host jump was found to be due to a single nucleotide polymorphism (SNP) in the core genome (Viana *et al.*, 2015). The single point mutation in the *dltB* gene was sufficient to convert a human *S. aureus* strain to a pathogenic rabbit *S. aureus* strain, therefore altering host tropism (Viana *et al.*, 2015). Gene decay of core genome genes is another important mechanism used by *S. aureus* to adapt to new ecological niches. For example, host-adaptation of *S. aureus* to ruminants is associated with the pseudogenisation of genes including toxins and lipoproteins (Guinane *et al.*, 2010). Similarly, a host-jump from humans into poultry was associated with pseudogene accumulation in human disease pathogenesis genes, such as protein A (Lowder *et al.*, 2009). Furthermore, genomic rearrangement of the core genome may also mediate *S. aureus* host-adaptation. For example, the hybrid *S. aureus* sequence type (ST) 171 occurred via large-scale recombination of CC97 and other lineages occupying the same ruminant niche, resulting in the acquisition of genes encoding innate immune evasion factors and collagen binding protein (Cna), involved in bovine extracellular matrix adherence (Spoor *et al.*, 2015). Recent evidence also identified distinct pathways present in the core genome, which are under positive selection, and are important for *S. aureus* host-adaptation (Richardson *et al.*, 2018). The enhanced utilisation of disaccharide lactose, a major carbohydrate in bovine milk, by bovine *S. aureus* clones, provided phenotypic evidence for host-adaptation (Richardson *et al.*, 2018).

1.2.2.2. Bacteriophages: key players in *S. aureus* host-adaptation

The majority of *S. aureus* bacteriophages are around 40 kb, belong to the *Siphoviridae* family and can be categorised according to 8 major integrase families, determining their site of integration into the genome (Brüssow, Canchaya & Hardt, 2004; Goerke *et al.*, 2009). They can lyse bacteria after infection but in *S. aureus* they typically integrate their DNA into the chromosome as a prophage (Goerke *et al.*, 2009). Bacteriophages encode genes which are important for their life cycle but also encode virulence factors, including toxins, regulatory factors and enzymes that can change bacterial components (Wagner & Waldor, 2002). These elements are often contained within "moron" elements, thus named as their addition adds "more on" the genome in which they are found (Juhala *et al.*, 2000). For example, β-converting prophage Sa3, inserted into the chromosome at the β-toxin, carries the immune evasion cluster 1 (IEC1), encoding genes associated with innate immune evasion (Van Wamel *et al.*, 2006). Bacteriophage-mediated gene transfer was originally found to be mediated by generalised and specialised transduction (Penadés *et al.*, 2015). More recent evidence demonstrated that bacteriophages undergo lateral transduction, whereby they replicate *in situ*, leading to the DNA packaging of both the prophage and large metameric spans of DNA flanking the prophage, which results in transfer of large regions of the *S. aureus* genome (Chen *et al.*, 2018a).

Bacteriophages have had a major impact on staphylococcal diversity and evolution. They have been revealed to be a major source of genomic variation between lineages (Lindsay, 2014). Apart from their capacity to spread chromosomally-encoded virulence factors, they can also mobilize SaPIs (Yarwood *et al.*, 2002; Xia & Wolz, 2014). For example, phage 80α mediates excision and transfer of SaPIs, which encode enterotoxins and toxic shock syndrome toxin 1 (TSST-1) (Fitzgerald *et al.*, 2001; Novick & Subedi, 2007). *S. aureus* bacteriophages have also been reported to induce chromosomal recombination when they are mobilized, which may increase *S. aureus* genetic diversity by creating novel genes (Goerke *et al.*, 2004). In addition, bacteriophages demonstrate extensive mosaicism due to recombination (Kwan *et al.*, 2005) and can be gained or lost, which also contributes to genome plasticity in *S. aureus* (Goerke & Wolz, 2004; Goerke *et al.*, 2009). Furthermore, integration of

prophages into the *S. aureus* genomes can disrupt genes, as exemplified by prophage Sa3 integrating into *hlb* and prophage NM4 integrating into *geh* (Van Wamel *et al.*, 2006; Goerke *et al.*, 2009).

Bacteriophages are important mediators of *S. aureus* host-adaptation (Figure 1.1), in part through immune evasion. For example, two prophages, Sa1 and Saeq1, are found respectively in bovine strains and equine strains, and contain host-specific genes *lukmf'* and *lukpq*, that encode leukocidins active against bovine and equine neutrophils, respectively (Vrieling *et al.*, 2016; Koop *et al.*, 2017).

Despite the fact that prophage Sa2 contains the lukS/lukF genes encoding Panton-Valentine leucocidin, it is only found in a small proportion isolates (Mccarthy & Lindsay, 2013). PVL is considered to be a phenotypic trait of human isolates as it is highly specific to human C5a receptors (Spaan *et al.*, 2013a). Similarly, human isolates exclusively carry prophage Sa3, encoding human-specific immune evasion genes *scn*, *chp*, *sak* and *sea* (Van Wamel *et al.*, 2006). Moreover, a similar prophage, inserted at the same chromosomal location, is present in avian isolates of *S. aureus*, and hypothesised to encode genes conferring a selective advantage in the poultry ecological niche (Lowder *et al.*, 2009).

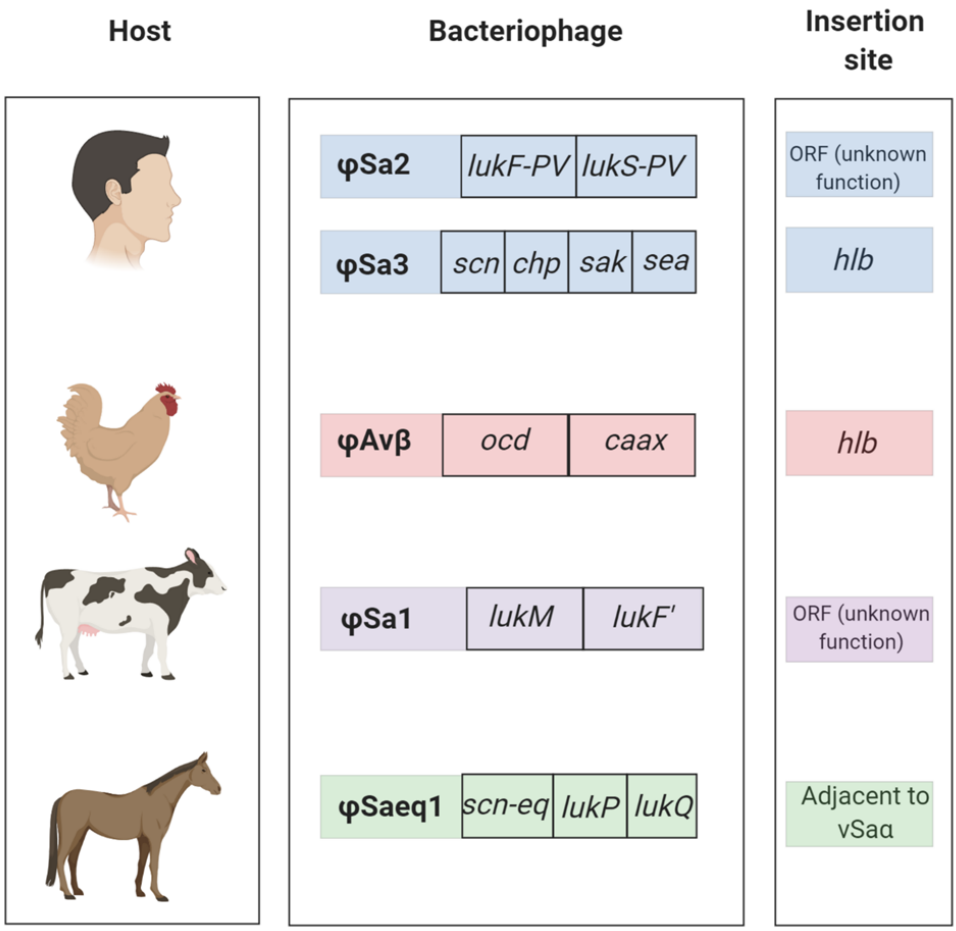

Figure 1.1. Bacteriophages are key mediators of *S. aureus* host-adaptation.

Bacteriophages in *S. aureus* integrated into the genome encode host-specific immune evasion genes that allow adaptation to a new ecological niche. The panel on the left depicts the species to which the bacterium is adapted, the middle panel depicts the different prophages and gene content and the panel on the right depicts the gene which is disrupted after integration of the prophage. Abbreviations: *caax (*putative CAAX-domain containing protease*), chp* (chemotaxis inhibitory protein of *S. aureus*), *hlb* (β-hemolysin), *luk* (leukocidin), *ocd* (putative ornithine cyclodeaminase), ORF (open reading frame), *sak* (staphylokinase), *scn* (staphylococcal complement inhibitor), *scneq* (equine staphylococcal complement inhibitor), *sea* (staphylococcal enterotoxin A), Vsaα (*S. aureus* genomic island). Figure created with BioRender.com.

1.2.2.3. *S. aureus* adaptation to poultry

At the population level, *S. aureus* poultry isolates show host-niche association. CC385 isolates have only been identified in avian isolates and are hypothesised to have long-term avian host restriction, with an estimated emergence in poultry approximately 600 years ago (Lowder *et al.*, 2009; Richardson *et al.*, 2018). In comparison, CC5 isolates are found in both poultry and mammals (Lowder *et al.*, 2009; Murray *et al.*, 2017a). Dissemination of CC5, one of the predominant lineages causing disease in poultry, occurred after a single human-to-poultry host jump around 50 years ago, associated with the gain of novel MGEs and loss of function of proteins involved in human disease (Lowder *et al.*, 2009). The poultry strain ED98 analysed in the study acquired two prophages, two plasmids and a SaPI, which are widely distributed in avian isolates but absent from human strains (Lowder *et al.*, 2009). The genes encoded on the novel MGEs may confer selective advantage in the avian ecological niche. For example, the novel cysteine protease ScpB, shown experimentally to be absent from porcine and bovine isolates (Takeuchi *et al.*, 2002b), is specifically found in poultry isolates (Lowder *et al.*, 2009). In addition, the loss of human-specific β-converting prophage Sa3 was accompanied with the gain of a novel β-converting prophage Avβ, encoding genes hypothesised to have avian niche-specific activities (Lowder *et al.*, 2009). Of note, these genomic alterations have led to an increased capacity of the avian CC5 isolate ED98 to evade innate immune killing compared to the basal human CC5 isolate MR1 (Lowder *et al.*, 2009).

Furthermore, a more recent study identified that the human-to-poultry host jump was followed by recombination within the CC5 clonal complex, leading to host-adaptation of *S. aureus* to poultry (Murray *et al.*, 2017). In addition, 47 genes were found more commonly in poultry CC5 isolates compared to human CC5 isolates, and these genes were identified to be common with other poultry lineages, suggesting horizontal gene transfer among poultry isolates (Murray *et al.*, 2017). Phenotypic analysis revealed enhanced growth of poultry isolates at 42°C, which is the avian body temperature, compared to human isolates, supporting the hypothesis that these genes are important for *S. aureus* adaptation to poultry (Murray *et al.*, 2017).

However, the molecular mechanisms underlying *S. aureus* host-adaptation in poultry are yet to be fully elucidated. Further understanding could reveal novel therapeutic targets for the control of *S. aureus* disease of poultry.

1.3. Avian innate immune response

The innate immune system is the first line of defence against *S. aureus* infections. The avian innate immune system differs from the mammalian innate immune system at the genetic, molecular and cellular level (Kaiser, 2010). However, our knowledge of the avian innate immune systems is still limited due to the lack of available tools, with most research carried out on the domestic chicken (Juul-Madsen *et al.*, 2003). The main avian innate immune responses to bacterial pathogens are discussed below and summarized in Figure 1.2.

1.3.1. The complement system

The complement system is an essential part of the innate immune system and acts as a first line of defence to staphylococcal infection (Merle *et al.*, 2015). The complement cascade leads to opsonisation of the pathogen and uptake by a phagocyte, stimulation of inflammatory cytokines and complement-mediated cytolysis (Merle *et al.*, 2015). There are three major pathways to the complement system. The 'classical' pathway is activated by antibody and C1q deposition on the staphylococcal surface (Geertsma *et al.*, 1994), the lectin pathway is activated by the association of lectins such as mannose-binding lectin (MBL) to staphylococcal carbohydrates (Ma *et al.*, 2004), and the 'alternative' pathway is activated by spontaneous breakdown of complement protein C3 (Verbrugh *et al.*, 1979). All three pathways lead to the proteolysis of C3 to generate C3b that can bind to microbial surfaces or antibodies. Furthermore, activation also leads to the generation of C3 convertase and C5 convertase, which cleave C3 and C5 into C3a, C3b, C5a and C5b. The cleavage of C3 is essential for downstream functions such as phagocytosis and enhancement of inflammation whilst the cleavage of C5 is essential for the creation of complement membrane attack complex (MAC), essential for killing Gram

negative bacteria (Merle *et al.*, 2015). *S. aureus* and other Gram positive bacteria are resistant to MAC, likely due to their thick peptidoglycan layer preventing insertion of MAC into their cell membrane (Berends *et al.*, 2013).

In the chicken complement system, C1q has been identified and presents a similar structure to the mammalian C1q (Yonemasu & Sasaki, 1986). Its proteolytic activity has been conserved but its role in the complement cascade remains to be elucidated (Yonemasu & Sasaki, 1986). Other components of the classical pathway, C2 and C4, have also been described, suggesting the classical pathway could exist in chickens (Wathen *et al.*, 1987; Kjalke, Welinder & Koch, 1993). MBL has also been identified in chickens, can activate the complement cascade and is up-regulated in response to viruses (Lynch *et al.*, 2005; Juul-Madsen *et al.*, 2003). In addition, chicken MBL exhibits binding to *S. aureus* in a dose-dependent manner and serum containing high levels of chicken MBL is highly bactericidal (Ulrich-Lynge *et al.*, 2015). The only major component of the alternative pathway to be identified in the avian complement system is chicken factor B (Kjalke, Welinder & Koch, 1993). Importantly, chicken C3 has been isolated, cloned and mapped, although in contrast to human C3, exists in three molecular forms (Laursen & Koch, 1989; Mavroidis, Sunyer & Lambris, 1995). mRNA expression of other complement molecules, such as C4b, C1r, and factor H has been detected, suggesting these components exist in the avian innate immune system (Inoue *et al.*, 2001). The avian MAC is predicted from the genome but experimental proof is lacking (Ohta *et al.*, 1984). Further work is needed to unravel the complete avian complement cascade and its role in immunity to *S. aureus* infections.

1.3.2. Heterophils

Mammalian neutrophils are central players in the host defence against *S. aureus*. These short-lived granulocytes are recruited to the site of infection by pro-inflammatory signals such as interleukin-8 (IL-8), which promote neutrophil adhesion and extravasation across the endothelium (Borregaard, 2010). Neutrophils are also important mediators of early phagocytosis during an *S. aureus* infection (van Kessel, Bestebroer & van Strijp, 2014). Phagocytosis is a mechanism whereby pathogens are taken up into the phagosome before phagolysosomal fusion, where the

pathogen is susceptible to killing mechanisms. These killing mechanisms include reactive oxygen species (ROS), such as myeloperoxidase (MPO), superoxide anion (O_{2-}), hydrogen peroxide (H_2O_2), hypochlorous acid (HOCl) and nitric oxide (NO), as well non-oxidative killing mechanisms including antimicrobial peptides (AMPs) and enzymes such as elastase and lysozymes (van Kessel, Bestebroer & van Strijp, 2014). Moreover, neutrophils can also release neutrophil extracellular traps (NETS), which form when the neutrophil releases extracellular DNA which can trap the pathogen (Brinkmann and Zychlinsky, 2012).

The avian counterparts of mammalian neutrophils are called heterophils. Our understanding of heterophil biology is mainly based on studies of the Gram negative *Salmonella* genus (Wigley, 2014). Similarly to neutrophils, they act early to engulf and destroy pathogens in the phagosome and release their granule content at the site of infection (Swaggerty *et al.*, 2003; Genovese *et al.*, 2013). They are capable of generating ROS, however, their oxidative burst is weakened due to the absence of MPO (Brune, Leffell & Spitznagel, 1972; Penniall & Spitznagel, 1975). AMPs likely play an important role in heterophil defence mechanisms due to their weak oxidative burst. The major classes of AMPs identified are: cathelicidin-like peptides and defensins. Unlike human neutrophils where α-defensins are the major antimicrobial peptide, only β-defensins appear to exist in chickens (Cuperus *et al.*, 2013), Furthermore, heterophils are also capable of killing pathogens via extracellular traps (Chuammitri *et al.*, 2009).

The avian heterophil response to *S. aureus* is similar to human neutrophils. For example, heterophil adherence, chemotaxis and phagocytic activity is increased during an *S. aureus in vivo* infection of chickens (Andreasen *et al.*, 1991). In addition, an important influx of heterophils in blood is reported during *S. aureus* bacteraemia *in vivo*, suggesting they play an important role in the first line of defence in chickens (Andreasen *et al.*, 1992). Avian defensins have been reported to be active against *S. aureus*. For example, cathelicidin-like peptide 2 (CATH2) binds to *S. aureus*, leading to membrane permeabilization and cell shrinkage (Schneider *et al.*, 2017). Moreover, intraperitoneal injection of CATH1 in neutropenic mice was protective against a lethal dose of MRSA, suggesting a potential therapeutic role (Bommineni *et al.*, 2010).

1.3.3. Macrophages

Macrophages are an essential component of the innate immune system, with a range of different functions, from defence against pathogens to tissue repair and homeostasis (Hume, 2015). In mammals, the growth and differentiation of macrophages depends on lineage-specific cytokines such as colony-stimulating factor 1 (CSF-1) (Hume, 2015). Tissue-resident macrophages are capable of recognising and phagocytosing invading pathogens and can also amplify the adaptive immune responses via antigen recognition by major histocompatibility complex II (MHC II) molecules and secretion of chemokines and cytokines (Gordon, 2003).

Mammalian macrophages play a key role in the host defence against *S. aureus* in mice models of infection (Brown *et al.*, 2015; Chan *et al.*, 2018). Recognition of *S. aureus* by macrophages leads to its engulfment, before phagosomal degradation by acidification and enzyme digestion (Kneidl *et al.*, 2012; Sedlyarov *et al.*, 2018). Mammalian macrophages possess an arsenal of antimicrobial killing mechanisms against *S. aureus* including ROS, lysozyme, cathepsins and phospholipase A2 (Miyauchi *et al.*, 1985; Müller *et al.*, 2014; Pernet *et al.*, 2015; Nandi *et al.*, 2015). The release of NO in response to staphylococcal lipoproteins has been described in mice (Nandi *et al.*, 2014; Bishayi *et al.*, 2014; Kim *et al.*, 2015). However, the expression and production of NO is host-species dependent. The macrophage production of NO for humans and some farm animals in response to bacterial challenge is absent or limited *in vitro* (Schneemann & Schoeden, 2007; Young *et al.*, 2018). Moreover, MHC II presentation by macrophages is essential for activation of T cells producing interferon gamma (IFNγ) and resolution of *S. aureus* infections in mice (Brown *et al.*, 2015).

Avian macrophages are similar in structure and function to mammalian macrophages (Kaspers & Kaiser, 2013). The proliferation and differentiation of macrophages also depends on signalling through the CSF1 receptor (Garceau *et al.*, 2010). The recent development of transgenic chickens with fluorescent myeloid cells under the control of the CSF-1 receptor should help to shed light on the spatial organisation and function of avian macrophages (Garceau *et al.*, 2015). Chicken macrophages are

capable of chemotaxis and also secrete the migration inhibition factor (MIF) (Morita *et al.*, 1976; Kim *et al.*, 2010). However, despite genetic description of chemokines and receptors, experimental proof is lacking (Hughes *et al.*, 2007; Kaiser *et al.*, 2005). Avian macrophages have been reported to phagocytose multiple bacterial pathogens, including *Salmonella enterica, Escherichia Coli* and *Campylobacter jejuni* (Kaspers & Kaiser, 2013) and possess a wide array of conserved killing mechanisms such as lysozyme and the respiratory burst. (Goethe & Phi, 1994; Lin, Chang & Mccormick, 1996; Wigley *et al.*, 2006). Interestingly, chicken macrophages are potent inducers of NO in response to different bacterial stimuli (Sung *et al.*, 1991; Lin, Chang & Mccormick, 1996; He & Kogut, 2003). Of note, chicken macrophages exhibit induction of NO in response to purified *S. aureus* lipotechoic acid (LTA) (He *et al.*, 2005).

Similarly to mammalian macrophages, avian macrophages express MHC II on their cell surface. However, mammals possess several distinct isotypes of highly polymorphic MHC genes whereas the chickens possess only one isotype of classical class II genes (Parker & Kaufman, 2017), suggesting a more compact MHC system. Of interest, MHC genotypes are strongly linked to disease resistance (Parker & Kaufman, 2017). MHC associations with moderately or highly pathogenic strains of *S. aureus* have been described in White Leghorn chickens (Cotter *et al.*, 1987). In addition, two MHC *B* complex genotypes, A4 and A12 are reported to be associated with increased susceptibility to *S. aureus* skeletal disease in broiler (Joiner *et al.*, 2005), suggesting a potential influence of MHC on the outcome of *S. aureus* infections.

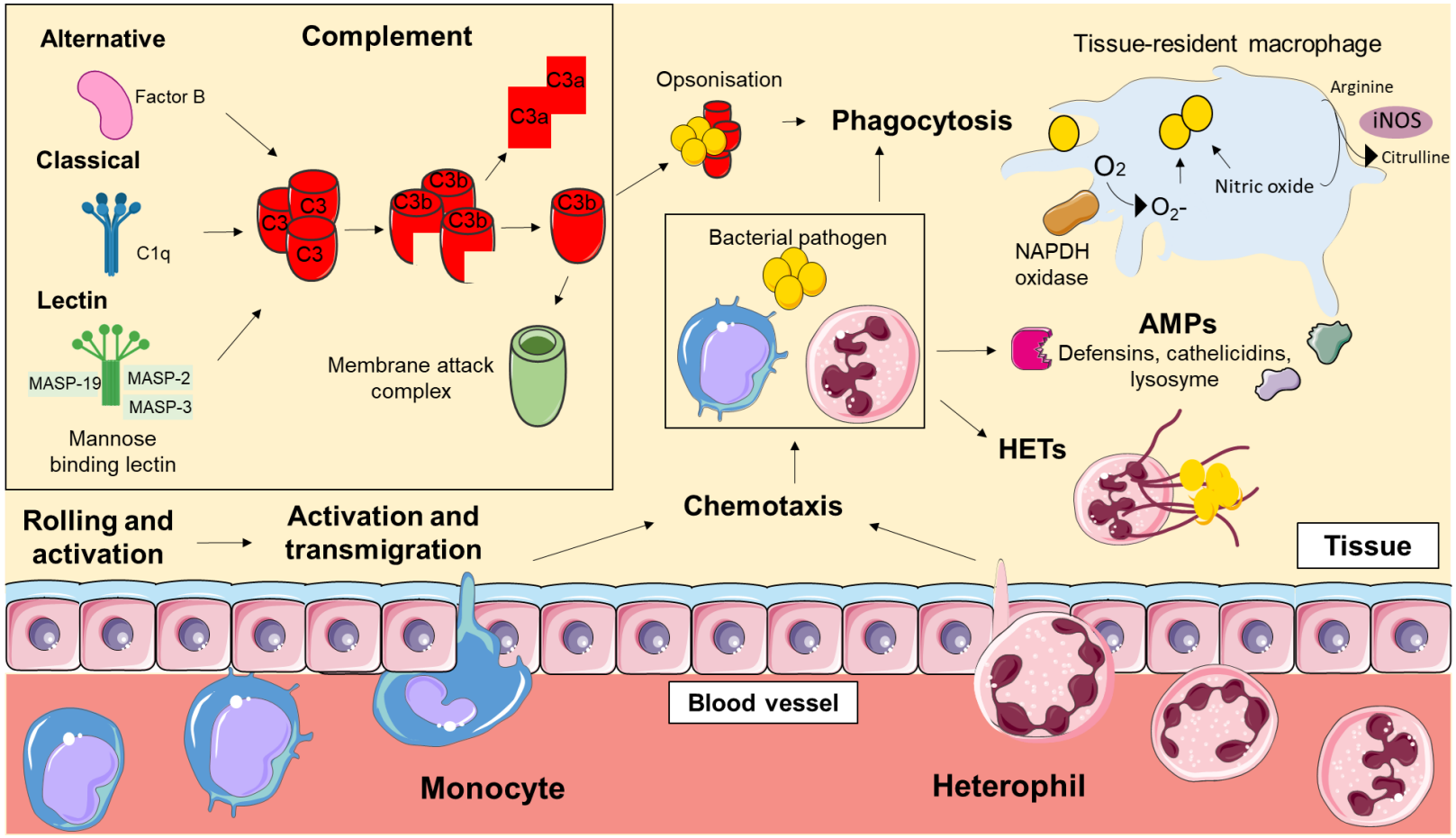
Alternative
Complement
Factor B
Classical
C1q
Lectin
MASP-19
MASP-2
MASP-3
Mannose binding lectin
C3
C3a
C3b
Membrane attack complex
Opsonisation
Phagocytosis
Bacterial pathogen
Tissue-resident macrophage
Arginine
iNOS
Citrulline
O_2
O_2-
Nitric oxide
NAPDH oxidase
AMPs
Defensins, cathelicidins, lysosyme
HETs
Chemotaxis
Rolling and activation
Activation and transmigration
Tissue
Blood vessel
Monocyte
Heterophil

Figure 1.2. The avian innate immune response to bacterial challenge.

When exposed to a bacterial pathogen, monocytes and heterophils are activated and recruited to the site of infection. The cells adhere and roll along the endothelium, before transmigrating and moving towards their target by chemotaxis. Heterophils recognise the bacterium via PRRs, followed by phagocytosis, killing by release of ROS, AMPs and release of HETs, leading to bacterial clearance. Tissue resident macrophages or recruited macrophages also recognise the pathogen which leads to phagocytosis and killing via ROS or NO. The complement system, present in the blood and tissues, can also clear *S. aureus* via three different pathways (classical, lectin and alternative). Figure created with images from Servier medical art.

1.3.4. Pattern recognition and signalling

Immune recognition of bacterial pathogens is crucial to initiate downstream antimicrobial cascades and cellular responses (Askarian *et al.*, 2018). In mammals, this is achieved by pattern recognition receptors (PRRs) of innate immune cells, which recognise pathogen-associated molecular patterns (PAMPs). These PRRs include Toll-like receptors (TLRs), retinoic acid-inducible gene-1 (RIG-I) like receptors (RLRs), nucleotide-binding oligomerisation domain (NOD)-like receptors (NLRs) and C-type lectin receptors (CLRs) family members. The PRRs are found at the cell surface, within membrane-bound vesicles or in the cytoplasm (Keestra *et al.*, 2013).

The recognition of *S. aureus* in mammalian host species has mainly been reported in mice and humans. For example, macrophages have been reported to recognize and phagocytose *S. aureus* via the cell surface receptors CD36, CD163 and C-type lectins, which leads to both induction and control of pro-inflammatory cytokines including TNFα and IL-12 (Stuart *et al.*, 2005; Kneidl *et al.*, 2014; Castleman, Febbraio & Hall, 2016; Mnich *et al.*, 2019). In addition, TLR2 has also been reported to be an important PRR in *S. aureus* infection. TLR2 binds to either diacyl lipopeptides in dimerization with TLR6 or triacycl lipopeptides in dimerization with TLR1 (Takeuchi *et al.*, 2001, 2002a). Studies suggest TLR2 can also bind LTA on the *S. aureus* cell surface (Schröder *et al.*, 2003a). However, the evidence is controversial due to potential contamination with lipoproteins (Dziarski & Gupta, 2005; Bunk *et al.*, 2010).

Binding of *S. aureus* to TLR2 on the cell surface of macrophage leads to activation of classical inflammatory cytokine pathways, including MYD88 signalling and production of pro-inflammatory cytokines TNFα, IL-6 and IL-1β (Feuerstein *et al.*, 2015). Conflicting evidence exists as to whether TLR2 is protective (Takeuchi, Hoshino & Akira, 2000; von Eiff *et al.*, 2001; Watanabe *et al.*, 2007; Hanzelmann *et al.*, 2016) or detrimental (Knuefermann *et al.*, 2004; Watanabe *et al.*, 2007) *in vivo* and is highly dependent on the models used.

Table 1.1 Comparison of human vs avian TLRs.

Human	Avian	Agonist	Reference
TLR1/6/10	TLR1 A/B	Lipoprotein	(Hume *et al.*, 2001; Fukui *et al.*, 2001)
TLR2	TLR2 A/B	Peptidoglycan	(Boyd *et al.*, 2001; Higuchi *et al.*, 2008)
TLR3	TLR3	dsRNA	(Schwarz *et al.*, 2007)
TLR4	TLR4	LPS	(Leveque *et al.*, 2003)
TLR5	TLR5	Flagella	(Iqbal *et al.*, 2005)
TLR7	TLR7	ssRNA	(Philbin *et al.*, 2005)
TLR8	Pseudogene	ssRNA	(Philbin *et al.*, 2005)
TLR9	TLR21	CpG	(Brownlie *et al.*, 2009; Keestra *et al.*, 2010)
Absent	TLR15	LPS/Lipoprotein/CpG	(Higgs *et al.*, 2006; De Zoete *et al.*, 2011; Boyd *et al.*, 2012; Zhou *et al.*, 2013)

However, individuals with TLR2 deficiencies are highly susceptible to *S. aureus* infection (von Bernuth *et al.*, 2012), underlining its importance in the *S. aureus* host response. Intracellular recognition of *S. aureus* in mammals has been reported for TLR8, TLR9 and NOD2 (Parker & Prince, 2012; Bergstrøm *et al.*, 2015; Hruz *et al.*, 2009; Volz *et al.*, 2010), leading to downstream activation of both classical inflammatory cytokines and type I interferons (Wolf *et al.*, 2011; Bergstrøm *et al.*, 2015).

In avian species, an increasing body of evidence has revealed the importance of TLRs for recognition of pathogens during infection (Kaiser, 2010). The avian TLR family members include both mammalian orthologues and avian specific TLRs, summarized in Table 1.1. The TLR1 family in the avian genome has tandemly duplicated genes, TLR1 A/B and TLR 2 A/B (Boyd *et al.*, 2001; Fukui *et al.*, 2001). Avian TLR1 and TLR2 families can form heterodimers to detect bacterial lipoproteins and peptidoglycan (Higuchi *et al.*, 2008).

Similarly to mammalian species, oxidative burst of heterophils in response to *S. aureus* LTA was inhibited by goat anti-TLR2 sera, suggesting a role for TLR2 in the avian response to *S. aureus* (Farnell *et al.*, 2003). Avian orthologues for TLR3 (Schwarz *et al.*, 2007), TLR4 (Leveque *et al.*, 2003), TLR5 (Iqbal *et al.*, 2005) and TLR7 (Philbin *et al.*, 2005) are also present in the chicken genome. Unlike the mammalian genome, TLR8 is pseudogenised and TLR9 is absent from the chicken genome (Philbin *et al.*, 2005). Two avian-specific TLRs are present: TLR21 and TLR15. TLR21 compensates for the absence of TLR9 as it is capable of detecting CpG motifs (Brownlie *et al.*, 2009; Keestra *et al.*, 2010). TLR15 can recognise microbial proteases and a range of PAMPs from bacterial pathogens such as *Salmonella Typhimurium* (Higgs *et al.*, 2006; De Zoete *et al.*, 2011). Downstream signalling of avian TLRs and intracellular PRRs are poorly characterised in chickens.

1.4. *S. aureus* immune evasion

When infecting a host, *S. aureus* must escape clearance by the host's immune system in order to survive. *S. aureus* has evolved a myriad of ways to evade the innate immune system, with over 35 staphylococcal immune evasion proteins identified so far, suggesting a high level of redundancy (summarized in Table 1.2).

1.4.1. Complement inhibition

S. aureus is capable of inhibiting complement at different stages of the cascade. In particular, *S. aureus* secretes proteins that can interfere with the deposition of C3 on the bacterial surface. For example, aureolysin, a metalloprotease, cleaves C3 to an inactive form (Laarman *et al.*, 2011a). In a similar way, the staphylococcal complement inhibitor (SCIN), encoded in the IEC2, associates with C3 and inhibits it, therefore blocking the downstream complement cascade (Jongerius *et al.*, 2007). Extracellular fibrinogen-binding protein (Efb) as well as extracellular complement-binding protein (Ecb), also encoded on IEC2, can modulate the alternative pathway of complement by binding to factor H and C3b, enhancing the inhibitory effect of factor H (Jongerius *et al.*, 2007). In addition, the staphylococcal binder of immunoglobulin (Sbi) can also associate with C3 and factor H to inhibit the alternative pathway. Furthermore, Sbi can interfere with C1q binding to immunoglobulin, through its Fcγ-domain, thereby blocking the classical complement pathway (Burman *et al.*, 2008). Finally, superantigen-like protein 7 (SSL7) binds to the Fc receptor of IgA and interferes with antibody recognition whilst the C-terminal grasp domain binds to C5 and inhibits complement activation (Laursen *et al.*, 2010; Bestebroer *et al.*, 2010).

1.4.2. Inhibition of chemotaxis

To prevent recruitment of immune cells, *S. aureus* produces a wide variety of proteins which inhibit chemotaxis. For example, *S. aureus* secretes the chemotaxis inhibitory protein (CHIPS), which inhibits the chemoattractant C5a and formyl peptide receptor (FPR1) (de Haas *et al.*, 2004). Moreover, members of the

staphylococcal superantigen-like toxin (SSL) family, encoded in the genomic island vSaα, also play an important role in the inhibition of immune cell chemotaxis (Fraser & Proft, 2008). For example, SSL5 inhibits neutrophil chemotaxis by binding both to complement receptors and chemokine receptors (Bestebroer *et al.*, 2007; Walenkamp *et al.*, 2010), as well as the matrix metalloproteinase 9 (MMP-9) on the surface of neutrophils (Itoh *et al.*, 2010a). Similarly, SSL10, SSL11 and SSL13 all interfere with neutrophil chemotaxis by binding to CXCR4, P-selectin and FPR1, respectively (Chung *et al.*, 2007a; Zhao *et al.*, 2018; Chen, Yang & Barbieri, 2019). Proteases can also inhibit chemotaxis, as reported for cysteine protease staphopain A (ScpA), which destroys CXCR2 (Laarman *et al.*, 2012).

1.4.3. Modulation of recognition and immune signalling

Recognition of *S. aureus* by phagocytes is an important step to initiate host immune responses, including phagocytic killing and activation of the adaptive immune system. *S. aureus* is capable of targeting cell surface receptors to evade recognition. For example, the bacterium targets TLR2 using SSL3, and to a less extent SSL4, which inhibit lipopeptide binding, as well as TLR2 heterodimerization with TLR1 and TLR6 (Bardoel *et al.*, 2012; Yokoyama *et al.*, 2012; Koymans *et al.*, 2018). Furthermore, *S. aureus* can also inhibit recognition by TLR2 by cleaving the lipoproteins on its cell surface (Chen & Alonzo, 2019). *S. aureus* is also capable of blunting TLR2-mediated recognition by the action of two moonlighting proteins: the lipoylated E2 subunit of pyruvate dehydrogenase and novel type-II CAAX protease MroQ (Grayczyk *et al.*, 2017; Marroquin *et al.*, 2019), although further work is required to determine the mechanism behind this immune modulation. Another tactic used by *S. aureus* to avoid immune recognition is the modification of its cell wall. For example, a significant proportion of *S. aureus* clones belonging to CC5 and CC398 contain prophages that encode an alternative wall techoic acid (WTA) glycosyltransferase (Gerlach *et al.*, 2018). The altered cell wall glycosylation leads to reduced antibody binding and therefore reduced immunogenicity (Gerlach *et al.*, 2018).

Table 1.1. Summary of immune evasion proteins and their proposed function.

Evasion mechanism	Virulence factor	Function	Reference
Chemotaxis inhibition	CHIPS	Binds C5aR receptor and formyl peptide receptor 1 and inhibits chemotaxis	(de Haas *et al.*, 2004)
	FLIPR	Binds formyl receptor 2 and inhibits chemotaxis	(Prat *et al.*, 2009)
	SSL1	Binds and inhibits MMPs, inhibiting neutrophil function	(Koymans *et al.*, 2016)
	SSL5	Binds to P-selectin, inhibiting neutrophil extravasation; Binds to N-terminus of chemokine and anaphylatoxin receptors to prevent leukocyte activation and migration; Binds and inhibits MMP-9, inhibiting neutrophil function; Binds to GPIbα and GPVI to activate and aggregate platelets for colonization	(Bestebroer *et al.*, 2007) (Walenkamp *et al.*, 2010) (Bestebroer *et al.*, 2009; De Haas *et al.*, 2009; Koymans *et al.*, 2016)) (Itoh *et al.*, 2010a)
	SSL6	Binds to CD47 on cells involved with migration and proliferation	(Fevre *et al.*, 2014)
	SSL8	Binds to extracellular matrix protein tenascin C and prevents attachment to P-selectin	(Itoh *et al.*, 2013a)
	SSL11	Binds to glycoproteins on neutrophils, prevents attachment to P-selectin and inhibits motility; Binds to FcαRI	(Chung *et al.*, 2007b; Chen, Yang & Barbieri, 2019)
	SSL13	Binds to formyl receptor 2, inhibiting neutrophil chemotaxis and inhibition	(Zhao *et al.*, 2018)

Evasion mechanism	Virulence factor	Function	Reference
Complement inhibition	Cna	Binds to C1q and blocks classical activation	(Kang *et al.*, 2013)
	Ecb	Modulates the alternative pathway of complement by binding to factor H and C3b, enhancing the inhibitory effect of factor H	(Jongerius *et al.*, 2007)
	Efb	Binds to C3b and fibrinogen and hides C3b deposition	(Ko *et al.*, 2013)
	Sbi	Binds to C3 and factor H to inhibit the alternative pathway; Interferes with C1q binding to immunoglobulin via Fcγ-domain, blocking the classical complement pathway	(Burman *et al.*, 2008)
	SdrE	Binds factor H and interacts with factor I to cleave C3b into inactive C3b	(Sharp *et al.*, 2012)
	SCIN	Binds C3 convertase and inhibits cleavage of C3. Humans specific variant and equine variant with broad host-specificity	(Jongerius *et al.*, 2007; De Jong *et al.*, 2018)
	SSL7	N-terminal OB domain binds to Fc receptor of IgA and interferes with recognition/opsonisation; C-terminal grasp binds to C5 and inhibits complement activation	(Laursen *et al.*, 2010) (Bestebroer *et al.*, 2010) (Langley *et al.*, 2005)
Inhibition of phagocyte mediated killing	DltABCD	D-alanylation of teichoic acids leading to a positive charge on the bacterial cell surface, interfering with binding of AMPs	(Peschel *et al.*, 1999)
	Eap	Inhibits neutrophil elastase, proteinase 3 and cathepsin G	(Stapels *et al.*, 2017)
	Hmp	Detoxifies NO in response to nitrosative stress	(Richardson, Dunman & Fang, 2006)

Evasion mechanism	Virulence factor	Function	Reference
	KatA	Detoxifies hydrogen peroxide	(Barria *et al.*, 2002)
	Ldh1	Produces L-lactate that helps maintain redox balance; Blocks NO from inhibiting respiration through fermentative activity	(Richardson *et al.* 2008)
	MprF	Decreases binding of AMPs by incorporating lysine residues into the lipid membrane	(Peschel *et al.*, 2001)
	OatA	Acetylates peptidoglycan, leading to lysozyme resistance	(Bera *et al.*, 2004)
	SodA and SodM	Catalyze superoxide into hydrogen peroxide which detoxifies reactive oxygen species	(Karavolos *et al.*, 2003)
	SPIN	Binds to and inhibits myeloperoxidase in human neutrophils	(Ploscariu *et al.*, 2018; M de Jong *et al.*, 2018)
	Staphylokinase (SAK)	Binds and inhibits α-defensins	(Jin *et al.*, 2004; Nguyen & Vogel, 2016)
	Staphyloxanthin	Involved in resistance to hydrogen peroxide produced by neutrophils	(Pelz *et al.*, 2005)
Inhibition of phagocytosis	Aureolysin	Degrades C3 and inhibits C3b opsonization	(Laarman *et al.*, 2011b)
	Capsule	Hides the bacterium from opsonization	(Thakker *et al.*, 1998)
	Protein A	Binds Fc region of IgG and prevents phagocytosis	(Dossett *et al.*, 1969)
	SAK	Plasminogen that degrades C3 and IgG	(Rooijakkers *et al.*, 2005)

Evasion mechanism	Virulence factor	Function	Reference
	Staphopain A/B	Secreted protease that degrade complement	(Kolar *et al.*, 2013)
	SSL10	N-terminal domain targets IgG1 and its C-terminal domain targets C4 for inhibition of opsonisation; Targets prothrombin and factor Xa to inhibit blood coagulation	(Patel *et al.*, 2010) (Itoh *et al.*, 2010b) (Itoh *et al.*, 2013b)
	V8	Protease that degrades complement and IgG	(Kolar *et al.*, 2013)
Host cell death			
	α-toxin	Targets a zinc-dependent metalloprotease ADAM-10 expressed as a transmembrane protein, found on the surface of epithelial, endothelial cells, monocytes, macrophages, B cells and T cells; Kills macrophages in an NLRP3-dependent manner	(Wilke & Wardenburg, 2010; Nygaard *et al.*, 2012; Becker *et al.*, 2014) (Craven *et al.*, 2009.; Kebaier *et al.*, 2012; Ezekwe *et al.*, 2016)
	HlgAB	Pore forming toxin; binds CXCR1, CXCR2 and CCR2 on neutrophils, monocytes and macrophages	(Spaan *et al.*, 2014)
	HlgCB	Pore forming toxin; binds C5aR1 and C5aR2 on neutrophils, monocytes and macrophages	(Spaan *et al.*, 2014)
	LukAB	Pore forming toxin; binds CD11b on human macrophages and neutrophils and kills human monocytes via NLRP3	(DuMont *et al.*, 2013) (Melehani *et al.*, 2015)
	LukED	Pore forming toxin; binds CCR5 and CXCR1 and 2 on macrophages, neutrophils, T cells and red blood cells	(Reyes-Robles *et al.*, 2013)
	LukMF’	Pore forming toxin; binds CCR1 on bovine neutrophils	(Vrieling *et al.*, 2016)

Evasion mechanism	Virulence factor	Function	Reference
Inhibition of immune cell activation and signalling	LukPQ	Pore forming toxin; binds CXCRA and CXCR2 on equine neutrophils	(Koop *et al.*, 2017)
	Non-ribosomal cylic dipeptide	Required for phagosomal escape and intracellular survival of *S. aureus*, as well as induction of host cell death	(Blättner *et al.*, 2016)
	α-PSMs	Small amphipathic peptide; may be involved in intracellular lysis of host cell, *S. aureus* phagosomal escape and immune cell modulation	(Wang *et al.*, 2007; Schreiner *et al.*, 2013; Surewaard *et al.*, 2013; Grosz *et al.*, 2014)
	PVL	Binds to C5aR, leads to host cell lysis; Kills human monocytes via NLRP3	(Spaan *et al.*, 2013a) (Holzinger *et al.*, 2012)
	Lipoic acid A	Suppresses immune activation of macrophages and limits NO release	(Grayczyk *et al.*, 2017; Grayczyk & Alonzo, 2019)
	Lipase	Inactivates lipoproteins leading to inhibition of immune cell activation	(Chen & Alonzo, 2019.)
	MroQ	Promotes TLR2 mediated activation of immune cells but prevents IL-1β secretion	(Cosgriff *et al.*, 2019)
	SSL3 and SSL4	Inhibitors of TLR2, inhibiting bacterial lipoprotein binding; Inhibitors of TLR2-4-6 heterodimerization	(Bardoel *et al.*, 2012; Koymans *et al.*, 2017)) (Hermans *et al.*, 2012)
	TarP	WTA glycosyltransferase; leads to avoidance of immune recognition	(Gerlach *et al.*, 2018)

1.4.4. Inhibition of phagocyte-mediated killing

As previously described, *S. aureus* can be phagocytosed by professional phagocytes, where it will come into contact with NO, reactive oxygen species, AMPs and proteolytic enzymes. *S. aureus* has evolved a wide array of mechanisms to evade these killing strategies. For example, *S. aureus* targets neutrophil oxidative defence by producing staphylococcal peroxidase inhibitor (SPIN), which directly inhibits MPO, blocking the production of HOCl (de Jong *et al.*, 2017; De Jong *et al.*, 2018). In addition, *S. aureus* also secretes the carotenoid pigment staphyloxanthin, which provides resistance to H_2O_2 produced by neutrophils (Pelz *et al.*, 2005).

In order to defend itself from NO, *S. aureus* synthesises lactate dehydrogenase (Ldh), allowing production of L-lactate, that helps maintain redox balance and leads to enhanced bacterial replication (Richardson, Libby & Fang, 2008b). The fermentative activity of Ldh also blocks NO from inhibiting respiration (Richardson, Libby & Fang, 2008a). Ldh is transcribed from flavohemoglobin (Hmp) which in itself can detoxify NO. Furthermore, *S. aureus* can also synthesise bacterial NO (bNOS) that is structurally similar to NO but lacking the reductase domain. This has been shown to promote cathelicidin resistance, NET killing resistance and increase intracellular survival within murine macrophages (Van Sorge *et al.*, 2013).

S. aureus also employs several virulence factors that target (AMPs). For example, D-alanylation of teichoic acids mediated by the Dlt operon (*DltACBD*) leads to a positive charge on the bacterial cell surface which interferes with binding of AMPs and increased susceptibility and increased killing by neutrophils is observed when D-alanylation is lost (Peschel *et al.*, 1999; Collins *et al.*, 2002). In addition, MprF can also modify the cell wall to repel cationic AMPs (Peschel *et al.*, 2001). Furthermore, Staphylokinase (SAK), an exoprotein that activates plasminogen, directly binds and inactivates α-defensins (Jin *et al.*, 2004).

1.4.5. Host cell death

Another important strategy used by *S. aureus* to manipulate the immune response is the induction of cell death via pore-forming toxins. These toxins disrupt the cell membrane and can be classified into two categories: the β-barrel pore-forming toxins and small α-helical peptides. The β-barrel forming proteins are found in monomeric forms and assemble in a heptamer to create a pore, leading to leakage and lysis (Berube *et al.*, 2013). α-toxin, also known as α-hemolysin, was the first β-barrel pore-forming toxin to be identified and is conserved in most *S. aureus* isolates (Wilke & Wardenburg, 2010). α-toxin targets a zinc-dependent metalloprotease ADAM-10 expressed as a transmembrane protein, found on the surface of epithelial and endothelial cells (Wilke & Wardenburg, 2010). It can also target monocytes, macrophages, B cells and T cells (Wilke & Wardenburg, 2010; Nygaard *et al.*, 2012). Furthermore, α-toxin can also trigger the inflammasome and induce programmed cell death in macrophages, both *in vitro* and in murine models of infection (Craven *et al.*, 2009; Kebaier *et al.*, 2012). Neutrophils can be resistant to α-toxin toxicity due to low expression of ADAM-10 on their cell surface (Nygaard *et al.*, 2012). α-toxin can also can inhibit macrophage phagocytosis (Scherr *et al.*, 2015) and affect downstream signalling of immune cells including neutrophils (Becker *et al.*, 2014). α-toxin has been identified as a key player in *S. aureus* pathogenesis in murine mice models and expression level correlates with the severity of infection (Inoshima *et al.*, 2011; Abtin *et al.*, 2014).

Bicomponent leukocidins are another group of the β-barrel pore-forming toxins that are widely distributed among *S. aureus* isolates (Koymans *et al.*, 2016). Leukocidins assemble from two subunits F and M into an octomeric pore once they have associated with the receptor on target myeloid cells and erythrocytes (Alonzo & Torres, 2014). The γ-hemolysin (expressed as HlgAB or HlgBC), present in all *S. aureus* strains, can lyse erythrocytes as well as promote lysis of neutrophils, monocytes and macrophages (Spaan *et al.*, 2014). Other leukocidins include LukED LukMF' and LukPQ (Reyes-Robles *et al.*, 2013; Vrieling *et al.*, 2016; Koop *et al.*, 2017). LukED binds to chemokine receptors CXCR1, CXCR2 and CCR5 on immune cells, as well as the Duffy antigen receptor for chemokines to lyse erythrocytes (Reyes-Robles *et al.*, 2013). LukMF' found in ruminant isolates also binds

chemokine receptors CCR1, CCR2 and CCR5 (Vrieling *et al.*, 2015). LukPQ, found in the majority of equine isolates, binds to equine CXCRA and CXCR2 (Koop *et al.*, 2017) These toxins all target and lyse immune cells such as neutrophils (Reyes-Robles *et al.*, 2013; Vrieling *et al.*, 2016; Koop *et al.*, 2017). The most divergent leucocidin LukAB targets human phagocytic cells and binds to the integrin CD11b rather than a chemokine receptor (DuMont *et al.*, 2013). It is the only leukocidin known to lyse neutrophils intracellular and can act together with α-toxin to inhibit macrophage phagocytosis, promoting their cell death (DuMont *et al.*, 2013; Scherr *et al.*, 2015).

Panton-Valentine leucocidin (PVL), another β-barrel pore-forming toxin, can bind to C5aR on neutrophils, monocytes and macrophages (Spaan *et al.*, 2013a) in a host-specific manner, exhibiting rapid activation in human and rabbit neutrophils but not mice (Bubeck Wardenburg *et al.*, 2007; Spaan *et al.*, 2013a). Despite only being secreted by 2% of *S. aureus* isolates, it is present in almost all CA-MRSA clones and is associated with necrotizing pneumonia (Gillet *et al.*, 2002). Furthermore, PVL can also act in synergy with other haemolysins such as LukED, β and γ toxins (Spaan *et al.*, 2013a).

The phenol-soluble modulins (PSM) belong to the family of small α-helical peptides that can lyse cells. These shorter monomeric peptides can be found in two forms, PSMα and PSMβ. PSMα are the most cytolytic and have a high affinity for lipids (Wang *et al.*, 2007), suggesting that they function intracellularly rather than extracellularly (Surewaard *et al.*, 2013). Furthermore, they can be neutralized by serum lipoproteins, limiting their capacity for extracellular activity (Surewaard *et al.*, 2012). Their location is linked to their function as they have been shown to be expressed inside the phagosome of phagocytes, helping *S. aureus* escape via lysis of the cell (Surewaard *et al.*, 2013; Grosz *et al.*, 2014). PSMs have also been reported to impact the adaptive immune system by inducing IL-10 secretion from T cells (Schreiner *et al.*, 2013).

β-toxin (also called the β-hemolysin) is a 35 kDa protein characterized as a sphingomyelinase, which can hydrolyse sphingomyelin, a specific membrane lipid, leading to cell lysis. It is capable of lysing red blood cells, leading to evasion of

immune system and scavenging of iron (Huseby *et al.*, 2007). β-toxin can also lyse monocytes, leading to pro-inflammatory cytokine release including IL-1β and IL-6 (Walev *et al.*, 1996), as well as neutrophils and T cells (Huseby *et al.*, 2007; Tajima *et al.*, 2009). β-toxin has also been reported to be involved in biofilm formation, skin colonisation and infective endocarditis (Huseby *et al.*, 2010; Katayama *et al.*, 2013; Herrera *et al.*, 2016, 2017).

Pore-forming toxins also have the capacity to kill myeloid cells via the inflammasome receptor NLRP3. For example, recent studies on α-toxin suggest that cell death occurs in an NLRP3-dependent manner (Craven *et al.*, 2009; Kebaier *et al.*, 2012; Ezekwe *et al.*, 2016). This intracellular receptor associates with a complex called ASC which leads to the inflammasome activation, resulting in the cleavage of IL-1 into its pro-inflammatory form (IL-1β) (Davis, Wen & Ting, 2011). Similarly, LukAB and PVL have also been identified to kill human monocytes via NLRP3 when found extracellularly (Holzinger *et al.*, 2012; Melehani & Duncan, 2016). Furthermore, studies of the CA-MRSA epidemic clone USA300 indicate that the inflammasome activation via NLPR3 is also linked to necroptosis. For example, Kitur *et al.* found that α-toxin, LukAB and PSMs can activate MLKL-mediated necroptosis and IL-1β expression via pore formation and inflammasome activation (Kitur *et al.*, 2016). In addition, another study in mouse alveolar macrophages also linked necroptosis and the inflammasome and suggested that α-toxin used potassium efflux to disrupt the membrane (González-Juarbe *et al.*, 2015). However, this is in contrast to previous work identifying apoptosis as the main mechanism for macrophage cell death (Wang, Zhou & He, 2010a), suggesting the mechanism underlying macrophage cell death by *S. aureus* is still unknown.

1.4.6. Internalisation of *S. aureus* as a strategy for dissemination

It is now well established that despite being an extracellular pathogen, *S. aureus* can survive intracellularly in certain circumstances. In non-phagocytic cells, internalisation is mainly mediated by surface adhesins including fibronectin binding proteins A and B (Sinha *et al.*, 2000). In phagocytic cells such as macrophages, once internalised, *S. aureus* is capable of surviving intracellularly and proliferating, leading to cell lysis (Kubica *et al.*, 2008; Grosz *et al.*, 2014; Hamza & Li, 2014). Similarly, Heinrichs *et al.* have also reported that phagocytosed USA300 MRSA strain can persist in the human and murine macrophage phagolysosome, where they initiate intracellular replication before killing macrophages, resulting in the release of viable staphylococci (Flannagan, Heit & Heinrichs, 2016). Further investigation of this phenotype revealed that the GraXRS two-component regulatory system enables *S. aureus* to survive in the acidic environment of the phagolysosome (Flannagan *et al.*, 2018). This finding was supported by a study suggesting intracellular persistence of *S. aureus* was linked to the disruption of lysosomal enzymes and requires phagosomal acidification to increase expression of virulence factors (Tranchemontagne *et al.*, 2015). In contrast, another study using a mouse model for *S. aureus* lung infection, as well as *in vitro* human cells, suggested that intracellular persistence results from overwhelming the macrophage microbicidal activity and impaired acidification of the phagosome (Jubrail *et al.*, 2016). The viable intracellular bacteria were observed to be maintained by a cycle of lysis and re-uptake (Jubrail *et al.*, 2016). Despite confounding evidence found in the literature, all the studies report that macrophages fail to phagocytose intracellular *S. aureus*, leading to cell death (Kubica *et al.*, 2008; Tranchemontagne *et al.*, 2015; Melehani *et al.*, 2015; Jubrail *et al.*, 2016; Flannagan, Heit & Heinrichs, 2016).

Discrepancies could be due to strain variation as well as difference between cellular models. It remains unclear whether *S. aureus* induces an anti-apoptotic programme and proliferates within the phagosome or whether it escapes the phagosome to remain in the cytosol (Wang, Zhou & He, 2010b; Grosz *et al.*, 2014; Koziel *et al.*, 2015). A recent finding suggests that *sae*-regulated toxins such as LukAB and PVL determine damage and escape from macrophages whereas PSMs are responsible for

the escape from the phagosome into the cytosol (Musenmayer *et al.*, 2016). However, the toxin responsible for disruption of the phagosomal membrane and whether phagosomal escape occurs is yet to be defined (Grosz *et al.*, 2014; DuMont *et al.*, 2013; Giese *et al.*, 2011).

1.4.7. Host-adaptation of immune evasion factors

Immune evasion virulence factors likely play an important role in *S. aureus* host-adaptation, as the new host's immune response presents a unique environment for the bacterium to survive in. An overview of the host-specific virulence factors secreted by *S. aureus* are shown in Figure 1.3.

Species-specific differences in immune responses play an important role in the host-specificity of *S. aureus* virulence factors. For example, bovine strains encode a novel leucocidin LukMF', which binds to the chemokine receptor CCR1 only expressed on bovine neutrophils, and is important for the development of bovine mastitis (Vrieling *et al.*, 2015, 2016). Similarly, equine strains of *S. aureus* encode LukPQ, which binds to the chemokine receptors CXCRA only expressed on equine neutrophils (Koop *et al.*, 2017). Furthermore, α-toxin exerts potent activity against both rabbit erythrocytes (Cassidy & Harshman, 1976; Hildebrand, Pohl & Bhakdi, 1991) and murine alveolar epithelial cells (Berube *et al.*, 2013), which is due to the high expression of the receptor ADAM10 on the cell surface. In contrast, α-toxin activity is low on human erythrocytes due to the low expression of ADAM10 on their cell surface (Bubeck Wardenburg *et al.*, 2007; Berube *et al.*, 2013).

The long-term association of *S. aureus* with humans has enabled the bacterium to become highly human-adapted and possess a wider range of human-specific virulence factors (Weinert *et al.*, 2012). For example, approximately 90% of human *S. aureus* isolates carry the β-converting prophage, which encodes the virulence factors SAK, SCIN, CHIPS and SEA, all reported to be highly human-specific (Van Wamel *et al.*, 2006). Other examples of human-specific virulence factors include SPIN, PVL, HlgCB and LukAB. SPIN is only active against human MPO but not murine, equine, bovine and rabbit MPO (de Jong *et al.*, 2017). PVL demonstrates rapid pore formation human and rabbit neutrophils but not mice (Bubeck

Wardenburg *et al.*, 2007; Spaan *et al.*, 2013a). HlgCB and LukAB are both unable to kill murine leukocytes, despite their strong activity against human and primate leukocytes (DuMont *et al.*, 2013; Spaan *et al.*, 2014). Thus, immune evasion virulence factors are crucial for *S. aureus* host-adaptation to humans.

In animal *S. aureus* isolates, allelic variants of immune evasion genes with specific function in their respective hosts have been identified. For example, ovine strains of *S. aureus* encode a variant of TSST-1 and SEA (Guinane *et al.*, 2010), superantigens capable of crosslinking MHC class II receptor with T cell receptors, leading to excessive immune activation. The ovine variant of TSST-1 has varying function compared to the human variant (Lee *et al.*, 1992), suggesting host-specific functional activity, but the host-specific function of ovine SEA is unknown. Similarly, the superantigen-like protein SELX has multiple allelic variants in human and ruminant isolates, with differing mitogenicity towards bovine or human T cells (Wilson *et al.*, 2011; Tuffs *et al.*, 2017). SCIN is another example of host-adapted virulence factor in animals, with two variants in bovine and equine strains (Viana *et al.*, 2010; De Jong *et al.*, 2018). Although the human variant of SCIN is human-specific, the equine variant functions in a wider range of hosts including horses, humans and pigs, but is mainly found in equine isolates (De Jong *et al.*, 2018). The function of the bovine variant of SCIN is unknown. A cysteine protease with similar properties to ScpA is produced in avian strains, suggesting potential for being a host-specific virulence factor, although functional studies of host-specificity are required (Takeuchi *et al.*, 1999).

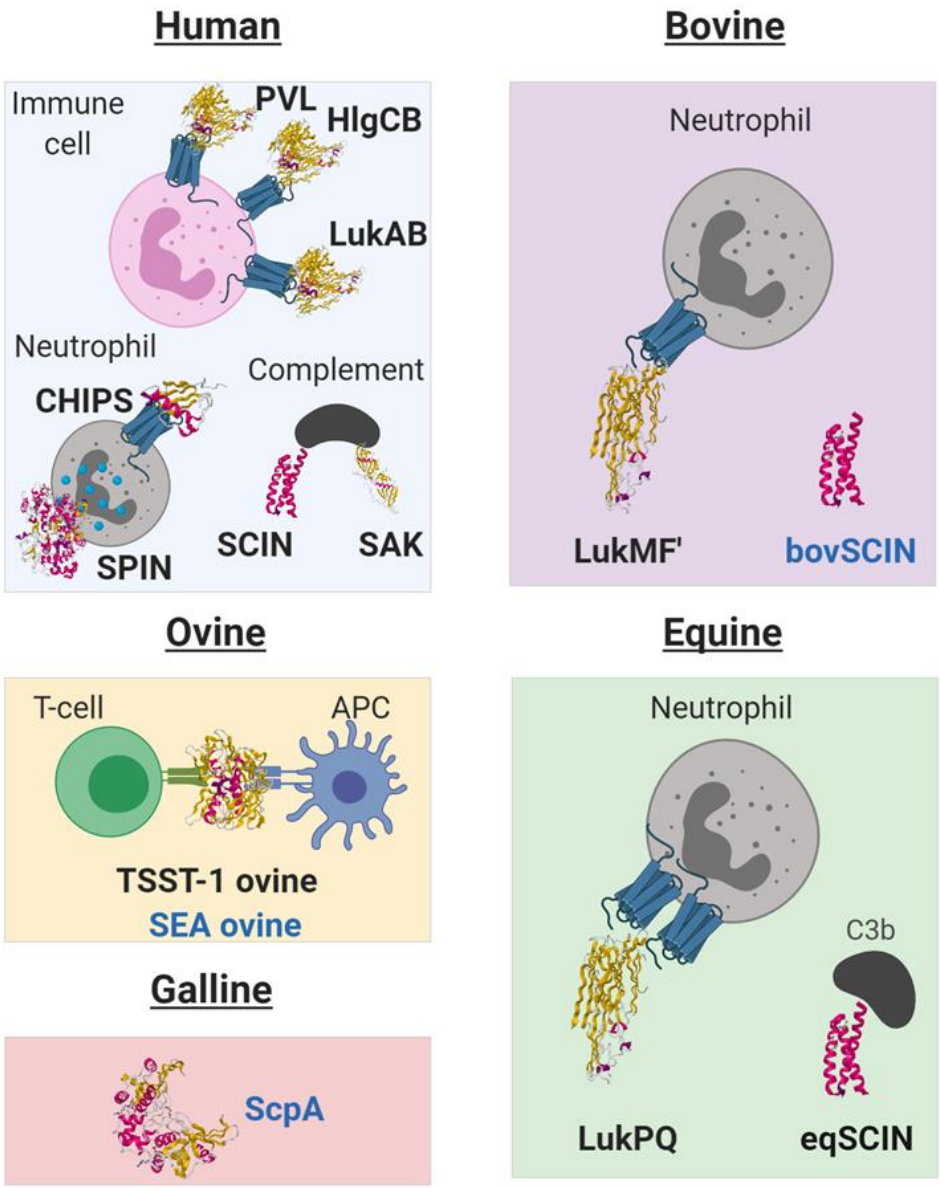

Figure 1.3. Host-specific *S. aureus* immune evasion proteins.

S. aureus possesses an array of host-specific virulence factors that play a role in evasion of their respective host's immune system. Shown are the different immune proteins that exhibit host-specific activity (black) or are hypothesised to exhibit host-specific activity (blue). Figure created with BioRender.com.

1.5. Hypothesis

Bacteriophages play an important role in *S. aureus* host-adaptation. β-converting prophage Sa3, found in approximately 90% of human isolates of *S. aureus*, contains IEC1, including genes associated with human-specific immune evasion (Van Wamel *et al.*, 2006). Comparative genomic analysis of *S. aureus* isolates from infected poultry has recently revealed an avian-specific subfamily of β-converting phages, called prophage Avβ (Lowder *et al.*, 2009). In prophage Avβ, the IEC1 is replaced with novel genes, hypothesised to play a role in *S. aureus* adaptation to the avian ecological niche. Further characterisation of the role of prophage Avβ in *S. aureus* avian host-adaptation could help to unravel the molecular mechanisms behind *S. aureus* pathogenesis in poultry. We propose that prophage Avβ and its encoded genes play a role in the evasion of avian innate immunity, thus allowing the survival and dissemination of *S. aureus* in the avian host.

1.6. Aims of this study

The aim of this project was to elucidate the role of prophage Avβ in *S. aureus* avian host-adaptation by:

- Evaluating the role of prophage Avβ in the evasion of avian innate immunity

- Investigating the distribution of prophage Avβ among avian isolates, characterising its gene content and functionally characterising the novel putative avian-specific genes

- Examining the early avian macrophage response to *S. aureus* and the role of prophage Avβ in this interaction

Chapter 2. General Materials and Methods

2.1. Ethics statement

All animal work was conducted in accordance with guidelines of the Roslin Institute and the University of Edinburgh and carried out under the regulations of the Animals (Scientific Procedures) Act 1986 under Home Office project license PPL 60/4420. Approval was obtained from the Protocols and Ethics Committees of the Roslin Institute and the University of Edinburgh.

Human venous blood was sampled from healthy donors recruited by passive advertising at the Roslin Institute (University of Edinburgh). Written informed consent was obtained from all volunteers before blood collection and after an outline of the risks was provided. Recruitment and sampling procedures were reviewed by the national research ethics service (NRES) committee London City and East under the research ethics committee reference 13/LO/1537. All blood collection samples were anonymized.

2.2. Bacterial culture conditions

S. aureus was routinely cultured in tryptone soy broth (TSB) (Oxoid) at 37°C with shaking at 200 rpm or plated on tryptone soy agar (TSA) (Oxoid) unless otherwise stated. All *Escherichia coli* strains were routinely cultured in Luria-Bertani (LB) broth (Melford Laboratories) at 37°C with shaking at 200 rpm or plated on LB agar. Where appropriate *E. coli* cultures were supplemented with 100 μg/ml ampicillin (Amp) (Formedium) or 15 μg/ml chloramphenicol (Cm) (Sigma-Aldrich) and *S. aureus* cultures were supplemented with 10 μg/ml chloramphenicol (Cm) or 1 μg/ml anhydrotetracycline (ATc) (Sigma-Aldrich).

2.3. Isolation and differentiation of chicken bone-marrow derived macrophages (chBMMs)

Femurs and tibias were collected from 3-week-old commercial Ross 308 broiler chickens. Bones were stripped of muscle with 70% (v/v) ethanol (Fisher Scientific). The bone were placed in a 60 mm petri dish (SLS) containing PBS (Lonza) before flushing the bone marrow using a 10 ml syringe (VWR), 18G blunt needle (VWR)

and RPMI-1640 medium (Gibco) under sterile conditions. Bone-marrow cells were passed through a 70 µm cell strainer (Thermo Fisher Scientific). Accurate cell numbers were obtained by live/dead counting with a haemocytometer (Neubaeur) and Trypan Blue (Life Technologies). Cells were frozen down by resuspending in heat-inactivated fetal bovine serum (FBS) (Thermo Fisher Scientific) + 10% (v/v) DMSO (Sigma-Aldrich) at $4x10^7$ cells/ml and stored at -155°C until further use.

To obtain chicken bone-marrow derived macrophages (chBMMs), the bone-marrow cells were thawed in a 37°C water bath and gently resuspended in 10 ml RPMI-1640 (Gibco) with 10% (v/v) FBS, 1% GlutaMAX (Gibco) and 1% (v/v) penicillin/streptomycin (Invitrogen) (complete RPMI). The bone-marrow cells were then centrifuged at 400xg for 5 min and re-suspended in complete RPMI. The cells were seeded at $2x10^7$ cells in 20 ml complete RPMI and 350 ng/µl recombinant chicken colony stimulating factor 1 (CSF-1) (Garceau *et al.*, 2010) in a sterilin 100mm square petri dish (SLS). The bone-marrow cells were cultured for 7 d at 41°C, 5% CO_2. On day 5, fresh media was supplemented with 350 ng recombinant chicken CSF-1. Differentiated macrophages were detached from plates by washing with PBS (Lonza) + 2% (v/v) FBS (Thermo Fisher Scientific), using a syringe and blunt 18G needle (VWR).

2.4. Molecular cloning

2.4.1. Genomic DNA extraction

Staphylococcal genomic DNA was routinely extracted from 500 µl of stationary phase culture using the PurEluteTM Bacterial Genomic Kit (Edge Biosystems). The manufacturer's instructions were followed except for the addition of 100 µg/ml lysostaphin (Ambi Products) to the Spheroplast Buffer followed by incubation for 30 min at 37°C. DNA pellets were suspended in 50 µl H_2O (Qiagen), and DNA was quantified using a NanoDropTM 1000 (Thermo Fisher Scientific).

2.4.2. Polymerase Chain Reaction

Custom oligonucleotides were purchased from Invitrogen, after design using software SnapGene Viewer (SnapGene). High-fidelity PCR reactions were performed with either *Pfu* Polymerase (Agilent Technologies) or Q5 polymerase (NEB). High fidelity polymerase reactions included 0.2 µM forward and reverse primers, approximately 100 ng of template DNA, 0.25 mM dNTPs (Promega), 1x PfuUltra^{TM} II reaction buffer (Agilent Technologies) or 1x Q5 reaction buffer (NEB), 1 U PfuUltra^{TM} II Fusion HS Polymerase (Agilent Technologies) or 1x Q5 high-fidelity polymerase and dH_2O to a final volume of 50 µl. For *Pfu* polymerase reactions, the thermocycler programme included an initial denaturation at 95°C for 2 min, followed by 30 cycles of denaturation at 95°C for 20 s, annealing at varying temperatures for 20 s, extension at 72°C for 15 s per kb, followed by final extension at 72°C for 3 min. For Q5 polymerase reactions, the thermocycler programme included an initial denaturation at 98°C for 30 s, followed by 30 cycles of denaturation at 98°C for 10 s, annealing at varying temperatures for 20 s, extension at 72°C for 20 s per kb, followed by final extension at 72°C for 2 min.

Low fidelity PCR reactions were performed using 0.625 U GoTaq® DNA polymerase (Promega), 0.2 µM forward and reverse primers, 0.25 mM dNTPs (Promega), 1.5 mM MgCl2 (Promega), 1 x GoTaq® Flexi Buffer (Promega), and dH_2O to a final volume of 25 µl. The thermocycler programme included, an initial denaturation at 95°C for 3 min, followed by 30 cycles of denaturation at 95°C for 30 s, annealing at varying temperatures for 30 s, extension at 72°C for 1 min per kb, followed by a final extension at 72°C for 5 min, unless otherwise stated.

For *E. Coli* colony PCR reactions, part of a colony was used to inoculate 10 µl of dH_2O and incubated at 95°C for 10 min. After centrifugation, 2 µl of this sample was used as template DNA following the same thermo-cycler conditions to those described previously.

For *S. aureus* colony PCR reactions, part of a colony was re-suspended in 50 µl lysis mix (H_2O containing 10 mg/ml lysostaphin (Ambi products), 10 mg/ml achromopeptidase (Sigma-Aldrich), 1% (w/v) 1M Tris-HCl pH 8 and 1% (w/v) 5M NaCl). The suspension was incubated at 37°C for 30 min then heated to 100°C for 5

min. 2 µl of this sample was used as template DNA following the same thermocycler conditions to those described previously.

2.4.3. Gel electrophoresis

Agarose gel electrophoresis of DNA fragments was carried out in 1 % (w/v) agarose (Melford Laboratories), with 1x Tris-acetate-EDTA (TAE) buffer (Thermo Fisher Scientific) containing either 1 x SYBR safe DNA gel stain (Life Technologies) or 1x Gel Red DNA stain (Biotium Limited, Cambridge Biosciences). Promega loading dye (Promega) was added to DNA samples before they were loaded onto the gel alongside a 1 kb DNA ladder (Promega), followed by electrophoresis at 110 V for 30 min. Gels were visualised using the UV transilluminator function on a G-box (Syngene).

2.4.4. Plasmid isolation and concentration

Plasmids were routinely extracted using the Monarch plasmid extraction kit (NEB) following the manufacturer's instructions except for the supplementation of buffer B2 with 5 mg/ml lysostaphin (Ambi Products) for *S. aureus* isolates, followed by incubation at 37°C for 30 min. Low copy number plasmids were concentrated using Pellet Paint® Co-precipitant (Novagen) following the manufacturer's instructions. Plasmid DNA was quantified using a NanoDropTM 1000 (Thermo Fisher Scientific).

2.4.5. Restriction digestion and ligation

Restriction digestion reactions were formulated as described in the manufacturer's instructions using restriction enzymes purchased from New England Biolabs (NEB). Reactions were incubated for at least 2 h at 37°C and heat inactivated if required. When necessary, re-ligation was prevented by incubating at 37°C for 30 min with 2 µl Antarctic Phosphatase Reaction Buffer and 5 U of Antarctic Phosphatase (NEB) and heat inactivated at 65°C for 5 min. Products of digestion were analysed by electrophoresis in a 1% (w/v) agarose gel and extracted using a Monarch Gel Extraction kit (NEB) following the manufacturer's instructions. Ligation reactions were performed using T4 DNA Ligase Reaction Buffer and T4 DNA Ligase (NEB)

following the manufacturer's instructions with the volume of plasmid and insert determined depending on a 3:1 molar ratio of insert: plasmid. Reactions were made up to 20 µl using nuclease-free dH_2O (Severn Biotech Ltd) and incubated overnight at 16°C. Before transformation the ligation plasmids were purified by dialysis using 0.025 µm filter circular discs (MilliPore) on MilliQ water at room temperature for 20 min.

2.4.6. Preparation of electrocompetent cells (*E. coli and S. aureus*)

E. coli competent cells were produced by inoculating 25 ml of LB broth (Melford Laboratories) with 250 µl of overnight culture followed by incubation at 37°C with shaking at 200 rpm until an OD600 of 0.6. Cells were placed on ice for 15 min and centrifuged at 4000 rpm for 10 min at 4°C. Cells were suspended once in an equal volume, once in a half volume, and once in a quarter volume of ice cold 10% (v/v) glycerol (Sigma-Aldrich) before final suspension in 2 ml ice cold 10% (v/v) glycerol. 50 µl aliquots were produced for storage at -80°C.

Electrocompetent *S. aureus* cells were prepared as follows: an overnight culture was diluted 1 in 25 in 25 ml TSB and grown at 37^{O}C, 200 rpm until OD600 of 0.8. Cells were centrifuged at 3000x *g* for 10 min and washed 3 times with an equal volume of sterile H_2O. Cells were then washed in 1/5 volume of 10% (v/v) glycerol, re-suspended in 1/10 volume of 10% (v/v) glycerol and incubated at 20^{O}C for 15 min before centrifugation and re-suspension in a final volume of 800 µl of 10% (v/v) glycerol. 70 µl aliquots were stored at -80^{O}C.

2.4.7. Electrotransformation of *E. coli* and *S. aureus*

Electrotransformation of *E. coli* cells was performed as follows: 5 µl of ligation reaction were mixed with 50 µl competent cells, in a 0.2 cm electroporation cuvette (Sigma-Aldrich) and electroporated at 100 Ω, 25 µF and 2.5 kV for 2 ms using a GenPulser XCell (Biorad). 250 µl of LB broth was immediately added and the cells allowed to recover at 37^{O}C, with shaking at 200 rpm for 1 h before plating on LB agar plates with the appropriate selective antibiotic.

Electrotransformation of competent *S. aureus* cells was performed as follows: competent cells were defrosted on ice for 5 min, incubated at 56^{O}C for 2 min, centrifuged at 5000x g for 1 min and re-suspended in 50 µl of 10% (v/v) glycerol (Sigma-Aldrich) with 500 mM sucrose (Sigma-Aldrich). 5 µl of plasmid were mixed and the cells transferred to a 0.1cm electroporation cuvette (Sigma-Aldrich), pulsed at 21 kV/cm, 100 Ω, and 25 µF for 2-2.4 ms. 1ml of TSB with 500 mM sucrose was immediately added and cells allowed to recover at 37^{O}C, 200 rpm for 2h before plating onto selective solid media.

2.4.8. Sanger sequencing

Sanger sequencing was performed by Edinburgh Genomics (University of Edinburgh) and Eurofins TubeSeq service (Eurofins). Chromatogram data from both strands was analysed for quality using FinchTV and 51 analysed using SeqMan Pro (DNASTAR Lasergene® Core Suite 9). To ensure accuracy of the sequence data, at least two reads were obtained for each nucleotide of the sequence.

2.5. Validation of mutant strains

Genomic DNA from *S. aureus* strains was isolated by MicrobesNG. Sequencing libraries were prepared using the Nextera XT library prep kit (Illumina, UK), as per the manufacturer's instructions, and sequenced on an Illumina HiSeq (Illumina, UK) using a 250 bp paired end protocol at MicrobesNG, Birmingham, UK.

Bioinformatic analysis of bacterial genome sequences was performed by Dr Bryan Wee or Dr Gonzalo Yebra. Variants were called by mapping to the reference genome using bwa (0.7.15) and freebayes (v1.0.2) as implemented in Snippy v3.1. Read alignments were visually inspected in IGV (v2.3.88). Gene content was analysed using the Roary pangenome analysis pipeline (v3.8.0) using assemblies from Spades v3.10 annotated with Prokka (v1.12-b).

Wild type and mutant strains were grown overnight in TSB at 37°C, with shaking at 200 rpm, diluted 1 in 1000 in fresh TSB or complete RPMI and 200 µl added to a 96-well Nunc^{TM}-treated plate. A growth curve was recorded in a FLUOstar Optima plate

reader (BMG labtech), with absorbance readings taken every 5 min with continuous shaking for 200 cycles. For measurement of sGFP, growth curves were recorded in a CLARIOstar plus plate reader (BMG labtech), with simultaneous measurement of OD_{600} and sGFP signal taken every 5 min with continuous shaking for 200 cycles. For measurement of sGFP signal, the gain was set at 1568 and filters to 485/520 (excitation/emission).

2.6. Flow cytometric analysis of *S. aureus* phagocytosis

chBMMs were plated at 5 x 10^5 /ml in a 00 mm square 25 compartment sterilin petri dish (SLS) on day 6 of differentiation. chBMMs were infected with *S. aureus* at an MOI of 1 by adding 100 µl to each well on day 7 of differentiation. 0.5% (v/v) H_2O_2 (Sigma-Aldrich) was used as a positive control for the live/dead staining and chBMM only as a negative control. After incubating at 41°C, 5% CO_2 for the appropriate timepoint, chBMMs were washed with PBS (Lonza) + 2% (v/v) FBS (Thermo Fisher Scientific), and detached using a syringe and 18G needle (VWR). The chBMMs were then centrifuged at 400x g for 5 min and the supernatant discarded. The chBMMs were re-suspended in PBS without FBS + Zombie Violet (Biolegend) at a dilution of 1:1000 for live/dead staining. The chBMMs were kept on ice for 30 min in the dark, before washing twice with PBS by centrifuging at 400x g for 5 min. The cells were then fixed in 4% (v/v) PFA (Thermo Scientific Fisher) on ice for 15 min and washed twice with PBS. The chBMMs were re-suspended in a minimum of 200 µl PBS and kept at 4°C in the dark before analysing by flow cytometry (Beckton Dickinson Fortessa). Unstained, single stained and fluorescence minus one (FMO) controls were included as controls.

2.7. chBMM cell death assay

chBMMs were plated at 5 x 10^5 /well in a 100 mm square 25 compartment sterilin petri dish (SLS) on day 6 of differentiation. chBMMs were infected with *S. aureus* at an MOI of 10 by adding 100 µl to each well on day 7. 0.5% (v/v) H_2O_2 (Sigma-Aldrich) was used as a positive control for the live/dead staining and chBMM only were used as a negative control. After incubating at 41°C for the appropriate timepoint, chBMMs were washed with PBS (Lonza) + 2% (v/v) FBS (Thermo Fisher

Scientific), and detached using a syringe and 18G needle. The chBMMs were then centrifuged at 400xg for 5 min and the supernatant discarded. The chBMMs were re-suspended in PBS without FBS + Zombie Violet (Biolegend) at a dilution of 1:1000 for live/dead staining. The chBMMs were kept on ice for 30 min in the dark, before washing twice with PBS by centrifuging at 400xg for 5 min. The cells were then fixed in 4% PFA (Thermo Scientific Fisher) on ice for 15 min and washed twice with PBS. After fixation, the cells were re-suspended in 200 µl of PBS and analysed by flow cytometry (Beckton Dickinson Fortessa). Unstained, single stained and fluorescence minus one (FMO) controls were included as controls.

2.8. Statistical analysis

Statistical analysis was performed using GraphPad Prism 8 software (GraphPad) or Minitab 18. All data was analysed for normality, using the Anderson-Darling test, and equal variance between experimental groups. Percentages were transformed using arcsine transformation. If these parameters were met, a one-way or two-way ANOVA analysis was performed depending on the number of variables analysed. Greisser-Greenhouse correction was applied when equal variance was not met. Multiple comparisons were performed when appropriate. If the data were not normally distributed and could not be successfully transformed, then nonparametric analysis was performed with Kruskal-Wallis analysis. For area under the curve analysis, growthcurver package (Sprouffske & Wagner, 2016) and one-way ANOVA analysis were performed in R.

Chapter 3. The role of prophage Avβ in *S. aureus* evasion of the avian innate immune evasion

3.1. Introduction

S. aureus host-adaptation is in part mediated by the gain of MGEs, which enable acquisition of host-specific virulence factors (Lowder *et al.*, 2009; Guinane *et al.*, 2010; Resch *et al.*, 2013; Spoor *et al.*, 2013). Of note, Lowder *et al.* previously identified an *S. aureus* host jump from humans into chickens, which was associated with the gain of MGEs (Lowder *et al.*, 2009), including prophage Avβ. This MGE is inserted into the *S. aureus* chromosome at the β-toxin gene, similarly to human-specific prophage Sa3 (Van Wamel *et al.*, 2006).

β-converting prophage Sa3 is associated with over 90% of human isolates and as such it is a hallmark of *S. aureus* host-adaptation in humans (Sung, Lloyd & Lindsay, 2008; Verkaik *et al.*, 2011). Sa3 encodes a cluster of genes at its 3' end associated with innate immune evasion: namely, *scn*, *sak*, *chp* and *sea* encoding SCIN, SAK, CHIPS and SEA. SCIN disrupts complement via C3 convertases (Rooijakkers *et al.*, 2005), SAK inhibits chemotaxis of neutrophils and inhibits α-defensins (Gladysheva *et al.*, 2003; Jin *et al.*, 2004), SEA activates T cells by MHC class crosslinking (Dohlsten *et al.*, 1993) and CHIPS is capable of chemotaxis inhibition (de Haas *et al.*, 2004). Each of these proteins contribute to evasion of the human innate immune system. Furthermore, both SCIN and SAK have been shown to have human restricted function, reinforcing their importance for human host-specific interactions (Gladysheva *et al.*, 2003; Rooijakkers *et al.*, 2005). In prophage Avβ, these innate immune evasion genes are replaced by a distinct complement of novel genes, which may contribute to avian host-adaptation (Lowder *et al.*, 2009).

The avian immune system differs drastically from the human innate immune system. For example, IgG in human serum, is replaced by IgY, which has an extra heavy chain constant domain and a single class compared to IgG (Carlander, Stålberg & Larsson, 1999). Unlike IgG, IgY does not bind to Protein A secreted by *S. aureus* (Ratcliffe & Härtle, 2013). In addition, the chicken BF-BL region, which functionally corresponds to the human MHC, is smaller and organised differently to the typical mammalian MHC (Parker & Kaufman, 2017). In effect, chickens only express two Class I and Class II alleles, which has led to close association between MHC type and resistance to infection (Wigley, 2017). Furthermore, heterophils, the

avian equivalent of neutrophils, do not possess myeloperoxidase, leading to weak oxidative killing and reliance on antimicrobial peptides and elastase for killing (Wells *et al.*, 1998). Thus, it is reasonable to hypothesise that *S. aureus* needs to utilise distinct innate immune evasion factors to survive the early stages of avian infection. This is reinforced by the observation that avian *S. aureus* strain ED98 exhibits increased resistance to avian heterophil, but not human neutrophil killing, compared to the basal human MR1 strain (Lowder *et al.*, 2009). However, the molecular mechanisms underpinning the immune evasion of *S. aureus* in chickens remain to be elucidated. In this study, we aimed to investigate whether, similarly to human-specific prophage Sa3 in humans, prophage Avβ plays a role in innate immune evasion in chickens.

3.2. Aims

The aims of this project were to:

- Investigate whether prophage Avβ plays a role in evasion of avian innate immune cell killing

- Construct a prophage Avβ deletion mutant with intact β-toxin and investigate its effect on *S. aureus*-macrophage interaction

3.3. Materials and Methods

3.3.1. Bacterial strains and growth conditions

Bacterial strains used are listed in Table 3.1. For *S. aureus* infection assays, a single colony of each bacterial strain was inoculated in 5 ml TSB and incubated overnight at 37°C with shaking at 200 rpm. Overnight cultures were diluted 1 in 10 into 25 ml fresh TSB media and incubated at 37°C with shaking at 200 rpm until $OD_{600} = 0.6$. Cultures were standardised to $OD_{600} = 0.6$ in 10 ml TSB before centrifugation at 5000 rpm for 7 min. The supernatants were discarded and the bacteria washed twice in PBS before resuspension in 10 ml RPMI-1640 (Gibco) containing 10% (v/v) heat-inactivated FBS (Thermo Fisher Scientific Scientific) and 1% (v/v) Glutamax (Gibco). Using the standardised bacterial suspensions, dilutions were made for a multiplicity of infection (MOI) of 0.1, 1 or 10 and an aliquot was taken for serial dilutions to perform viable counts.

3.3.2. Isolation of chicken heterophils

Blood was collected from day-old chicks, following dislocation and decapitation. Blood from 3 to 5 chicks was pooled together to obtain enough heterophils. Heterophils were isolated as previously described (Kogut *et al.*, 1995, 2005). 1% methycellulose (w/v) (Sigma-Aldrich) in RPMI-1640 (Gibco) was added to the blood before centrifuging at 4°C for 25 min at 25 x g to sediment the red blood cells. The supernatant was removed and made up to 50 ml with 1x $HBSS^{+/+}$ (Life Technologies) and 25 ml was added to a dual layer Ficoll gradient (15 ml of a density 1.119 g/ml histopaque solution (Sigma-Aldrich) with 10 ml of density 1.077 g/ml ficoll-hypaque solution (GE healthcare) layered on top. The tubes were then centrifuged at 250 x g for 1 h at room temperature (slow acceleration and brakes off). The top fraction was removed and the heterophils recovered from the second interface, washed by centrifuging at 4°C for 15 min at 300 x g, and cells counted using a TC20 automated cell counter (Biorad).

3.3.3. Isolation of human neutrophils

50 ml tubes of venous blood was drawn and mixed with 6 ml of acid-citrate-dextran (ACD) (25 g D-glucose (Sigma-Aldrich) and 20.5 g trisodium citrate (Sigma-Aldrich) added to 1 L of ddH_2O). Blood was mixed 1:1 in 1x PBS (Mg^{2+} Ca^{2+} free) (Gibco) and 25 ml was layered onto a dual layer Ficoll gradient (12 ml of a density 1.119 g/ml histopaque solution in a 50 ml tube with 10 ml of density 1.077 g/ml ficoll-hypaque solution layered on top). Tubes were then centrifuged for 20 min at 396 x g without brakes. Plasma was aspirated before the polymorphonuclear neutrophil (PMN) layer was recovered and each cell type was washed with RPMI-1640 (Gibco) containing 0.05 % (v/v) human serum albumin (RPMI+HSA) (Sigma-Aldrich). Cells were pelleted by centrifugation at 400 x g for 10 min at 4°C. Contaminating red blood cells were removed from the PMN pellet by hypertonic lysis and the pellet was re-suspended in 9ml of ice cold ddH_2O followed by incubation for 30 s. Isotonic conditions were restored by the addition of 1 ml of 10x PBS (Mg^{2+} Ca^{2+} free) (Gibco) before washing in RPMI+HSA and then centrifugation at 300 x g for 10 min at 4°C. Cells were counted using a TC20 automated cell counter (Biorad) and re-suspended to a concentration of 1 x 10^7 cells/ml.

3.3.4. Isolation and differentiation of human blood monocyte-derived macrophages

Fresh human blood (270 ml) was sampled from healthy donors, recruited by passive advertising, and mixed with acid-citrate-dextran solution (Sigma-Aldrich). The whole blood was transferred to a 50 ml falcon tube and centrifuged for 15 min at 1200 x g without application of break. The plasma was removed and discarded, and the buffy coat aspirated from 2 samples, pooled together and diluted in RPMI-1640 (Gibco) into 50ml falcon tubes. The diluted blood was gently overlaid onto 15 ml Ficoll (GE healthcare) and centrifuged for 45 min at 200 x g without brake, after which the mononuclear cell layer was harvested and washed with RPMI-1640 (Gibco). The cells were centrifuged for 10 min at 300 x g at 10°C and the supernatant was carefully discarded. The cells were collated in 50 ml PBS (Sigma-Aldrich) + 2% (v/v) FBS and counted using a haemocytometer (Sigma-Aldrich). The CD14+ monocytes were purified using magnetic activated cell sorting (MACS) positive

selection, according to the manufacturer's guidelines (Miltenyi Biotech, Germany). After isolation, CD14+ monocytes were resuspended to $1x10^6$ cells/ml in complete RPMI containing rhCSF-1 10^4 U/ml (Hume laboratory), seeded in 96-well NuncTM-treated plates (Fisher Scientific) and incubated at 37ºC. On day 5, the cells were topped up with 50% complete medium containing 3x target concentration of rh-CSF1 and on day 6, the media was removed and replaced. The macrophages were fully differentiated by day 7 and used between day 7 and 12.

3.3.5. Neutrophil/Heterophil killing assay

Bacterial suspension ($1x10^4$ cfu in 225 µl) was added to neutrophils or heterophils ($1x10^5$ cfu in 25 µl) in an Eppendorf tube and incubated at 41 °C (chicken body temperature) or 37 °C (human body temperature) for 30 min with vigorous shaking. Simultaneously, a bacterial suspension for each strain of interest was incubated with 25 µl of $HBSS^{+/+}$ (Life Technologies) without neutrophils or heterophils. The neutrophils or heterophils were then lysed with 0.1% (v/v) Triton X-100 (Sigma-Aldrich), and ten-fold dilutions made in $HBSS^{+/+}$ (Life Technologies), followed by plating on TSA and incubated at 37 °C for 14 to 16 h before determination of colony counts. Killing of bacteria was expressed as the percent reduction in colony count in the co-culture compared with the colony count of the bacteria alone.

3.3.6. Macrophage survival assay

Differentiated chicken bone-marrow macrophages (chBMM) were plated at 5 $x10^4$ /well in a 96-well Nunc™-treated plate (Fisher Scientific) on day 6 of differentiation and infected with 100 µl *S. aureus* on day 7 at an MOI of 1, before incubating at 41°C, 5% CO_2. At each timepoint, the supernatant was collected, and the cells lysed with 50 µl 0.1% (v/v) Triton X-100 (Sigma-Aldrich). The lysate was combined with the supernatant and serial dilutions were performed, before plating on TSA plates. For bacteria only CFU counts, bacteria were incubated at 41°C, 5% CO_2 in complete RPMI. All results are shown as a fold change compared to the inoculum, which was serially diluted and plated after infection.

3.3.7. Construction of allelic replacement plasmid pMAD::intact *hlb*

Bacterial strains, plasmids and primers used in this part of the study are listed in Tables 3.1, 3.2 and 3.3 respectively.

Allelic replacement was employed to generate a strain deficient of Avβ with an intact *hlb.* PCR products of approximately 500 bp flanking the left (A and B) and right (C and D) region of prophage Avβ were amplified using high fidelity polymerase *Pfu*. The thermocycler programme included an initial denaturation at 95°C for 2 min, followed by 30 cycles of denaturation at 95°C for 20 s, annealing at varying at 50°C for 20 s, extension at 72°C for 20 s, followed by final extension at 72°C for 3 min. PCR products were purified using Monarch PCR and DNA clean-up kit (New England biolabs) as per the manufacturer's instructions. 1 µl of both the AB and CD products were spliced together using a *Pfu* overlapping PCR, with an annealing temperature of 50°C and extension time of 34s.

The PCR product was blunt cloned into pSC-B blunt using a Blunt end cloning kit (Agilent) as per the manufacturer's instructions, with selection by Amp. White colonies were selected and cultured overnight in LB with 100µg/ml Amp at 37^{O}C, with shaking at 200 rpm. Plasmid DNA was extracted as described before digestion with *Bam*HI and *Eco*RI and resolution by electrophoresis in a 1% (w/v) agarose gel, the appropriate bands excised, and the DNA purified with a Monarch DNA Extraction kit (New England Biolabs) as described previously.

Digested PCR products were quantified as described previously and ligated into pMAD as described previously. Ligations were transformed into electro-competent *E. coli* DH5α cells as described previously and plated on LB + 100 µg/ml Amp followed by incubation overnight at 37^{O}C. Colonies were screened by colony PCR with multiple cloning site (MCS) primers of pMAD and positive colonies were grown overnight at 37^{O}C, with shaking at 200 rpm before plasmid DNA extraction. Plasmid DNA was concentrated and transformed into an intermediate *S. aureus* competent host strain RN4220, before transforming into *S. aureus* strain CIX2 ΔAvβ, and plating onto TSA containing 10 µg/ml Cm and 2% (w/v) X-gal for blue/white screening. Blue positive colonies were grown overnight at 30^{O}C in TSA

containing 10 μg/ml Cm, with shaking at 200 rpm. Plasmid extracted as described previously and screened using GoTaq PCR, with an annealing temperature of 50°C and extension time of 3 min.

3.3.8. Allelic replacement using pMAD

One colony of *S. aureus* containing the pMAD deletion construct of interest was inoculated into 10ml TSB containing 10 μg/ml Cm at 42 °C for 48 h to select for integration of the plasmid into the chromosome through homologous recombination. The culture was then plated on TSA containing 2% (w/v) XGal (Sigma-Aldrich) and 10 μg/ml Cm and incubated at 42°C overnight. Colonies which grew at this temperature were sub-cultured to single colonies on TSA containing Cm at 42 °C to ensure a pure culture. To excise the plasmid from the chromosome, a single blue colony was re-suspended in 100 μl of TSB and a 2 μl volume of this was added to 10 ml of TSB without antibiotics at 30°C with shaking at 200 rpm for 24 h. The 30°C culture was diluted to an OD_{600} of 0.2 in 1 ml of TSB. To generate double cross-over excisants, 2 μl of this was added to 10 ml of TSB without antibiotics and kept at 42°C for two days without shaking. 10-fold serial dilutions were plated onto TSA containing X-gal and incubated on TSA at 42°C overnight. Colonies were then screened for sensitivity on Cm plates (inferring loss of the plasmid) and screened for WT or mutated forms of the genes by colony PCR with OUT primers upstream and downstream of *hlb* (annealing temperature of 50°C and extension time of 3 min). The resulting mutant strain which has gained a non-truncated *hlb* was verified by PCR analysis for no amplification with pMAD MCS primers. Positive colonies were confirmed by PCR with gDNA template using OUT primers, Sanger sequencing and whole genome sequencing as described previously in Chapter 2.

Table 3.1. List of strains used in this study.

Strain	Description	Reference
S. aureus		
ED98	Broiler infecting *S. aureus* strain from skeletal infection	(Lowder *et al.*, 2009)
MR1	Human infecting *S. aureus* strain from wound infection	(Lowder *et al.*, 2009)
CIX2	Wild type chicken infecting *S. aureus* strain	(Lowder *et al.*, 2009)
CIX2 ΔAvβ	Deletion of prophage Avβ	(Provan, 2011)
CIX2-sGFP	Wild-type with integration of *sarA*_P1-sGFP-Term downstream pseudogene CIX2_000363	This study
CIX2 ΔAvβ-sGFP	Deletion of prophage Avβ with integration of *sarA*_P1-sGFP-Term downstream pseudogene CIX2_000363	This study
E. coli		
Strataclone solopack	lacZΔM15, *endA*, *recA*-deficient	Stratagene
DH5α	FΦ80*lac*ZΔM15Δ(lacZYAargF)U169 *rec*A1 *end*A1 *hsd*R17(rK,mK+) *pho*A *sup*E44λ*thi*1 *gyr*A96 *rel*A1	Invitrogen
DC10B	DH10B background, Δ*dcm*	(Monk et al., 2012)

Table 3.2. List of plasmids used in this study.

Plasmid	Description	Digestion sites	Resistance marker	Reference
pSC-B	Vector for blunt end ligation	-	Amp	Stratagene
pMAD	Thermosensitive gene replacement plasmid	-		(Arnaud *et al.*, 2004)
pMAD::intact *hlb*	β-toxin repair plasmid	*Bam*HI + *Eco*RI	Cm	This study
pTH100	pJB38-NWMN29-30 + *sarA*_P1-sGFP-Term	-	Cm	(De Jong *et al.*, 2017)

Table 3.3. List of primers used in this study.

Primer name	Sequence	Function	Annealing temperature
Hlb A F/*Bam*HI	GGCCGGATCCTGGCACTTGAACATTTGCTT	pMAD::intact *hlb*	50°C
Hlb B R	TTATAATAAAAGTCTCCAGTTTGGATAC	pMAD::intact *hlb*	50°C
Hlb C F	gtatccaaactggagacttttattataaGTGTATCCAAACT GGGGAC	pMAD::intact *hlb*	50°C
Hlb D R/*Eco*RI	GCGAATTCGGTCTGGTGAAAACCAATGTA GA	pMAD::intact *hlb*	50°C
pMAD 2m	AAGCGAGAATCATAATGGG	Transformation screen	50°C
pMAD 2c	CTTGCTCCAACTGAAAATCCC	Transformation screen	50°C
Intact *hlb* OUT F	CGCTGTGTAAATACCTGATTTC	Integration PCR	50°C
Intact *hlb* OUT R	GGCGAAAGATAATTTCACAACC	Integration PCR	50°C
Hlb seq F	AGTGCCAAAGCCGAATCTAA	AD PCR product sanger sequencing	55°C
Hlb seq R	ATTATCGAATCCACAACCGC	AD PCR product sanger sequencing	54°C
pTH100 MCS F	CATAATGTGTTGTAAACATTTTTTTTG	Transformation screen	55°C
pTH100 MCS R	TATGTCACTTATCCTTTTGGAAATG	Transformation screen	55°C

Primer name	Sequence	Function	Annealing temperature
Newman RS00185 F OUT	CGCTAATGTGATATATGCAAC	Integration PCR	54°C
Newman 30 R OUT	GAGATAAGCCAGAACAGTTCC	Integration PCR	54°C
sGFP seq primer F	GACGTGTCAGTGTTGTGTTTAT	sGFP integration for sanger sequencing	55°C
sGFP seq primer R	TACGACAATTCAAGAGCTTGC	sGFP integration for sanger sequencing	55°C

Underlined sequences represent restriction digestion sites (BamHI/EcoRI) and lower-case sequences represent complementary sequence in allelic replacement primers. Restriction digestion enzymes employed are provided alongside the primer name.

3.3.9. PCR screen of prophage φAvβ excision

Overnight cultures of CIX2, CIX2 ΔAvβ and CIX2 ΔAvβ + *hlb* were subcultured into 25 ml TSB with and without 1 mM H_2O_2 (Signa-Aldrich) until OD_{600} = 0.6. Both exponential and overnight cultures were pelleted by centrifugation (5000 rpm for 7 min) and the pellets resuspended in of lysis buffer (960 µl dH_2O, 10 µl 1M Tris-HCl pH8, 10 µl 5M NaCl, 10 µl lysostaphin (10 mg/ml, Ambi Products) and 10 µl achromopeptidase (10 mg/ml, Sigma-Aldrich)). The tubes were then incubated at 37°C for 50 min and then heated to 100°C for 5 min. The suspensions were centrifuged at 13 000 rpm for 2 min and the supernatant was retained and used neat for the PCR. PCR primers were adapted from Tran *et al.* 2019 and performed using GoTaq DNA polymerase as described previously, at an annealing temperature of 50°C and an extension time of 1 min. The fragments amplified were: excised ϕAvβ with primer set ϕAvβ Excised F/R, integrated ϕAvβ with primer set Avβ Int F/R and intact *hlb* with primer set hlb F/R. All primer sequences are listed in table 3.4.

3.3.10. Viable count analysis for assessment *S. aureus* phagocytosis by chBMMs

Differentiated chicken bone-marrow macrophages were plated at 5 x10^4 /well in a 96-well Nunc^{TM} plate (Fisher Scientific) on day 6 of differentiation. The chBMMs were infected with *S. aureus* on day 7 at an MOI of 1. 100 µl of bacterial inoculum was added to each well, before centrifuging the plate at 300 x g for 5 min to promote bacterial interaction with the macrophages. After 1 h of incubation, the supernatant was collected and discarded and the cells were incubated with 100 µg/ml of gentamicin for 30 min at 41°C 5% CO_2 to kill extracellular bacteria. The chBMMs were then washed twice with 1 x PBS (Mg^{2+} Ca^{2+} free) (Gibco) and lysed with 100 µl 0.1% (v/v) Triton X-100 (Sigma-Aldrich) and serial dilutions were performed, before plating on TSA plates. TSA plates were left overnight at 37°C and colony forming unit (CFU) counts were performed the next day.

Table 3.4. PCR screen of prophage φAvβ excision.

Primer name	Sequence	Annealing temperature
ϕAvβ Excised F	ACTCTACAAGCTATCAATAACGC	50°C
ϕAvβ Excised R	AGTCGCTACACCACTCATAC	50°C
ϕAvβ Integrated F	GCGTTATTGATAGCTTGTAGAGT	50°C
ϕAvβ Integrated R	ATTATCGAATCCACAACCGC	50°C
Hlb F	CAACGTGAATCTTCAGATTGTG	50°C
Hlb R	TCCTGTTGATGCTATAACGC	50°C

3.3.11. Integration of sGFP into *S. aureus* chromosome using plasmid pTH100

Allele replacement was used to integrate sGFP into the *S. aureus* chromosome. Plasmid pTH100 integrates into the chromosome between genes NWMN_ RS00185 and NWMN_0030 and allows stable markerless expression of sGFP (De Jong *et al.*, 2017). Firstly, a BLASTn search was performed on *S. aureus* strains CIX2 and CIX2 ΔAvβ genomes to ensure homology of the NWMN RS00185-30 locus in these strains. The plasmid pTH100 was introduced by electroporation into the strains of interest and transformants were plated on TSA supplemented with 10 μg/ml Cm and incubated overnight at the replication-permissive temperature of 30°C. Single colonies were picked and introduction of the plasmid was confirmed by PCR. Subsequently, colonies were plated on TSA containing 7.5 μg/ml Cm and incubated overnight at 43°C for integration of the plasmid by homologous recombination. Large colonies were considered to have undergone a single recombination event and were re-streaked on TSA containing 7.5 μg/ ml Cm and incubated overnight at 43°C. These single recombinants were inoculated in 5 ml TSB and incubated at 30°C without antibiotics. Cultures were diluted 1:1000 and subcultured 5 times to promote double crossover events and plasmid loss. Cultures were plated on TSA with 200 ng/ml anhydrotetracycline and incubated at 37°C to select for double crossover mutants. The resulting colonies were replica plated onto TSA without antibiotics and TSA with 10 μg/ml Cm. Colonies that had lost the ability to grow on Cm plates (double crossover mutants) were analysed by PCR using high fidelity polymerase Q5 (New England Biolabs). The thermocycler programme included an initial denaturation at 98°C for 30 s, followed by 30 cycles of denaturation at 98°C for 10 s, annealing at 54°C for 20 s, extension at 72°C for 2 min, followed by final extension at 72°C for 2 min. sGFP integration was confirmed by whole genome sequencing as described in Chapter 2, section 2.5.

3.4. Results

3.4.1. The *S. aureus* prophage Avβ is not associated with increased resistance to heterophil killing

Previously, avian CC5 strain ED98 was demonstrated to exhibit increased resistance to heterophil killing compared to a closely-related human CC5 strain (MR1) (Lowder *et al.*, 2009). We hypothesised that this could be due to the gain of β-converting prophage Avβ, since the human β-converting prophage Sa3 is associated with evasion of human neutrophil killing (Rooijakkers *et al.*, 2005). To investigate this hypothesis, we used an avian strain of *S. aureus* CIX2 and its previously generated prophage deletion mutant CIX2 ΔAvβ. CIX2 is a CC5 *S. aureus* strain that harbours both prophage Avβ and plasmid pAvY, whilst CIX2 ΔAvβ is lacking prophage Avβ, as well as 370 bp of *hlb* (β-toxin gene). The 370 bp of the β-toxin were deleted to control for the fact that β-converting prophages are inserted at the β-toxin gene *hlb*, truncating it and rendering it non-functional. Thus, deleting a fragment of *hlb* ensured that the Avβ deletion mutant also possessed a non-functional β-toxin (Provan, 2011).

To study the role of prophage Avβ in resistance to human neutrophil or avian heterophil killing, *S. aureus* strains ED98, MR1, CIX2 and CIX2 ΔAvβ were first opsonised with either human plasma or chicken plasma. Following testing of neutrophils and macrophages for purity (Figure 3.1A,B), each strain was incubated with either human neutrophils at 37°C (normal human body temperature) or chicken heterophils at 41°C (normal chicken body temperature) for 30 min at a MOI of 0.1. Our results indicate that the avian ED98 strain is more resistant to heterophil killing than the basal MR1 strain, confirming previous findings (Figure 3.1C). However, we observed no statistical difference in either neutrophil or heterophil killing between CIX2 and CIX2 ΔAvβ (Figure 3.1C). This suggests that the previously identified resistance to heterophil killing in avian strain ED98 is not due to prophage Avβ but most likely due to another MGE acquired after *S. aureus* host jump from humans into chickens.

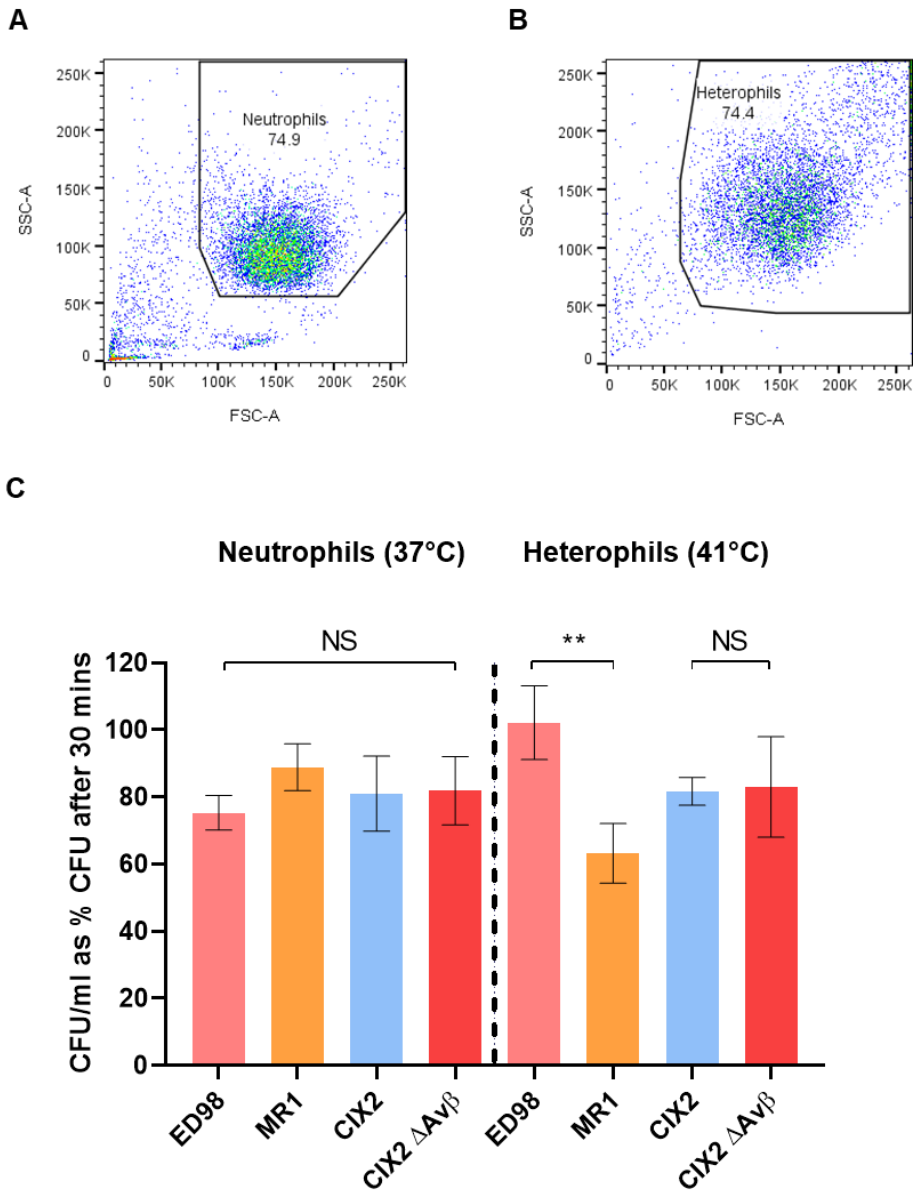

Figure 3.1. Prophage Avβ does not enhance *S. aureus* resistance to human neutrophil or avian heterophil killing.

A) Representative FACS plot of purity check for human neutrophils **B)** Representative FACS plot of purity check for avian heterophils **C)** Neutrophil/heterophil bacterial survival assays presented as bacterial CFU/ml as percentage CFU compared to bacteria only after 30 min. Each point represents the mean of technical replicates and each bar represents the mean of 3 individual donors (either human or broiler chicken), ± standard deviation. Statistical analysis was performed using one-way ANOVA with Tukey's post-comparison test.

3.4.2. Prophage Avβ contributes to survival of *S. aureus* in the presence of chicken macrophages

Macrophages are crucial players in the first line response to *S. aureus* (Brown *et al.*, 2015) and therefore we next chose to assess whether prophage Avβ plays a role in evasion of macrophage killing. To achieve this, chicken bone-marrow derived macrophages (chBMMs) were incubated with either CIX2 or CIX2 ΔAvβ for up to 8 h at a MOI of 1. At each timepoint, total recovered bacterial counts (combined supernatants and lysed cells) were assessed. We observed a 100-fold increase in total recovered bacteria in CIX2 infected chBMMs compared to CIX2 ΔAvβ infected chBMMs at 8 h of infection (Figure 3.2A). To exclude that our results were not due to bacteria growing at different rates in complete RPMI, we included a bacteria only control, where bacteria were incubated in complete RPMI alone and bacterial CFU counts were performed at each timepoint. No difference was seen between the two strains (Figure 3.2B), suggesting that prophage Avβ indeed enhances survival of *S. aureus* in chBMMs.

3.4.3. Generation of a prophage Avβ deletion with an intact β-toxin

As mentioned previously, prophage Avβ is inserted at the β-toxin gene, leading to its truncation. Prophage Sa3 has been reported to excise from the chromosome under conditions of stress such as reactive oxygen species killing leading to a sub-population of bacteria capable of expressing the β-toxin (Salgado-Pabón *et al.*, 2014). To confirm whether the phenotype observed in chBMMs was solely due to presence of prophage Avβ and not the presence of an intact β-toxin, we aimed to construct a new prophage deletion mutant with an intact *hlb* gene by repairing the missing 370 bp segment of *hlb* in strain CIX2 ΔAvβ using allelic replacement (Figure 3.3A). This was attempted using allelic replacement plasmid pMAD and confirmed by PCR (Figure 3.3B). However, whole genome sequencing (WGS) revealed that 30 bp of prophage DNA is present in the repaired *hlb* gene, which

introduces a stop codon towards the start of the protein (Figure 3.3C). The β-toxin is therefore likely not functional and this new deletion mutant is not an effective control.

3.4.4. φAvβ incompletely excises from the chromosome

Due to the lack of effective β-toxin control, we were unable to rule out the possibility of transient β-toxin expression due to excision of prophage Avβ during the course of an infection. Thus, we next aimed to assess whether prophage Avβ is capable of excision from the chromosome using PCR. Primers were designed to detect excised φAvβ, integrated φAvβ and intact *hlb* (Table 3.4). Excised φAvβ was detected by amplification across the bacterial and phage attachment sites, which are restored after prophage excision. Integrated φAvβ was detected by amplification of the bacterial DNA-integrated prophage junction. Intact *hlb* was detected by amplification of the region of *hlb,* only present in absence of the integrated prophage. *S. aureus* strains CIX2, CIX2 ΔAvβ and CIX2 ΔAvβ + *hlb* were either grown in TSB overnight or TSB to exponential growth phase. To induce bacterial stress, strains were also grown in TSB with 1mM H_2O_2 during exponential growth phase. As reported previously for human φSa3 (Tran *et al.*, 2019), φAvβ excised from CIX2 during exponential growth, with and without the presence of H_2O_2, but not after overnight growth (Figure 3.4A). In addition, we observed that even though φAvβ can be excised, a proportion of prophage remains integrated, as indicated by the band at 614 bp in Figure 3.4B. Excision of φAvβ in a subpopulation of *S. aureus* during culture is supported by weak amplification of intact β-toxin gene in wild type CIX2 in all conditions (Figure 3.4C). These data suggest that φAvβ is capable of incomplete excision from the chromosome, supporting a scenario whereby low levels of β-toxin and phage-encoded proteins may be expressed simultaneously.

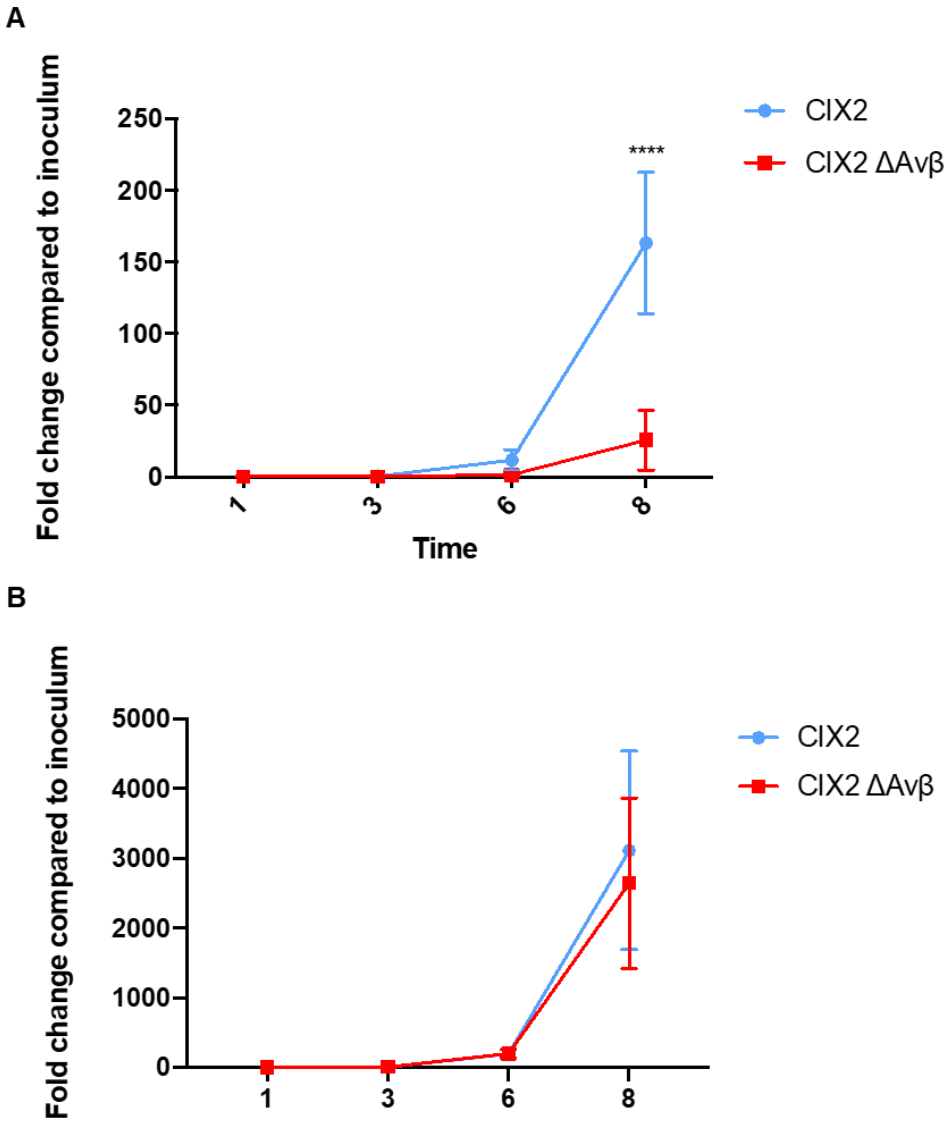

Figure 3.2. Prophage Avβ enhances bacterial survival after chBMM infection

A) Total recovered bacteria after infection of chBMMs **B)** Bacterial CFU counts after incubation in complete RPMI. Data is shown as fold change compared to the inoculum. Each point represents the mean of three biological replicates, ± standard error of the mean. Each experiment was performed with technical triplicates. Statistical analysis was performed using two-way RM ANOVA with Geisser-Greenhouse correction and Tukey's post-comparison test, represented by ***p ≤0.001.

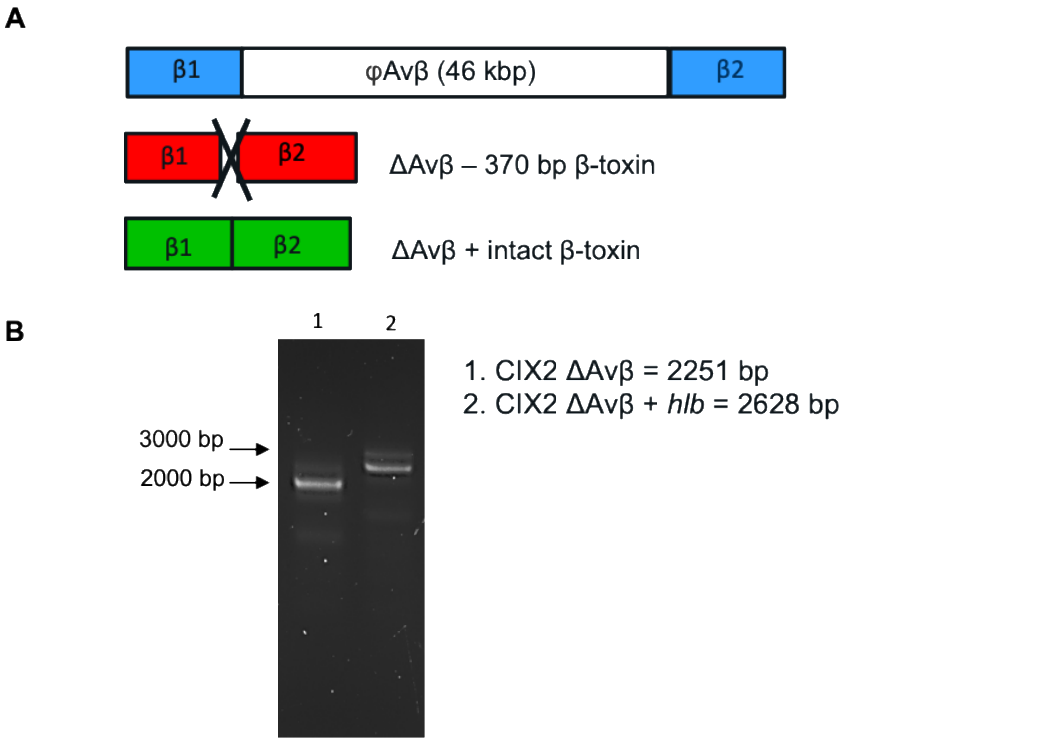

Figure 3.3. Genotypic validation of intact *hlb* deletion mutant.

A) Schematic representation of wild type (CIX2), prophage deletion mutant with disrupted *hlb* gene (CIX2 ΔAvβ) and prophage deletion mutant with repaired *hlb* gene (CIX2 ΔAvβ + *hlb*) **B)** Agarose gel electrophoresis of genomic DNA produced by PCR amplification to confirm gene deletion. Primer pairs were located outside of the flanking region used for repair of *hlb* **C)** Amino acid sequence of the repaired β-toxin in CIX2 ΔAvβ + *hlb*. The stop codon is denoted by a red asterisk.

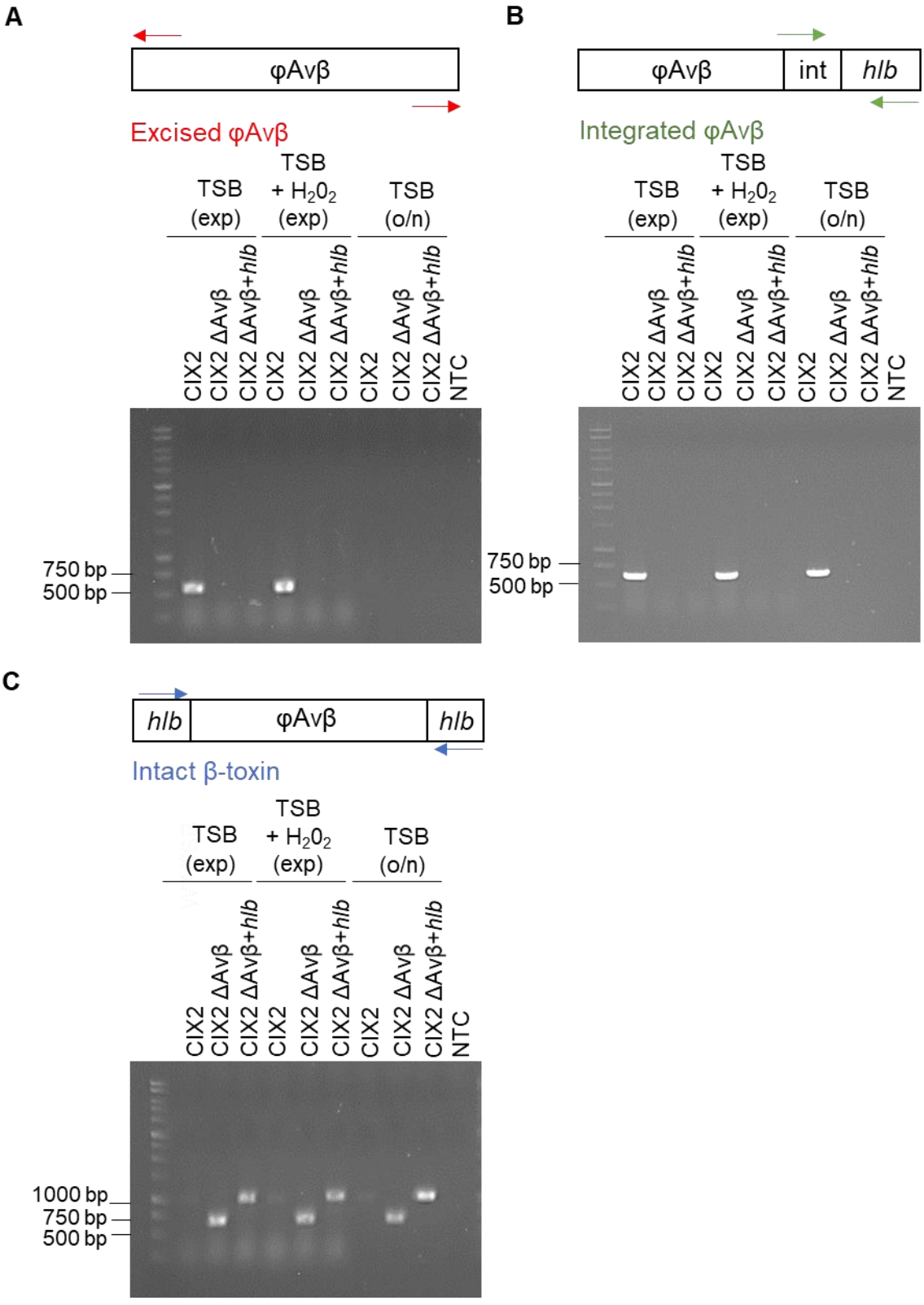
A
φAvβ
Excised φAvβ
TSB (exp)
TSB + H2O2 (exp)
TSB (o/n)
CIX2
CIX2 ΔAvβ
CIX2 ΔAvβ+hlb
NTC
750 bp
500 bp
B
φAvβ
int
hlb
Integrated φAvβ
C
hlb
φAvβ
hlb
Intact β-toxin
1000 bp
750 bp
500 bp

Figure 3.4. Incomplete excision of prophage φAvβ occurs at exponential phase and in presence of H_2O_2.

Agarose gel electrophoresis of PCR analysis of prophage excision in CIX2, CIX2 ΔAvβ, CIX2 ΔAvβ + *hlb* grown until OD_{600} = 0.6 in TSB or TSB + 1mM H_2O_2, and overnight in TSB **A)** PCR across circularised prophage, only present in excised prophage DNA (expected size = 530 bp) **B)** PCR across the integration site, only present in integrated prophage (expected size = 614 bp) **C)** PCR across the *hlb* gene, only present in the absence of integrated prophage (expected size: CIX2 ΔAvβ = 673 bp , CIX2 ΔAvβ+*hlb* = 1050 bp).

3.4.5. Enhanced survival in chBMMs associated with prophage Avβ-encoded genes, or restoration of β-toxin expression, is specific to chicken macrophages

In order to investigate whether prophage Avβ-encoded genes, or restoration of β-toxin expression, leads to a host specific increase in bacterial survival, we next performed the macrophage bacterial survival assays in human blood monocyte-derived macrophages (hMDMs). The graph is Figure 3.5 shows no significant difference in bacterial survival between CIX2 and CIX2 ΔAvβ strains in hMDMs. This demonstrates that prophage Avβ or the β-toxin provide an advantage during chBMM infection but not hMDM infection, suggesting a host-specific role of either prophage Avβ or the β-toxin.

3.4.6. Presence of prophage Avβ, or an intact β-toxin, lead to increased early phagocytosis of *S. aureus* by chBMMs

To further investigate the role of prophage Avβ-encoded genes, or an intact β-toxin, in bacterial survival during macrophage infection, we next sought to determine whether macrophage phagocytosis is affected by deletion of prophage Avβ. chBMMs were infected with CIX2 and CIX2 ΔAvβ for 1 h at a MOI of 1. After infection, the supernatant was removed, extracellular bacteria killed with 100 μg/ml of gentamicin and intracellular bacteria enumerated by lysing the chBMMs. The results show a 10% increase in phagocytosis of strain CIX2 compared to CIX2 ΔAvβ (Figure 3.6), suggesting that either presence prophage Avβ, or restoration of β-toxin expression due to prophage Avβ excision, is associated with increased phagocytosis by chBMMs. We were unable to assess phagocytosis at later timepoints, due to the presence of *S. aureus* clumped to the surface of chBMMs, even after gentamicin treatment (data not shown).

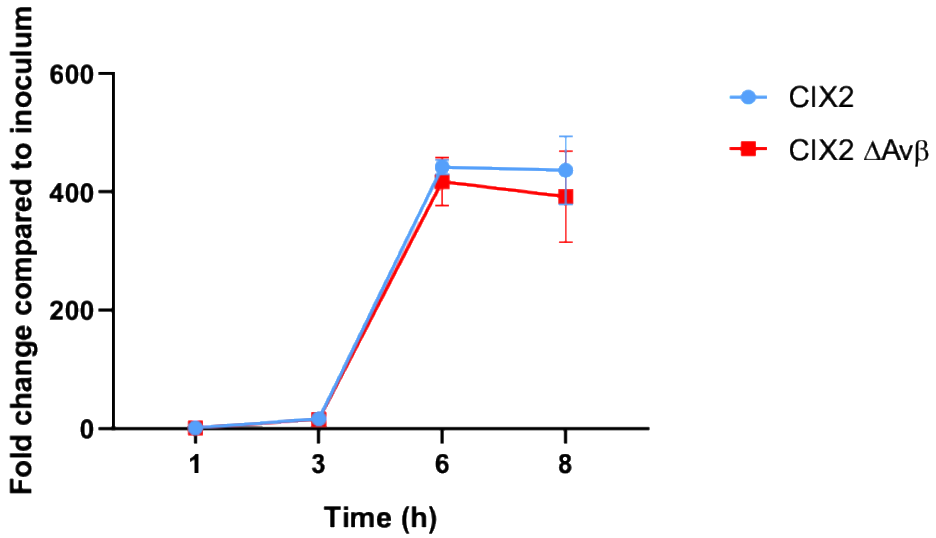

Figure 3.5. Prophage Avβ is not associated with increased resistance to human bone-marrow derived macrophages.

Bacterial CFU counts after infection of hMDMs. Data is shown as fold change compared to the inoculum. Each point represents the mean of three human donors, ± standard deviation. Each experiment was performed with technical triplicates. Statistical analysis was performed using two-way RM ANOVA with Tukey's post-comparison test. Experiments were performed by Dr Joana Alves.

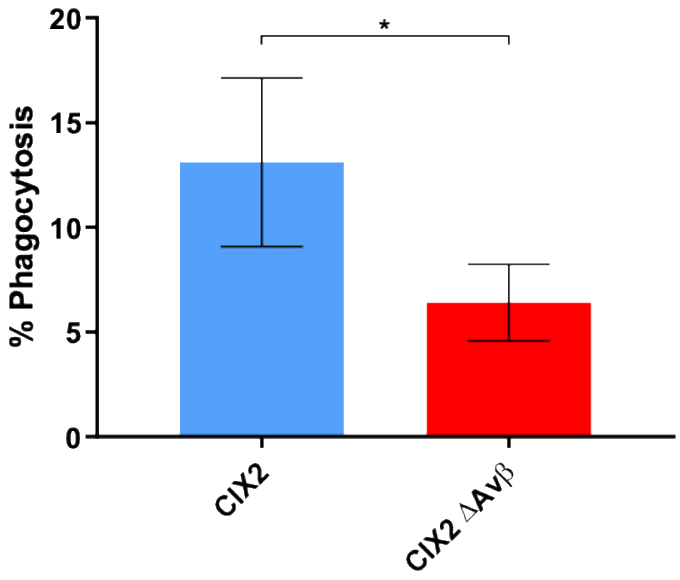

Figure 3.6. The deletion of prophage Avβ is associated with decreased early phagocytosis of *S. aureus* by chBMMs.

chBMMs were infected with *S. aureus* strains CIX2 and CIX2 ΔAvβ at an MOI of 1 for 1 h. Intracellular counts were performed after 1 h phagocytosis and gentamicin treatment to kill extracellular bacteria. Each point represents a biological replicate, ± standard deviation. Statistical analysis was performed using one-way RM ANOVA test with Tukey's post comparison and Geisser-Greenhouse correction, represented by *$p<0.05$.

3.4.7. Generation of sGFP-expressing strains for analysis of phagocytosis and intracellular bacteria

In order to assess phagocytosis of *S. aureus* by chBMMs during the course of an infection, constitutive sGFP-expressing strains were generated for use in flow cytometry experiments. Allelic replacement was used to integrate sGFP, driven by the *sarA* P1 promoter (PsarA_sGFP), into an intergenic region of *S. aureus* strains CIX2 and CIX2 ΔAvβ. Integration of PsarA_sGFP was confirmed by PCR and WGS (Figure 3.7A). No difference in growth rate was observed for any strain in either TSB or complete RPMI, at 37°C or 41°C (Figure 3.7B).

sGFP expression was assessed over a 12 h time-course in a fluorescent plate reader by measuring the relative fluorescent intensity (RFU). CIX2 exhibits increased sGFP fluorescence intensity compared to CIX2 ΔAvβ, both at 37°C and 41°C (Figure 3.7B) during the course of a growth curve. The OD_{600} and sGFP signal of the strains were measured simultaneously, with no difference in growth rate observed (Figure 3.7B), suggesting that this effect is not due to differences in bacterial density. The data reveal higher expression of the sarA P1 promoter driving sGFP expression in strain CIX2, compared to CIX2 ΔAvβ, suggesting that either prophage Avβ or an intact β-toxin influence *S. aureus sarA* expression.

Taken together, these data demonstrate the successful integration of PsarA_sGFP into *S. aureus* strains CIX2 and CIX2 ΔAvβ, with no effect on growth. However, the constitutive expression of sGFP differs between the strains during bacterial growth and therefore subsequent comparison of fluorescence intensity is not feasible.

A

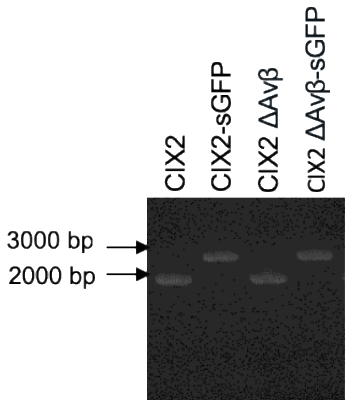
CIX2
CIX2-sGFP
CIX2 ΔAvβ
CIX2 ΔAvβ-sGFP
3000 bp
2000 bp

B

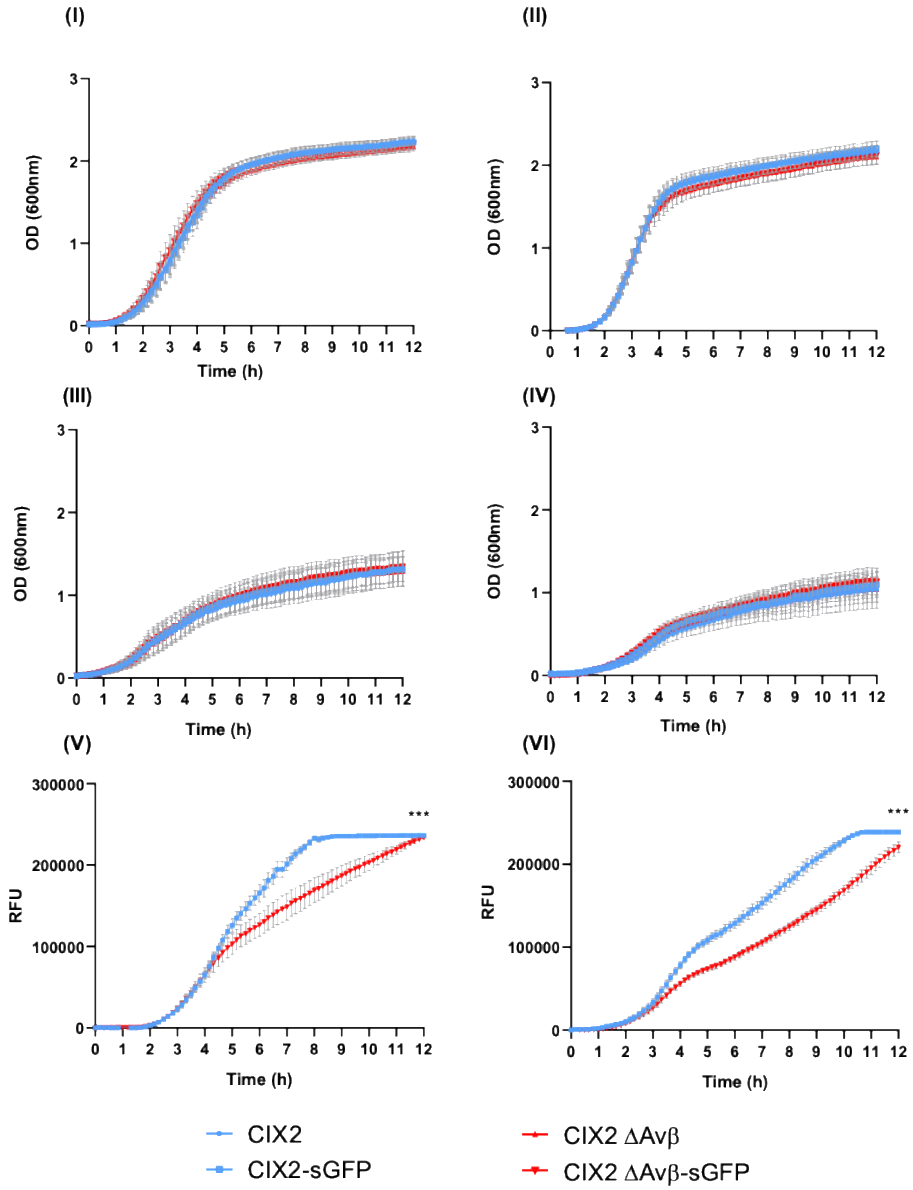
(I)
(II)
(III)
(IV)
(V)
(VI)
OD (600nm)
RFU
Time (h)
***
CIX2
CIX2-sGFP
CIX2 ΔAvβ
CIX2 ΔAvβ-sGFP

Figure 3.7. Genotypic and phenotypic validation of sGFP-expressing strains.

A) Agarose gel electrophoresis of genomic DNA produced by PCR amplification to confirm sGFP integration. Primer pairs were located outside of the flanking region used for integration of sGFP **B)** Growth curves were performed in TSB at 37°C (I,V), TSB at at 41°C (II,VI), complete RPMI at 37°C (III) and complete RPMI 41°C (IV), with measurements every 5 min for 12h. OD_{600} measurement (I,II,III,IV) and sGFP fluorescence intensity measurement shown (V,VI) as relative fluorescence intensity (RFU) are shown here. For RFU, the gain was set at 1708 and filters to 485/520 (excitation/emission). The data was blanked to both TSB and wild-type *S. aureus* strains lacking integration of sGFP. Each point represents the mean of biological replicates, performed in triplicate ± standard error of the mean; n =3.

3.4.8. Longitudinal analysis reveals that deletion of prophage Avβ leads to decreased phagocytosis of *S. aureus* by chBMMs

To elucidate whether prophage Avβ, or an intact β-toxin, play a role in *S. aureus* phagocytosis during prolonged infection, we infected chBMMs at a MOI 1 for 1, 3 and 5 h with CIX2-sGFP and CIX2 ΔAvβ-sGFP. At each timepoint, percentage GFP^+ cells and cell death was assessed using flow cytometry. The gating strategy is shown in Figure 3.8. Our results show a significant decrease in phagocytosis of CIX2 ΔAvβ-sGFP compared to the wild type CIX2-sGFP, at both 1 and 3 h post-infection (Figure 3.9A). This was not associated with increased cell death, but there is a trend towards increased cell death in chBMMs infected with CIX2-sGFP compared to CIX2 ΔAvβ-sGFP at 5 h post-infection (Figure 3.9B). In addition, cell death compared to the uninfected chBMMs was observed during infection with both strains of *S. aureus* (Figure 3.9B). These data indicate that either prophage Avβ, or the restoration of β-toxin expression due to prophage Avβ excision, promote enhanced phagocytosis of *S. aureus* by chBMMs. In addition, these data also suggest a potential role for either prophage Avβ or a functional β-toxin in the increased cell death of chBMMs.

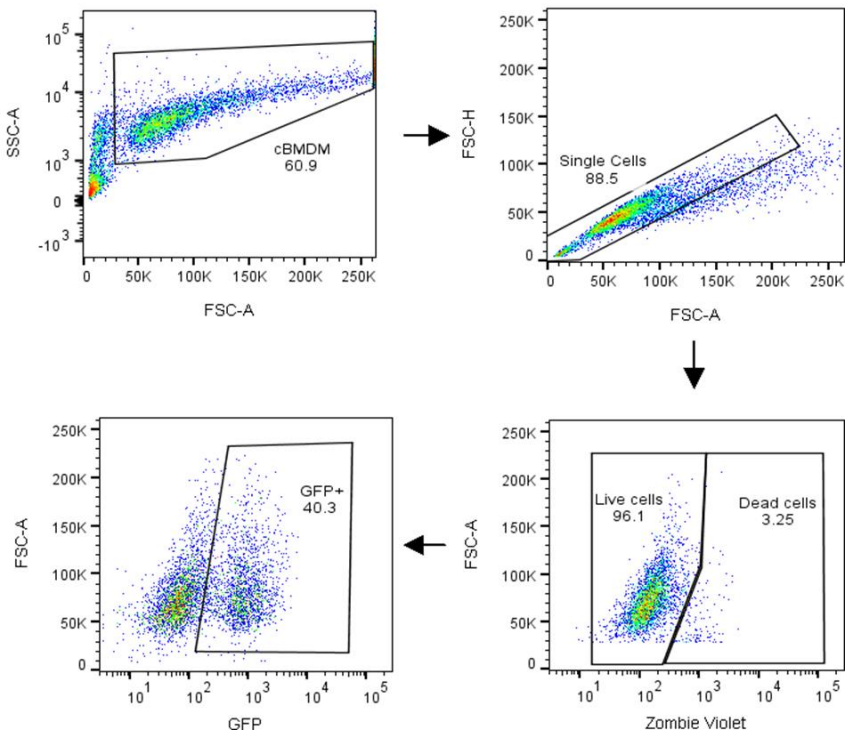

Figure 3.8. Gating strategy for flow cytometry analysis of *S. aureus* phagocytosis and chBMM viability.

chBMMs were first gated using FSC and SSC and then gated on single cells using FSC-H. Percentage cell death was determined by staining with a live/dead Zombie Violet stain. chBMMs were gated on live cells then percentage phagocytosis was defined as GFP^+ chBMMs.

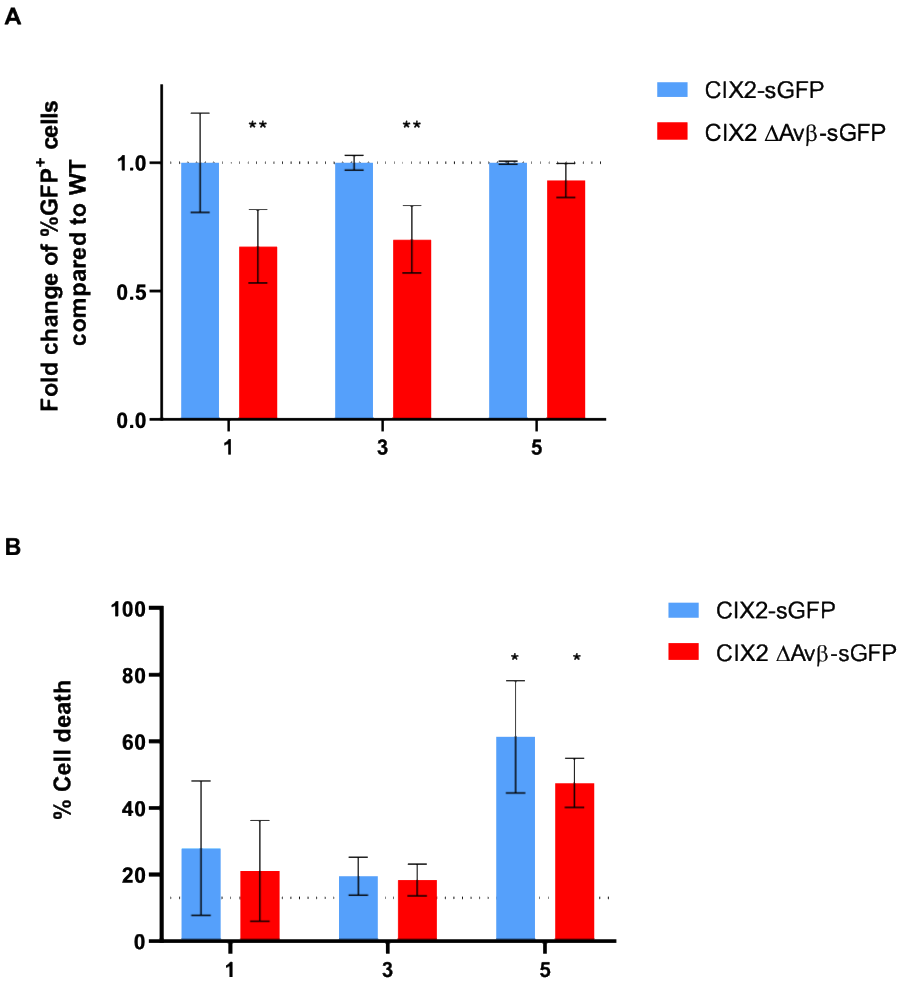

Figure 3.9. The deletion of prophage Avβ leads to decreased phagocytosis of *S. aureus* by chBMMs but not increased chBMM cell death at low MOI.

A) Phagocytosis of *S. aureus* strains CIX2-sGFP and CIX2 ΔAvβ-sGFP by chBMMs, presented as fold change of percentage GFP^+ cells compared to the wild type CIX2-sGFP. Each point represents a biological replicate, ± standard deviation; n = 5. Statistical analysis was performed using two-way RM ANOVA with Dunnett's post-comparison test (compared to wild type CIX2-sGFP) and represented by **p ≤0.01. **B)** chBMM cell death after infection with *S. aureus* at a MOI of 1. Data is presented as percentage dead cells after staining with live/dead zombie violet. Each point represents a biological replicate, ± standard deviation; n = 4. Statistical analysis was performed using two-way RM ANOVA with Tukey's post-comparison test (compared to uninfected chBMMs), where *p<0.05.

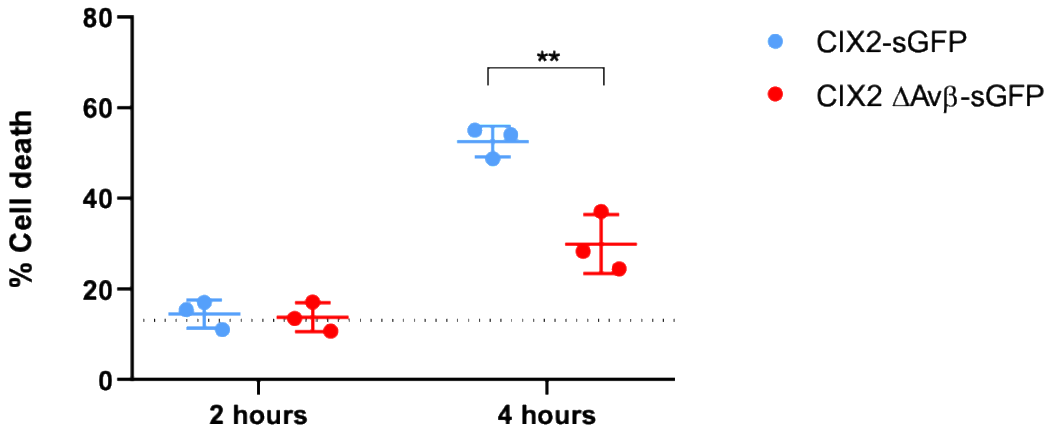

Figure 3.10. Presence of prophage Avβ is associated with increased cell death of chBMMs at a higher bacterial density of *S. aureus*.

Macrophage cell viability after infection with *S. aureus* at a MOI of 10. Data is presented as percentage live cells after staining with live/dead Zombie Violet. The dotted line represents the level of cell death for control uninfected chBMMs. Each point represents a biological replicate, ± standard deviation; n = 3. Statistical analysis was performed between groups using two-way RM ANOVA with Tukey's post-comparison test.

3.4.9. Presence of prophage Avβ, or an intact β-toxin, are associated with increased cell death of chBMMs by *S. aureus*

To further investigate whether prophage Avβ plays a role in chicken macrophage cell death after infection with *S. aureus*, we infected the chBMMs with *S. aureus* strains CIX2-sGFP and CIX2 ΔAvβ-sGFP at a higher MOI (10) for 2 and 4 h. Our results demonstrate a 20% increase in cell death of chBMMs by CIX2-sGFP compared to CIX2 ΔAvβ-sGFP (Figure 3.10), suggesting that either prophage Avβ, or the restoration of β-toxin expression due to the excision of prophage Avβ, play a role in chBMM intoxication by *S. aureus* at higher bacterial density

Together, these data demonstrate a role for either prophage Avβ or an intact β-toxin in avian innate immune evasion. Presence of prophage Avβ does not enhance resistance to heterophils but does enhance bacterial survival of *S. aureus* in chBMM infection. This phenotype did not occur in hMDMs, consistent with avian host-specificity. However, we were unable to determine whether the observed phenotypes in chicken macrophages are due to the genes encoded on prophage Avβ or due to the restoration of β-toxin expression, which occurs when prophage Avβ excises from the chromosome. Furthermore, prophage-encoded genes or expression of the β-toxin in *S. aureus* also led to increased phagocytosis by chBMMs. Finally, prophage-encoded genes or expression of the β-toxin lead to enhanced cell death of chBMMs by *S. aureus* at higher bacterial density.

3.5. Discussion

Previous studies have demonstrated that proteins carried on the human-specific prophage Sa3, such as SAK, lead to resistance of human neutrophil killing (Jin, Bokarewa & Tarkowski, 2005). Therefore, we hypothesised that genes encoded on prophage Avβ could lead to resistance of avian heterophil killing but this was not the case. Therefore, the previously observed enhanced resistance of avian *S. aureus* to heterophil killing is likely due to other bacterial determinants (Lowder *et al.*, 2009). SaPIs have also been shown to encode host-specific virulence factors, such as bovine, ovine and equine variants of the *vwbp* gene, allowing host-specific plasma coagulation (Jacobsson *et al.*, 2002; Guinane *et al.*, 2010; Viana *et al.*, 2010). It is therefore tempting to speculate that SaPIAv harboured by avian *S. aureus* isolates could be involved in host-specific resistance of heterophil killing.

Macrophages are key players in response to *S. aureus* host response and thus we investigated whether prophage Avβ affects the *S. aureus*-macrophage interaction. Deletion of the prophage resulted in enhanced bacterial survival after infection of chicken macrophages. No gentamicin treatment was included to kill extracellular bacteria, suggesting the observed phenotype in the presence of prophage Avβ could either be due to faster extracellular replication of *S. aureus* or resistance to macrophage killing. In effect, our data demonstrates that bacteria grown in cell culture medium alone grew at the same rate, suggesting that prophage Avβ-encoded genes likely enhances survival to macrophage killing.

However, the observed phenotype in macrophages could also be due to the presence of an intact β-toxin in a subpopulation of bacteria. In effect, we identified that φAvβ is capable of incomplete excision from the chromosome, likely leading to a small sub-population of *S. aureus* encoding an intact β-toxin. In addition, the lack of effective *hlb* control in this study suggests that excision of prophage Avβ, leading to the restoration of β-toxin expression, rather than genes encoded on prophage Avβ, could be responsible for the observed phenotype in macrophages. A previous study

has revealed that excision of the human adapted β-converting phage Sa3 leads to intracellular β-toxin expression in keratinocytes, which enables more effective colonization of murine ears, due to increased killing of keratinocytes (Katayama *et al*., 2013). Furthermore, the β-toxin is capable of killing monocytes and has also been associated with intracellular escape of *S. aureus* from endothelial cells (Walev *et al.*, 1996; Giese *et al.*, 2011). Therefore, excision of prophage Avβ during macrophage infection, leading to the β-toxin expression, could provide an advantage for *S. aureus* due to intracellular killing. Further experiments with an effective *hlb* control would determine whether the phenotype is due to prophage Avβ or due to excision of prophage Avβ, leading to the restoration of β-toxin activity.

Despite potent macrophage antimicrobial mechanisms, *S. aureus* is capable of surviving intracellularly after initial phagocytosis (Schnaith *et al.*, 2007; Kubica *et al.*, 2008; Tuchscherr *et al.*, 2011; Flannagan, Heit & Heinrichs, 2016; Jubrail *et al.*, 2016). Here, we report that either prophage Avβ or the β-toxin lead to enhanced phagocytosis of *S. aureus* by chicken macrophages. It remains unclear whether this increase in phagocytosis is due to increased resistance to intracellular killing leading to intracellular replication or if it is due to increased uptake of *S. aureus* by the macrophages, eventually overwhelming macrophage killing but *S. aureus* is capable of using both strategies. For example, *S. aureus* can evoke changes in gene expression to survive in the acidified phagolysosome to resist killing by macrophages (Flannagan *et al.*, 2018). *S. aureus* has also been shown to deplete macrophage killing by continued cycles of lysis and uptake (Jubrail *et al.*, 2016). Further experiments would be valuable to dissect which pathway is most affected by either prophage Avβ or the β-toxin.

Our findings indicate that either prophage Avβ-encoded genes or β-toxin expression are associated with increased chicken macrophage cell death. Firstly, we identified a trend towards increased macrophage cell death at 5 h post-infection; occurring after increased phagocytosis at 3 h post-infection and at a lower MOI. This finding suggests that chicken macrophages are overwhelmed by the increased bacterial load associated with increased phagocytosis, leading to macrophage cell death and potential further dissemination. This finding would confirm previous reports reporting that *S. aureus* can escape from the intracellular compartment of phagocytes

by the intracellular killing action of PSMα (Surewaard *et al.*, 2013; Grosz *et al.*, 2014). Our data also demonstrate that significant macrophage cell death occurs at higher bacterial density in the presence of prophage Avβ or an intact β-toxin, reinforcing previous work suggesting dose-dependent induction of cell death, due to accumulation of intracellular bacteria leading to cell lysis *(*Kubica *et al., 2008;* Yun Pang *et al.*, 2010; Wang, Zhou & He, 2010; Jubrail *et al.*, 2016).

However, *S. aureus* is also capable of killing macrophages from the extracellular environment, with the actions of toxins such as LukAB and α-toxin (Melehani *et al.*, 2015; Scherr *et al.*, 2015). Therefore, the observed increase in chicken macrophage cell death could be due to either the action of intracellular or extracellular bacteria. Furthermore, macrophage cell death by *S. aureus* has been shown to require both bacterial phagocytosis and extracellular killing (Jubrail *et al.*, 2016). Cells found in chickens exhibit high expression of ADAM-10, the receptor for α-toxin and secretion of α-toxin is associated with avian CC5 isolates (Hall & Erickson, 2003; Monecke *et al.*, 2013), suggesting α-toxin is active against chicken cells and could be involved in chicken macrophage cell death. In addition, the β-toxin exhibits cytotoxicity towards monocytes (Walev *et al*., 1996), suggesting the observed cell death could be due to prophage Avβ excision and subsequent activity of the restored β-toxin. It remains to be elucidated whether enhanced macrophage cell death associated with prophage Avβ or the β-toxin is due to an overwhelming bacterial burden or toxin-mediated lysis.

Integration of the sGFP gene led to the discovery that prophage Avβ may influence chromosomal gene expression. The constitutive sGFP expression is driven by the SarA P1 promoter and as such it is tempting to speculate that prophage Avβ regulates expression of the global regulator SarA, either directly or indirectly. SarA has been implicated in the regulation of superoxide dismutase and its deletion leads to transcriptional dysregulation in response to nitric oxide (Ballal & Manna, 2009; Grosser *et al.*, 2016). Thus, regulation of SarA by genes encoded on prophage Avβ could allow increased resistance of *S. aureus* to intracellular killing. In addition, SarA regulates cell surface protein expression, which could help to explain the increased phagocytosis observed in the presence of prophage Avβ (Dunman *et al.*, 2001). However, SarA is reported to be dispensable during *S. aureus* intracellular

survival (Kubica *et al.*, 2008; Tranchemontagne *et al.*, 2015b). In addition, the lack of effective *hlb* control leaves the possibility for the β-toxin to be the main driver of macrophage killing evasion and therefore the potential regulation of SarA expression by prophage Avβ may play an alternative role in avian host-adaptation. It would be interesting to further explore the impact of Avβ on global gene expression of *S. aureus* and its impact on innate immune evasion.

The ability of *S. aureus* to adapt to different hosts is largely dependent on its ability to circumvent the host's innate immune system. In this study, we identified a role for prophage Avβ-encoded genes or the β-toxin in the host adaptation of *S. aureus* to avian innate immunity. The presence of prophage Avβ led to increased survival of chicken macrophage killing but not human macrophage killing. This suggests that the prophage Avβ-encoded genes may have a host-restricted function, in the same way that SCIN, CHIPS and SAK on Sa3 are human restricted (de Haas *et al.*, 2004; Rooijakkers *et al.*, 2005; Spaan *et al.*, 2014). However, the macrophages used in these experiments were differentiated from circulating blood monocytes, as opposed to bone-marrow. Circulating monocytes can be pre-activated and present a more heterogenous population compared to bone-marrow derived macrophages (Boyette *et al*., 2017; Zhao *et al*., 2017), suggesting the human and avian macrophages in this study may not be an effective pairwise comparison. In addition, further experiments on additional host species would help to identify whether the effect of prophage Avβ-encoded genes, or the β-toxin, on *S. aureus*-macrophage interaction is truly host-specific.

In summary, our data demonstrate a role for either prophage Avβ-encoded genes or the β-toxin in *S. aureus* evasion of avian innate immunity. Our finding provides more evidence that MGEs likely facilitate host adaptation of *S. aureus*. Further functional characterisation of the role of prophage Avβ and the β-toxin in *S. aureus*-macrophage interaction would help to dissect the molecular mechanism behind host-adaptation, as well as deepen our understanding of *S. aureus*-macrophage interactions.

Chapter 4. Genomic analysis of prophage Avβ-encoded genes and characterization of their role in avian host-adaptation

4.1. Introduction

The genome diversity of *S. aureus* is in part due to variation in the presence of MGEs, such as plasmids, pathogenicity islands, bacteriophages and transposons (Fitzgerald & Holden, 2016). Bacteriophages are key mediators of HGT, mobilising and transferring chromosomal DNA between strains, including genomic islands. Phage transduction is the main route by which phage-mediated HGT occurs. Historically, transduction was thought to occur by two mechanisms: generalized and specialized transduction (Ning *et al.*, 2019). However, recent evidence points to the capacity for *S. aureus* temperate bacteriophages to undergo lateral transduction, whereby *in situ* replication of the phage creates multiple prophage genomes, allowing DNA packaging and phage maturation to occur simultaneously, generating high titres of transducing particles and high-frequency gene transfer (Chen *et al.*, 2018a).

Acquisition of bacteriophages by *S. aureus* can influence pathogenesis. For example, *S. aureus* bacteriophages encode for virulence factors such as Panton-Valentine leucocidin or exfoliative toxin A (Kaneko *et al.*, 1998; Yamaguchi *et al.*, 2001; Boakes *et al.*, 2011; Kahánková *et al.*, 2010). In addition, bacteriophages are capable of disrupting chromosomal virulence factors such as the β-toxin (*hlb*) or lipase (*geh*) (Lee & Buranen, 1989; Van Wamel *et al.*, 2006).

In *S. aureus*, bacteriophages are a driving force for host-adaptation. For example, bacteriophages ϕSa1 and ϕSaeq1 encode for LukMF' and LukPQ, essential for bovine and equine specific immune modulation, respectively (Vrieling *et al.*, 2016; Koop *et al.*, 2017). β-converting prophage Sa3, associated with 90% of human isolates, encodes genes important for human innate immune evasion (*scn, sak, chp* and *sea*) (Van Wamel *et al.*, 2006). However, Sa3 is not strictly found in human isolates as it has been described in livestock isolates, which could be a relic of recent host jumps from humans into animals (Spoor *et al.*, 2013).

β-converting prophage Avβ found in avian infecting *S. aureus* strains is inserted at the same location as prophage Sa3. Instead of human innate immune evasion genes, prophage Avβ encodes a set of putative avian virulence factors (Lowder *et al.*, 2009). Variants of prophage Avβ have also been detected in pig isolates that recently jumped from an avian host (Lowder *et al.*, 2009; Price *et al.*, 2012).

Despite the prevalence of Avβ among avian *S. aureus* strains, a full genomic and structural characterisation of prophage Avβ is lacking to date. In this study, we aimed to characterise prophage Avβ in avian infecting isolates of *S. aureus* and dissect the molecular mechanism behind its potential role in avian innate immune evasion.

4.2. Aims

The aims of this project were to:

- Characterise the structure and gene content of prophage Avβ
- Determine the distribution of prophage Avβ and its encoded genes among avian *S. aureus* isolates
- Investigate the role of specific prophage Avβ genes in avian innate immune evasion

4.3. Materials and methods

4.3.1. Phylogenetic analysis and identification of prophage Avβ in avian strains of *S. aureus*

To examine the distribution of prophage Avβ in avian isolates, 348 whole genome sequences of avian strains of *S. aureus* were sourced from the SHAC and Fitzgerald laboratory databases by Dr Gonzalo Yebra. These were used to generate a core SNP genome alignment and maximum-likelihood tree using Parsnp (Treangen *et al.*, 2014). Avian strain ED98 was used as a reference (accession number CP001781). Closely related sequences were removed to avoid redundancy and improve clarity. The remaining 117 avian *S. aureus* strains were used to generate a new core SNP genome alignment and maximum-likelihood tree with Parsnp (Treangen *et al.*, 2014). Prophage Avβ was identified on contigs for each strain using blastable (https://github.com/bawee/blastable) to search for intact and truncated β-toxin phage integrase, human immune evasion genes (*scin*, *chips*, *sak* and *sea*) and putative avian immune evasion genes (*ocd*, *caax* and *mbl*). ITOL was used to generate the final figure (Letunic & Bork, 2019).

4.3.2. Bioinformatic analysis of prophage Avβ-encoded genes

To identify candidate genes responsible for immune evasion in prophage Avβ, we re-annotated genes using InterProScan (Jones *et al.*, 2014), BLAST searches against the Conserved Domain Database (Marchler-Bauer & Bryant, 2004) or Pfam protein families database (Finn *et al.*, 2016). Further characterisation was carried out using the following online bioinformatic tools: SignalP to detect signal peptides (Petersen *et al.*, 2011), EffectiveDB to predict secreted proteins (Eichinger *et al.*, 2016), LipoP to predict lipoproteins (Rahman *et al.*, 2008), a TMHMM transmembrane predictor to detect membrane proteins (Krogh *et al.*, 2001), Cofactory for identification of Rossmann folds (Geertz-Hansen *et al.*, 2014), and TA finder to detect presence of toxin/antitoxin systems (Xie *et al.*, 2018). Phaster was used to functionally assign genes according to phage life cycle function (Arndt *et al.*, 2016). EasyFig was used to generate a summary figure of hits (Sullivan, Petty & Beatson, 2011).

4.3.1. Amino acid sequence analysis

Protein alignments of putative avian immune evasion genes were performed in Clustal Omega (EMBL-EBI) and the sequences used are found in Table 4.1. Structural modelling was performed using Phyre2 (Kelley *et al.*, 2015).

4.3.2. Construction of allelic replacement plasmids pIMAY::*ocd*, pIMAY::*caax* and pIMAY::*mbl*

Bacterial strains, plasmids and primers used in this part of the study are listed in Tables 4.2, 4.3 and 4.4, respectively.

Primers for Gibson assembly (New England Biolabs) were generated using NEBuilder Assembly Tool (New England Biolabs). Allelic replacement was employed to generate single mutant strains deficient in Avβ-encoded putative ornithine cyclodeaminase (*ocd*), CAAX domain protease (*caax*) and putative metallo β-lactamase (*mbl*), respectively. PCR products of approximately 500 bp flanking the left (A and B) and right (C and D) region of each gene were amplified from the wild type gDNA using high fidelity polymerase Q5. The thermocycler programme included an initial denaturation at 98°C for 30 s, followed by 30 cycles of denaturation at 98°C for 10 s, annealing at 53°C for 20 s, extension at 72°C for 20 s, followed by final extension at 72°C for 2 min. Plasmid pIMAY was digested with enzymes *Kpn*I and *Sac*I and treated with Antarctic Phosphatase (NEB) as described in Chapter 2 (section 2.4.5). After PCR purification as described previously, the products were quantified using a NanoDrop1000 spectrophotometer (NanoDrop). Next, the amplified sequences were assembled and introduced into pIMAY by Gibson assembly (New England Biolabs) as per manufacturer's instructions.

The ligated construct was transformed into DC10B by heat shock transformation. Briefly, 2 µl of the undiluted assembled fragments were added to DC10B competent cells before incubation on ice for 30 min, 42°C for 1 min and 2 min on ice. 950 µl of super optimal broth (SOB) was added at room temperature (RT), followed by incubation for 1 h at 37°C with shaking at 200 rpm. Next, the bacterial suspension was spun down at 5000 x g for 1 min, 900 µl of the supernatant removed and the remaining 100 µl plated on LB + Amp before overnight incubation at 37°C,

Table 4.1. List of protein sequences analysed in this study.

Organism/Strain	Gene	Genbank reference	Reference
S. aureus MR1	Core genome-encoded OCD	ACZQ00000000.1	(Lowder et al., 2009)
S. aureus Newman	Core genome-encoded OCD	PVG34558.1	(Kobylarz *et al.*, 2014)
S. aureus CIX2	Core genome-encoded OCD	-	This study
S. aureus CIX2	Putative Avβ encoded OCD	-	This study
F. tularensis	OCD	ABK90312.1	(Rohmer *et al.*, 2007)
P. putida	OCD	NP_745670.1	(Goodman *et al.*, 2004)
A. fulgidus	AlaDH	AAB89583.1	(Gallagher *et al.*, 2004)
H. sapiens	μ-crystallin	AAF77139.1	(Kim, Gassert & Wistow, 1992)
S. aureus NCTC 8325	SpdA	YP_500401.1	(Frankel *et al.*, 2010)
S. aureus NCTC 8325	SpdB	YP_501049.1	(Frankel *et al.*, 2010)
S. aureus NCTC 8325	SpdC	YP_500738.1	(Poupel *et al.*, 2018)
S. aureus USA300	MroQ	ABD20720.1	(Cosgriff *et al.*, 2019; Marroquin *et al.*, 2019)

and screening by colony GoTaq PCR, with an annealing temperature of 60°C and extension time of 1 min 20 s. Plasmid DNA was extracted, concentrated and transformed into CIX2-sGFP as described previously.

4.3.3. Allelic replacement using pIMAY

For plasmid integration, confirmed transformants were suspended into 200 µl of TSB and diluted 1:10 000. 100 µl of this dilution was plated onto TSA supplemented with 10 µg/ml Cm and incubated at 37°C overnight. 18 large colonies were streaked onto TSA 10 µg/ml Cm and incubated at 37°C overnight. Colonies were screened for integration by high fidelity colony PCR as described previously, using the A and D cloning primers and OUT primers (Figure 4.2) with annealing temperature of 54°C and extension time of 1 min 40 sec.

To excise the plasmid, colonies representing putative integrants were inoculated into 10 ml TSB and incubated at 30°C, with shaking at 200 rpm overnight. The broths were diluted 1:10 to 10^{-6} and 100 µl plated onto TSA containing 10 µg/ml ATc. Plates were incubated at 30°C for 48h. Large colonies were replica plated onto TSA and TSA containing 10 µg/ml Cm followed by incubation at 37°C overnight. To screen for double cross-over events colonies with Cm sensitivity were tested for gene loss using colony PCR and then confirmed by PCR of gDNA template using OUT primers, and Sanger sequencing as described previously.

Table 4.2 List of strains used in this study.

Strain	Description	Reference
S. aureus		
CIX2	Wild-type	(Lowder *et al.*, 2009)
CIX2 ΔAvβ	Deletion of prophage Avβ	(Provan, 2011)
CIX2-sGFP	Wild-type with integration of *sarA*_P1-sGFP-Term downstream pseudogene CIX2_000363	This study
CIX2 ΔAvβ-sGFP	Deletion of prophage Avβ with integration of *sarA*_P1-sGFP-Term downstream pseudogene CIX2_000363	This study
CIX2-sGFP Δ*ocd*	Deletion of prophage-encoded putative ornithine cyclodeaminase	This study
CIX2 Δ*caax*	Deletion of prophage-encoded CAAX protease	This study
CIX2 Δ*mbl*	Deletion of prophage-encoded putative metallo β-lactamase	This study
E. coli		
DC10B	DH10B background, Δ*dcm*	(Monk *et al.*, 2012)

Table 4.3 List of plasmids used in this study.

Plasmid	Description	Digestion sites	Resistance marker	Reference
pIMAY	Thermosensitive gene replacement plasmid	-	Amp *E.coli* Cm *S. aureus*	(Monk *et al.*,2012)
pIMAY::*ocd*	*Ocd* deletion plasmid	*Kpn*I + *Sac*I	Cm	This study
pIMAY::*caax*	*Caax* deletion mutant	*Kpn*I + *Sac*I	Cm	This study
pIMAY::*mbl*	*Mbl* deletion mutant	*Kpn*I + *Sac*I	Cm	This study

Table 4.4. List of primers used in this study.

Primer name	Sequence	Function	Annealing temperature
ocd A F (*Kpn*I)	*AGGGAACAAAAGCTGGGTAC*CAGTAACTAGTATGAGTGG	pIMAY::*ocd*	53°C
ocd B R	*GAGGTATATT*GATGAAAATAAAGAGTAGTAGTAAAATATTTTTC	pIMAY::*ocd*	53°C
ocd C F	*TTATTTTCATC*AATATACCTCCTTTTTAAAGAGGTG	pIMAY::*ocd*	53°C
ocd D R (*Sac*I)	*CGACTCACTATAGGGCGAATTGGAGCT*CATTACTCTCTCAAGTTGAAATG	pIMAY::*ocd*	53°C
caax A F (*Kpn*I)	*AGGGAACAAAAGCTGGGTAC*TGATTGGATAAACAAGGGATG	pIMAY::*caax*	53°C
caax B R	*AGAGAAGTCA*TTTTGATGATTTGGATTCATTTTAAC	pIMAY::*caax*	53°C
caax C F	*CAAATCATCAAAA*TGACTTCTCTCCTTATTCTTTATTATC	pIMAY::*caax*	53°C

Primer name	Sequence	Function	Annealing temperature
caax D R (*Sac*I)	*CGACTCACTATAGGGCGAATTG*GAGCTCACTACAAGTATGACG	pIMAY::*caax*	53°C
mbl A F (*Kpn*I)	*AGGGAACAAAAGCTGG*GGTACTCTCTTCATTAACTTCAACCG	pIMAY::*mbl*	53°C
mbl B R	*AGAGTAAACA*GGAGAATAAAAGATGACATTAGAAC	pIMAY::*mbl*	53°C
mbl C F	*CTTTTATTCTCC*TGTTTACTCTCCTTACTATGTTTTATTG	pIMAY::*mbl*	53°C
mbl D R (*Sac*I)	*CGACTCACTATAGGGCGAATTG*GAGCTGCCATTAGAGAAGTTAACG	pIMAY::*mbl*	53°C
pIMAY MCS	TACATGTCAAGAATAAACTGCCAAAGC	Transformation check	60°C
pIMAY MCS	AATACCTGTGACGGAAGATCACTTCG	Transformation check	60°C
ocd OUT F	GGACTCGAGACCCTACAT	Integration PCR for *ocd*	55°C

Primer name	**Sequence**	**Function**	**Annealing temperature**
ocd OUT R	GGTTGCCTCAGATAGTATGACA	Integration PCR for *ocd*	55°C
caax out F	CATCCAGTGACATGCTTAGATGG	Integration PCR for *caax*	55°C
caax out R	CGTTAGATAGCAATGGTGTACC	Integration PCR for *caax*	55°C
mbl out F	GCGTTCTTGATTTCTGATATGTG	Integration PCR for *mbl*	55°C
mbl out R	GCTACTTGTTGGAGCAAGTAA	Integration PCR for *mbl*	55°C

Underlined sequences represent restriction digestion sites KpnI and SacI. Italic blue sequences represent complementary sequence to plasmid pIMAY and italic green sequences represent complementary sequences to AB or CD fragments for Gibson assembly. Restriction digestion enzymes employed are provided alongside the primer name.

4.3.4. Biofilm assay

Biofilm assays were performed using strains *S. aureus* strains CIX2-sGFP, CIX2 ΔAvβ-sGFP and CIX2-sGFP Δ*caax*. Strains were grown overnight, in either TSB supplemented with 0.5% (v/v) glucose + 3% (v/v) NaCl or BHI supplemented with 1% (v/v) glucose, at 37°C with shaking. The bacteria were diluted to OD_{600} of 0.01 in 200 µl of appropriate media in a 96-well plate (MaxiSorp, Nunc). The plates were incubated at 42°C for 24 h in a static incubator. The plates were washed gently three times with PBS and fixed for 30 min at room temperature with 100 µl of 25% (v/v) formaldehyde (Sigma). After fixation the plates were washed three times with PBS and stained with 50 µl of 0.05% (v/v) crystal violet for 3 min at room temperature. The plates were washed again 3 times with PBS, followed by incubation with 100 µl of 5% (v/v) acetic acid (Sigma) for 10 min to solubilize. Plates were analysed using a Synergy HT plate reader (BioTek) reading at 450 nm wavelength. Biofilm assays were performed by Dr Amy Pickering.

4.4. Results

4.4.1. Genomic and structural characterisation of prophage Avβ

To identify potential candidate effector proteins that play a role in evasion of avian innate immune responses, prophage Avβ gene nucleotide and amino acid sequences were analysed using online bioinformatics tools detailed in the Methods section.

Firstly, we identified that prophage Avβ is part of the *Siphoviridae* family, as identified by its genome organisation. Similarly to other *Siphoviridae* bacteriophages (Kahánková *et al.*, 2010), the double-stranded DNA genome of prophage Avβ can be divided into different functional modules: host cell lysis, tail morphogenesis, DNA packaging and head assembly, DNA metabolism and lysogeny (Figure 4.1A). However, over 40% of genes could not be assigned a function, due to the poor annotation of other prophages in this family (Figure 4.1B).

To investigate which proteins could be potential virulence factors associated with avian immune evasion, we next examined where virulence factor genes are typically located in *Siphoviridae* phages, downstream of the lysis module, at the 3′ end of the prophage (Hendrix, 2003). As described previously identified in Lowder *et al.* 2009, instead of encoding human-specific immune evasion genes in this region, two new putative virulence factors are encoded including a hypothetical ornithine cyclodeaminase (*ocd*) and predicted CAAX-domain containing protease (*caax*) (Lowder *et al.*, 2009). In addition, virulence factors have also been found to be encoded in *S. aureus* phages between the lysogeny and DNA metabolism modules (Bae *et al.*, 2006). In prophage Avβ, this region contains three genes encoding novel hypothetical proteins. Of note, human prophage Sa3 has been found to contain two putative enterotoxins (*seg2* and *sek2*) between the phage repressor and integrase genes, which is replaced by two putative mRNA interferases in prophage Avβ. The genes are predicted to be similar to toxins found in toxin-antitoxin systems, but no corresponding antitoxins were identified (Figure 4.1B)

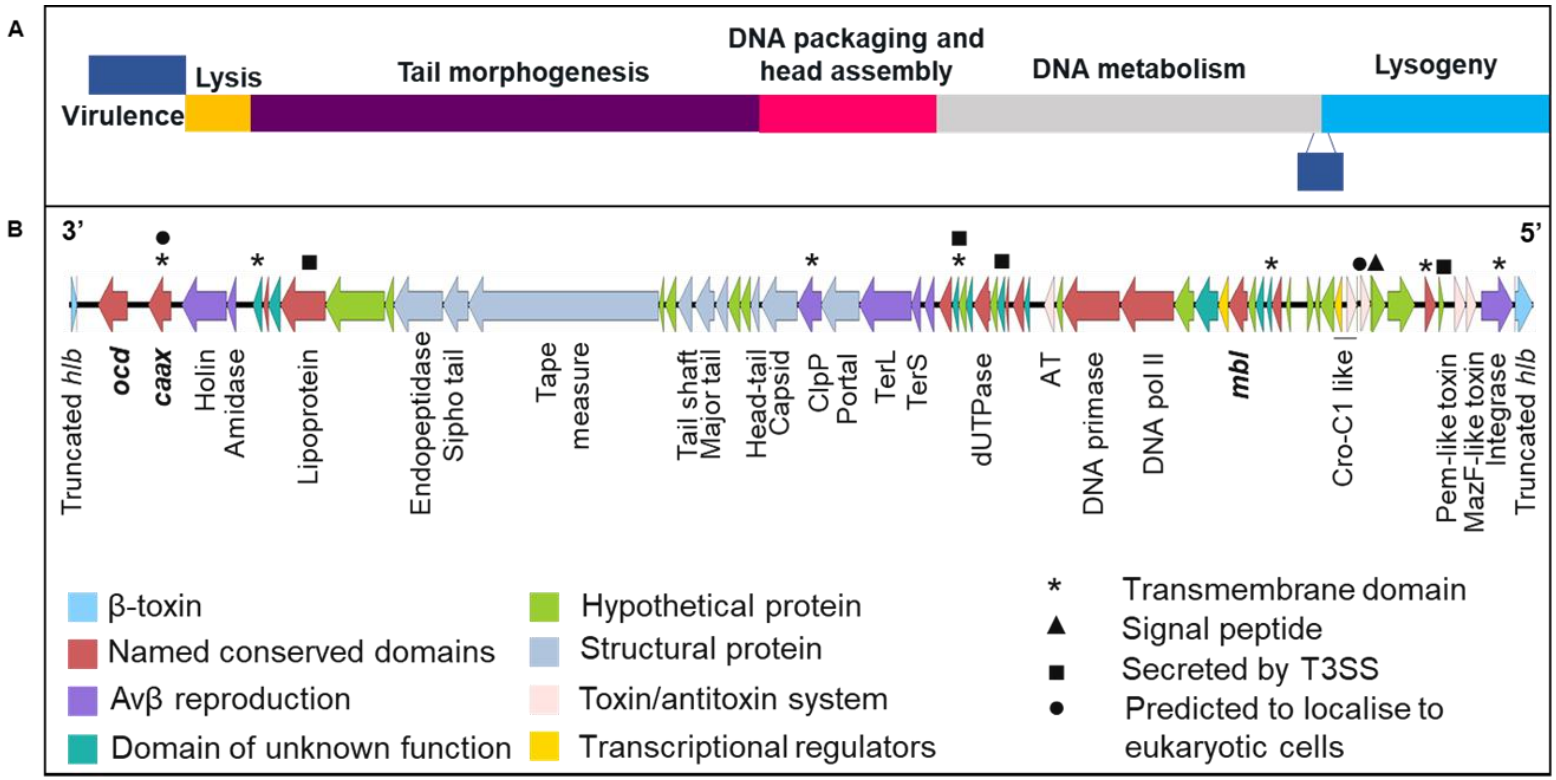

Figure 4.1. Schematic representation of prophage Avβ from strain CIX2.

A) Coloured boxes represent functional modules of prophage Avβ **B)** Gene arrangement, size, direction of transcription (arrows) and putative function are shown. Data are based on nucleotide sequence analysis using BLAST search and other online protein prediction tools.

Given the clear chicken macrophage cell death associated with either prophage Avβ or the β-toxin in *S. aureus* (Chapter 3), we searched for secreted proteins encoded on the prophage using SignalP, with a single hypothetical protein predicted to have a signal peptide (Figure 4.1B). Other proteins of interest encoded on prophage Avβ include a hypothetical lipoprotein gene in the tail morphogenesis module specific for a protein with a YkyA domain with 40% amino acid identity with *S. aureus* protein IspA, recently shown to suppress macrophage activation and be responsible for production of farnesyl pyrophosphates (Krute *et al.*, 2015; Grayczyk *et al.*, 2017). Furthermore, prophage Avβ also encodes a hypothetical metallo-β-lactamase, previously shown to be secreted by *S. aureus* avian strain CIX2 and not its prophage deletion mutant CIX2 ΔAvβ (unpublished work, Fitzgerald laboratory).

4.4.2. The majority of avian *S. aureus* strains contain prophage Avβ

In order to investigate the distribution of prophage Avβ in avian *S. aureus* strains and assess whether the prophage-encoded genes are conserved, we first performed phylogenetic analysis on 117 poultry isolates, representative of the breadth of diversity within this species. This was followed by a BLASTn nucleotide search for presence/absence of human or avian type integrase and presence of intact β-toxin and presence/absence of human prophage Sa3 encoded genes (*scn, chps, sak, sea*) or avian prophage Avβ encoded genes (*ocd, caax, mbl*).

Phylogenetic indicates that 80% of avian *S. aureus* strains contain the avian prophage Avβ (Figure 4.2). The majority of strains in clades CC5 and CC385 carry prophage Avβ, which is inserted at the β-toxin gene. Furthermore, 100% of isolates carrying prophage Avβ encode putative ornithine cyclodeaminase *ocd*, 99% encode putative CAAX-domain protease *caax* and 91.4% encode putative metallo-β-lactamase *mbl*. CC5 and CC385 have previously been shown to be the major avian-associated clonal complexes (Lowder *et al.*, 2009), and therefore the presence of prophage Avβ and its

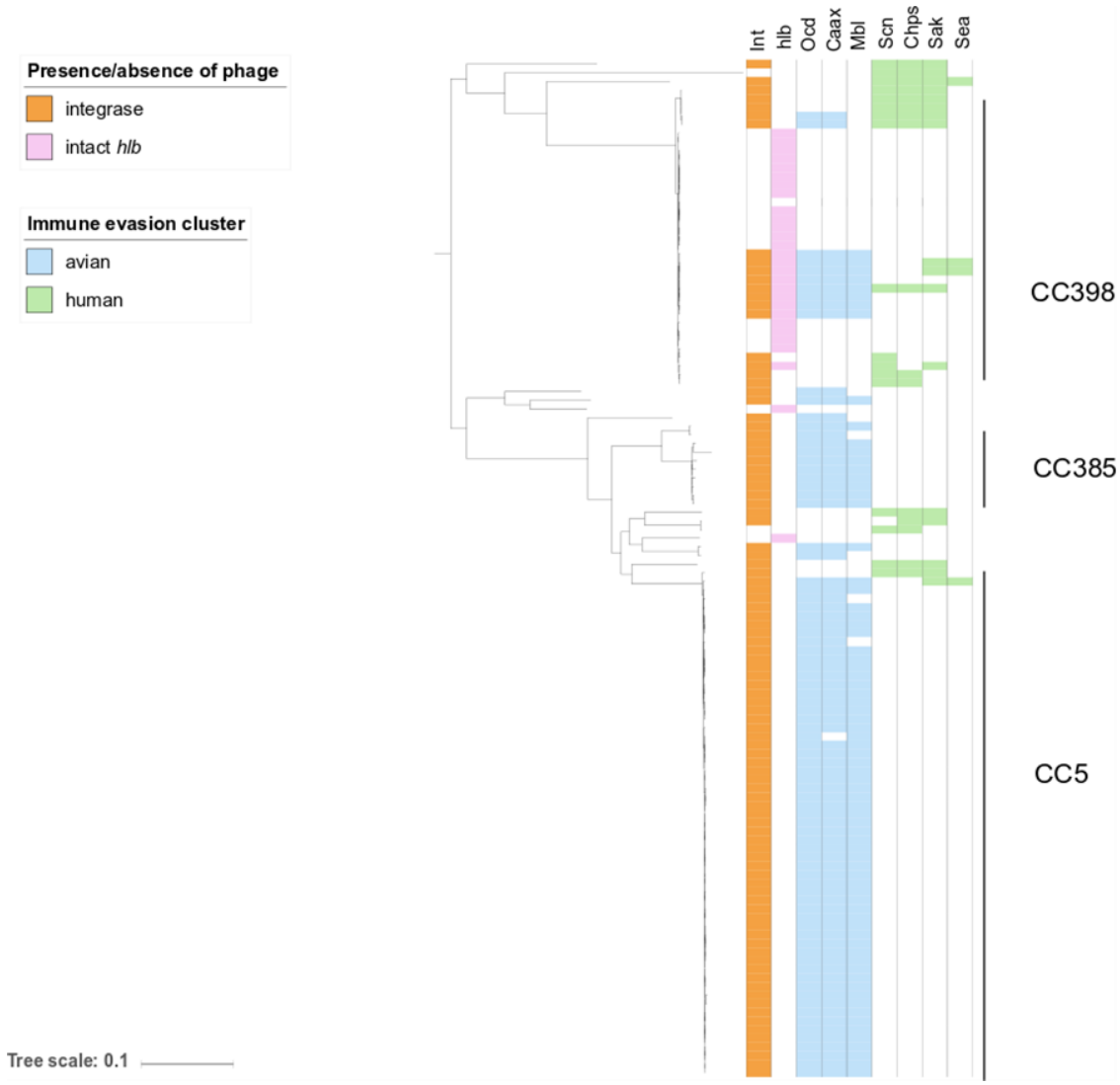

Figure 4.2 80% of avian *S. aureus* strains contain prophage Avβ.

Maximum-likelihood phylogenetic tree was constructed using a core SNP genome alignment. Fixed columns represent presence of avian or human type integrase (orange), presence of intact β-toxin, Avβ encoded genes (blue: *ocd*, *caax*, *mbl*) and Sa3 encoded genes (green: *scn*, *chps*, *sak*, *sea*). Scale bar indicates the mean number of nucleotide substitutions per site.

encoded genes in the majority of strains in these clades suggests a role in avian host-adaptation.

In contrast, clade CC398 contains prophage Avβ in a different gene encoding a putative transporter MSF1. In addition, a small proportion of strains in this clade do not carry prophage Avβ. 3% of strains in this clade carry both the human prophage Sa3, inserted at the β-toxin, and avian prophage Avβ, inserted within the MSF1 gene. The presence of both MGEs may reflect the host promiscuity of CC398 (Price *et al.*, 2012)

Moreover, the strains carrying human prophage Sa3 show some correlation with core SNP phylogeny, with all strains of sequence types ST45, ST1027 and ST15 containing the human prophage Sa3. Interestingly, strains belonging to ST45 and one strain belonging to ST15 contained Sa3 without an integrase gene, which implies a loss of ability to excise from the genome (Figure 4.2).

4.4.3. Generation of candidate phage effector gene deletion mutants

In order to investigate whether hypothetical virulence factors *ocd* and *caax* are linked to evasion of avian innate immunity, single gene deletion mutants were constructed using allelic replacement. As described previously mentioned, proteomic analysis in the Fitzgerald laboratory has identified that the *mbl* gene product, putative metallo-β-lactamase, encoded on prophage Avβ is the only protein solely expressed in *S. aureus* strain CIX2 *in vitro* compared to its prophage deletion mutant CIX2 ΔAvβ. As such, a gene deletion mutant of the *mbl* gene was also constructed. Assessing phagocytosis and chBMM cell death was previously achieved using sGFP-tagged strains (Chapter 3). Therefore, for subsequent analysis, isogenic deletion mutants were constructed in the CIX2-sGFP background.

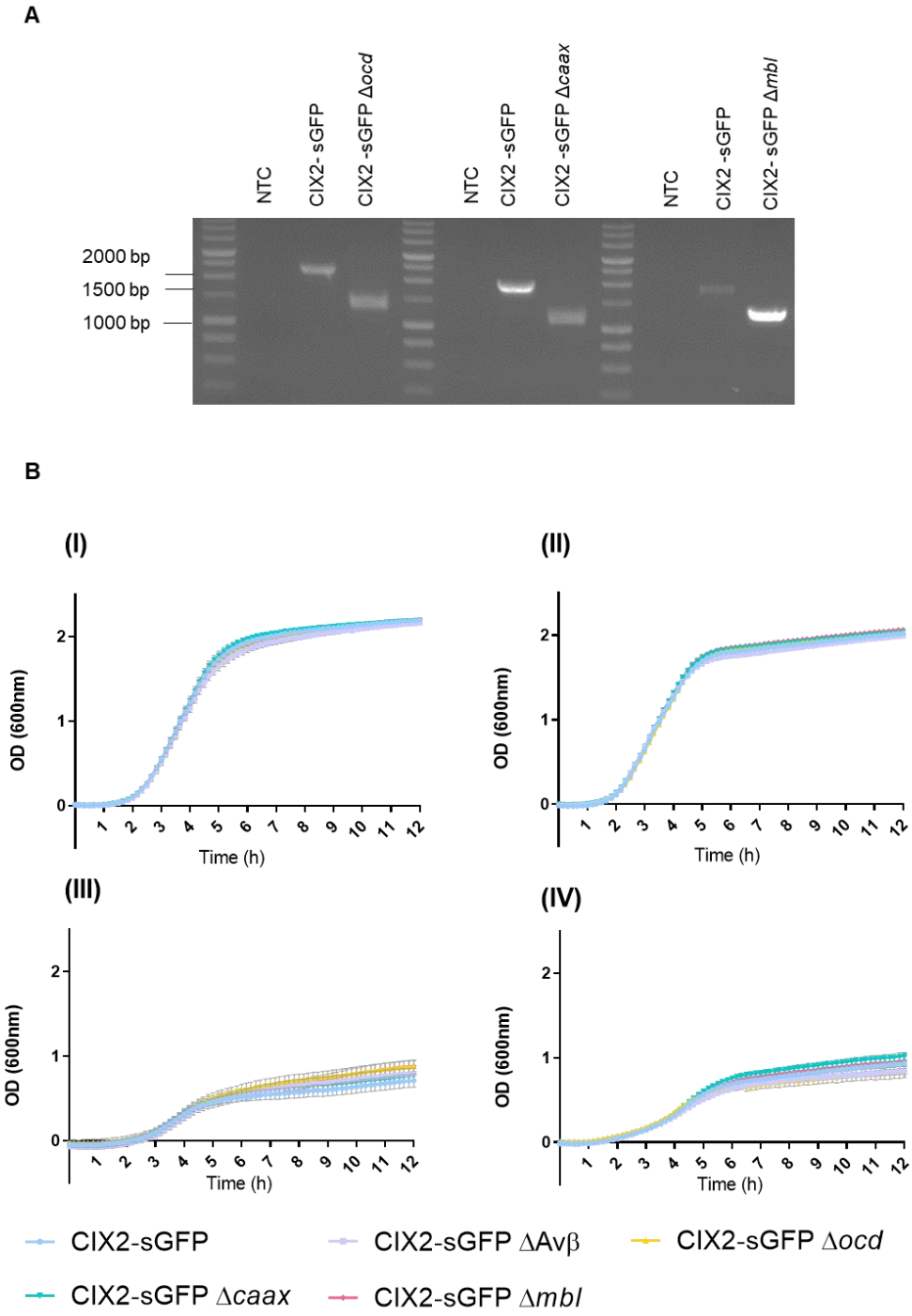

Figure 4.3. Genotypic and phenotypic validation of candidate effector prophage gene deletion mutants.

A) Agarose gel electrophoresis of genomic DNA produced by PCR amplification to confirm gene deletion. Primer pairs were located outside the flanking region of the gene of interest (*ocd*, *caax* or *mbl*) **B)** Growth curves were performed in TSB at 37°C (I) and 41°C (II), and complete RPMI at 37°C (III) and 41°C (IV), with measurements every 5 min for 12 h. Each point represents the mean of biological repeats performed in triplicate ± standard error of the mean; n =3.

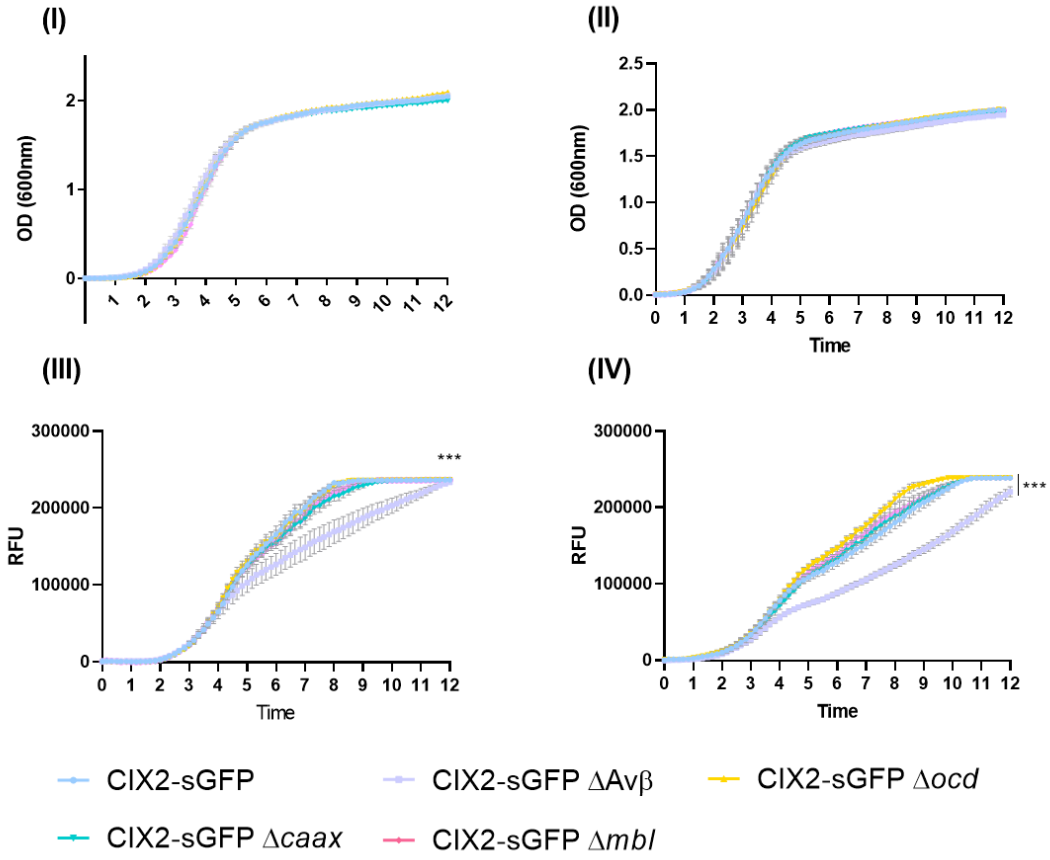

Figure 4.4. Validation of sGFP expression in *S. aureus* strains.

Growth curves were performed in TSB at 37°C (I, III) and 41°C (II, IV), with absorbance (I, II) and fluorescence measurements (III, IV) every 5 min for 12 h. Absorbance was measured at OD_{600} and fluorescence was measured at 485/520 (excitation/emission), shown as relative fluorescence intensity (RFU). The data was blanked to both TSB and wild-type *S. aureus* strains lacking integration of sGFP. Each point represents the mean of biological repeats performed in triplicates ± standard error of the mean; n = 3.

Deletion of *ocd*, *caax* and *mbl* was confirmed by PCR and whole genome sequencing (Figure 4.3A). No difference in growth rate was observed in either TSB or complete RPMI, at 37°C or 41°C (Figure 4.3B). As previously mentioned in Chapter 3, integration of sGFP in the prophage deletion mutant *S. aureus* strain CIX2 ΔAvβ-sGFP led to differential expression of sGFP compared to its wild type CIX2-sGFP. However, no difference was observed with the three new deletion mutants (Figure 4.4), suggesting that this phenotype is not due to *ocd*, *caax* or *mbl* genes.

4.4.4. The role of prophage Avβ in *S. aureus*-chBMM interaction is not due to *ocd*, *caax* or *mbl*

To investigate whether prophage-encoded genes *ocd*, *caax* and *mbl* play a role in *S. aureus*-chicken macrophage interaction, all strains were incubated with chBMMs at an MOI of 1 and phagocytosis was assessed at 3 and 5 h post-infection. The results show a decrease in phagocytosis at 3 and 5 h when chBMMs were infected with CIX2 ΔAvβ-sGFP compared to its wild type, but no difference was observed with CIX2-sGFP Δ*ocd*, CIX2-sGFP Δ*caax* or CIX2-sGFP Δ*mbl* (Figure 4.6). In a similar way, increased chBMM cell death was observed when infected with *S. aureus* wild type CIX2-sGFP compared to its prophage deletion mutant CIX2 ΔAvβ-sGFP, but no difference was observed with strains CIX2-sGFP Δ*ocd*, CIX2-sGFP Δ*caax* or CIX2-sGFP Δ*mbl* (Figure 4.6). These genes are therefore not responsible for the previously identified effect of the presence of prophage Avβ, or restoration of β-toxin expression, on *S. aureus*-chicken macrophage interactions.

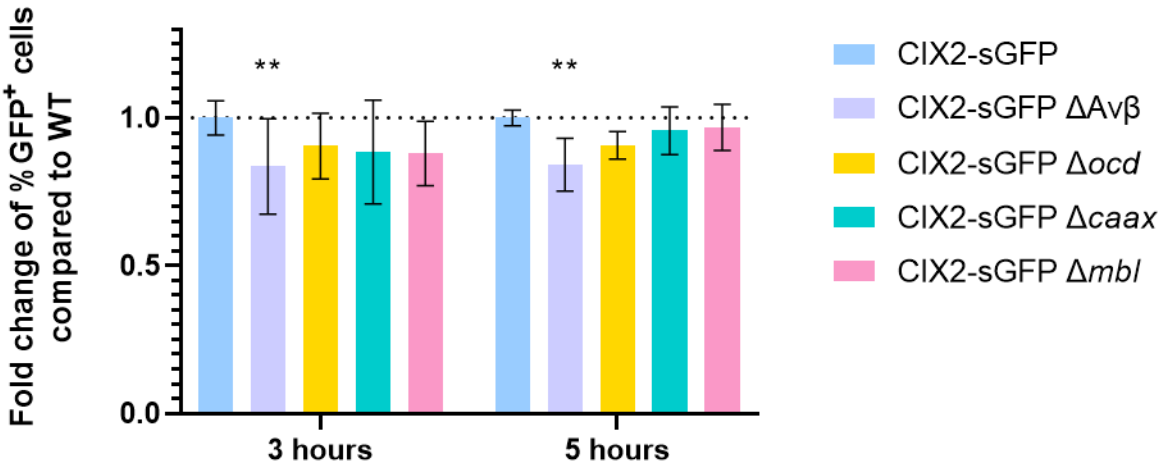

Figure 4.5. Deletion of candidate phage effector genes does not lead to reduced phagocytosis of *S. aureus* by chBMMs.

Phagocytosis of *S. aureus* strains by chBMMs, presented as fold change of percentage GFP^+ cells compared to the wild type CIX2-sGFP. Each point represents a biological replicate, ± standard deviation; n = 7. Statistical analysis was performed using two-way RM ANOVA with Dunnett's post-comparison test (compared to wild type CIX2-sGFP) and represented by ** $p \leq 0.01$.

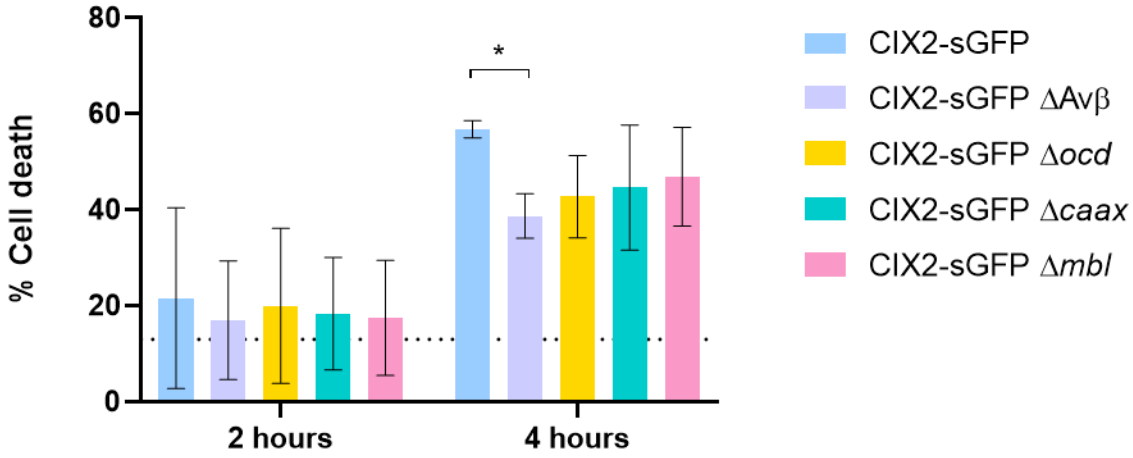

Figure 4.6 Deletion of candidate effector genes does not lead to reduced chBMM cell death by *S. aureus*

chBMM cell death after infection with *S. aureus* at a MOI of 10. Data is presented as percentage dead cells after staining with live/dead zombie violet stain. Each point represents a biological replicate, ± standard deviation; n = 4. Statistical analysis was performed using two-way RM ANOVA with Tukey's post-comparison test, where * $p<0.05$.

4.4.5. Putative ornithine cyclodeaminase encoded on prophage Avβ does not play a role in iron-limited conditions

Core genome-encode OCD enzymes in *S. aureus* have previously been linked with survival in low iron conditions (Friedman *et al.*, 2006). Moreover, siderophore SbnB shares sequence similarity to bacterial OCDs (Beasley, Cheung & Heinrichs, 2011). To assess whether the putative prophage-encoded OCD plays a role in *S. aureus* growth in iron limited conditions, growth curves in RPMI only, a media low in iron, were performed on strains CIX2-sGFP, CIX2-sGFP ΔAvβ and CIX2-sGFP Δ*ocd* in a plate reader at both 37°C and 41°C for 12 h. Differences in growth between the strains was measured by calculating the area under the curve (AUC) for growth. No difference was observed between the three strains at 37°C (Figure 4.7A). However, a decrease in bacterial growth was observed in the absence of prophage Avβ but not in the absence of prophage Avβ-encoded *ocd* (Figure 4.7B). These data suggest that either prophage Avβ or excision of prophage Avβ, leading to β-toxin expression, enhances bacterial growth during iron limited conditions, and this effect was significant at 41°C. This phenotype is not due to the putative prophage-encoded *ocd*, suggesting another prophage-encoded factor or a functional β-toxin are involved in *S. aureus* growth in iron limited conditions.

4.4.6. Sequence analysis of putative ornithine cyclodeaminase

In order to further identify a potential role for the hypothetical avian virulence proteins encoded by prophage Avβ, structural predictions and sequence alignments were performed on the putative ornithine cyclodeaminase (OCD) and CAAX-domain protease.

Firstly, an initial structural prediction using Phyre2 predicted the putative ornithine cyclodeaminase to be structurally related to ornithine cyclodeaminase-like proteins (OCD), archaeal alanine dehydrogenase (AlaDH) and mammalian μ-crystallin. The defining feature of these proteins is the presence of a NAD/NADP binding domain with a core Rossman-type fold, consisting of three layers alpha/beta/alpha where the six beta strands are parallel (Geertz-Hansen *et al.*, 2014).

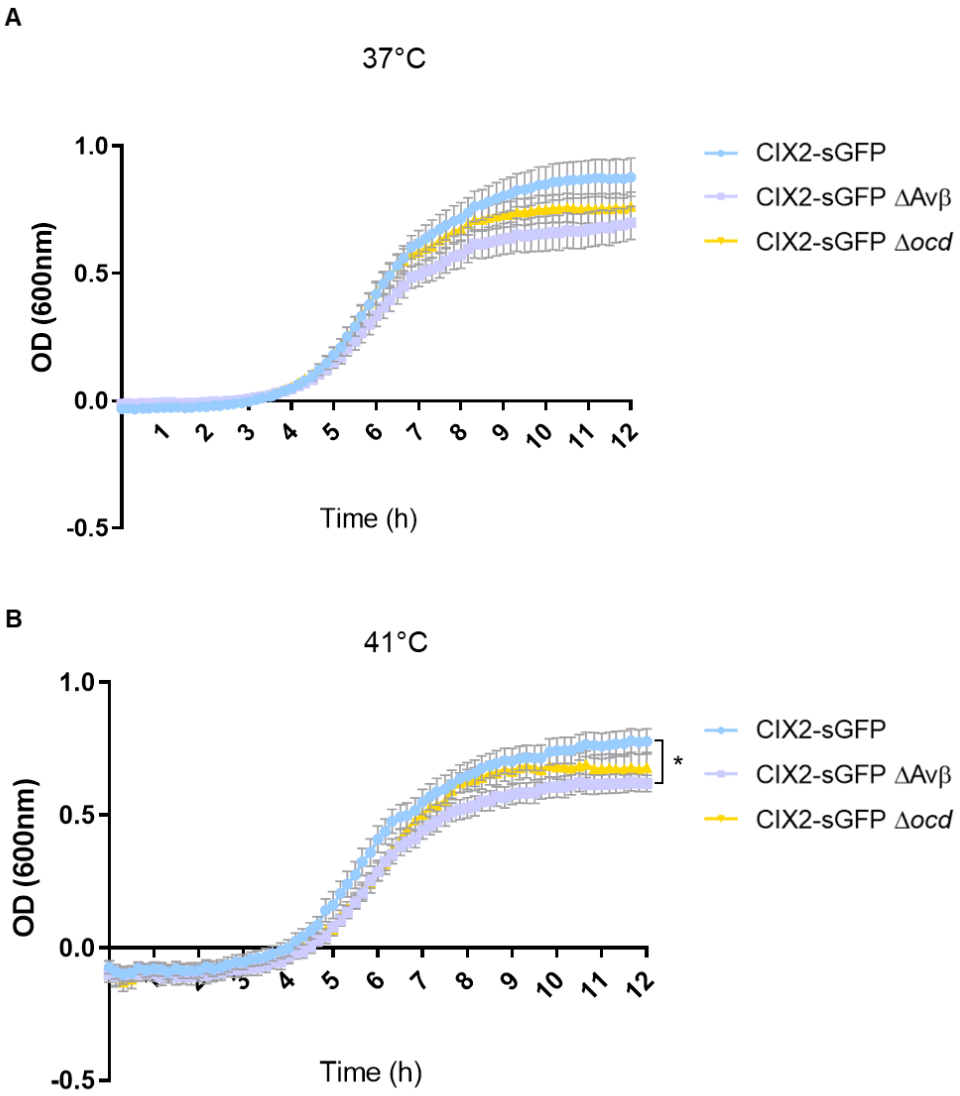

Figure 4.7. Prophage Avβ enhances S. aureus growth during iron-limited conditions, independent of *ocd*.

Growth curves were performed in RPMI only at **A)** 37°C and **B)** 41°C, with absorbance readings every 5 min for 12 h. Absorbance was measured at OD_{600}. The data was blanked to RPMI only. Each point represents the mean of biological repeats performed in triplicate ± standard error of the mean; n = 3. Statistical analysis was performed by measuring the area under the curve using growthcurver package in R, followed by one-way ANOVA analysis, represented by * $p < 0.05$.

We next aimed to determine protein motifs and residues in the putative ornithine cyclodeaminase that may contribute to its function. An amino acid alignment was performed against bacterial proteins confirmed to have CCD activity, as well as the structurally related mammalian μ-crystallin and archael AlaDH (Figure 4.8). In addition, we included proteins annotated as ornithine cyclodeaminase encoded in the *S. aureus* core genome. Our results show that at the amino acid level, the prophage-encode putative OCD is more similar to the archaeal AlaDH (34.55% aa identity) than to known bacterial OCDs (~22% aa identity) or core genome-encoded putative OCDs (~22% aa identity).

Ornithine cyclodeaminase catalyses the conversion of l-ornithine to l-proline via an NAD^+ transfer reaction, resulting in secretion of ammonia (Lee *et al.*, 2010). To assess whether the prophage-encoded putative OCD has a similar function, we used a previously characterised crystal structure of *Pseudomonas putida* OCD and identified the key amino acid residues essential for binding to l-ornithine (Goodman *et al.*, 2004); namely, Arg45, Lys69 and Arg112. Glu56 has also been identified to be important for substrate binding, and Asp228 directly interacts with the α-amino leaving group during the deamination of ornithine (Goodman *et al.*, 2004). Our results indicate that multiple key residues (Arg45, Glu56 and Asp228) are not conserved in the prophage encoded putative OCD (Figure 4.8). Furthermore, the core Rossman-type fold motif in bacterial OCDs has the sequence GXGXXS whereas the archaeal alanine dehydrogenase, μ-crystallin and prophage encoded putative OCD have the sequence GXGXXA and the core-encode putative OCDs have the sequence GXGXXG (Figure 4.8). Finally, bacterial OCDs have an extended C-terminus and conserved basic lysine residue, which is absent in the phage-encoded putative ornithine cyclodeaminase (Figure 4.8). These sequence differences suggest that the prophage-encoded putative OCD is unlikely to have the same enzymatic functions as previously characterised bacterial OCDs but likely acts as a NAD(P) binding enzyme of unknown function.

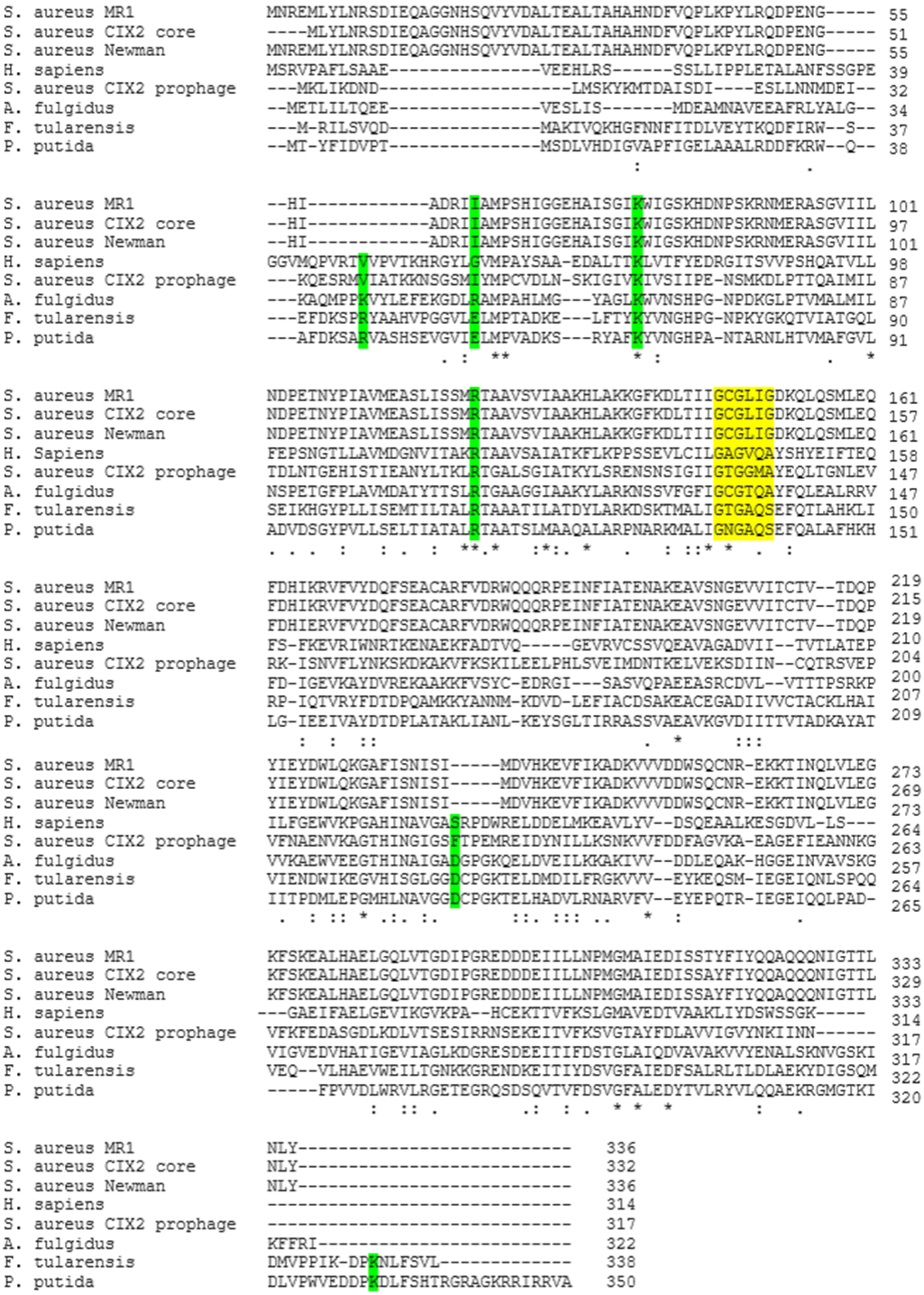

Figure 4.8 Amino acid sequence alignment of OCD enzymes, AlaDH and μ-crystallins.

Regions of identity (*), conservation (:) and similarity (*) are indicated below the alignments. Residues highlighted in green have been found to essential for L-ornithine binding in P. putida crystal structure. Residues highlighted in yellow indicate the conserved sequence of the Rossman fold (GXGXXG/A/S).

4.4.7. Sequence analysis of predicted CAAX-domain protease

One of the prophage-encoded putative virulence factors is predicted to be a type II CAAX protease. In eukaryotes, these proteases are involved in post-translational modifications through prenylation. involving addition of an isoprenyl group to the Cys residue on the CAAX motif of a protein, after which the CAAX protease cleaves the AAX tripeptide (Pei & Grishin, 2001). However, only a few bacterial proteins contain this motif, suggesting that prenylation is not conserved in prokaryotes (Krute *et al.*, 2015). Although previously thought to play a role in immunity against phages, two CAAX-domain proteases, SpdC and MroQ, have recently been identified to be involved in protein display, regulation of virulence factors and biofilm formation in *S. aureus* (Frankel *et al.*, 2010; Cosgriff *et al.*, 2019; Marroquin *et al.*, 2019).

To investigate a potential role for the prophage-encoded CAAX-domain protease, amino acid alignments were performed against known CAAX-domain proteases of *S. aureus* (SpdA, SpdB, SpdC, MroQ) using Clustal Omega. Consistent with its annotation, this protease contains the conserved diglutamate motif EEXXXR, as well as the FXXXH motif and single histidine, proposed to be involved in metal coordination (Figure 4.9A).

The second glutamic acid in motif 1 has been identified as the catalytic residue and is conserved in prophage-encoded CAAX-domain protease (Frankel *et al.*, 2010), suggesting a proteolytic role for this protein. Similarly to SpdC and MroQ, Phyre2 analysis suggests a topology containing eight transmembrane helices with both the N and C terminus position in the extracellular space (Figure 4.9B). These data suggest a potential for prophage-encoded CAAX-domain protease to have a similar role as other *S. aureus* CAAX-domain proteases.

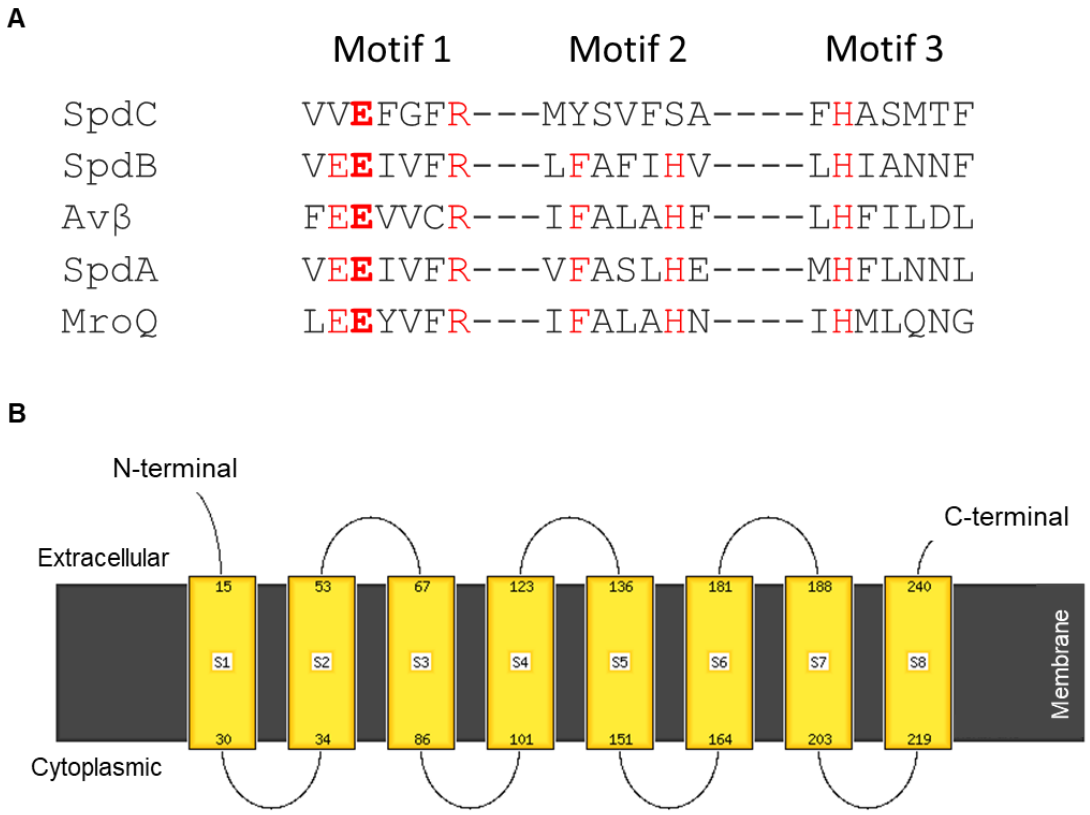

Figure 4.9. Sequence and structure analysis of CAAX-domain protease encoded on prophage Avβ.

A) Amino acid sequence alignment of the conserved residues from the three motifs of CAAX domain-containing *S. aureus* proteins. Highlighted in red are residues with high sequence conservation among CAAX domain-containing proteins. The catalytic glutamic acid residue (E) is highlighted in bold **B)** Phyre 2 topology prediction of putative CAAX protease. Yellow boxes indicated transmembrane domains, with the corresponding amino acids numbered.

4.4.8. Prophage Avβ-encoded genes, or an intact β-toxin, influence biofilm formation independent of putative CAAX-domain protease

Previously identified *S. aureus* CAAX-domain proteases SpdC and MroQ have been shown to play a role in biofilm formation (Poupel *et al.*, 2018; Marroquin *et al.*, 2019). Deletion of SpdC led to decreased biofilm formation whilst deletion of MroQ led to enhanced biofilm formation (Poupel *et al.*, 2018; Marroquin *et al.*, 2019). In both cases, this was due to the regulation of the abundance of cell surface proteins. Given the amino acid similarities between these proteins and prophage-encoded CAAX-domain protease, we hypothesised that the prophage-encoded CAAX-domain protease would also play a role in *S. aureus* biofilm formation.

To explore this hypothesis, *S. aureus* strains CIX2-sGFP, CIX2-sGFP ΔAvβ and CIX2-sGFP Δ*caax* were grown statically at 41°C in either TSB supplemented with glucose and NaCl or BHI supplemented with glucose. In TSB, strain CIX2-sGFP ΔAvβ exhibited increased biofilm formation compared to the wild type CIX2-sGFP and *caax* deletion mutant CIX2-sGFP Δ*caax* (Figure 4.10A). A similar phenotype was observed in BHI and was more pronounced compared to strains grown in TSB (Figure 4.10B). Previous biofilm studies have identified that *S. aureus* biofilms formed in TSB supplemented with glucose and NaCl are polysaccharide-dependent whereas *S. aureus* biofilms formed in BHI supplemented with glucose are protein-protein interaction-dependent (Sadovskaya *et al.*, 2005). Therefore, these data suggest that either the prophage Avβ or an intact β-toxin play a role in biofilm formation, particularly in biofilms dependent on protein-protein interactions and this is not dependent on prophage-encoded CAAX-domain protease.

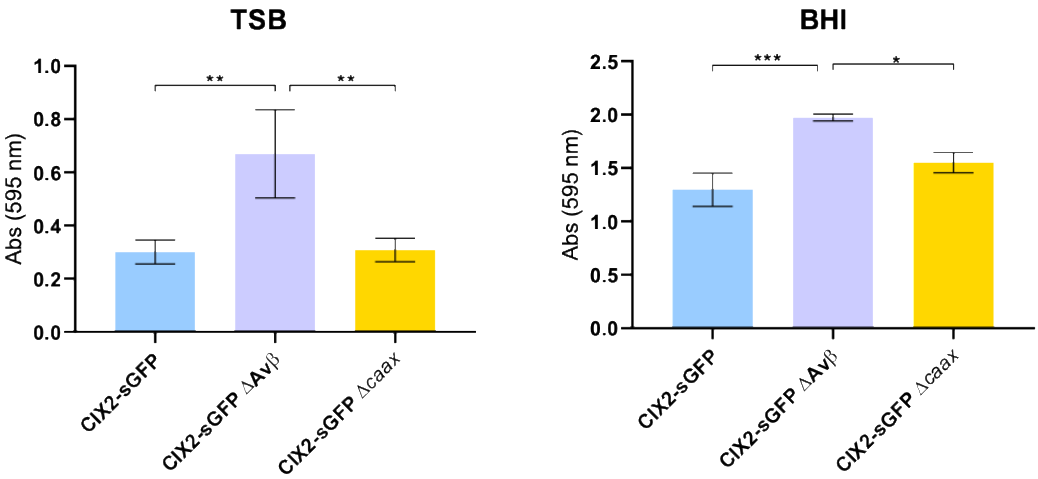

Figure 4.10. Absence of prophage Avβ leads to an increased capacity to form a biofilm.

Strains were grown for 24 h at 41°C in either **A)** TSB supplemented with 0.5% glucose and 3% NaCl or **B)** BHI supplemented with 1% glucose. Biofilm formation was quantified with crystal violet staining, followed by solubilisation using acetic acid and OD_{450} measurement. Assays were performed in biological triplicates and technical triplicates. Error bars represent SD. Statistical analysis was performed using one-way ANOVA with Tukey's post-comparison test, where * $p < 0.05$, ** $p < 0.01$, *** $p < 0.001$.

To summarise, we investigated the genomic structure, content and distribution of prophage Avβ in avian infecting *S. aureus* strains. We assessed the role of three candidate effector genes on avian innate immune evasion with the use of single gene deletion mutants. Importantly, we discovered a potential role for either prophage Avβ or an intact β-toxin in *S. aureus* growth in iron-limited conditions and biofilm formation, suggesting a pleiotropic role in disease-relevant conditions.

4.5. Discussion

Bacteriophages of *S. aureus* are important drivers of evolution and host-adaptation (Hendrix, 2003). Despite their importance, studies focusing on their genome structure and content are limited. Here, we characterized the genome structure and content of Avβ. Genomic analysis revealed a similar gene organization to other *S. aureus Siphoviridae* bacteriophages, with genes organised into six distinct functional modules. However, most genes encoded on prophage Avβ have a putative functional annotation and experimental evidence is required to assign further function. Of note, similarly to human prophage Sa3, avian prophage Avβ lacks a *xis* gene excisionase, which raises the question of how these β-converting bacteriophages initiate excision from the genome (Sumby & Waldor, 2003).

Population analysis revealed that prophage Avβ is carried by the majority of avian *S. aureus*. The presence of prophage Avβ in most of the isolates in this clade suggests that prophage Avβ plays an important role in avian host-adaptation. Moreover, this is emphasised by the fact that prophage Avβ is also present in all of the strains belonging to CC385, specific for avian hosts (Lowder *et al.*, 2009; Murray *et al.*, 2017a). Interestingly, strains belonging to CC398 demonstrated either carriage of prophage Avβ, carriage of human-specific prophage Sa3 and carriage or loss of both prophages. The presence of prophage Avβ reinforces the findings of a previous phylogenetic analysis, which identified that prophage Sa3 was lost during CC398 adaptation to a non-human isolates and was associated with the gain of prophage Avβ in turkey CC398 isolates (Price *et al.*, 2012). CC398 has a mixed host

distribution, with isolates found both in humans and livestock (Price *et al.*, 2012; Ward *et al.*, 2014). Loss of prophage Sa3 in CC398 turkey isolates has been suggested to be associated with secondary transmission from pig isolates, which have lost prophage Sa3 (Monecke *et al.*, 2013), which could also explain the loss of prophage Sa3 in our CC398 isolates. In contrast, the presence of human prophage Sa3 in some isolates could be due to a closer relationship of these avian isolates to humans compared to livestock isolates.

Human-specific prophage Sa3 contains an immune evasion cluster (IEC), encoding a combination of *scn, sak, chps* and *sea* genes (Van Wamel *et al.*, 2006). Previous work reported that instead of the human immune evasion cluster, prophage Avβ encodes novel genes *ocd* and *caax*, hypothesised to be involved in avian niche host-adaptation (Lowder *et al.*, 2009). Our analysis revealed that both *ocd* and *caax* are conserved in avian isolates carrying prophage Avβ, but single gene deletion mutants of *ocd* and *caax* demonstrated that these candidate effector genes are not associated with the previously identified phenotype in chicken macrophages.

Phage-associated virulence factors are not limited to the immune evasion cluster. This is exemplified by an alternative glycotransferase TarP, encoded near human-specific prophage Sa3's integrase, which alters *S. aureus* WTA glycosylation and inhibits antibody recognition, leading to reduced immunogenicity (Gerlach *et al.*, 2018). We therefore investigated whether *mbl*, previously identified to encode a secreted protein, was associated with avian innate immune evasion. However, single deletion of *mbl* did not lead to a change in *S. aureus* phagocytosis or chicken macrophage killing. Further bioinformatic analysis of prophage-encoded genes allowed us to identify other potential candidate effector genes involved in avian innate immune evasion. Of interest, prophage Avβ encodes two genes at its 5′, which contain domains associated with mRNA interferases MazF and PemK.

These mRNA inteferases are usually encoded by toxin-antitoxin systems, associated with bacterial growth control and plasmid maintenance (Schuster & Bertram, 2016). Under resting conditions, the mRNAse toxin component is repressed by the antitoxin whilst under stress conditions, the antitoxin is degraded, freeing the mRNAse, inducing cell stasis or death (Schuster & Bertram, 2016). Given their location, these

genes could be involved in the transition from lysogenic to lytic growth of prophage Avβ (Bae *et al.*, 2006). Phage-encoded virulence factors are often found close to the host chromosome, with could be acquired during previous aberrant excision events (Wagner & Waldor, 2002; Novick, 2003). For example, enterotoxin genes *seg2* and *sek2* have been found at this location in human-specific prophage Sa3 (Sumby & Waldor, 2003).

In *S. aureus*, both MazF and PemK have been associated with regulation of *S. aureus* virulence factors in a sequence specific manner (Fu *et al.*, 2009; Bukowski *et al.*, 2013). For example, MazF leads to steady state expression of *sarA*-regulated mRNAs but cleaves both *hla* and *sigB* regulated transcripts. (Fu *et al.*, 2009; Schuster *et al.*, 2015). In a similar way, PemK targets mRNAs related to metabolism and transmembrane transport while preserving virulence genes and therefore may function as a regulator of gene expression (Bukowski *et al.*, 2013). Therefore, it is tempting to speculate that the prophage-encoded toxins could be also involved in regulation of *S. aureus* virulence mRNA transcripts. However, PemK and MazF are both regulated by an antitoxin, found adjacent to the toxin, which is lacking in prophage Avβ (Fu *et al.*, 2009; Bukowski *et al.*, 2013). This might suggest an additional role for these prophage-encoded genes and further characterisation would help to elucidate whether they function as mRNA interferases and play a role in evasion of avian innate immunity.

Modification of metabolism in response to nutrient availability is an important host-adaptive trait (Richardson *et al.*, 2018). OCD-like proteins in bacteria have been identified to catalyse the conversion of l-ornithine into proline, suggesting a role in bacterial metabolism. The synthesis of proline could be useful for *S. aureus*, as the bacterium uses proline as a primary substrate for glutamate in low-glucose environments, such as inside macrophage phagosomes (Halsey *et al.*, 2017). In addition, an OCD-like protein encoded in the core genome of *S. aureus* is repressed by the ferric uptake regulator (Fur) and involved in synthesis of staphyloferrin B (Friedman *et al.*, 2006; Kobylarz *et al.*, 2014), suggesting a role in *S. aureus* survival during iron-limited conditions. Thus, we hypothesised that the prophage-encoded putative OCD could be associated with *S. aureus* growth in low-iron conditions. However, our findings demonstrate that *S. aureus* growth in iron-limited conditions

is only impaired in an Avβ-deficient strain and not in the *ocd*-deficient strain. Further comparative sequence analysis identified that that despite structural similarity to OCD-like proteins, the prophage-encoded putative OCD is more similar to the archaeal alanine dehydrogenase AlaDH. For example, both proteins demonstrate a lack of conserved substrate binding site residues and lack of extended C-terminus. Furthermore, the core Rossman-fold domain of both AlaDH and prophage-encoded putative OCD is GXGXXA, as opposed to GXGXXS in bacterial OCDs. These amino acid differences suggest that prophage-encoded OCD does not have the same function as previously characterised bacterial OCDs and therefore could explain why *ocd* is not involved in *S. aureus* growth in iron-limited conditions.

Importantly, the impaired growth of the Avβ-deficient strain in iron-limited conditions was observed to be temperature-dependent, occurring at 41°C but not 37°C. Given the fact that the intracellular environment of a macrophage is iron-limited (Haley & Skaar, 2012), our findings suggest that the previously identified phenotype in chicken macrophages could be due to enhanced growth of *S. aureus* in iron-limited conditions. The excision of human-adapted prophage Sa3 was previously identified to be suppressed when *S. aureus* was grown in RPMI-1640 (Tran *et al.*, 2019), which suggests that excision of prophage Avβ and restoration of β-toxin expression may not be responsible for the observed enhanced growth in iron-limited media. Furthermore, the observed temperature-dependent phenotype suggests that prophage Avβ could also play a role in *S. aureus* adaptation to the higher body temperature found in birds.

Finally, our study revealed that the CAAX-domain protein encoded on prophage Avβ is likely to have a similar function as other CAAX-domain proteases of *S. aureus*. Structural and sequence analysis revealed that the second glutamic acid residue of motif 1, believed to be the essential catalytic residue, is conserved in the prophage-encoded protein (Frankel *et al.*, 2010). However, in previously characterised CAAX-domain proteases found in Gram-positive bacteria, their regulatory role and interaction with histidine kinases was not dependent on their proteolytic activity (Firon *et al.*, 2013; Poupel *et al.*, 2018). For example, in *S. aureus*, SpdC interacts with the histidine kinase WalK via its membrane spanning domain, independently of its catalytic residues, leading to coordination of cell envelope division (Poupel *et al.*,

2018). In contrast, the regulation of *agr* quorum sensing by recently characterised CAAX-domain protease MroQ is dependent on the conserved active site residues (Cosgriff *et al.*, 2019; Marroquin *et al.*, 2019). Therefore, although this prophage-encoded protease is likely proteolytically active, it may have an alternative mechanism of action.

Given the sequence similarities to both SpdC and MroQ, which have been shown to be involved in *S. aureus* biofilm formation (Poupel *et al.*, 2018; Marroquin *et al.*, 2019), we investigated whether prophage-encoded CAAX-domain protease was also involved in biofilm formation. Our findings revealed that the Avβ-deficient *S. aureus* strain leads to increased biofilm formation compared to its wild type, but this effect was not dependent on presence of *caax*. However, the increased biofilm formation after prophage Avβ deletion is comparable to what was observed in an *mroQ* or *agr* deletion mutant (Boles & Horswill, 2008; Marroquin *et al.*, 2019). This was proposed to be due to an initial increase in MSCRAMM production and decrease in virulence factor production, leading to increased initial biofilm formation but loss of dispersal (Boles & Horswill, 2008; Marroquin *et al.*, 2019). Therefore, prophage Avβ-dependent control of biofilm formation could be due to the regulation of cell surface proteins, supported by the fact that the biofilms are likely dependent on protein-protein interactions.

However, biofilm formation could also be dependent on restoration of β-toxin expression, as the toxin is capable of cross-linking DNA, leading to the formation of a biofilm matrix (Huseby *et al.*, 2010). Recent evidence points to the capacity for human-adapted prophage Sa3 to excise during biofilm growth (Tran *et al.*, 2019), suggesting that prophage Avβ may also excise during biofilm conditions, leading to restoration of β-toxin expression, which is capable of increasing biofilm formation. However, the enhanced biofilm formation in our study only occurred in the Avβ-deficient strain with non-functional β-toxin and not the wild-type, suggesting that excision of prophage Avβ and restoration of β-toxin expression may lead to decreased biofilm formation. The β-toxin is regulated post-exponentially by *agr* (Cheung *et al.*, 1992), and *agr* deficient strains exhibit increased biofilm formation (Boles & Horswill, 2008), suggesting that decreased β-toxin expression can lead to thicker biofilm formation. Therefore, the presence of a functional β-toxin due to

prophage Avβ excision could be responsible for the decreased biofilm formation observed in our study. Further experiments which include an effective *hlb* control are required to dissect the mechanism behind the influence of prophage Avβ or the β-toxin on *S. aureus* biofilm formation.

Overall, these findings suggest a pleiotropic role for prophage Avβ or the β-toxin in *S. aureus* virulence and metabolism, which is likely important for *S. aureus* host-adaptation to birds. This study provides more evidence for the key role of MGE in host-adaptation of *S. aureus*.

Chapter 5. Transcriptomic analysis of the chicken macrophage response to *S. aureus* infection

5.1. Introduction

Macrophages play a crucial role in the recognition of *S. aureus* leading to innate immune signalling and recruitment of the adaptive immune cells (Brown *et al.*, 2015). TLR2 has been identified as the main PRR for the recognition of *S. aureus* in mice and humans, leading to classical cytokine activation (Takeuchi, Hoshino & Akira, 2000; von Bernuth *et al.*, 2012). *S. aureus* can also be recognised intracellularly by TLR8, which induces expression of interferon response genes (Bergstrøm *et al.*, 2015). Most studies on the macrophage recognition of *S. aureus* have been carried out in mice and humans, and it is known that the recognition of bacterial pathogens can vary according to host species (Kapetanovic *et al.*, 2012; Schroder *et al.*, 2012; Young *et al.*, 2018). Knowledge of how chicken macrophages recognise and respond to bacterial pathogens is limited due to the lack of specific tools available in avian immunology (Kaiser & Stäheli, 2013). High-throughput profiling of transcriptomes using RNA-seq has enabled investigations into the complex changes in gene expression following bacterial infection (Wang, Gerstein & Snyder, 2009). However, the response of chicken macrophages to the avian pathogen *S. aureus* has yet to be examined.

The current study has identified a role for either prophage Avβ-encoded genes or prophage Avβ excision leading to β-toxin expression, in evasion of macrophage killing. However, the mechanism underlying this phenotype remains to be elucidated. *S. aureus* has adapted strategies to avoid recognition by innate immune cells during human infection. For example, core encoded SSL3 can directly bind to TLR2 to avoid cytokine signalling (Bardoel *et al.*, 2012), and PSMs can stimulate shedding of bacterial lipoproteins to avoid recognition by TLR2 (Hanzelmann *et al.*, 2016). Human-specific β-converting prophages encode genes capable of manipulating the recognition of *S. aureus* by innate immune cells. For example, TarP is an alternative glycosyltransferase able to modify the immunogenicity of wall techoic acid and therefore evading immune recognition (Gerlach *et al.*, 2018). Similarly, both CHIPS and SAK inhibit leukocyte chemotaxis (Gladysheva *et al.*, 2003; de Haas *et al.*, 2004). Considering recognition of *S. aureus* by macrophages is an important player

in coordinating the innate immune response, we hypothesised that the prophage Avβ would influence host-macrophage interactions leading to altered transcriptional response of chBMMs to *S. aureus*, associated with immune evasion. In the current study, RNA-seq was employed to investigate the early chBMM transcriptional response to *S. aureus*, as well as the role of prophage Avβ in this response.

5.2. Aims

- Analyse the early transcriptional response of chicken bone-marrow derived macrophages to infection with avian *S. aureus*

- Investigate the influence of the *S. aureus* prophage Avβ on the response of chicken bone-marrow derived macrophage to infection

5.3. Materials and Methods

5.3.1. KUL01 staining of chBMMs

chBMM cells were plated in a 100 mm square Sterilin Petri Dish (SLS) at a concentration of 2 x 10^7 cells/plate in 20 ml on day 5 of differentiation. On day 6 or day 7 of differentiation, chBMMs were washed with PBS + 2% FBS (Gibco) and detached using a syringe and 18G needle (SLS). The chBMMs were then centrifuged at 400xg for 5 min and the supernatant discarded, before resuspending in PBS without FBS + Zombie Violet (Biolegend) at a dilution of 1:1000 for live/dead staining. The chBMMs were kept on ice for 30 min in the dark, before washing twice with PBS by centrifuging at 400xg for 5 min, followed by fixing in 4% PFA on ice for 15 min and washing twice with PBS. After fixation, the chBMMs were blocked for 15 min on ice with PBS + 1% goat serum (Sigma Aldrich), and then stained with KUL01-PE (Cambridge Bioscience) at a dilution of 1:800 in PBS + 1% goat serum. After washing twice, the chBMMs were re-suspended in a minimum of 200 µl PBS and kept at 4°C in the dark before analysing by flow cytometry (Beckton Dickinson Fortessa).

5.3.2. Infection of chBMMs with *S. aureus* for FACS sorting

For the FACS sorting experiments, chBMMs were plated in 100 mm square Sterilin Petri Dishes (SLS) at a concentration of 2 x 10^7 cells/plate in 20 ml on day 5 of differentiation. On Day 6, chBMM were infected with 1 ml of CIX2-sGFP or CIX2 ΔAvβ-sGFP at a MOI of 1. After a 2 h incubation at 41°C 5% C02, the supernatant was removed and the chBMMs were detached using PBS + 2% PBS. The chBMMs were centrifuged at 400 x g for 5 min, re-suspended in PBS (Gibco) and counted using a TC20 cell counter (Biorad). Between 1x10^7 cells and 2x10^7 cells, re-suspended in PBS +1% goat serum (Sigma Aldrich) were added to a 12x75mm FACS tube (Beckton Dickinson) and blocked on ice for 10 min. The chBMMs were centrifuged again and re-suspended in PBS + 0.5% BSA (Sigma) + 1:800 KUL01-PE (Cambridge Bioscience) for 30 min on ice in the dark. The chBMMs were washed

twice with PBS+0.5% BSA and filtered using a 70 µM cell strainer (SLS). The chBMMs were re-suspended at $1x10^7$ cells/ml in PBS + 0.5% BSA. Controls= single stain GFP, PE, Unstained.

5.3.3. FACS sorting of infected chBMMs

chBMMs were gated on forward/side scatter and doublets excluded. Gates were set on $KUL01^+$ GFP^- vs $KUL01^+$ GFP^+ cells based on KUL01 staining and GFP intensity. Cells were sorted under continuous cooling to 4°C by a BD FACS Aria III and collected in 15 ml Falcon tubes (BD) containing 100 µl PBS + 0.5% BSA. The samples were kept on ice during the duration of the FACS sorting. Finally, samples were centrifuged at 400 x g for 5 min at 4°C and re-suspended in 1 ml Trizol (Life Technologies) before freezing at -80°C until subsequent analysis.

5.3.4. RNA extraction

RNA isolation from chBMMs was performed using a Trizol-based method. chBMMs were lysed after FACS sorting by adding 1 ml of Trizol (Life Technologies). 500 µl of chloroform (Sigma) was added to the suspension and the samples were vortexed for 30 s and incubated at room temperature for 3 min. Following centrifugation at 12 000 x g for 15 min, the upper aqueous layer was collected and precipitated with isopropanol (Fisher) at a ratio of 1:1. The mixture was incubated at room temperature for 10 min and centrifuged at 12 000 x g for 10 min at 4°C. The obtained RNA pellet was washed twice with 75% ethanol (Fisher), and after air-drying, the pellets were re-suspended in 50 µl RNAse-free molecular grade water with heating at 65°C for 5 min. The RNA was DNAse-treated with Turbo-DNA-free-kit (Ambion) as per the manufacturer's instructions. The RNA purity and concentration were checked by analysis on an Agilent 2200 Tapestation (Agilent), and then immediately stored at -80°C.

5.3.5. RNA sequencing

RNA-seq libraries were generated and sequenced by Edinburgh Genomics. All libraries were prepared using the Illumina TruSeq Stranded library protocol for total RNA libraries (Illumina). TruSeq Stranded mRNA libraries were sequenced at a depth of >250 million with 50 bp paired-end reads on the Novaseq 6000 platform. The quality of raw sequencing data was evaluated using the software FastQC.

Adapter sequences were trimmed using the software FastP to a minimum length of 15 bp (Chen *et al.*, 2018b).

5.3.6. RNA-seq analysis

The short reads were aligned to the chicken genome sequence (Gallus_gallus.5.0) using STAR aligner (Dobin *et al.*, 2013). Multi-mapping sequences were discarded. Mapped reads were collapsed using samtools (Li *et al.*, 2009) and counted using the featureCounts command in Rsubread package (Liao, Smyth & Shi, 2014). Raw mapped read counts were normalized using the trimmed mean of M-values normalization method (TMM) and filtered using a counts-per-million (CPM) threshold of 0.3, where at least 3 samples pass the threshold. Differential gene expression analysis was performed in edgeR (Robinson, McCarthy & Smyth, 2010). A generalised linear model with matched pairwise comparisons was used, incorporating the batch effect as a variable. Statistical analysis was performed with a quasi likelihood F test, Benjamini-Hochberg post-comparison test (FDR <0.05). Differentially expressed genes (DE genes) were filtered at an FDR (False discovery rate) of 0.05, $\log_2$ fold change >1. Functional analysis of differentially expressed gene sets (KEGG pathway enrichment) was performed using KOBAS 3.0 (Mao *et al.*, 2005).

5.3.7. qRT-PCR

RNA was reverse transcribed to cDNA using the Revert Aid H Minus First Strand cDNA synthesis kit (Thermo Scientific). 100 ng of isolated RNA was used as a template in a 20 µl reaction with oligo(dT) primers. qRT-PCR was performed using FastStart Universal Sybr Green Rox mastermix (Roche) with a lightcycler 480 (Roche) and cDNA diluted 1 in 10. qRT-PCR primer sequences are described in Table 5.1. All samples were amplified in triplicate with a no template control (NTC) and no RT controls. The thermocycling conditions were 48°C for 30 min for 1 cycle, 10 min at 95°C for 1 cycle, followed by 45 cycles of 20 s at 95°C, 20 s at 60°C and 20 s at 72°C with fluorescence measured at the end of each annealing step. Data were

normalised against the housekeeping gene GAPDH. The fold change in the uninfected vs infected chBMMs was calculated using the $2^{-\Delta\Delta Ct}$ method where:

$\Delta C_T = C_{T\,(gene\ of\ interest)} - C_{T(GAPDH)}$ (Eq. 1)
$\Delta\Delta C_T = \Delta C_{T\,(infected)} - \Delta C_{T\,(Uninfected)}$ (Eq. 2)

Statistical analysis was performed with GraphPad Prism with an unpaired t-test and Welch's correction.

Table 5.1. List of primers used in this study.

Gene target	Forward	Reverse	Reference
AvBD 2	TCTGCAGCCATGAGGATTC	TAAAGCACATGCCTGGAAGAAAT	(Hong *et al.*, 2012)
AvBD 7	GCTGTCTGTCCTCTTTGTGGTG	ATTTGGTAGATGCAGGAAGGAT	(Hong *et al.*, 2012)
CATH1	GCTGTGGACTCCTACAACCAAC	GGAGTCCACGCAGGTGACATC	(Achanta *et al.*, 2012)
CATH3	GCTGTGGACTCCTACAACCAAC	TGGCTTTGTAGAGGTTGATGC	(Achanta *et al.*, 2012)
SQLE	AGAACGATCGCTTAAGGACTATG	CACTCATTCCTCCACCAGTAAG	This study
FDPS	CACCGACATCCAGGACAATAA	CTCATACAGCTCCTTCACCTTC	This study
DHCR7	AGCCAGTTACCAGTGAATTAGAG	AAGCCTCCTTCAGAGCATTAC	This study
GAPDH	GACGTGCAGCAGGAACACTA	TCTCCATGGTGGTGAAGACA	This study

5.4. Results

5.4.1. KUL01 as a chBMM cell surface marker

In order to analyse the chicken macrophage response to *S. aureus*, the first step was to tackle the problem of heterogeneous macrophage infection by *S. aureus*. Previous experiments have demonstrated that not all macrophages contain bacteria after an infection and this is independent of the MOI used (data not shown). This leads to the presence of bystander macrophages, which are exposed to *S. aureus* but not infected. To separate infected and bystander macrophages, we used a FACS sorting approach.

We first needed to identify a chicken macrophage cell surface marker that would enable us to sort a pure population of macrophages. The monoclonal antibody KUL01 was used as it has been shown to specifically recognise the mannose receptor on chicken monocytes and macrophages (Staines *et al.*, 2014). We tested the antibody on chBMMs differentiated to day 6 and day 7, as day 6 differentiated macrophages have been shown to be more efficient at phagocytosis (Weiler & Von Bülow, 2008). The gating strategy for analysis of $KUL01^+$ chBMMs is shown in figure 5.1A. Over 90% of the chBMMs were positive for KUL01. This cell surface marker was used for subsequent optimisation (Figure 5.1B).

5.4.2. Day 6 chBMMs display increased phagocytosis of *S. aureus* compared to Day 7 chBMMs

To assess the phagocytosing ability of day-6-differentiated chBMMs compared to day-7-differentiated chBMMs, the chBMMs were infected with *S. aureus* CIX2-sGFP, at a MOI of 1, 5 or 10 for 2 h. GFP-tagged bacteria were used to easily identify bacteria using flow cytometry. The percentage of phagocytosis was determined by gating on $KUL01^+$ GFP^+ chBMMs (Figure 5.2A). The day-6-differentiated chBMMs showed a 10 to 15% increase in phagocytosis of CIX2-sGFP compared to day-7-differentiated chBMMs. This occurred at every MOI tested (Figure 5.2B). In order to obtain a pure population of $KUL01^+$ GFP^+ macrophages,

we used day-6-differentiated chBMMs with higher phagocytosis abilities were used for downstream experiments.

5.4.3. Optimisation of infection conditions for FACS sorting

In order to determine the best MOI and timepoint for gene expression analysis, chBMMs were infected with CIX2-sGFP and CIX2 ΔAvβ-sGFP for 2 and 4 h, at a MOI of 1 or 10. The timepoints were chosen based on a previous RNA-seq study in murine bone-marrow derived macrophages infected with *S. aureus,* which suggested that most immune related genes were induced between 1 and 3 h (Scumpia *et al.*, 2017). In addition, previous experiments showed that rapid proliferation of *S. aureus* can quickly overtake chBMM cultures so earlier timepoints were preferable (data not shown). Although higher phagocytosis was achieved at later timepoints and at a higher MOI (Figure 5.3A), this was confounded by the higher levels of cell death (Figure 5.3B). To focus on immune pathways and minimize the effect of cell death, an MOI of 1 was used at a time point of 2 h. Furthermore, this MOI and time point showed a clear increase in phagocytosis in CIX2-sGFP compared to CIX2 ΔAvβ-sGFP (Figure 5.3A), confirming previous results on day-7-differentiated chBMMs and thus allowing investigation of the impact of prophage Avβ or an intact β-toxin on chBMM gene expression.

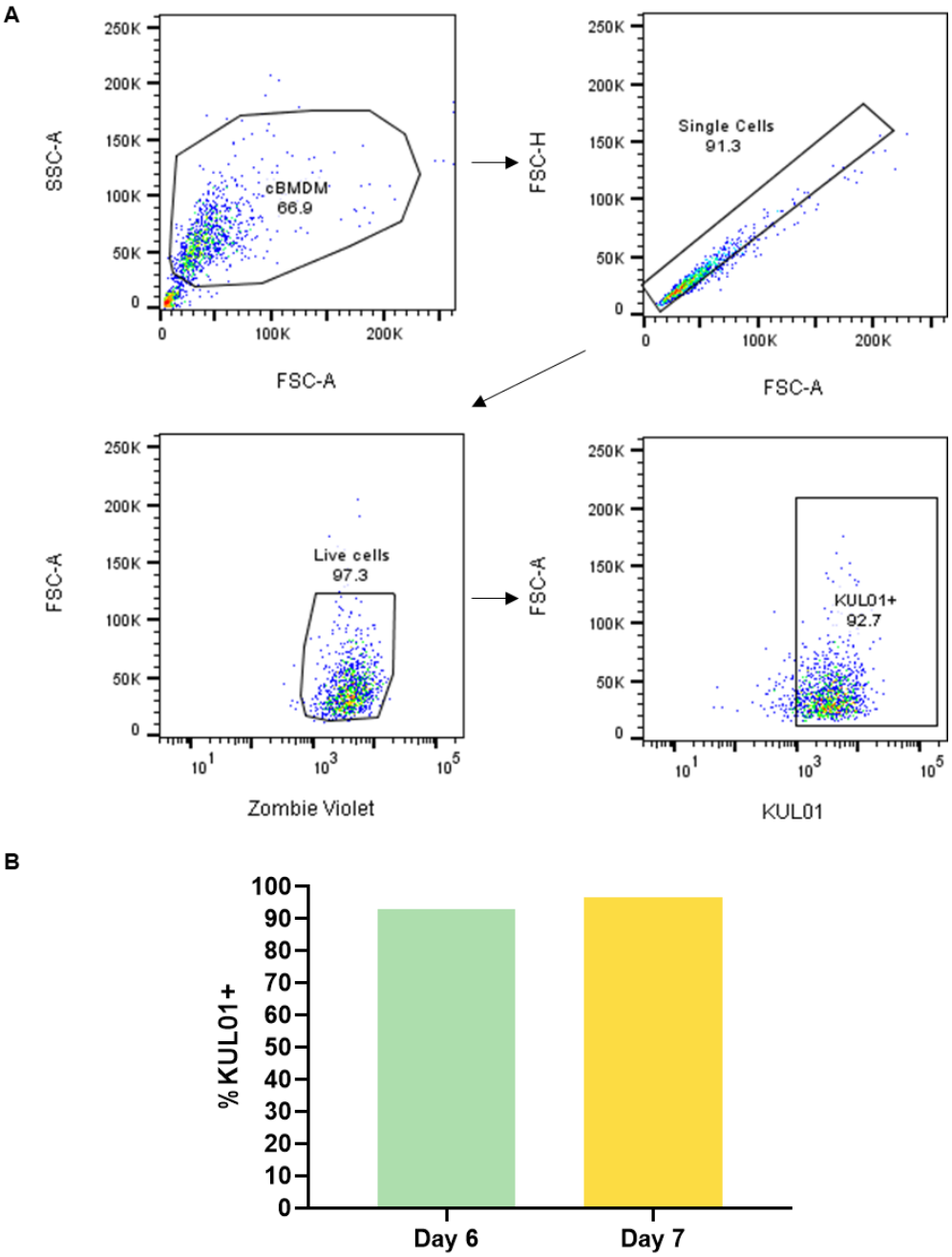

Figure 5.1. chBMMs are KUL01^{+}.

A) Gating strategy used to define KUL01^{+} chBMMs. chBMMs were first gated using FSC and SSC and then gated on single cells using FSC-H. Live cells were identified by staining with live/dead Zombie Violet stain. A PE-KUL01 antibody was used to identify KUL01^{+} cells. **B)** Percentage of KUL01^{+} chBMMs on day-6-differentiated compared to day-7-differentiated chBMMs. Results are representative of one biological replicate.

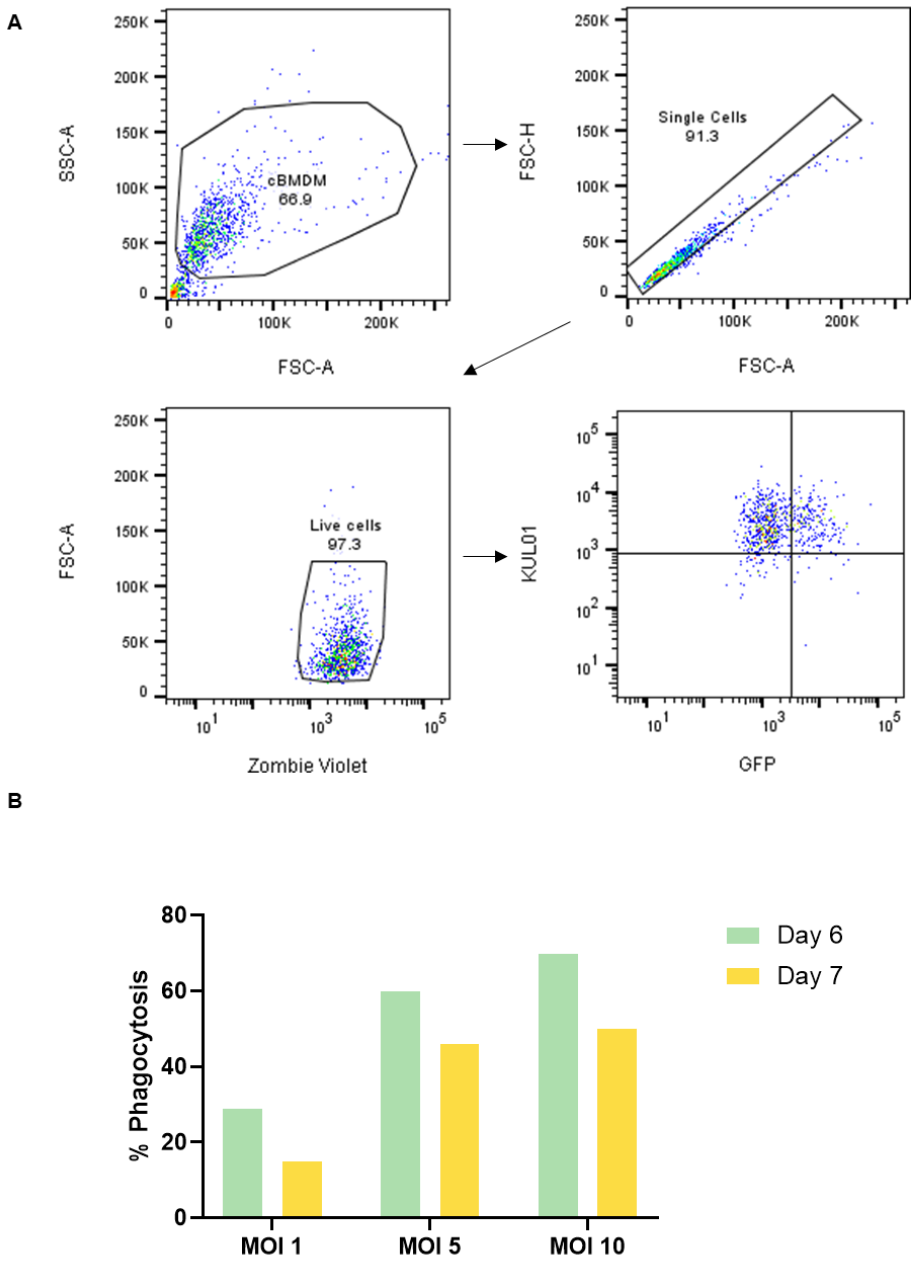

Figure 5.2. Day-6-differentiated chBMMs exhibit increased phagocytosis of CIX2-sGFP compared to day-7-differentation chBMMs.

A) Gating strategy used to define KUL01^{+} GFP^{+} chBMMs. chBMMs were first gated using FSC and SSC and then gated on single cells using FSC-H. Live cells were identified by staining with live/dead Zombie Violet stain. A PE-KUL01 antibody was used to identify KUL01^{+} cells and GFP-tagged CIX2 to identify *S. aureus*. **B)** Percentage of KUL01^{+} GFP^{+} chBMMs at MOI 1, 5 or 10 at 2 h. Results are representative of one experiment performed in triplicate.

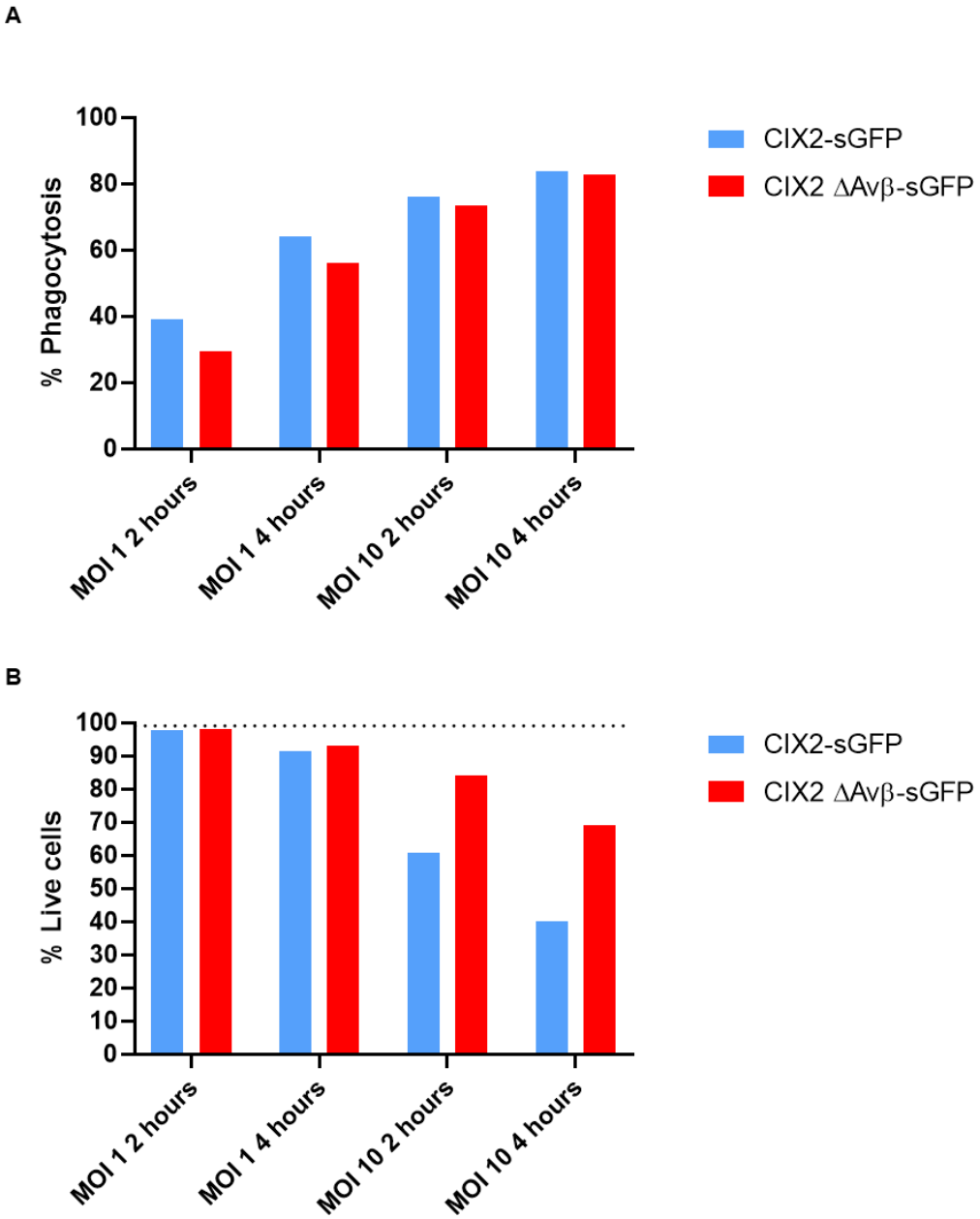

Figure 5.3. Optimisation of chBMM infection with *S. aureus* for FACS sorting.

A) Percentage phagocytosis by chBMMs of *S. aureus* CIX2 and CIX2 ΔAvβ-sGFP at different timepoints and MOIs determined by gating on KUL01^{+} GFP^{+} chBMMs. **B)** Percentage live cells of chBMMs infected with *S. aureus* CIX2 and CIX2 ΔAvβ-sGFP determined by Zombie Violet live/dead stain. Dotted line represents percentage of live cells for an uninfected control. Data is representative of the three broilers tested.

5.4.4. FACS sorting of infected chBMMs

Bone-marrow cells from three different 3-week-old broilers (broiler IDs: #379, #401. #391) were differentiated to day 6, infected to a MOI of 1 for 2 h and FACS sorted. Uninfected controls were also FACS sorted to ensure appropriate comparison. A typical FACS plot in shown in Figure 5.4 (pre-sort panel). To evaluate the purity of the sorted fractions, the samples were re-analysed using the same settings (Figure 5.4, post-sort panel). The purity check revealed that the $KUL01^{+}$ GFP^{+} fraction also contained a small fraction (~10-15%) of $KUL01^{+}$ GFP^{-} chBMMs. This could be due to the mechanical force applied to the chBMMs during sorting which can lead to cell death and loss of intracellular bacteria. However, this fraction was negligible compared to the $KUL01^{+}$ GFP^{+} fraction. For all three birds, a trend towards increased phagocytosis of CIX2-sGFP compared to CIX2 ΔAvβ-sGFP was observed (Figure 5.5), consistent with data from previous experiments (Chapter 3).

5.4.5. RNA-seq data quality control

In order to analyse the chicken macrophage response to *S. aureus*, RNA from sorted chBMM fractions was extracted and sent for RNA-seq. Before performing differential gene expression analysis, RNA-seq data quality control was performed. Quality-filtered sequencing reads were mapped against the chicken reference genome (Gallus.Gallus.v5) and multi-mapping reads were removed. This step confirmed that the majority of reads could be mapped to the reference (Figure 5.6).

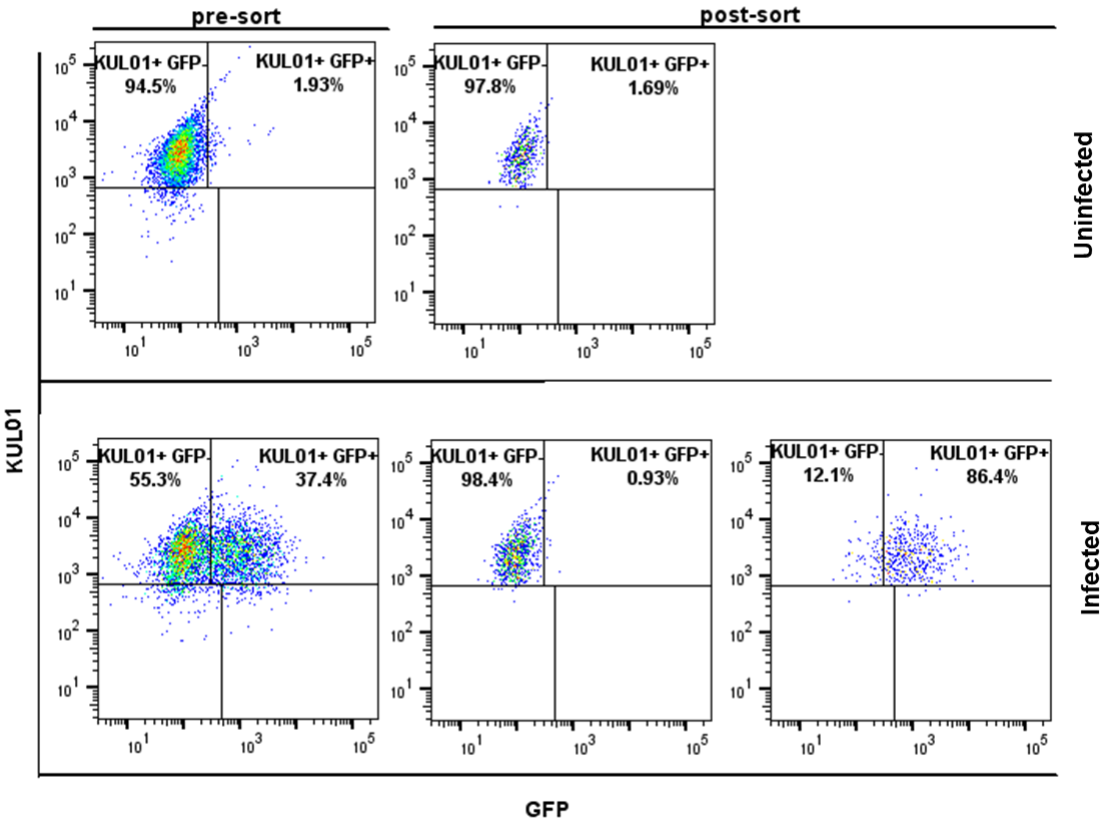

Figure 5.4. FACS sorting of chBMMs infected with GFP-tagged S. aureus results in a high enrichment of KUL01$^+$ GFP$^+$ chBMMs.

Representative FACS plot of *S. aureus* infected chBMMs at 2 h, MOI of 1 (pre-sort). Purity of sorted fractions was assessed (post-sort). Data is representative one biological replicate.

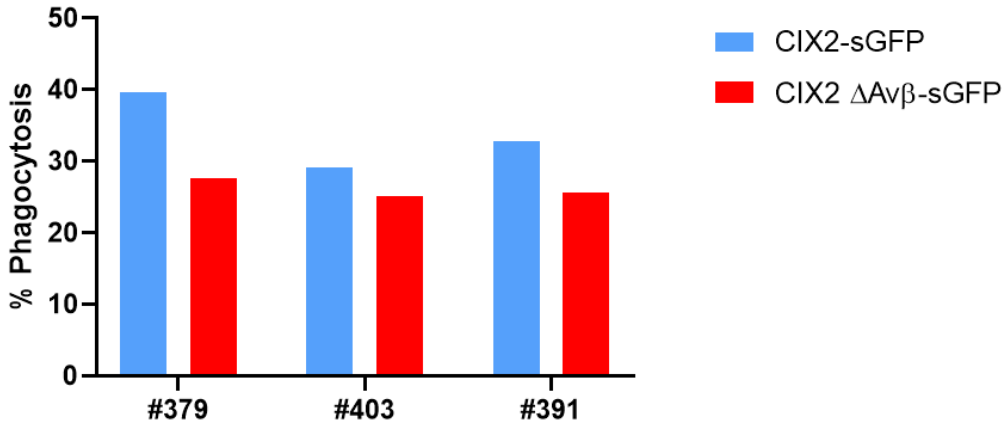

Figure 5.5. Infection of chBMMs with S. aureus CIX2-sGFP results in higher levels of phagocytosis compared to infection with CIX2 ΔAvβ-sGFP.

Percentage phagocytosis of chBMMs infected with *S. aureus* CIX2-sGFP or CIX2 ΔAvβ-sGFP for 2 h at a MOI of 1. Percentage phagocytosis was determined by gating on $KUL01^+$ GFP^+ chBMMs. The experiments were performed in three biological replicates, represented on the x-axis by the broiler ID (#379, #403, #391).

Table 5.2. Mapping statistics of RNA reads to Gallus Gallus v5 reference genome.

Sample	Percentage Mapped
Uninfected (#379)	89.73%
CIX2 (#379)	90.15%
CIX2 ΔAvβ (#379)	89.5%
Uninfected (#403)	88.67%
CIX2 (#403)	88.38%
CIX2 ΔAvβ (#403)	86.37%
Uninfected (#391)	90.57%
CIX2 (#391)	89.07%
CIX2 ΔAvβ (#391)	77.25%

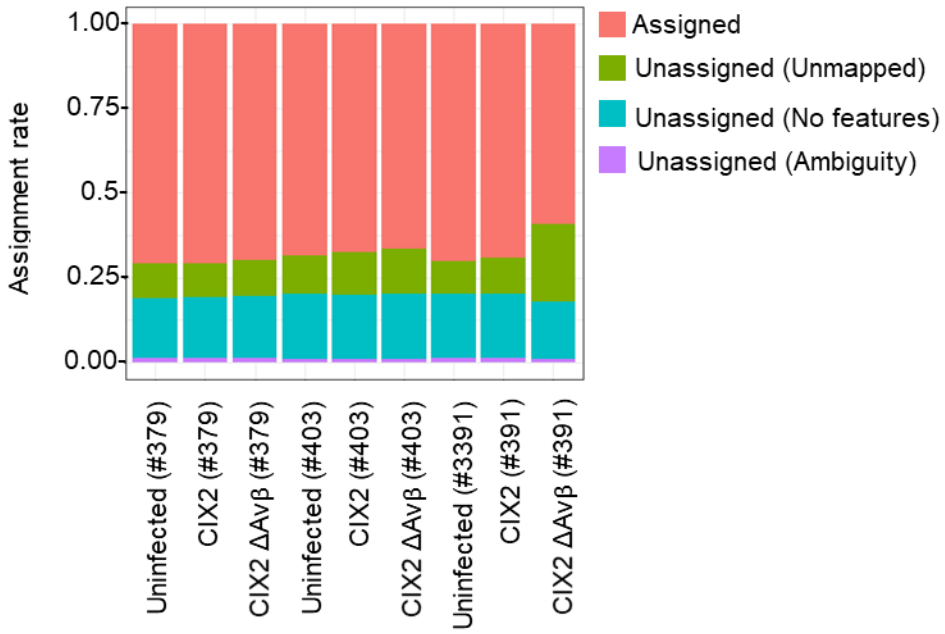

Figure 5.6. RNA-seq reads showed a high gene assignment rate.

RNA-seq reads post-mapping were assigned to a gene using featureCounts in Rsubread package. Assignment rate is shown here, with assigned reads representing the reads assigned to a gene feature in the annotation file, 'Ambiguity' representing reads that could be assigned to more than one gene, 'No features' representing reads assigned to an unannotated region and 'Unmapped' representing genes that are unable to map to the reference.

Counts per gene were generated using featureCounts in the RSubread package. Most reads could be assigned to a gene (Table 5.2). Those that were mapped but unassigned likely reflect the current state of genome annotation. The proportion is similar to recent global analysis of the chicken transcriptome (Bush *et al.*, 2018). Some reads were unmapped, which is likely due to their small size after trimming (Figure 5.6). The sample infected with CIX2 ΔAvβ-sGFP from bird #391 showed a lower proportion of assigned reads, which is due to the lower relative sequencing quality of this sample. Overall, the RNA-seq data was of good quality and suitable for downstream analysis

5.4.6. Multi-dimensional scaling of gene expression revealed sample separation by infection status and bird

To gain an overview of differential gene expression between uninfected and infected chBMMs, exploratory analysis of the data was performed using a multi-dimensional scaling analysis. Clustering analysis revealed that samples segregated according to infection status (uninfected versus infected), with a clear within group reproducibility. In contrast, there were no global differences in gene expression between samples infected with the wild type *S. aureus* strain CIX2-sGFP compared to the prophage deletion mutant CIX2 ΔAvβ-sGFP. The analysis also revealed clear clustering according to each individual broiler (i.e. biological repeat) (Figure 5.7). This effect was therefore taken into account in subsequent differential gene expression analysis. This is not necessarily a batch effect, since recent studies of the response of chicken BMDM to the TLR4 agonist lipopolysaccharide (LPS) also reveal significant variation between birds (DAH, Ms under review).

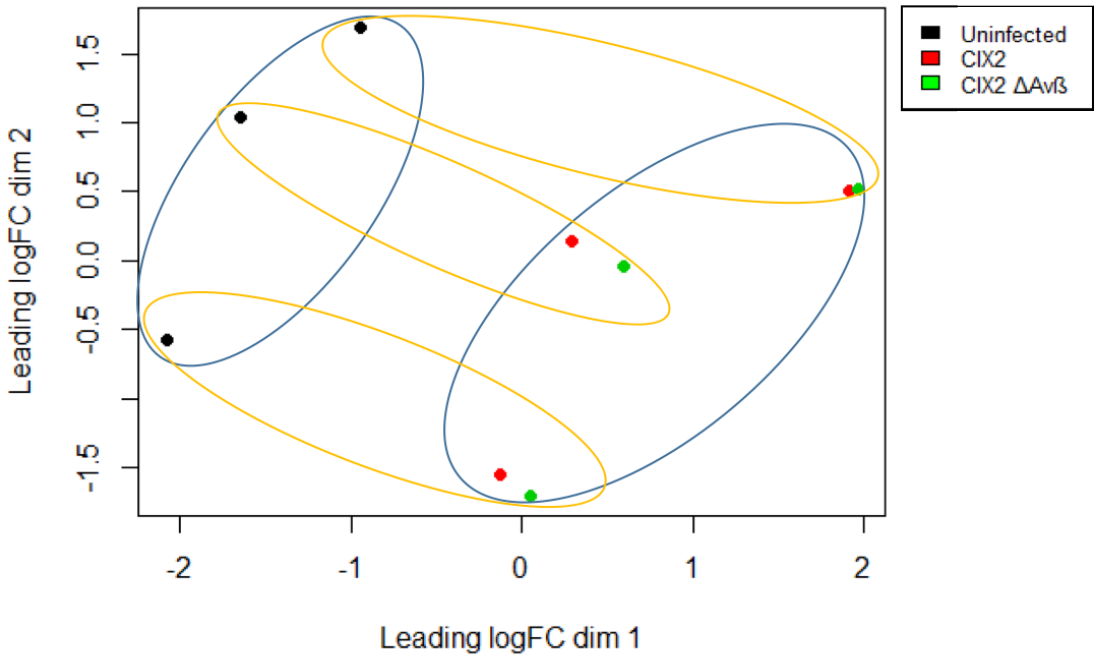

Figure 5.7. Multi-dimensional scaling plot revealing clustering according to infection status and batch.

Multi-dimensional scaling plot was performed using EdgeR. Distances between samples on the plot represent 'leading fold change', defined as the root-mean-square average of the log-fold-changes for the genes best distinguishing each pair of samples. Colours of dots represent infection status (uninfected, infected with CIX2-sGFP and infected with CIX2 ΔAvβ-sGFP). Samples cluster by infection status (blue ellipse) or by biological repeat (yellow ellipse).

5.4.7. Differential gene expression analysis identifies up-regulation of immune-related genes in response to *S. aureus* CIX2-sGFP

In order to investigate transcriptional changes between uninfected and CIX2-sGFP infected samples, differential gene expression analysis was performed using EdgeR. The bird-specific variation was incorporated as a variable and a generalised linear model with matched pairwise comparisons was used. The analysis identified 799 differentially expressed genes (DEGs), of which 583 were up-regulated and 216 were down-regulated, with good within group/bird reproducibility (Figure 5.8).

The top 20 up-regulated genes included well-known pro-inflammatory cytokines (IL1B, CCL4, IL8L1), genes involved in pro-inflammatory cytokine regulation (RNF19B and NFKB1) and a gene involved in type I interferon response (PLSCR1). Anti-inflammatory genes such as SOCS3, IL13RA1 and PPARD were also highly up-regulated. In addition, the apoptosis-associated gene CASP8 and the necroptosis associated gene MLKL were also up-regulated. In contrast, two apoptosis-promoting genes (BMF and PTPN13) were among the top down-regulated genes, revealing that that both anti-apoptotic and pro-apoptotic genes are induced by *S. aureus* infection of chBMMs. Interestingly SNX10, a marker of late phagosome maturation (Lou *et al.*, 2017), was also among the highest up-regulated genes, suggesting that *S. aureus* CIX2-sGFP may reside among maturing phagosomes at this time point (Figure 5.9).

In comparison, no pattern was identified for the top down-regulated genes (Figure 5.9). Many of the down-regulated genes, such as ABAT, PTDSS2 and GLDC, are associated with metabolism, which is a common feature of macrophage bacterial infection (Liu *et al.*, 2010). Genes encoding solute carrier transporter proteins (SLC38A2, SLC45A3, SLC49A3) were also among the top down-regulated genes. Similarly to other studies (Scumpia *et al.*, 2017; Thänert *et al.*, 2017), infection of chBMMs with *S. aureus* leads to a shift in hypoxia-related genes, as seen by the down-regulation of CITED2, a negative regulator of HIF-A induced genes (Chen *et al.*, 2012).

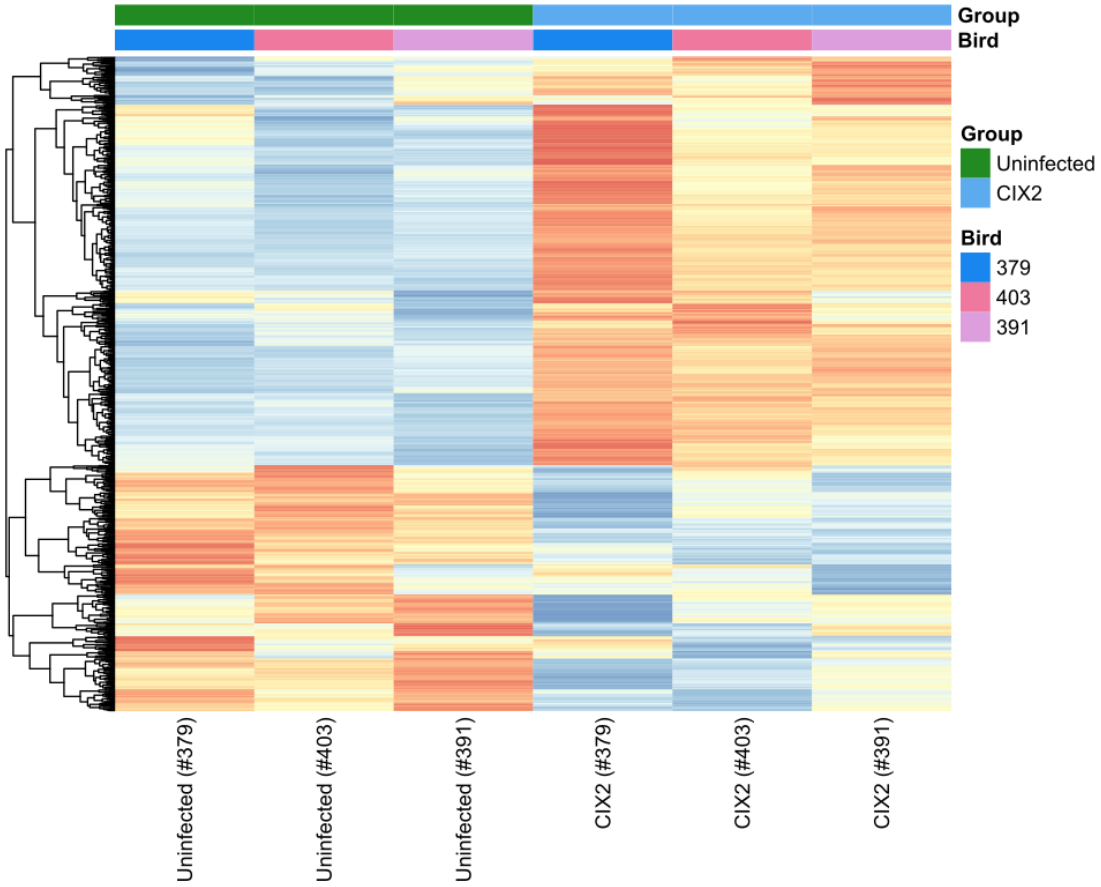

Figure 5.8. Gene expression analysis of *S. aureus* CIX2-sGFP infected chBMMs compared to uninfected chBMMs.

Heat map of the $\log_2$ fold change >1, FDR <0.05 DEGs determined between CIX2-sGFP infected and uninfected chBMMs. Down-regulated DEGs are represented in blue and up-regulated DEGs in red.

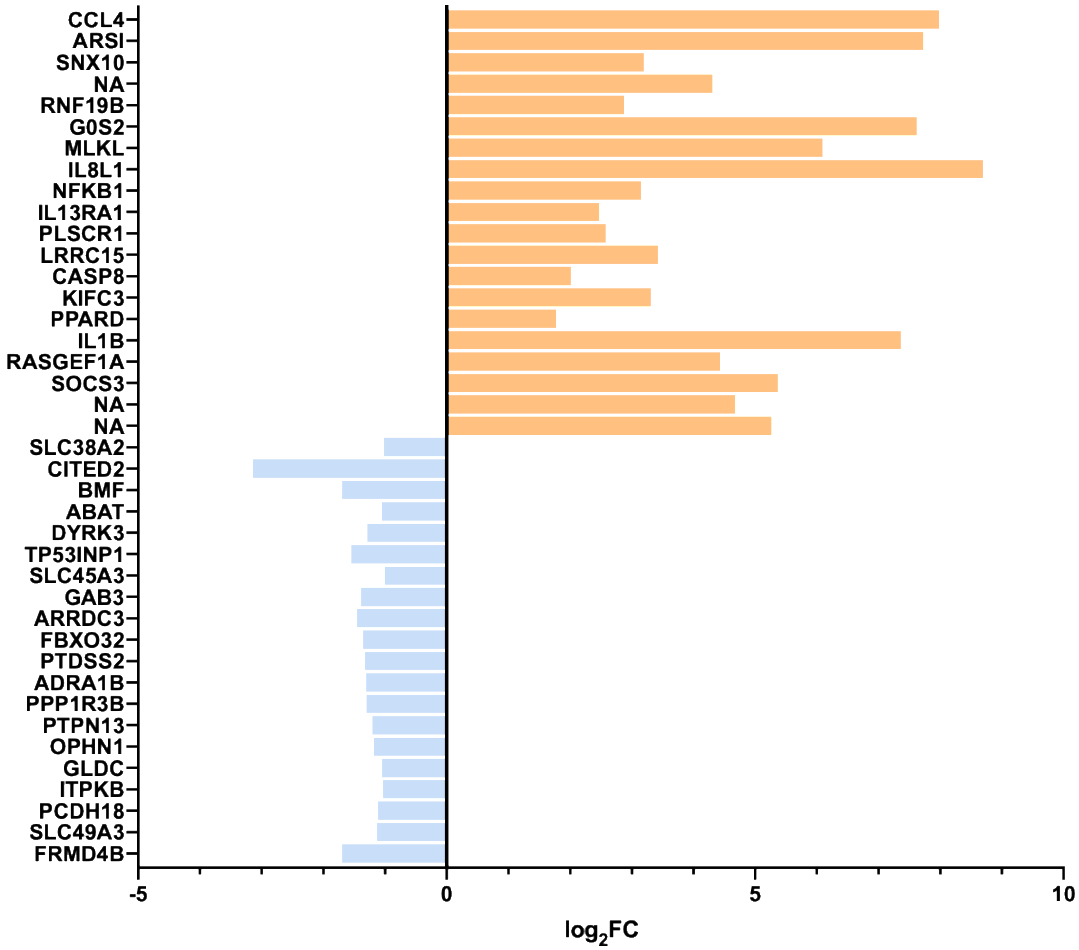

Figure 5.9. Top 20 up and down-regulated DEGs when comparing *S. aureus* CIX2-sGFP chBMMs to uninfected chBMMs.

Threshold used was $\log_2$ fold change >1, FDR <0.05. Up-regulated DEGs are shown in orange and down-regulated DEGs in blue. All data reflect biological replicates.

We next examined whether the chBMMs responded to *S. aureus* in a manner similar to BMMs from other host species (Lewandowska-Sabat *et al.*, 2013; Scumpia *et al.*, 2017; Thänert *et al.*, 2017; Sun *et al.*, 2018). *S. aureus* CIX2-sGFP induced an up-regulation of inflammatory mediators, including the pro-coagulants SERPINE2 and F3, the bradykinin BDKRB1 and prostaglandin receptor PTGER4 (Figure 5.10). In addition, CIX2-sGFP induces common antimicrobial mechanisms in the chBMMs including phagosome-associated lysozyme (LYZ) and phospholipase A2 (PLA2G6), both previously reported to contribute to *S. aureus* intracellular and extracellular killing, respectively (Miyauchi *et al.*, 1985; Wu *et al.*, 2010) (Figure 5.11). Moreover, nutritional immunity also plays an important role in controlling *S. aureus* infections (Cassat & Skaar, 2012), consistent with the observed up-regulation of genes including the siderocalin ExFABP, ferrireductase STEAP3/4 and the zinc transporter SLC39A8 (Figure 5.11). In addition, TRPM2, previously shown to regulate phagosomal acidification of macrophages to kill *S. aureus* (Di *et al.*, 2017), was also up-regulated. Of note, the nitric oxide gene NOS2 was only induced by one of the three birds (data not shown). Previously, nitric oxide was reported to be induced in chicken macrophages in response to LPS (Wu *et al.*, 2016) but this is a relatively late response, dependent upon upstream induction of the Myd88-independent endogenous interferon pathway.

Taken together, these data suggest conservation across host species of the early response of macrophages to *S. aureus*, with the induction of pro and anti-inflammatory cytokine genes, cell death, inflammatory mediators and antimicrobial mechanisms.

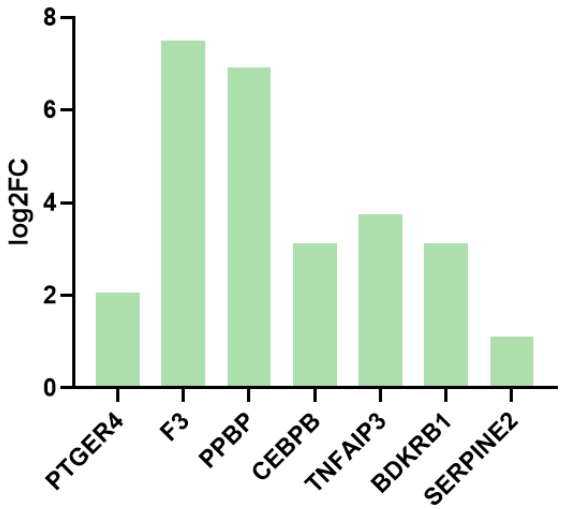

Figure 5.10. Inflammation mediators are up-regulated in chBMMs after infection with *S. aureus*.

Up-regulated DEGs related to inflammation in CIX2-sGFP infected chBMMs compared to uninfected chBMMs are shown.

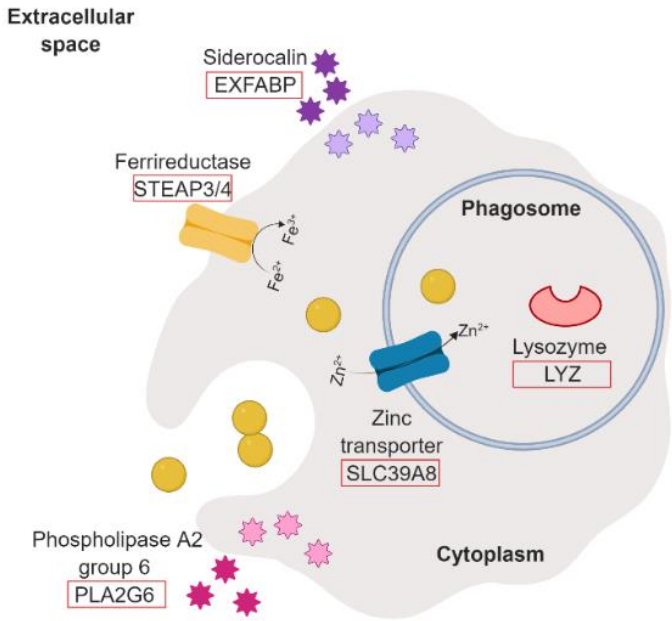

Figure 5.11. Schematic representation of genes up-regulated during S. aureus infection that are associated with antimicrobial mechanisms (red boxes).

Figure created with BioRender.com.

5.4.8. KEGG pathway enrichment analysis

Functional classification of the DEGs using KEGG (Kyoto Encyclopedia of Genes and Genomes) pathway enrichment revealed that 'cytokine-cytokine receptor interaction' was the main pathway to be up-regulated in CIX2-sGFP infected chBMMs compared to uninfected chBMMs (Figure 5.12). Most genes in this pathway are pro-inflammatory cytokines such as IL-1B, IL-6, IL-8 and TNFSF15 (Figure 5.13A) and leukocyte chemoattractants including CCL4 and CCL20 (Figure 5.13B). However, there is also an important up-regulation of anti-inflammatory cytokines and their receptors such as IL-10 and IL13RA2. (Figure 5.13A).

Other KEGG pathways significantly enriched include those involved in innate immune recognition such as 'toll-like receptor signalling pathway', 'NOD-like receptor signalling pathway' and 'RIG-I like signalling pathway' (Figure 5.12). *S. aureus* has been shown to activate a wide range of toll-like receptors, both extracellular and endosomal, which is reflected in these enriched pathways (Askarian *et al.*, 2018). The main TLRs up-regulated in CIX2-sGFP infected chBMMs are TLR1 type 1 and 2 and TLR15. These cell surface receptors activate pro-inflammatory cytokines (IL6, IL1B, IL12B, IL8, IL8L1 and TNFSF15) via activation of NF-KB (NFKB1, NFKB2) (Figure 5.14). TLR3 and TLR7 signalling pathways were also up-regulated. Both NOD-like receptor signalling and RIG-I like signalling pathways involve intracellular recognition of *S. aureus* and lead to the activation of interferon regulatory factor IRF7, which enables transcription of Type I interferons (Figure 5.14).

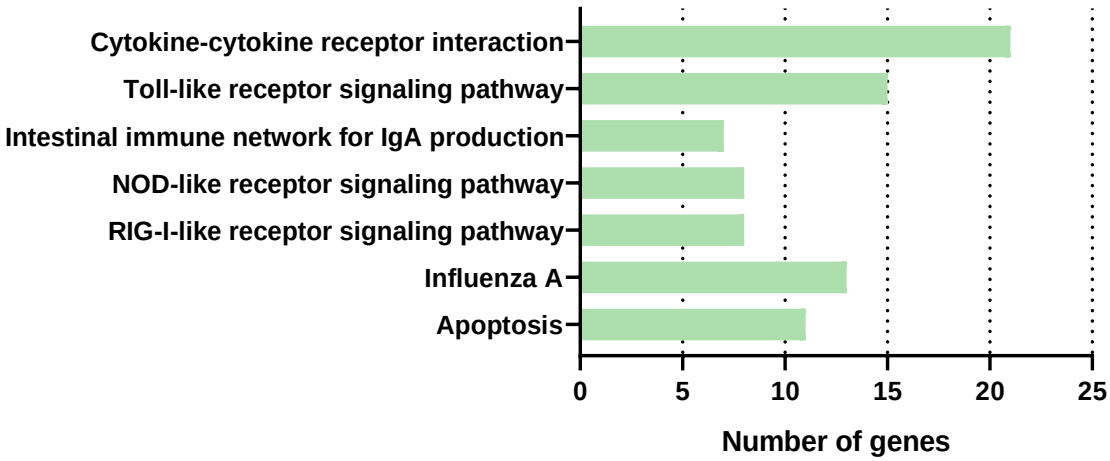

Figure 5.12. KEGG pathways enriched in S. aureus CIX2-sGFP infected chBMMs.

Significantly enriched KEGG pathways of DEGs (log_2 fold change of >1, FDR <0.05). Pathways are displayed by FDR value (from top to bottom).

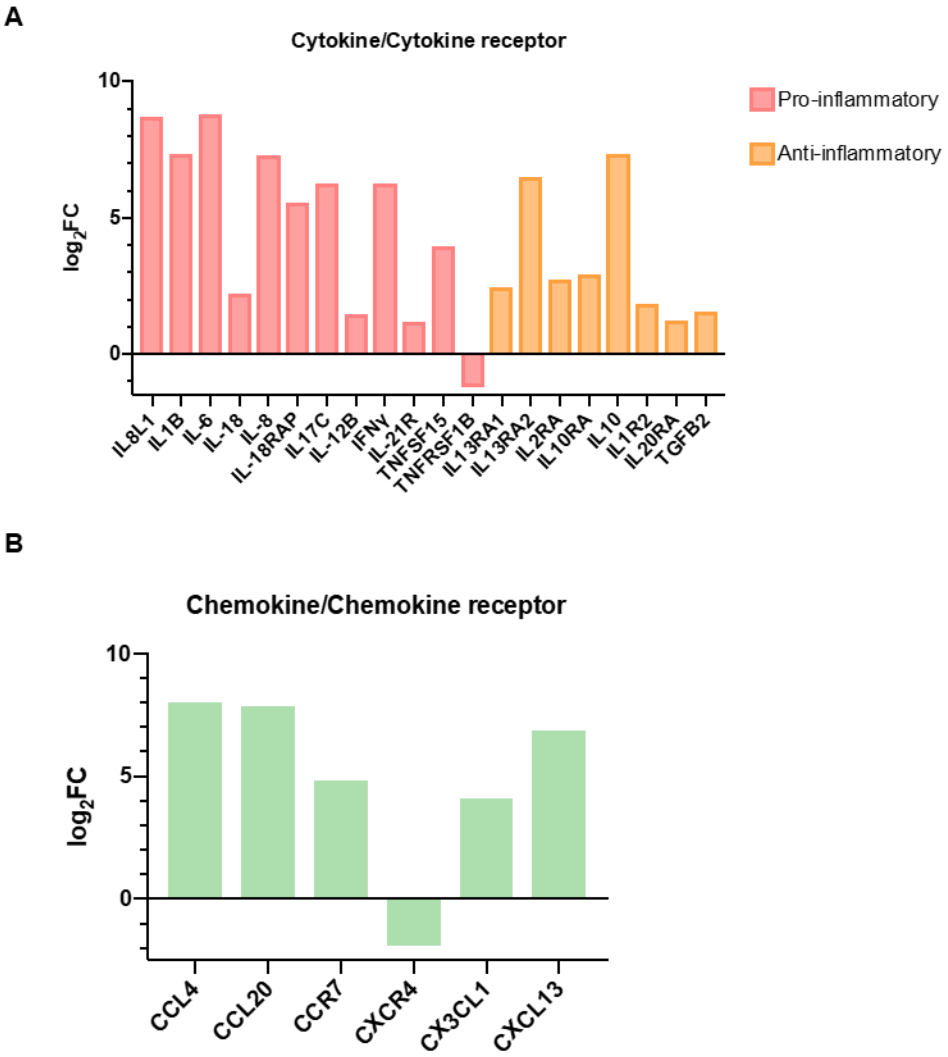

Figure 5.13. Genes belonging to top KEGG enriched pathway 'cytokine-cytokine receptor interaction'.

A) Genes belonging to 'Cytokine/Cytokine receptor' pathway, coloured by 'pro-inflammatory' and 'anti-inflammatory' status **B)** Genes belonging to 'Chemokine/Chemokine receptor' pathway

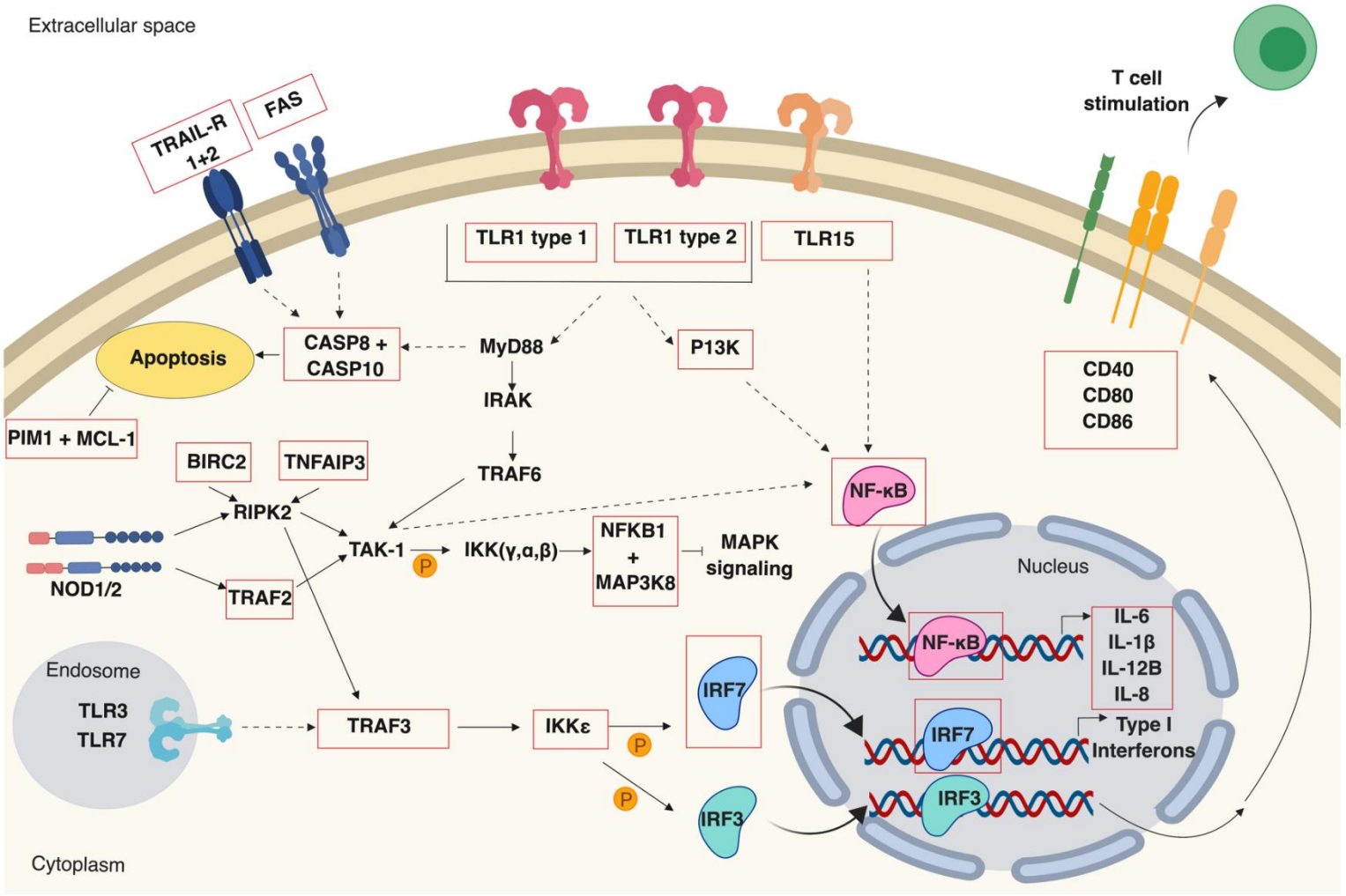
Extracellular space
TRAIL-R 1+2
FAS
TLR1 type 1
TLR1 type 2
TLR15
T cell stimulation
Apoptosis
CASP8 + CASP10
MyD88
P13K
IRAK
CD40
CD80
CD86
PIM1 + MCL-1
BIRC2
TNFAIP3
TRAF6
NF-κB
RIPK2
TAK-1
P
IKK(γ,α,β)
NFKB1 + MAP3K8
MAPK signaling
NOD1/2
TRAF2
Nucleus
NF-κB
IL-6
IL-1β
IL-12B
IL-8
Endosome
TLR3
TLR7
TRAF3
IKKε
IRF7
Type I Interferons
IRF3
Cytoplasm

Figure 5.14. Schematic representation of pathway enrichment analysis.

Up-regulated DEGs in enriched pathways are represented by red boxes. *S. aureus* up-regulation of TLRs (TLR1 type 1 and 2, TLR15), which activates NFκB, leading to up-regulation of pro-inflammatory cytokines IL-1β, IL-6 and IL-8. *S. aureus* is also recognised by an unknown intracellular receptor, which up-regulates NFκB and IRF7 signalling pathways. Both pro (TRAILR, FAS, CASP8/10) and anti-apoptotic genes (PIM-1, MCL-1) are up-regulated in the apoptotic pathway. Finally, immune signalling also leads to up-regulation of cell surface receptors CD40, CD80 and CD86, which are involved in T cell stimulation. Figure created with BioRender.com.

Finally, the ‘apoptosis’ pathway was also enriched including cell death receptors TRAIL and FAS as well as caspase genes (CASP8 and CASP10) suggesting that recognition of *S. aureus* by chBMMs leads to the extrinsic apoptosis pathway (Figure 5.12,14). However, pro-survival genes PIM1 and MCL-1, which inhibit mitochondrial cell death, were also up-regulated. It is therefore unclear from these data whether *S. aureus* induces a pro or anti-apoptotic signalling pathway in chBMMs.

These data suggest that *S. aureus* is recognised by chBMMs through multiple different pathogen associated molecular patterns, both extracellular and endosomal. Furthermore, *S. aureus* drives NF-KB and IRF7 activation, leading to an array of cytokine and chemokine production similar to other host species.

5.4.9. The deletion of the prophage Avβ results in an increase in inducible gene expression in chBMMs

In order to investigate if the prophage Avβ affects the transcriptional response of chBMMs to *S. aureus*, either due to its encoded genes or excision leading to β-toxin expression, we compared the response of chBMMs to *S. aureus* CIX2 and its Avβ-deficient derivative. Differential gene expression analysis revealed that 923 genes were differential expressed, 667 up-regulated and 256 down-regulated. 715 DEGs were shared between CIX2-sGFP infected chBMMs and CIX2 ΔAvβ-sGFP infected chBMMs, providing an effective indication of the robustness of the data (Figure 5.15). 84 DEGs detected only in CIX2-sGFP infected chBMMs and 208 only in CIX2 ΔAvβ-sGFP infected chBMMs (Figure 5.15). Together these data infer that either prophage Avβ or an intact β-toxin contribute to suppression of inducible gene expression of chBMMs in response to *S. aureus*.

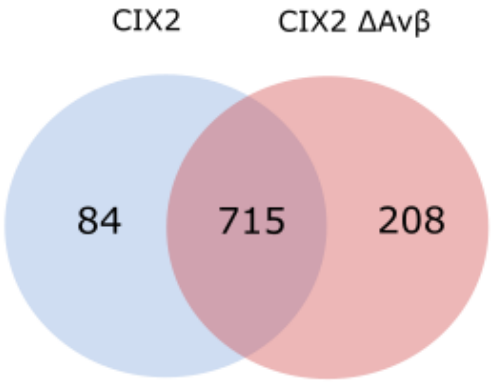

Figure 5.15. Infection of chBMMs with wild type CIX2-sGFP results in overall reduced gene induction compared to prophage deletion mutant CIX2 ΔAvβ-sGFP.

Venn diagram showing degree of overlap between genes which meet expression threshold criteria (log_2 fold change >1, FDR <0.05) in chBMMs in response to CIX2-sGFP and CIX2 ΔAvβ-sGFP.

5.4.10. There are no prophage Avβ or β-toxin dependent significantly enriched pathways in chBMMs

To further investigate the impact of prophage Avβ or an intact β-toxin on chBMM gene expression, differential gene expression analysis was performed comparing CIX2-sGFP infected chBMMs to CIX2 ΔAvβ–sGFP infected chBMMs. Based upon the observed effect of prophage Avβ or an intact β-toxin on *S. aureus* survival and chBMM killing (Chapters 3 and 4), a functional analysis on the DEGs present in CIX2-sGFP vs CIX2 ΔAvβ–sGFP infected chBMMs was carried out with a p-value cut-off of <0.05. KEGG pathway enrichment analysis identified two enriched pathways related to metabolism: 'steroid biosynthesis pathway' and 'terpenoid backbone pathway'. Genes enriched in these pathways are depicted in Figure 5.16A. The expression of the genes present in these pathways appeared lower in CIX2-sGFP infected chBMMs compared to CIX2 ΔAvβ–sGFP infected chBMMs. The terpenoid backbone pathway, specifically the mevalonate pathway, acts upstream of the steroid biosynthesis pathway. However, the mevalonate pathway is also important for protein prenylation, a post-translational modification essential for proteins of the autophagy pathway (Miettinen & Björklund, 2015). Studies on statins, including HMG-CoA reductase inhibitors, have shown that the downregulation of protein prenylation affects the autophagic pathway and activates caspase-1 inflammasome dependent cell death (Chan, Oza & Siu, 2003; Chen, Huang & Lin, 2006).

The deletion of prophage Avβ leads to reduced chBMM cell death (Chapter 3). In addition, the CAAX domain protease often carried by prophages is hypothesised to be involved in eukaryotic protein prenylation due to similar functions in other CAAX domain proteases (Pei & Grishin, 2001). Thus, prophage Avβ could up-regulate the terpenoid and steroid biosynthesis pathways in chBMMs in order to block autophagy. This would lead to an increase in cell death, accelerating intracellular escape (Figure 5.16A).

To determine whether the genes in these pathways were up-regulated, qRT-PCR was performed on the RNA extracted from FACS sorted infections previously sent for RNA-seq. The three genes chosen for validation were farnesyl diphosphate (FDPS), an intermediate between the mevalonate and steroid pathway, squalene epoxidase (SQLE) involved in the first step of steroid biosynthesis and 7-Dehydrocholesterol reductase (DHCR7) that catalyses the production of cholesterol. There was no significant difference in gene expression between CIX2-sGFP infected and CIX2 ΔAvβ–sGFP infected chBMMs (Figure 5.16B). Together these data indicate that there are no significantly enriched pathways between these two conditions, confirming RNA-seq differential gene expression analysis.

A

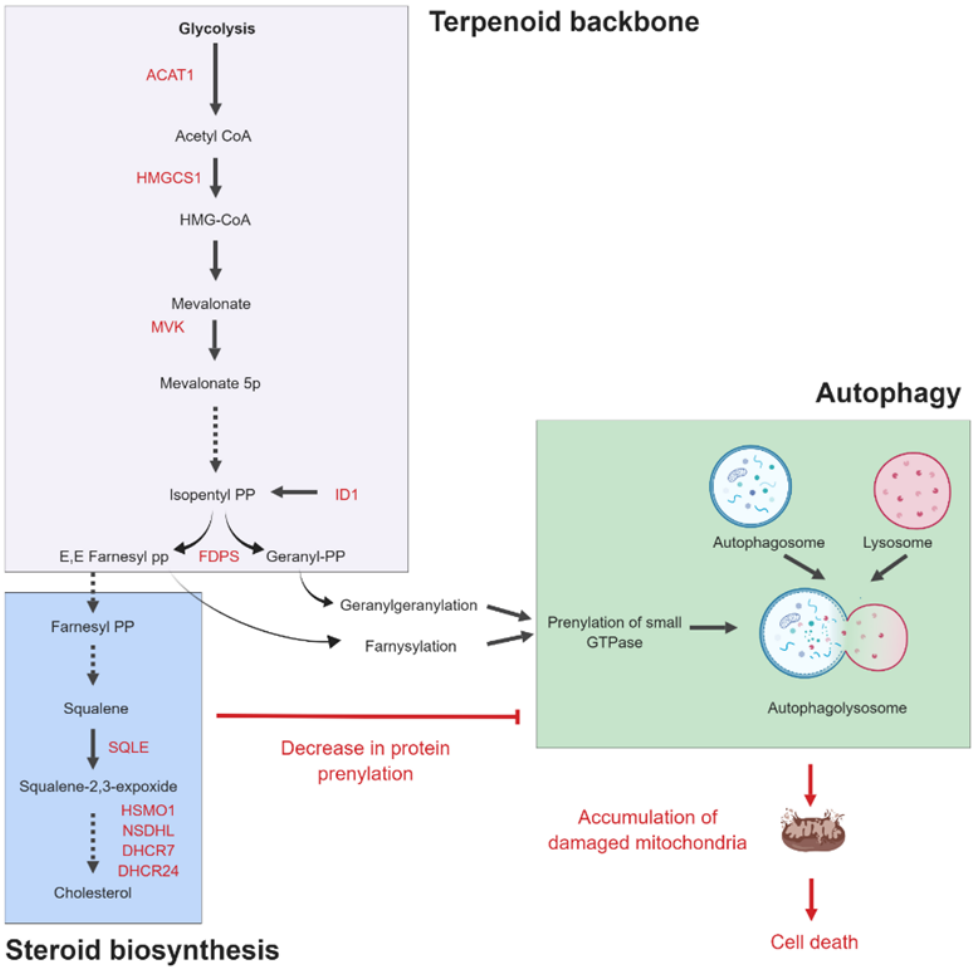
Terpenoid backbone
Glycolysis
ACAT1
Acetyl CoA
HMGCS1
HMG-CoA
Mevalonate
MVK
Mevalonate 5p
Isopentyl PP
ID1
E,E Farnesyl pp
FDPS
Geranyl-PP
Farnesyl PP
Squalene
SQLE
Squalene-2,3-expoxide
HSMO1
NSDHL
DHCR7
DHCR24
Cholesterol
Steroid biosynthesis
Geranylgeranylation
Farnysylation
Autophagy
Autophagosome
Lysosome
Prenylation of small GTPase
Autophagolysosome
Decrease in protein prenylation
Accumulation of damaged mitochondria
Cell death

B

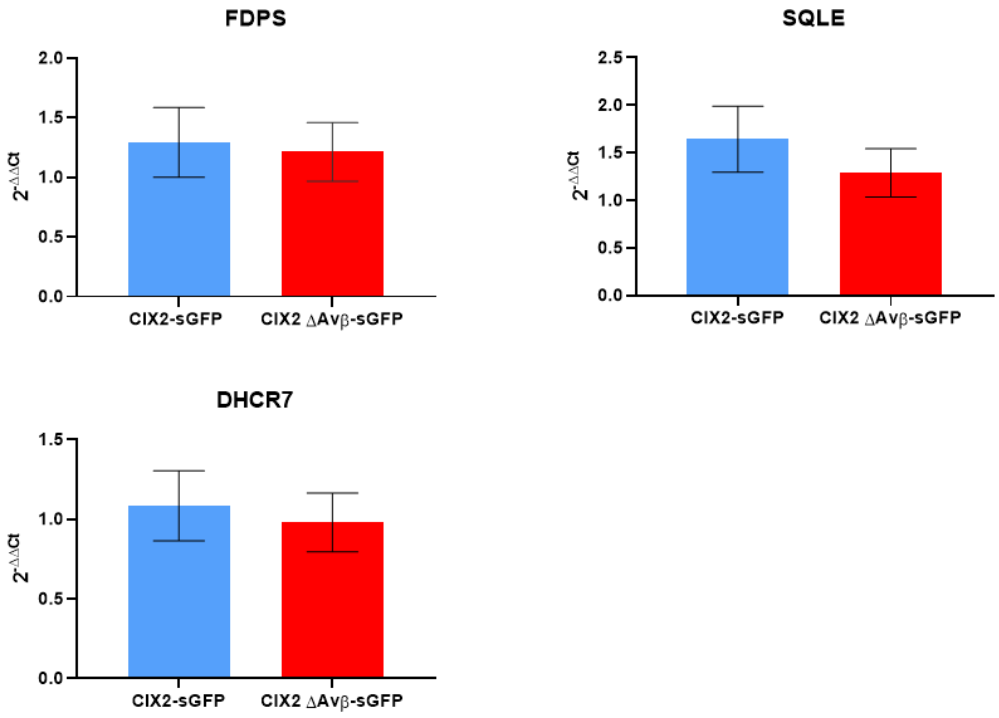
FDPS
SQLE
DHCR7
2^-ΔΔCt
CIX2-sGFP
CIX2 ΔAvβ-sGFP

Figure 5.16. No significantly enriched pathways between wild type CIX2-sGFP and prophage deletion mutant CIX2 ΔAvβ-sGFP in chBMMs.

A) Schematic representation of the putative role of genes enriched in the 'terpenoid backbone' and 'steroid biosynthesis' pathways. Genes up-regulated in CIX2-sGFP infected chBMMs compared to CIX2 ΔAvβ-sGFP are present in red. **B)** qRT-PCR of up-regulated genes (SQLE, FDPS, DHCR7) present in KEGG enriched pathways. Data was normalised to GAPDH and fold change compared to uninfected chBMMs was calculated using $2^{-\Delta\Delta}$Ct method. Data is presented as mean of three biological replicates ± the standard deviation of the mean.

5.4.11. Deletion of prophage Avβ is associated with up-regulation of antimicrobial peptides in chBMMs

Consistent with the lack of a global difference in response, only 54 genes appeared to be differentially expressed in response to the two bacterial strains; with 40 down-regulated in the CIX2-sGFP infected chBMMs compared to CIX2 ΔAvβ-sGFP infected chBMMs (Table 5.3). Notably, among the down-regulated genes, four antimicrobial peptides are down-regulated (CATHL1, CATHL3, AvBD2, AvBD7) (Table 5.3). The presence of prophage Avβ, or the excision of prophage Avβ leading to an intact β-toxin, was associated with an increase in total recovered bacteria after chBMM infection (Chapter 3). Antimicrobial peptides are capable of killing *S. aureus* (Derache *et al.*, 2009; Bommineni *et al.*, 2007, 2014) and therefore their down-regulation could lead to increased *S. aureus* survival. To further investigate this, expression profiles were analysed and revealed a clear trend towards up-regulation of antimicrobial peptides in CIX2 ΔAvβ-sGFP infected chBMMs compared to CIX2-sGFP infected chBMMs (Figure 5.17). qRT-PCR analysis confirmed a significant difference in gene expression for all 4 AMP genes (Figure 5.18), indicating that either prophage Avβ or excision of prophage Avβ, leading to an intact β-toxin, are associated with a down-regulation of avian antimicrobial peptides.

Table 5.3 List of annotated DEGs in CIX2-sGFP vs CIX2 ΔAvβ-sGFP infected chBMMs that meet fold change >2 and p-value <0.05 threshold.

Gene name [1]	logFC	PValue	FDR
ALKAL2	-1.617348	0.0011212	0.9996831
BD7	-2.355982	0.0041091	0.9996831
CATHL1	-1.693625	0.0089569	0.9996831
COL6A3	-1.100509	0.0102311	0.9996831
RF00334	-1.611999	0.011941	0.9996831
AvBD2	-1.471039	0.0121945	0.9996831
MAPK10	-1.569133	0.0135295	0.9996831
GAS1	-1.241519	0.0193841	0.9996831
ACKR3	-1.608645	0.0206192	0.9996831
PHLDB2	-1.461499	0.0238324	0.9996831
DOK4	-1.067541	0.025733	0.9996831
NR0B2	-1.552772	0.0273806	0.9996831
CATHL3	-1.461212	0.0305504	0.9996831
MOK	1.100832	0.033862	0.999683
FST	-1.737641	0.034876	0.9996831
Y-LEC1	-1.411187	0.0358325	0.9996831
ADRA2B	-1.072041	0.0364028	0.9996831
C21orf58	-1.144999	0.0373255	0.9996831
SLC44A3	-1.198873	0.0373332	0.9996831
MIRLET7I	-1.591755	0.0383844	0.9996831
PIANP	-1.129342	0.039016	0.9996831
FAM163B	-1.043214	0.0434209	0.9996831
REEP1	1.31477	0.044032	0.9996831
HEPACAM2	1.74984	0.048868	0.9996831

[1] Red boxes indicate up-regulated DEGs and blue boxes indicate down-regulated DEGs in CIX2-sGFP vs CIX2 ΔAvβ-sGFP infected chBMMs

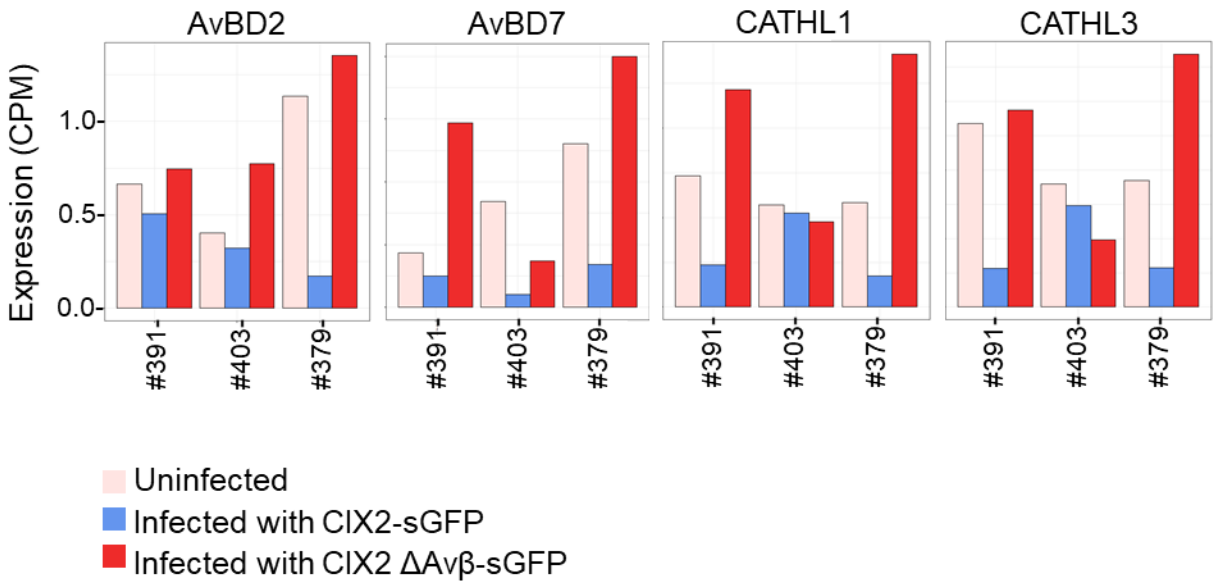

Figure 5.17. Expression of antimicrobial peptides after infection of chBMMs with *S. aureus*.

Expression is shown as normalized counts-per-million for each broiler (#379, #403, #391) with uninfected chBMMs in pink, CIX2-sGFP infected chBMMs in blue and CIX2 ΔAvβ-sGFP infected chBMMs in red.

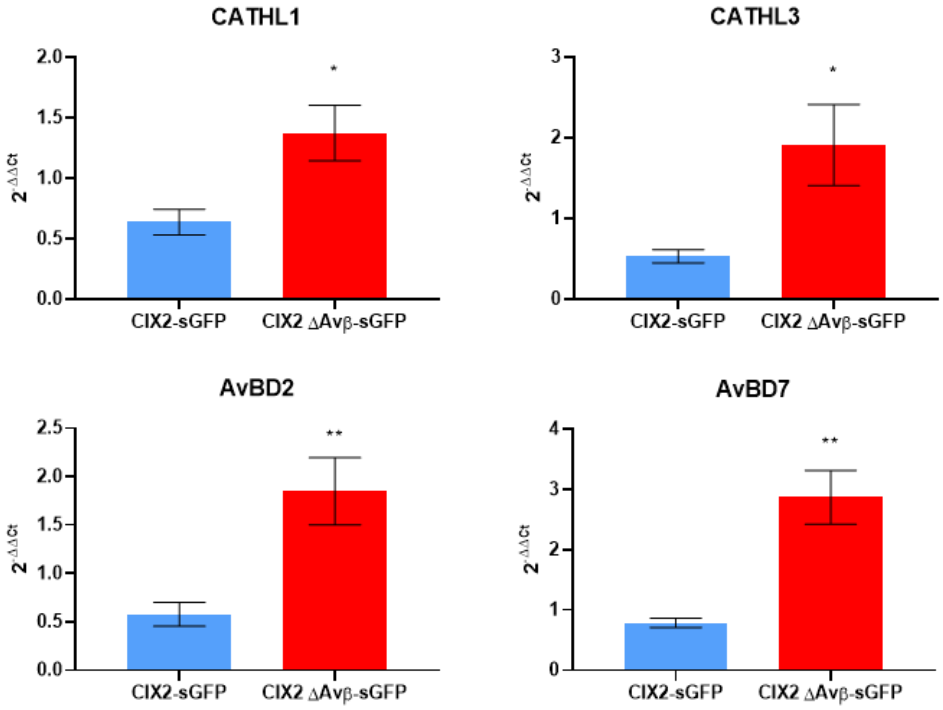

Figure 5.18. qRT-PCR confirms up-regulation of antimicrobial peptides in the Avβ-deficient strain.

Expression analysis of antimicrobial peptides (AvBD2, AvBD2, CATHL1, CATHL3) present in KEGG enriched pathways by qRT-PCR. Data was normalised to GAPDH and fold change compared to uninfected chBMMs was calculated using $2^{-\Delta\Delta Ct}$ method. Results are the mean of three biological replicates ± the standard deviation of the mean. Statistical analysis was performed using an unpaired t-test with Welch's correction, where $p<0.05$ = *, $p<0.01$ = **.

In summary, wild type CIX2-sGFP leads to a general decrease in inducible gene expression profiles in chBMMs compared to its prophage Avβ deletion mutant. We were unable to identify significantly enriched pathways in the CIX2-sGFP infected chBMMs compared to the CIX2 ΔAvβ-sGFP infected chBMMs. However, biological inference allowed us to identify the significant down-regulation of antimicrobial peptide mRNA expression in the presence of prophage Avβ, either due to prophage-encoded genes or excision of the prophage Avβ leading to restoration of the β-toxin expression.

5.5. Discussion

In this study, we investigated the early transcriptional chicken macrophage response to *S. aureus.* Using RNA-seq analysis, we analysed how *S. aureus* is recognised by PRRs and what effect this has on downstream cytokine signalling. In addition, we also investigated the role of prophage Avβ in this transcriptional response, providing new insights into the avian host-adaptation of *S. aureus*.

The recognition of *S. aureus* by pattern recognition receptors (PRRs) on the macrophage cell surface is crucial for initiation of the innate immune response (Kawai & Akira, 2010). In macrophages originating from mice and humans, TLR2 has been identified as the main PRR, recognising both peptidoglycan and lipoproteins PAMPs (Schröder *et al.*, 2003b; Roach *et al.*, 2005). TLR2 can recognise diacyl lipopeptides of *S. aureus* by heterodimer formation with TLR6 (Takeuchi 2001) and triacyl lipopeptides by heterodimer formation with TLR1 (Takeuchi 2002). In contrast, we identified that the early chicken macrophage response to *S. aureus* is initiated by TLR1 1LA/LB and TLR 15 but not TLR2. TLR1LA and TLR1LB are orthologs of the mammalian TLR1/TLR6 heterodimer but these individual receptors do not form heterodimers (Temperley *et al.*, 2008). Despite the lack of TLR2 up-regulation, this PRR can still play a role in *S. aureus* recognition as chicken TLR2 can form a complex with TLR1LA to recognise *S. aureus* peptidoglycan (Keestra *et al.*, 2013) or form a complex with

TLR1LA/TLR1LB to recognise tri or di-acetylated lipoproteins of *S. aureus* (Higuchi *et al.*, 2008).

Interestingly, TLR1LA, TLR1LB and TLR15 are all unique to chickens. TLR15 has been shown to recognise microbial proteases and activates downstream NF-κB activation (De Zoete *et al.*, 2011) but knowledge of TLR15 ligands is limited. This study is the first to identify live *S. aureus* recognition by TLR15. To identify the chicken macrophage response to *S. aureus,* we focused on an avian-adapted strain (CIX2) of *S. aureus*. Further studies with both avian adapted and human adapted *S. aureus* would help to identify whether interaction with avian specific TLRs occurs in a host-dependent manner.

Macrophages from mice and humans play an important role in the tight control of the immune system by switching between pro and anti-inflammatory phenotypes (Bowdish *et al.*, 2015). Similarly, in this study, the clear up-regulation of inflammatory mediators and cytokines in *S. aureus* infected chBMMs is counteracted by the important cytokine signalling repressor SOCS3 and the anti-inflammatory cytokine IL-10 amongst others. Furthermore, the transcription factor NF-κB is an essential step for regulation of the innate response (Naumann, 2000). For example, evidence shows it is required for phagocytosis *S. aureus* in mice by induction of pro-inflammatory cytokines (Zhu, Yue & Wang, 2014). On the other hand, the up-regulation of PPARD, which senses lipids from apoptotic cells, leading to a switch to anti-inflammatory type phenotype, is also dependent on NF-κB (Zingarelli *et al.*, 2010). In effect, we demonstrate that chicken macrophages play a role in the fine tuning of the innate immune system, to avoid damage from inflammation and cytokine dysregulation during *S. aureus* infection.

Intracellular recognition of *S. aureus* is also a crucial component of the innate immune system, as *S. aureus* is capable of surviving intracellularly after phagocytosis (Flannagan, Heit & Heinrichs, 2016; Jubrail *et al.*, 2016). This can be achieved by endosomal PRRs TLR 8 or 9 or cytosolic receptors such as NOD2 (Bergstrøm *et al.*, 2015; Volz *et al.*, 2010; Kitur *et al.*, 2016). In this study, we determined that NOD-like and RIG-I-like signalling played a role in the early response of chicken macrophages to *S. aureus*. This was characterized by the up-

regulation of TRAF3, IKKε and IRF7, which traditionally leads to transcriptional activation of type I interferons (Boxx & Cheng, 2016). However, we were unable to identify the intracellular PRR responsible for this downstream signalling.

The lack of NOD-like receptor up-regulation could be due to the fact that NOD-dependent signalling is poorly characterized in chBMMs. NOD1 is the only receptor present in the chicken genome and despite evidence suggesting it recognises peptidoglycan (Volz *et al.*, 2010), it is unclear whether it activates type I interferons in the same way as other host species. Furthermore, both TLR8 and TLR9 are absent in the chicken genome (Philbin *et al.*, 2005; Kannaki *et al.*, 2019). In addition, RIG-I, another endosomal PRR, is also not present in the chicken genome (Zou *et al.*, 2009). Chicken MDA-5 can recognise both short and long dsRNA which can compensate for the lack of other receptors but this was not found to be up-regulated in our study (Hayashi *et al.*, 2014). TLR3 and TLR7 are also present in the chicken genome, and although they have been identified to play a role in viral infections, they could be responsible for IRF7 induction (Philbin *et al.*, 2005; Schwarz *et al.*, 2007).

However, it is also likely that IRF7 induction is due to the c-GAS/STING pathway since STING is conserved in the chicken genome (Cheng *et al.*, 2015) and a previous study has identified a role for this pathway in murine macrophage host defence against *S. aureus* (Scumpia *et al.*, 2017). Notably, further evidence for a role of STING in chBMM response to *S. aureus* was seen by the presence of PLSCR1 up-regulation, previously shown to be induced by the STING/IRF3 cascade, allowing protection from α-toxin damage by increasing the IFN response (Lizak & Yarovinsky, 2012; Kodigepalli & Nanjundan, 2015). Despite up-regulation of IRF7 in *S. aureus* infected chBMMs, no induction of type I interferons was observed. This could be due to the choice of time point, as expression of type I interferons against *S. aureus* have been identified at later timepoints (Martin *et al.*, 2009; Scumpia *et al.*, 2017). Evidence of NLRC5 up-regulation, involved in type I interferon regulation in chicken macrophages, also indicates a potential for later type I interferon expression (Lian *et al.*, 2012).

An important limitation of this study is the inability to discriminate between bacterial recognition by macrophage PRRs and active manipulation of the immune response.

S. aureus has been shown to be able to manipulate TLR2 by structural mimicry to overstimulate it, blocking it via the TIR domain protein and by the binding of SSL3 and SSL4 (Watanabe *et al.*, 2007; Askarian *et al.*, 2014; Bardoel *et al.*, 2012). Therefore, there is potential for up-regulation of TLRs or other immune signalling to be due to the bacterial manipulation, rather than the chicken macrophage response. Previous work suggests that heat-killed *S. aureus* activates TLRs whereas live *S. aureus* activates both TLR and STING through cGAS recognition of DNA (Scumpia *et al.*, 2017), which suggests *S. aureus* actively manipulated different immune recognition pathways. It is likely that a similar phenotype would occur in chicken macrophages as we have observed both up-regulation of TLRs and type I interferon signalling response.

An important mechanism that *S. aureus* uses to evade the macrophage killing is the induction of cell death. This study provides evidence for both the induction of pro and apoptotic pathways in chicken macrophage in response to *S. aureus*, as well as induction of necroptotic pathways. The cytoprotectivity of *S. aureus* infection has previously been identified in human macrophages, with overexpression of both BCL2 and MCL-1 genes (Koziel *et al.*, 2015). This mechanism allows *S. aureus* to survive intracellularly, thus avoid killing by other cells and potentially increasing further bacterial dissemination. However, the up-regulation of CASP8 confirms previous reports showing that *S. aureus* actively induces the caspase-dependent apoptotic pathway (Flannagan, Heit & Heinrichs, 2016; Winstel, Missiakas & Schneewind, 2018). Furthermore, the up-regulation of MLKL, a marker of necroptosis, confirms previous findings in mice and humans that *S. aureus* can induce both apoptotic and necroptotic cell death pathways (Kitur *et al.*, 2016; Flannagan, Heit & Heinrichs, 2016). These pathways in other host species have been shown to be activated by *S. aureus* toxins, particularly α-toxin (Melehani *et al.*, 2015). Macrophage cell death mechanisms in chicken macrophages are less well characterized and therefore the exact cell pathway induced by *S. aureus* in chicken macrophages remains to be elucidated.

This study provides evidence for conservation across species of antimicrobial killing mechanisms against *S. aureus.* After initial phagocytosis, *S. aureus* has been shown

to rapidly reside in mature phagosomes, where they can be killed by antimicrobial mechanisms (Flannagan, Heit & Heinrichs, 2016). Evidence in this study points to *S. aureus* also residing in mature phagosomes in chicken macrophages. For example, RNF19B, shown to localize to the phagosome and ubiquinate phagosomal proteins in mice is up-regulated (Lawrence & Kornbluth, 2018). In the same way, SNX10, shown to promote bactericidal activity and late phagosomal maturation against *Listeria monocytogenes* was also up-regulated (Lou *et al.*, 2017). The up-regulation of both lysozyme and phospholipase A2 confirms previous reports identifying antimicrobial activity against *S. aureus* (Wellman-Labadie, Picman & Hincke, 2008; Karray *et al.*, 2011). Furthermore, markers of inflammation were significantly up-regulated in infected chBMMs, which is also an important marker of host response to bacterial infection. This study also reinforces the importance of iron sequestration as an antimicrobial mechanism to contain *S. aureus*. This was seen by the up-regulation of exFABP siderocalin shown to retain iron and stop intracellular growth of *E.coli* and *B.subtilis* and STEAP3, a metalloreductase capable of decreasing iron availability in the cytosol in mouse macrophages (Zhang *et al.*, 2012).

We also established that either prophage Avβ, or restoration of β-toxin expression, in an avian strain of *S. aureus* is associated with down-regulation of avian antimicrobial peptides. Antimicrobial peptides are crucial in the first line of host defence against *S. aureus.* In humans they have been identified to kill *S. aureus* directly, with the positively charged residues interacting with the negatively charged cell membrane, leading to cell membrane disruption and bacterial death (Powers & Hancock, 2003). In addition, they also have immunomodulatory functions such as enhanced phagocytosis or cytokine signalling (Bowdish & Hancock, 2005). In the chicken genome, both β-defensins and cathelicidins have been described , with similar role to mammalian antimicrobial peptides (Lynn *et al.*, 2004; Bommineni *et al.*, 2007; Meudal *et al.*, 2011).

Both avian β-defensin 2 and 7 (AvBD2 and AvBD7), as well as avian cathelicidin 1 and 2 (CATHL1 and CATHL3) have previously been shown to be expressed in chicken bone marrow cells (Derache *et al.*, 2009; Achanta *et al.*, 2012; Zhao *et al.*, 2001; Xiao *et al.*, 2004). However, this is the first study to identify gene expression

in chicken macrophages in response to *S. aureus*. This finding contradicts a mass spectrometry study where AvBD2 was only found in heterophils but not chicken macrophages (Kannan *et al.*, 2009). This contradiction could be explained by the fact that we used live bacteria as opposed to TLR agonists to induce expression of avian β-defensins.

All the antimicrobial peptides identified to be down-regulated in this study have been found to be active against *S. aureus* (Derache *et al.*, 2009; Bommineni *et al.*, 2007, 2014) and therefore it is likely *S. aureus* downregulates the peptides to avoid intracellular killing by chicken macrophages. This is supported by our previous data showing that *S. aureus* carrying prophage Avβ is able to survive better when incubated with chBMMs than the prophage deletion mutant. However, avian antimicrobials are also capable of modulating the immune system. For example, AvBD2 and CATHL1 have both been shown to be potent chemoattractants for neutrophils and T cells (Soman, Arathy & Sreekumar, 2009; Bommineni *et al.*, 2014). In the same way, avian CATHL3 is capable of inducing pro-inflammatory cytokines in murine macrophages (Bommineni *et al.*, 2007). Therefore, *S. aureus* could also be avoiding immune activation by down-regulation of antimicrobial peptides.

S. aureus avoids antimicrobial killing by changing its bacterial cell surface charge, proteolytic inactivation or activating transporters that can remove antimicrobial peptides from the cell wall (Peschel & Sahl, 2006). In addition, the human adapted β-converting prophage Sa3 encodes staphylokinase which can bind to and induce α-defensin secretion in neutrophils (Jin *et al.*, 2004). α-defensins are not present in chicken macrophages and therefore it is possible that the avian β-converting prophage Avβ encodes a protein with similar action to staphylokinase but active against avian antimicrobial peptides. However, since we observe a down-regulation of expression of antimicrobial peptides and an overall down-regulation of gene expression in response to prophage Avβ, we hypothesise that either prophage Avβ or an intact β-toxin are affecting upstream signalling of antimicrobial peptide production and not directly binding to them.

Antimicrobial peptides can be induced by TLR signalling (Kannan *et al.*, 2009; Wanke *et al.*, 2011) or by activation of the vitamin D3 receptor (Schauber *et al.*, 2007; Zhang *et al.*, 2016). Due to its sphingomyelinase activity, the β-toxin can cleave sphingomyelin on the cell surface, generating ceramide, which in turn is capable of regulating signalling pathways such as NF-κB (Luberto *et al.*, 2000). In addition, the β-toxin exhibits anti-inflammatory activity, down-regulating both IL-8 mRNA and protein production via the MAPK pathway (Tajima *et al.*, 2009). Thus, excision of prophage Avβ, leading to the restoration of β-toxin expression, may lead to down-regulation of signalling pathways controlling antimicrobial peptide expression. However, we were unable to identify a significantly up-regulated pathway in CIX2 infected chBMMs compared to the prophage deletion mutant that would enable us to identify how avian antimicrobial peptide expression is regulated. This could be due to the large variation between biological replicates and further replicates, which include an effective *hlb* control, could elucidate which pathway leads to antimicrobial peptide down-regulation.

In summary, this study highlights the importance of *S. aureus* recognition in the early chicken macrophage response to *S. aureus*. Our data provide the first evidence for the importance of TLR signalling, NF-κB activation and type I interferon response in chicken macrophage host defence to *S. aureus.* Finally, we demonstrated that acquisition of prophage Avβ modulates the transcriptional chicken macrophage response by down-regulating avian antimicrobial peptides, which is either due to prophage-encoded genes or restoration of β-toxin expression.

Chapter 6. General discussion

The success of a pathogen depends on its ability to survive, adapt, replicate and spread to a new host. Numerous selective pressures shape the genome of bacterial populations to mediate adaptation to a new host, including the immune system, nutrient availability, predators and microbial competitors (Bliven & Maurelli, 2016). Dawkins *et al.* postulated that conflicting drives between a host and a pathogen have led to an evolutionary arms race, whereby the host evolves defences against the pathogen, leading to evolution of pathogen defences, forcing the host to develop new strategies and so on (Dawkins & Krebs, 1979). From the bacterium's perspective, horizontal gene transfer plays an important role in this arms race. The capacity of *S. aureus* to infect and adapt to multiple host-species is driven in part by large genome changes via the acquisition of MGEs that target the host's immune system (Malachowa & DeLeo, 2010). Understanding the molecular mechanisms underpinning host-adaptation is crucial to understand how specific lineages can cross the species barrier and infect new host species, as well as for the development of novel targeted therapeutic strategies. In this thesis, we provide new insights into the mechanisms of *S. aureus* avian innate immune evasion and host-adaptation.

6.1. Prophage Avβ-encoded genes, or the excision of prophage Avβ restoring β-toxin expression, mediate *S. aureus* evasion of macrophage killing

Recent comparative genomic analysis of *S. aureus* isolates from infected poultry revealed an avian-specific subfamily of β-converting phages (Lowder *et al.*, 2009). We hypothesised that, similarly to β-converting phages found in human-adapted *S. aureus* isolates, the avian β-converting phage Avβ would play role in evasion of avian innate immunity and therefore be an important mediator of *S. aureus* host-adaptation to avian species. Our study revealed that presence of prophage Avβ is associated with increased bacterial survival, phagocytosis and chicken macrophage cell death during *S. aureus*-chicken macrophage infections, demonstrating a potential role in evasion of avian innate immunity. However, the lack of effective *hlb* control resulted in the inability to determine whether the observed role of prophage Avβ in *S.*

aureus-macrophage interactions is due to prophage-encoded genes or due to excision of prophage Avβ, leading to the restoration of β-toxin expression.

Investigation of innate immune responses against *S. aureus* has largely been focused on neutrophils, as these short lived granulocytes are the first line of defence against *S. aureus* infection and *S. aureus* possesses an array of virulence factors to counteract these defences (Spaan *et al.*, 2013b). However, our findings suggest that prophage Avβ-encoded genes, or β-toxin expression, are important for evasion of macrophage killing but not heterophil killing, supporting an important role for macrophages during *S. aureus* infections.

Macrophages have been identified as a centre for intracellular persistence for *S. aureus* during infections. For example, in a zebrafish model of infection, macrophages were found to harbour persistent *S. aureus* and acted as "Trojan Horses", whereby *S. aureus* can hide from other immune mechanisms, before being trafficked to a new site of infection by neutrophils (Pollitt *et al.*, 2018). However, this phenotype was only observed at lower doses of *S. aureus*, as at higher doses the macrophage defences were overloaded, suggesting that above a certain threshold of bacteria, macrophages are unable to contain *S. aureus* intracellularly (Pollitt *et al.*, 2018). We identified a similar phenotype in our study, whereby at lower doses, *S. aureus* harbouring prophage Avβ was continually phagocytosed by chicken macrophages without significant cell death but at higher doses, significant macrophage cell death was induced.

This could reflect a scenario whereby during the initial stages of an infection, prophage Avβ-encoded genes allow *S. aureus* to survive intracellularly and persist. At this stage of the infection, protecting macrophage viability may enable *S. aureus* to survive killing by other immune factors. However, as the infection progresses, increasing numbers of *S. aureus*, due either to intracellular replication or increased phagocytosis, overwhelms macrophage microbicidal defences, leading to cell death and dissemination. Study of avian salmonellosis has suggested that the avian-adapted serovar *S. Pullorum* may persist in low numbers within macrophages in the liver or spleen of a bird, allowing bacterial persistence, and suggesting that this may be a common strategy for bacterial adaptation to chickens (Wigley *et al.*, 2001).

However, it is also possible that the observed phenotype is due to concentration-dependent expression of the β-toxin. Investigation of neutrophil cell death induced by *S. aureus* has revealed a concentration dependent action of α-toxin intracellularly, acting only at an MOI above 1 (Pang *et al.*, 2010). Similarly, to achieve β-toxin lethality in a rabbit model of infective endocarditis, a high bacterial inoculum was necessary (Herrera *et al*., 2016). Thus, intracellular action of the β-toxin may be dependent on bacterial density. Furthermore, we identified that excision of prophage Avβ occurs after exposure to H_2O_2, and therefore prophage Avβ may excise once *S. aureus* is phagocytosed by macrophages and exposed to reactive oxygen species, leading to β-toxin expression. Analysis of prophage Sa3 excision dynamics has revealed that despite important excision under conditions of stress such as H_2O_2, a sub-population of *S. aureus* harbouring prophage Sa3 was always present. In addition, excision was time-dependent and β-toxin expression reached a peak around 2 hours post-exposure to H_2O_2 (Tran *et al.*, 2019). Therefore, β-toxin mediated toxicity of macrophages could also be dependent on the *S. aureus* β-toxin expressing sub-population density. However, evidence on β-toxin mediated cytotoxicity of macrophages is lacking and further work is required to dissect whether prophage-encoded genes or the β-toxin play a role in *S. aureus*-macrophage interactions.

6.2. The evolutionary relationship between prophage Avβ and *S. aureus*

Bacteriophages are estimated to outnumber bacterial cells by an order of magnitude and are the most abundant biological entities (Bergh *et al.*, 1989). Phages can control bacterial populations by killing and lysing them, thus reducing bacterial numbers. However, once a bacteriophage infects a bacterium, its survival is dependent on the host (Wagner & Waldor, 2002). Ensuring that the host adapts to new ecological niches is therefore critical for their own survival. For example, the carriage of φSa3, which encodes beneficial human-specific immune evasion genes, allows both survival of *S. aureus* and spread of the bacteriophage to over 90% of human-associated isolates (Van Wamel *et al.*, 2006). In this study, we identified that prophage Avβ is present in the majority of poultry isolates, reinforcing that it is

likely exerting a selective advantage in *S. aureus*. The ubiquitous distribution of prophage Avβ in the CC5 population may also suggest that integration into the *S. aureus* chromosome is beneficial for the bacteriophage's lifecycle, highlighting that the relationship between bacteriophages and bacteria can be more symbiotic rather than parasitic (Cumby, Davidson & Maxwell, 2012).

Additional prophage-encoded moron elements, not associated with the bacteriophage's life cycle, have been identified in permitting a symbiotic relationship between bacteriophages and bacterial populations (Brüssow, Canchaya & Hardt, 2004). Sequence analysis of prophage Avβ identified three genes (*ocd, caax, mbl*) which could be classified as moron elements and could be responsible for prophage Avβ's role in *S. aureus*-macrophage interaction. However, no difference in bacterial survival or phagocytosis was observed by single gene deletion of these three candidate effectors genes compared to the wild type. Despite the importance of prophage-encoded morons on bacterial virulence, it is possible that the effect of prophage Avβ on *S. aureus*-macrophage interaction is due to genes associated with its own lifecycle and not bacteriophage-encoded morons. For example, enterohemorrhagic *E. coli* (EHEC) carries lamboid bacteriophages encoding the Shiga-toxin (Stx) that reside dormantly within the bacterial chromosome during its lysogenic cycle. Phage-repressor CI and anti-repressor Cro are essential proteins involved in the switch between lysogeny and lytic cycles (Oppenheim *et al.*, 2005). Studies have revealed that the Cro protein is involved in the regulation of chromosomally-encoded virulence factors and metabolic genes of EHEC during its lysogenic cycle (Chen *et al.*, 2005; Juan Hernandez-Doria and Vanessa Sperandio ,2018). This is associated with increased bacterial virulence in a mouse model (Juan Hernandez-Doria and Vanessa Sperandio, 2018), suggesting bacteriophage life cycles can enhance bacterial pathogenicity by controlling bacterial virulence factors. Prophage Avβ encodes Cro-CI like proteins and a transcriptional regulator of unknown function and therefore these elements could lead to changes in virulence factors affecting *S. aureus*-macrophage interaction.

Gain of virulence factors is not the only mechanism by which bacterial pathogenicity evolves. Loss of gene function is also important for bacterial host-adaptation (Sheppard, Guttman & Fitzgerald, 2018). However, our study revealed that prophage

Avβ is capable of incomplete excision from the chromosome, potentially allowing the conditional expression of the β-toxin and therefore inactivation of β-toxin may not promote bacterial adaptation. Transient expression of the β-toxin could be a strategy used by prophage Avβ to promote bacterial survival, as restoring β-toxin expression in response to environmental cues can be beneficial to *S. aureus*, as observed in a rabbit model of pneumonia (Salgado-Pabón *et al.*, 2014). In addition, human-specific φSa3 has been revealed to act as a phage regulatory switch, whereby it induces phage excision under certain environmental stresses to restore the expression of the β-toxin, suggesting φSa3 helps *S. aureus* adapt to new environments (Tran *et al.*, 2019). Similarly, prophage excision in *Listeria monocytogenes* restores comK activity, leading to enhanced phagosomal escape (Rabinovich et al., 2012), which suggests that intracellular prophage excision may be an important bacterial immune evasion strategy. Excision of prophage Avβ may also modulate immune evasion gene expression, as *in situ* replication of the prophage before excision could be leading to enhanced prophage-encoded gene expression, as observed with prophage Sa3 (Sumby & Waldor, 2003). Therefore, excision could also be an evolutionary strategy employed by prophage Avβ to replicate and spread, which affects *S. aureus* virulence, directly or indirectly impacting *S. aureus*-macrophage interactions.

6.3. A potential role for prophage Avβ-encoded genes, or the β-toxin, in modulation of macrophage immune signalling

Recognition of *S. aureus* and downstream activation of signalling pathways by macrophages is essential to activate antimicrobial mechanisms (Kawai & Akira, 2010). Our data suggest a potential role for prophage Avβ-encoded genes, or an intact β-toxin, in modulation of macrophage signalling pathways, enabling *S. aureus* to survive intracellularly.

Deletion of prophage Avβ was associated with increased formation of biofilms, likely due to increased protein-protein interactions. Cell surface proteins are

important in the initial development of *S. aureus* biofilm formation (Yarwood *et al.*, 2004), which could suggest that prophage Avβ-encoded genes lead to the down-regulation of cell surface proteins or proteins involved in the formation of the cell wall. The formation of biofilms by *S. aureus* has been revealed to be important in evading immune cell killing and modulating the macrophage response (Scherr *et al.*, 2013, 2015). However, modifying the cell wall or down-regulating cell surface proteins could also be an important mechanism utilized by *S. aureus* to avoid immune recognition. RNAIII, a regulatory RNA central to the *agr* regulatory system that binds target mRNA to prevent initiation of translation, can repress the synthesis of major *S. aureus* surface proteins such as Sbi or FNBPs, or proteins involved in peptidoglycan turnover such as LytM (Bronesky *et al.*, 2016). This allows a switch between the expression of surface proteins and synthesis of excreted toxins, which could mediate transition from colonisation to invasiveness of *S. aureus* (Bronesky *et al.*, 2016). It is tempting to speculate that prophage Avβ-encoded genes lead to a similar switch between expression of cell surface proteins and synthesis of toxins, favouring toxin production.

This hypothesis is supported by the transcriptomic analysis of infected macrophage, which revealed that infection with the Avβ-deficient strain of *S. aureus* led to an increase in differentially expressed genes compared to the strain harbouring prophage Avβ, which could be due to decreased immune recognition associated with this proposed down-regulation of cell surface proteins. However, it is also possible that the restoration of β-toxin expression modulates macrophage signalling pathways. In effect, the β-toxin exhibits inhibition of endothelial IL-8 production, which is due to upstream inhibition of the MAPK signalling pathway (Tajima *et al.*, 2009). Thus, the observed decrease in differentially expressed genes in the *S. aureus* strain harbouring prophage Avβ, as well as the down-regulation of AMP mRNA expression, may be due to excision of prophage Avβ and restoration of β-toxin expression.

Furthermore, an important aspect of macrophage biology highlighted in this study is the capacity to induce both a pro and anti-inflammatory responses. Macrophages exhibit a high level of phenotypic plasticity in response to environmental stimuli (Bowdish *et al.*, 2015). Bacterial pathogens have evolved to exploit different

macrophage activation states. For example, *S. aureus* biofilm formation in an *in vivo* mouse model of infection was associated with down-regulation of macrophage induced pro-inflammatory cytokines (Thurlow *et al.*, 2011). Similarly, *M. tuberculosis* has been revealed to skew the macrophage response by activating neutral sphingomyelinases, leading to excessive ROS production, inhibition of autophagy and cell death, which enables the bacterium to survive longer intracellularly (Liu *et al.*, 2016). Different states of macrophage activation and their modulation are poorly characterised in poultry (Kaspers & Kaiser, 2013). It is unclear whether the observed mRNA expression of both pro and anti-inflammatory cytokines is due to macrophage immunoregulation to avoid excessive inflammation or if it is induced by *S. aureus*. It would be interesting to investigate whether *S. aureus* can skew the avian macrophage response to promote an anti-inflammatory response to avoid antimicrobial killing and determine whether this is promoted by prophage Avβ or the β- toxin.

6.4. Species-specific interaction between avian macrophages and *S. aureus*

Macrophage responses to bacterial challenges can be host-species dependent, which could be a driver of bacterial host-adaptation (Buchan, Foster & Renshaw, 2019). For example, macrophage production of NO and arginine metabolism in response to bacterial challenge is divergent across different species and due to *cis*-acting regulatory elements (Young *et al.*, 2018). In order to adapt to a new host, bacteria may have to overcome these species-specific differences and develop distinct strategies for immune evasion. Transcriptomic analysis of *S. aureus*-infected chicken macrophages in this study revealed the importance of TLR signalling, NF-κB activation and type I interferon response in the early chicken macrophage response to *S. aureus*. This response confirms previous findings in mice (Scumpia *et al.*, 2017), suggesting likely conservation of immune responses to *S. aureus* across these two species. In addition, microarray studies in both bovine and human macrophages revealed a similar up-regulation of pro and anti-inflammatory cytokines in response to *S. aureus* (Sun *et al.*, 2018; Lewandowska-Sabat *et al.*, 2013), reinforcing the concept that global strategies of innate immune responses against *S. aureus* are

widely conserved. However, our study highlighted the up-regulation of specific avian TLRs, TLR1A/B and TLR15, in response to *S. aureus*, suggesting that the bacterium may have to overcome inter-species variation of signalling receptors in order to survive within macrophages. Moreover, other transcriptomic studies performed differ in MOI, *S. aureus* strain and timepoints used. Comparative analysis under identical conditions across different species would be necessary to dissect host-specific differences in response to *S. aureus* and would help our understanding of how the bacterium adapts to different host species.

Differences in the innate immune responses in avian and mammalian species are mainly characterised by their divergence in receptor-specificity, cellular responses and types of antimicrobial compounds produced (Kaiser, 2010). An important finding of our study was the observed down-regulation of AMP mRNA expression in chicken macrophages infected with *S. aureus* harbouring prophage Avβ. Down-regulation of AMPs by bacterial pathogens has been reported as an immune evasion strategy in both human-infecting and avian-infecting bacteria. For example, LL37 expression was reported to be suppressed during both *Shigella dysenteriae* and *Neisseria gonorrhoeae* in humans (Islam *et al.*, 2001; Bergman *et al.*, 2005). In poultry, *Campylobacter jejuni* infection represses expression of avian β-defensins (Meade *et al.*, 2009; Li *et al.*, 2012). In human macrophages, the gene encoding cathelicidin is TLR inducible via the vitamin D dependent pathway, suggesting a role for TLRs in regulation of AMP production (Liu *et al.*, 2006). This was observed to be species-dependent as up-regulation of the vitamin D receptor was not observed in mice (Liu *et al.*, 2006). In poultry, defensin gene expression was reported to be affected by vitamin D3 concentrations in feed but this has not yet been linked to TLR activation (Zhang *et al.*, 2011). Although classes of AMPs are largely conserved across species, gene sequences, numbers and tissue distribution varies (Dimitrov & White, 2016). Therefore, it is possible that prophage Avβ enables *S. aureus* to adapt to these host species-dependent differences in both AMP regulation and production, which is either due to prophage-encoded genes or excision of prophage Avβ leading to restoration of β-toxin expression .

β-toxin activity on macrophages may also be host-specific. For example, erythrocytes from ruminants have a high content of sphingomyelin in their plasma

membrane (Titball et al., 1993), which may explain why *S. aureus* strains isolated from bovine isolate preferentially produce the β-toxin rather than harbour human-adapted prophage Sa3 (Aerestrup *et al.*, 1999; Larsen *et al.*, 2002). Sphingomyelin content is high in chicken livers and egg yolk (Weihrauch *et al*., 1993), and therefore it is tempting to speculate that prophage Avβ preferentially excises to enable β-toxin mediated toxicity. However, sphingomyelin content on the macrophage cell membrane across host species has not been established and it remains to be determined whether the β-toxin plays a role in *S. aureus*-macrophage interactions.

The transcriptomic analysis in this study also highlighted the high level of variation that occurs between macrophages from different individuals. Recent RNA-seq analysis of chBMMs isolated from the progeny of sibling matings from broiler and layer lines revealed regulatory variation that impacted the transcriptome of immune cells from different birds (Freem *et al.* 2019, unpublished). It is possible that the variation observed in our study is due to similar *trans*-acting regulatory elements in the individual birds. Exploiting this variation further could help to identify susceptible vs resistant macrophages and uncover the mechanisms by which chicken macrophages eliminate *S. aureus*, but also how *S. aureus* can evade the avian innate immune response. For example, gene expression analysis of macrophages from either resistant or susceptible chicken lines has revealed that the rapid expression of pro-inflammatory cytokines and chemokines is essential for immunity to *Salmonella* (Beal *et al.*, 2004; Wigley *et al.*, 2006). Furthermore, our results also highlight the unintended consequences of intensive selective breeding in the poultry industry. Breeding programs directed towards accelerated growth and feed conversion efficiency may have resulted in reduced responses to bacterial pathogens (Swaggerty *et al.*, 2009), which could be exploited by *S. aureus* to expand into the avian host.

6.5. Proposed models for the role of prophage Avβ and an intact β-toxin in evasion of avian innate immunity

Taken together, our data allows us to develop a model for either the role of prophage Avβ-encoded genes, or excision of prophage Avβ leading to restoration of an intact β-toxin, in evasion of avian innate immunity (Figure 6.1).

Initial contact of chicken macrophages with *S. aureus* harbouring prophage Avβ leads to increased phagocytosis compared to the Avβ-deficient strain, suggesting either that the chicken macrophages are less capable of killing *S. aureus* or that *S. aureus* is actively enhancing phagocytosis to become intracellular and avoid other components of the immune system. We hypothesise that down-regulation of cell surface proteins or modification of the cell wall by prophage Avβ-encoded genes enable *S. aureus* to bypass recognition by chicken macrophages, leading to the down-regulation of avian AMP mRNA expression and avoidance of intracellular killing (Figure 6.1A). However, it is also possible that increased phagocytosis is due to prophage Avβ excision, leading to restoration of β-toxin expression. In this scenario, we hypothesise that the β-toxin activity is restored after ROS exposure, which skews the microbicidal response and leads to overall down-regulation of antimicrobial killing, including AMPs (Figure 6.1B).

Regardless of the mechanism, *S. aureus* is capable of avoiding macrophage killing due to either the presence of prophage Avβ-encoded genes or an intact β-toxin. We propose that intracellular accumulation, leads to macrophage lysis, either by the overwhelming of macrophage microbicidal function or by actively inducing intracellular or extracellular toxin-mediated lysis, allowing *S. aureus* to disseminate further during an infection (Figure 6.1A,B).

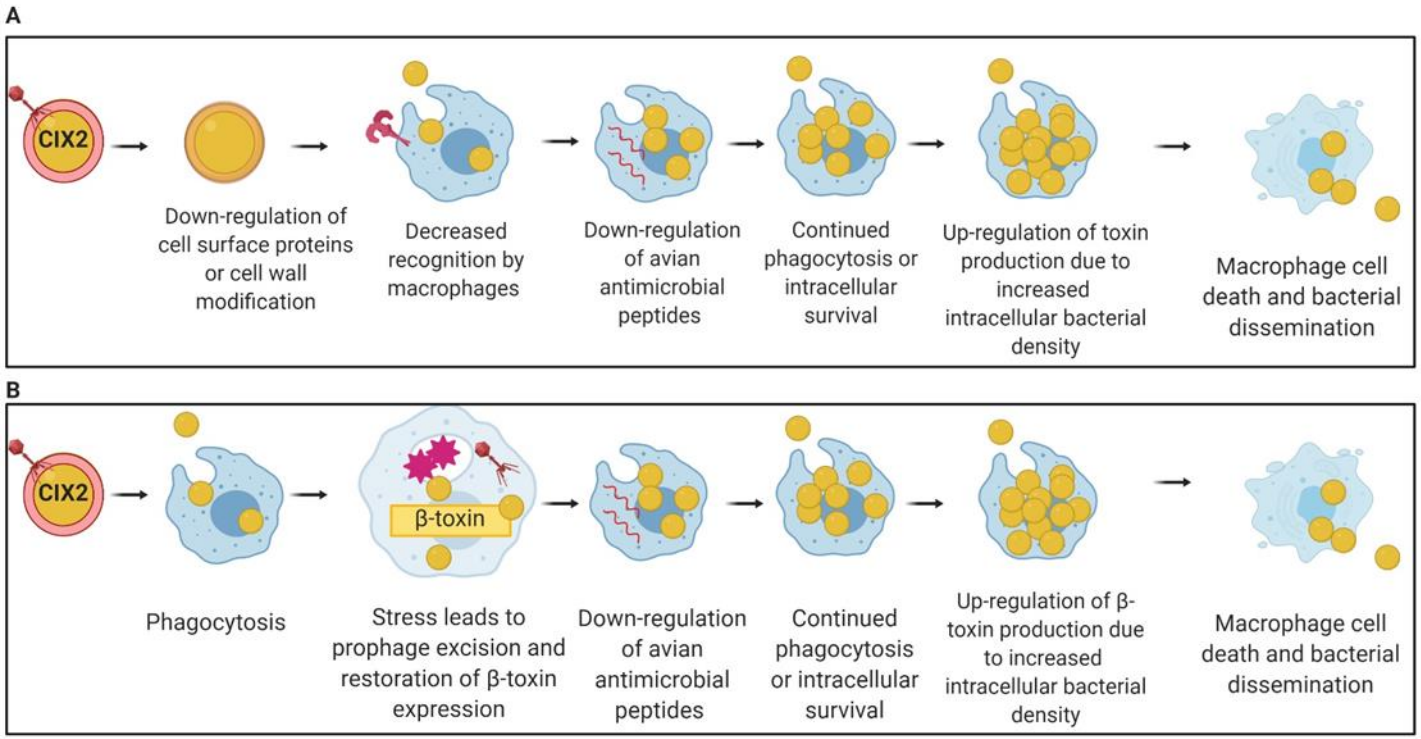
A
CIX2
Down-regulation of cell surface proteins or cell wall modification
Decreased recognition by macrophages
Down-regulation of avian antimicrobial peptides
Continued phagocytosis or intracellular survival
Up-regulation of toxin production due to increased intracellular bacterial density
Macrophage cell death and bacterial dissemination
B
CIX2
β-toxin
Phagocytosis
Stress leads to prophage excision and restoration of β-toxin expression
Down-regulation of avian antimicrobial peptides
Continued phagocytosis or intracellular survival
Up-regulation of β-toxin production due to increased intracellular bacterial density
Macrophage cell death and bacterial dissemination

Figure 6.1. Proposed model of the role of prophage Avβ in *S. aureus*-macrophage interaction.

A) Prophage Avβ-encoded genes promote avoidance of *S. aureus* recognition by avian macrophages, leading to the down-regulation of AMP mRNA expression. This allows either continued increased phagocytosis or intracellular survival and replication. Increasing numbers of intracellular bacteria lead to macrophage cell death and potential further bacterial dissemination. B) The restoration of β-toxin expression, after *S. aureus* contact with ROS inside macrophages, leads to down-regulation of antimicrobial mechanisms, including AMP mRNA expression. This allows either continued increased phagocytosis or intracellular survival and replication. Increasing numbers of intracellular bacteria with an intact β-toxin lead to macrophage cell death via β-toxin membrane disruption and potential further bacterial dissemination. Figure created with BioRender.com.

6.6. Future work

Despite identifying a role for prophage Avβ in evasion of avian macrophage killing, the molecular mechanism driving this phenotype remains unclear. To assess whether prophage Avβ-encoded genes or restoration of β-toxin expression are responsible for evasion of avian innate immunity, construction of an Avβ-deficient with restored β-toxin is required. In addition, deletion of the prophage Avβ integrase gene, which would inhibit prophage Avβ excision, would determine whether the phenotype is dependent on prophage Avβ excision. Analysis of the bacterial transcriptome using RNA-seq analysis could also provide insights into phage dynamics, as transcription of all prophage-encoded genes could be assessed. Furthermore, to further investigate the role of avian AMP mRNA down-regulation in evasion of avian macrophage killing, assessment of AMP protein production is required. This could be achieved with the use of immunohistochemistry or mass spectrometry. To further investigate the role of prophage Avβ in chicken macrophage cell death, the use of bacterial supernatants in chicken macrophage cell death assays could help to decipher whether

the cell death is mediated by the β-toxin or another *S. aureus* toxin. In addition, the use of microscopy could help to unravel the intracellular fate of avian-adapted *S. aureus* and the role of prophage Avβ, or the β-toxin, in this interaction. For example, confocal microscopy time course analysis of the fluorescently-tagged bacteria contained within chicken macrophages may identify whether the observed increased phagocytosis is due to intracellular replication or continued cycles of phagocytosis and whether chicken macrophage cell death is induced by intracellular *S. aureus*. Finally, our study was performed *in vitro* and further characterisation *in vivo* would enable us to assess the impact of macrophage dysfunction associated with prophage Avβ, or the β-toxin, on disease outcome. *S. aureus* infections in poultry often occur after a breach to the skin, followed by system infection (Peton & Le Loir, 2014). Thus, intradermal infection of the broiler footpad and monitoring subsequent systemic infection would a good natural model of infection (Zhu, Wu and Hester, 2001). This model would enable us to assess the role of prophage Avβ, or the β-toxin, in *S. aureus* survival against early infiltration of monocytes and macrophages to the site of infection as well as in *S. aureus* dissemination to other organs (Mölne & Tarkowski, 2000). Furthermore, an *in vivo* model of infection in poultry would help dissect the role of macrophages in activating the adaptive immune system and investigate whether prophage Avβ or the β-toxin play a role in this interaction.

6.7. Conclusion

In conclusion, this study has revealed a role for the prophage Avβ in evasion of chicken macrophage-mediated killing, either due to its encoded genes or its excision, leading to restoration of β-toxin expression. Future work unravelling the mechanisms involved will provide important new insights into how *S. aureus* undergoes host-adaptation. Furthermore, our data highlight how the development of integrative approaches are required to understand how phages, bacterial genetics and the immune system interact to drive the host-adaptive evolution of bacterial pathogens.

References

Abtin, A., Jain, R., Mitchell, A.J., Roediger, B., Brzoska, A.J., Tikoo, S., Cheng, Q., Ng, L.G., Cavanagh, L.L., Von Andrian, U.H. and Hickey, M.J., 2014. Perivascular macrophages mediate neutrophil recruitment during bacterial skin infection. *Nature immunology*. 15(1), 45.

Achanta, M., Sunkara, L.T., Dai, G., Bommineni, Y.R., *et al.*, 2012. Tissue expression and developmental regulation of chicken cathelicidin antimicrobial peptides. *Journal of animal science and biotechnology*. 3 (1), 15.

Alibayov, B., Baba-Moussa, L., Sina, H., Zdeňková, K., *et al.*, 2014. *Staphylococcus aureus* mobile genetic elements. *Molecular Biology Reports*. 41 (8), 5005–5018.

Alonzo, F. and Torres, V.J., 2014. The bicomponent pore-forming leucocidins of *Staphylococcus aureus*. *Microbiol. Mol. Biol. Rev.*. 8(2), 199-230.

Anderson, K.L., Roberts, C., Disz, T., Vonstein, V., *et al.*, 2006. Characterization of the *Staphylococcus aureus* heat shock, cold shock, stringent, and SOS responses and their effects on log-phase mRNA turnover. *Journal of bacteriology*. 188 (19), 6739–6756.

Andreasen, C.B., Latimer, K.S., Harmon, B.G., Glisson, J.R., *et al.*, 1991. Heterophil function in healthy chickens and in chickens with experimentally induced staphylococcal tenosynovitis. *Veterinary pathology*. 28 (5), 419–427.

Andreasen Jr, J.R., Andreasen, C.B., Anwer, M. and Sonn, A.E., 1993. Heterophil chemotaxis in chickens with natural staphylococcal infections. In *Avian diseases*, 284-289.

Arndt, D., Grant, J.R., Marcu, A., Sajed, T., *et al.*, 2016. PHASTER: a better, faster version of the PHAST phage search tool. *Nucleic Acids Research*. 44 (W1), W16–W21.

Askarian, F., Van Sorge, N.M., Sangvik, M., Beasley, F.C., Henriksen, J.R., Sollid, J.U., Van Strijp, J.A., Nizet, V. and Johannessen, M., 2014. A Staphylococcus aureus TIR domain protein virulence factor blocks TLR2-mediated NF-κB signaling. *Journal of innate immunity*. 6(4), 485-498.

Askarian, F., Wagner, T., Johannessen, M. & Nizet, V., 2018. *Staphylococcus aureus* modulation of innate immune responses through Toll-like (TLR), (NOD)-like (NLR) and C-type lectin (CLR) receptors. *FEMS Microbiology Reviews*. 025, 656–671.

Bae, T., Baba, T., Hiramatsu, K. and Schneewind, O., 2006. Prophages of Staphylococcus aureus Newman and their contribution to virulence. *Molecular microbiology*. 62(4), 1035-1047.

Ballal, A. & Manna, A.C., 2009. Regulation of superoxide dismutase (sod) genes by

SarA in *Staphylococcus aureus*. *Journal of bacteriology*. 191 (10), 3301–3310.

Bardoel, B.W., Vos, R., Bouman, T., Aerts, P.C., *et al.*, 2012. Evasion of Toll-like receptor 2 activation by staphylococcal superantigen-like protein 3. *Journal of Molecular Medicine*. 90 (10), 1109–1120.

Barrière, C., Brückner, R., Centeno, D. and Talon, R., 2002. Characterisation of the katA gene encoding a catalase and evidence for at least a second catalase activity in Staphylococcus xylosus, bacteria used in food fermentation. *FEMS microbiology letters*, 216(2), 277-283.

Beal, R.K., Powers, C., Wigley, P., Barrow, P.A., *et al.*, 2004. Temporal dynamics of the cellular, humoral and cytokine responses in chickens during primary and secondary infection with *Salmonella enterica* serovar Typhimurium. *Avian Pathology*. 33 (1), 25–33.

Beasley, F.C., Cheung, J. and Heinrichs, D.E., 2011. Mutation of L-2, 3-diaminopropionic acid synthase genes blocks staphyloferrin B synthesis in *Staphylococcus aureus*. *BMC microbiology*. 11(1), 199.

Becker, R.E., Berube, B.J., Sampedro, G.R., DeDent, A.C. and Wardenburg, J.B., 2014. Tissue-specific patterning of host innate immune responses by *Staphylococcus aureus* α-toxin. *Journal of innate immunity*, 6(5), 619-631.

Bera, A., Herbert, S., Jakob, A., Vollmer, W., *et al.*, 2004. Why are pathogenic staphylococci so lysozyme resistant? The peptidoglycan O-acetyltransferase OatA is the major determinant for lysozyme resistance of *Staphylococcus aureus*. *Molecular Microbiology*. 55 (3), 778–787.

Berends, E.T.M., Dekkers, J.F., Nijland, R., Kuipers, A., *et al.*, 2013. Distinct localization of the complement C5b-9 complex on Gram-positive bacteria. *Cellular microbiology*. 15 (12), 1955–1968.

Bergh, Ø., BØrsheim, K.Y., Bratbak, G. & Heldal, M., 1989. High abundance of viruses found in aquatic environments. *Nature*. 340 (6233), 467–468.

Bergman, P., Johansson, L., Asp, V., Plant, L., *et al.*, 2005. *Neisseria gonorrhoeae* downregulates expression of the human antimicrobial peptide LL-37. *Cellular Microbiology*. 7 (7), 1009–1017.

Bergstrøm, B., Aune, M.H., Awuh, J.A., Kojen, J.F., *et al.*, 2015. TLR8 Senses *Staphylococcus aureus* RNA in Human Primary Monocytes and Macrophages and Induces IFN-β Production via a TAK1-IKKβ-IRF5 Signaling Pathway. *Journal of immunology*. 195 (3), 1100–1111.

von Bernuth, H., Picard, C., Puel, A. & Casanova, J.L., 2012. Experimental and natural infections in MyD88- and IRAK-4-deficient mice and humans. *European Journal of Immunology*. 42 (12) 3126–3135.

Berube, B., Wardenburg, J., Berube, B.J. & Wardenburg, J.B., 2013. *Staphylococcus aureus* α-Toxin: Nearly a Century of Intrigue. *Toxins*. 5 (6), 1140–1166.

Bestebroer, J., Aerts, P.C., Rooijakkers, S.H.M., Pandey, M.K., *et al.*, 2010. Functional basis for complement evasion by staphylococcal superantigen-like 7.

Cellular Microbiology. 12 (10), 1506–1516.

Bestebroer, J., Kessel, K.P.M. van, Azouagh, H., Walenkamp, A.M., *et al.*, 2009. Staphylococcal SSL5 inhibits leukocyte activation by chemokines and anaphylatoxins. *Blood*. 113 (2), 328–337.

Bestebroer, J., Poppelier, M.J.J.G., Ulfman, L.H., Lenting, P.J., *et al.*, 2007. Staphylococcal superantigen-like 5 binds PSGL-1 and inhibits P-selectin-mediated neutrophil rolling. *Blood*. 109 (7), 2936–2943.

Bishayi, B., Bandyopadhyay, D., Majhi, A. & Adhikary, R., 2014. Possible Role of Toll-like Receptor-2 in the Intracellular Survival of *Staphylococcus aureus* in Murine Peritoneal Macrophages: Involvement of Cytokines and Anti-Oxidant Enzymes. *Scandinavian Journal of Immunology*. 80(2), 127-143.

Blättner, S., Das, S., Paprotka, K., Eilers, U., *et al.*, 2016. *Staphylococcus aureus* Exploits a Non-ribosomal Cyclic Dipeptide to Modulate Survival within Epithelial Cells and Phagocytes. *PLOS Pathogens*. 12 (9), e1005857.

Bliven, K.A. & Maurelli, A.T., 2016. Evolution of Bacterial Pathogens within the Human Host. *Microbiology spectrum*. 4 (1).

Boakes, E., Kearns, A.M., Ganner, M., Perry, C., *et al.*, 2011. Distinct bacteriophages encoding Panton-Valentine leukocidin (PVL) among international methicillin-resistant *Staphylococcus aureus* clones harboring PVL. *Journal of clinical microbiology*. 49 (2), 684–692.

Boles, B.R. & Horswill, A.R., 2008. agr-Mediated Dispersal of *Staphylococcus aureus* Biofilms. *PLoS Pathogens*. 4 (4), e1000052.

Bommineni, Y.R., Achanta, M., Alexander, J., Sunkara, L.T., *et al.*, 2010. A fowlicidin-1 analog protects mice from lethal infections induced by methicillin-resistant *Staphylococcus aureus*. *Peptides*. 31 (7), 1225–1230.

Bommineni, Y.R., Dai, H., Gong, Y.-X., Soulages, J.L., *et al.*, 2007. Fowlicidin-3 is an α-helical cationic host defense peptide with potent antibacterial and lipopolysaccharide-neutralizing activities. *FEBS Journal*. 274 (2), 418–428.

Bommineni, Y.R., Pham, G.H., Sunkara, L.T., Achanta, M., *et al.*, 2014. Immune regulatory activities of fowlicidin-1, a cathelicidin host defense peptide. *Molecular Immunology*. 59 (1), 55–63.

Borregaard, N., 2010. Neutrophils, from Marrow to Microbes. *Immunity*. 33 (5), 657–670.

Boyette, L.B., Macedo, C., Hadi, K., Elinoff, B.D., Walters, J.T., Ramaswami, B., Chalasani, G., Taboas, J.M., Lakkis, F.G. and Metes, D.M., 2017. Phenotype, function, and differentiation potential of human monocyte subsets. *PloS one*, 12(4), e0176460.

Hume, D.A., 2015. The many alternative faces of macrophage activation. *Frontiers in immunology*. 6, p.370.

Bowdish, D.M.E. & Hancock, R.E.W., 2005. Anti-endotoxin properties of cationic

host defence peptides and proteins. *Journal of Endotoxin Research*. 11 (4), 230–236.

Boxx, G.M. & Cheng, G., 2016. The Roles of Type I Interferon in Bacterial Infection. *Cell Host & Microbe*. 19 (6), 760–769.

Boyd, A.C., Peroval, M.Y., Hammond, J.A., Prickett, M.D., *et al.*, 2012. TLR15 is unique to avian and reptilian lineages and recognizes a yeast-derived agonist. *Journal of immunology*. 189 (10), 4930–4938.

Boyd, Y., Goodchild, M., Morroll, S. & Bumstead, N., 2001. Mapping of the chicken and mouse genes for toll-like receptor 2 (TLR2) to an evolutionarily conserved chromosomal segment. *Immunogenetics*. 52 (3–4), 294–298.

Bradley, A.J., Leach, K.A., Breen, J.E., Green, L.E., *et al.*, 2007. Survey of the incidence and aetiology of mastitis on dairy farms in England and Wales. *The Veterinary record*. 160 (8), 253–257.

Bronesky, D., Wu, Z., Marzi, S., Walter, P., *et al.*, 2016. *Staphylococcus aureus* RNAIII and Its Regulon Link Quorum Sensing, Stress Responses, Metabolic Adaptation, and Regulation of Virulence Gene Expression. *Annual Review of Microbiology*. 70 (1), 299–316.

Brown, A.F., Murphy, A.G., Lalor, S.J., Leech, J.M., *et al.*, 2015. Memory Th1 Cells Are Protective in Invasive *Staphylococcus aureus* Infection. *PLoS Pathogens*. 11(11), p.e1005226.

Brownlie, R., Zhu, J., Allan, B., Mutwiri, G.K., *et al.*, 2009. Chicken TLR21 acts as a functional homologue to mammalian TLR9 in the recognition of CpG oligodeoxynucleotides. *Molecular Immunology*. 46 (15), 3163–3170.

Brune, K., Leffell, M.S. & Spitznagel, J.K., 1972. Microbicidal Activity of Peroxidaseless Chicken Heterophile Leukocytes. *Infection and Immunity*. 5 (3), 283.

Brüssow, H., Canchaya, C. & Hardt, W.-D., 2004. Phages and the evolution of bacterial pathogens: from genomic rearrangements to lysogenic conversion. *Microbiology and molecular biology reviews : MMBR*. 68 (3), 560–602.

Bubeck Wardenburg, J., Bae, T., Otto, M., DeLeo, F.R., *et al.*, 2007. Poring over pores: α-hemolysin and Panton-Valentine leukocidin in *Staphylococcus aureus* pneumonia. *Nature Medicine*. 13 (12), 1405–1406.

Buchan, K.D., Foster, S.J. & Renshaw, S.A., 2019. *Staphylococcus aureus*: setting its sights on the human innate immune system. *Microbiology*. 165 (4), 367–385.

Bukowski, M., Lyzen, R., Helbin, W.M., Bonar, E., Szalewska-Palasz, A., Wegrzyn, G., Dubin, G., Dubin, A. and Wladyka, B., 2013. A regulatory role for *Staphylococcus aureus* toxin–antitoxin system PemIK Sa. *Nature communications*. *4*, p.2012.

Bunk, S., Sigel, S., Metzdorf, D., Sharif, O., *et al.*, 2010. Internalization and Coreceptor Expression Are Critical for TLR2-Mediated Recognition of Lipoteichoic Acid in Human Peripheral Blood. *The Journal of Immunology*. 185 (6), 3708–3717.

Burman, J.D., Leung, E., Atkins, K.L., O'Seaghdha, M.N., *et al.*, 2008. Interaction of human complement with Sbi, a staphylococcal immunoglobulin-binding protein: indications of a novel mechanism of complement evasion by *Staphylococcus aureus*. *The Journal of biological chemistry*. 283 (25), 17579–17593.

Bush, S.J., Freem, L., MacCallum, A.J., O'Dell, J., *et al.*, 2018. Combination of novel and public RNA-seq datasets to generate an mRNA expression atlas for the domestic chicken. *BMC genomics*. 19 (1), 594.

Bystroń, J., Molenda, J., Bania, J., Kosek-Paszkowska, K., *et al.*, 2005. Occurrence of enterotoxigenic strains of *Staphylococcus aureus* in raw poultry meat. *Polish journal of veterinary sciences*. 8 (1), 37–40.

Bystroń, J., Podkowik, M., Piasecki, T., Wieliczko, A., *et al.*, 2010. Genotypes and enterotoxin gene content of *S. aureus* isolates from poultry. *Veterinary Microbiology*. 144 (3–4), 498–501.

Carlander, D., Stålberg, J. & Larsson, A., 1999. Chicken Antibodies. *Upsala Journal of Medical Sciences*. 104 (3), 179–189.

Cassat, J.E. & Skaar, E.P., 2012. Metal ion acquisition in *Staphylococcus aureus*: overcoming nutritional immunity. *Seminars in Immunopathology*. 34 (2), 215–235.

Cassidy, P. and Harshman, S., 1976. Studies on the binding of staphylococcal 125I-labeled α-toxin to rabbit erythrocytes. Biochemistry, 15(11), 2348-2355.

Castleman, M.J., Febbraio, M. & Hall, P.R., 2016. CD36 Is Essential for Regulation of the Host CD36 Is Essential for Regulation of the Host Innate Response to *Staphylococcus aureus* a-Toxin–Mediated Dermonecrosis. *The Journal of Immunology*. 195(5), 2294-2302.

Chan, K.K.W., Oza, A.M. & Siu, L.L., 2003. The statins as anticancer agents. *Clinical cancer research : an official journal of the American Association for Cancer Research*. 9 (1), 10–19.

Chan, L.C., Rossetti, M., Miller, L.S., Filler, S.G., *et al.*, 2018. Protective immunity in recurrent *Staphylococcus aureus* infection reflects localized immune signatures and macrophage-conferred memory. *Proceedings of the National Academy of Sciences of the United States of America*. 115 (47), E11111–E11119.

Chen, C., Bentham, J., Cosgrove, C., Braganca, J., *et al.*, 2012. Functional significance of SRJ domain mutations in CITED2. *PloS one*. 7 (10), e46256.

Chen, C., Yang, C. & Barbieri, J.T., 2019. Staphylococcal Superantigen-like protein 11 mediates neutrophil adhesion and motility arrest, a unique bacterial toxin action. *Scientific Reports*. 9 (1), 4211.

Chen, J.-C., Huang, K.-C. & Lin, W.-W., 2006. HMG–CoA reductase inhibitors upregulate heme oxygenase-1 expression in murine RAW264.7 macrophages via ERK, p38 MAPK and protein kinase G pathways. *Cellular Signalling*. 18

(1), 32–39.

Chen, J., Quiles-Puchalt, N., Chiang, Y.N., Bacigalupe, R., Fillol-Salom, A., Chee, M.S.J., Fitzgerald, J.R. and Penadés, J.R., 2018a. Genome hypermobility by lateral transduction. *Science*, *362*(6411), 207-212.

Chen, S., Zhou, Y., Chen, Y. & Gu, J., 2018b. Fastp: An ultra-fast all-in-one FASTQ preprocessor. *Bioinformatics*. i884–i890.

Chen, X. & Alonzo, F., 2019. Bacterial lipolysis of immune-activating ligands promotes evasion of innate defenses. *Proceedings of the National Academy of Sciences of the United States of America*. 116 (9), 3764–3773.

Chen, Y., Golding, I., Sawai, S., Guo, L., *et al.*, 2005. Population Fitness and the Regulation of Escherichia coli Genes by Bacterial Viruses Matt Waldor. *PLoS Biology*. 3 (7), e229.

Cheng, Y., Sun, Y., Wang, H., Yan, Y., *et al.*, 2015. Chicken STING Mediates Activation of the IFN Gene Independently of the RIG-I Gene. *Journal of immunology*. 195 (8), 3922–3936.

Chiang, Y.N., Penadés, J.R. and Chen, J., 2019. Genetic transduction by phages and chromosomal islands: The new and noncanonical. *PLoS pathogens*, 15(8), e1007878.

Chuammitri, P., Ostojić, J., Andreasen, C.B., Redmond, S.B., *et al.*, 2009. Chicken heterophil extracellular traps (HETs): Novel defense mechanism of chicken heterophils. *Veterinary Immunology and Immunopathology*. 129 (1–2), 126–131.

Chung, M.C., Wines, B.D., Baker, H., Langley, R.J., *et al.*, 2007. The crystal structure of staphylococcal superantigen-like protein 11 in complex with sialyl Lewis X reveals the mechanism for cell binding and immune inhibition. *Molecular Microbiology*. 66 (6), 1342–1355.

Collins, L.V., Kristian, S.A., Weidenmaier, C., Faigle, M., *et al.*, 2002. *Staphylococcus aureus* Strains Lacking D- Alanine Modifications of Teichoic Acids Are Highly Susceptible to Human Neutrophil Killing and Are Virulence Attenuated in Mice. *The Journal of Infectious Diseases*. 186(2), 214-219.

Cosgriff, C.J., White, C.R., Teoh, W.P., Grayczyk, J.P. and Alonzo, F., 2019. Control of *Staphylococcus aureus* quorum sensing by a membrane-embedded peptidase. *Infection and immunity*, 87(5), e00019-19.

Cotter, P.F., Taylor Jr, R.L., Wing, T.L. and Briles, W.E., 1987. Major histocompatibility (B) complex-associated differences in the delayed wattle reaction to staphylococcal antigen. *Poultry science*. 66(2), 203-208.

Craven, R.R., Gao, X., Allen, I.C., Gris, D., *et al.*, 2009. *Staphylococcus aureus* α-hemolysin activates the NLRP3-inflammasome in human and mouse monocytic cells. *PLoS ONE*. 4 (10). e7446.

Cumby, N., Davidson, A.R. & Maxwell, K.L., 2012. The moron comes of age. *Bacteriophage*. 2 (4), 225–228.

Cuny, C., Friedrich, A., Kozytska, S., Layer, F., *et al.*, 2010. Emergence of methicillin-resistant *Staphylococcus aureus* (MRSA) in different animal species. *International Journal of Medical Microbiology*. 300 (2–3), 109–117.

Cuperus, T., Coorens, M., van Dijk, A. and Haagsman, H.P., 2013. Avian host defense peptides. *Developmental & Comparative Immunology*, *41*(3), 352-369.

Davis, B.K., Wen, H. & Ting, J.P.-Y., 2011. The Inflammasome NLRs in Immunity, Inflammation, and Associated Diseases. *Annual Review of Immunology*. 29 (1), 707–735.

Dawkins, R. & Krebs, J.R., 1979. Arms races between and within species. *Proceedings of the Royal Society of London. Series B. Biological Sciences*. 205 (1161), 489–511.

Dehbi, M., Moeck, G., Arhin, F.F., Bauda, P., *et al.*, 2009. Inhibition of transcription in *Staphylococcus aureus* by a primary sigma factor-binding polypeptide from phage G1. *Journal of bacteriology*. 191 (12), 3763–3771.

DeLeo, F.R. & Chambers, H.F., 2009. Reemergence of antibiotic-resistant *Staphylococcus aureus* in the genomics era. *The Journal of clinical investigation*. 119 (9), 2464–2474.

Derache, C., Labas, V., Aucagne, V., Meudal, H., *et al.*, 2009. Primary structure and antibacterial activity of chicken bone marrow-derived beta-defensins. *Antimicrobial agents and chemotherapy*. 53 (11), 4647–4655.

Derache, C., Meudal, H., Aucagne, V., Mark, K.J., Cadène, M., Delmas, A.F., Lalmanach, A.C. and Landon, C., 2012. Initial insights into structure-activity relationships of avian defensins. Journal of Biological Chemistry, 287(10), 7746-7755.

Di, A., Kiya, T., Gong, H., Gao, X., *et al.*, 2017. Role of the phagosomal redox-sensitive TRP channel TRPM2 in regulating bactericidal activity of macrophages. *Journal of cell science*. 130 (4), 735–744.

Dimitrov, V. & White, J.H., 2016. Species-specific regulation of innate immunity by vitamin D signaling. *Journal of Steroid Biochemistry and Molecular Biology*. 164.246–253.

Dobin, A., Davis, C.A., Schlesinger, F., Drenkow, J., *et al.*, 2013. Sequence analysis STAR: ultrafast universal RNA-seq aligner. 29 (1), 15–21.

Dohlsten, M., Björklund, M., Sundstedt, A., Hedlund, G., *et al.*, 1993. Immunopharmacology of the superantigen staphylococcal enterotoxin A in T-cell receptor V beta 3 transgenic mice. *Immunology*. 79 (4), 520–527.

Dossett, J.H., Kronvall, G., Williams, R.C. & Quie, P.G., 1969. Antiphagocytic effects of staphylococcal protein A. *Journal of immunology*. 103 (6), 1405–1410.

DuMont, A.L., Yoong, P., Day, C.J., Alonzo, F., *et al.*, 2013. *Staphylococcus aureus* LukAB cytotoxin kills human neutrophils by targeting the CD11b subunit of the integrin Mac-1. *Proceedings of the National Academy of Sciences*. 110 (26), 10794–10799.

Dunman, P.M., Murphy, E., Haney, S., Palacios, D., *et al.*, 2001. Transcription profiling-based identification of *Staphylococcus aureus* genes regulated by the agr and/or sarA loci. *Journal of bacteriology*. 183 (24), 7341–7353.

Dupre, J.M., Johnson, W.L., Ulanov, A. V., Li, Z., *et al.*, 2019. Transcriptional profiling and metabolomic analysis of *Staphylococcus aureus* grown on autoclaved chicken breast. *Food Microbiology*. 82, 46–52.

Dziarski, R. & Gupta, D., 2005. *Staphylococcus aureus* peptidoglycan is a toll-like receptor 2 activator: a reevaluation. *Infection and immunity*. 73 (8), 5212–5216.

Eichinger, V., Nussbaumer, T., Platzer, A., Jehl, M.A., *et al.*, 2016. EffectiveDB - Updates and novel features for a better annotation of bacterial secreted proteins and Type III, IV, VI secretion systems. *Nucleic Acids Research*. 44 (D1), D669–D674.

von Eiff, C., Becker, K., Machka, K., Stammer, H., *et al.*, 2001. Nasal Carriage as a Source of *Staphylococcus aureus* Bacteremia. *New England Journal of Medicine*. 344 (1), 11–16.

Ezekwe, E., Weng, C., Duncan, J., Ezekwe, E.A.D., *et al.*, 2016. ADAM10 Cell Surface Expression but Not Activity Is Critical for *Staphylococcus aureus* α-Hemolysin-Mediated Activation of the NLRP3 Inflammasome in Human Monocytes. *Toxins*. 8 (4), 95.

Farnell, M.B., Crippen, T.L., He, H., Swaggerty, C.L., *et al.*, 2003. Oxidative burst mediated by toll like receptors (TLR) and CD14 on avian heterophils stimulated with bacterial toll agonists. *Developmental and Comparative Immunology*. 27 (5), 423–429.

Fevre, C., Bestebroer, J., Mebius, M.M., de Haas, C.J.C., *et al.*, 2014. *S taphylococcus aureus* proteins SSL6 and SElX interact with neutrophil receptors as identified using secretome phage display. *Cellular Microbiology*. 16 (11), 1646–1665.

Finn, R.D., Coggill, P., Eberhardt, R.Y., Eddy, S.R., *et al.*, 2016. The Pfam protein families database: towards a more sustainable future. *Nucleic Acids Research*. 44 (D1), D279–D285.

Firon, A., Tazi, A., Da Cunha, V., Brinster, S., *et al.*, 2013. The Abi-domain Protein Abx1 Interacts with the CovS Histidine Kinase to Control Virulence Gene Expression in Group B *Streptococcus*. *PLoS Pathogens*. 9 (2), e1003179.

Fitzgerald, J.R. & Holden, M.T.G., 2016. Genomics of Natural Populations of *Staphylococcus aureus*. *Annual Review of Microbiology*. 70, 459-478.

Fitzgerald, J.R., Monday, S.R., Foster, T.J., Bohach, G.A., *et al.*, 2001. Characterization of a Putative Pathogenicity Island from Bovine *Staphylococcus*

aureus Encoding Multiple Superantigens. *Journal of Bacteriology*. 183 (1), 63–70.

Flannagan, R.S., Heit, B. & Heinrichs, D.E., 2016. Intracellular replication of *Staphylococcus aureus* in mature phagolysosomes in macrophages precedes host cell death, and bacterial escape and dissemination. *Cellular Microbiology*. 18 (4), 514–535.

Flannagan, R.S., Kuiack, R.C., McGavin, M.J. and Heinrichs, D.E., 2018. *Staphylococcus aureus* uses the GraXRS regulatory system to sense and adapt to the acidified phagolysosome in macrophages. *MBio*, *9*(4), e01143-18.

Frankel, M.B., Wojcik, B.M., DeDent, A.C., Missiakas, D.M. and Schneewind, O., 2010. ABI domain- containing proteins contribute to surface protein display and cell division in *Staphylococcus aureus. Molecular microbiology*, *78*(1), 238-252.

Fraser, J.D. & Proft, T., 2008. The bacterial superantigen and superantigen-like proteins. *Immunological Reviews*. 225 (1), 226–243.

Friedman, D.B., Stauff, D.L., Pishchany, G., Whitwell, C.W., Torres, V.J. and Skaar, E.P., 2006. S*taphylococcus aureus* redirects central metabolism to increase iron availability. *PLoS pathogens*, *2*(8), e87.

Fu, Z., Tamber, S., Memmi, G., Donegan, N.P., *et al.*, 2009. Overexpression of MazFsa in *Staphylococcus aureus* induces bacteriostasis by selectively targeting mRNAs for cleavage. *Journal of bacteriology*. 191 (7), 2051–2059.

Fukui, A., Inoue, N., Matsumoto, M., Nomura, M., *et al.*, 2001. Molecular cloning and functional characterization of chicken toll-like receptors. A single chicken toll covers multiple molecular patterns. *The Journal of biological chemistry*. 276 (50), 47143–47149.

Gallagher, D.T., Monbouquette, H.G., Schröder, I., Robinson, H., *et al.*, 2004. Structure of alanine dehydrogenase from Archaeoglobus: Active site analysis and relation to bacterial cyclodeaminases and mammalian mu crystallin. *Journal of Molecular Biology*. 342(1), 119-130.

Garceau, V., Balic, A., Garcia-Morales, C., Sauter, K.A., *et al.*, 2015. The development and maintenance of the mononuclear phagocyte system of the chick is controlled by signals from the macrophage colony-stimulating factor receptor. *BMC Biology*. 13 (1), 12.

Garceau, V., Smith, J., Paton, I.R., Davey, M., *et al.*, 2010. Pivotal Advance: Avian colony-stimulating factor 1 (*CSF-1*), interleukin-34 (*IL-34*), and *CSF-1* receptor genes and gene products. *Journal of Leukocyte Biology*. 87 (5), 753–764.

Geertsma, M.F., Nibbering, P.H., Haagsman, H.P., Daha, M.R., *et al.*, 1994. Binding of surfactant protein A to C1q receptors mediates phagocytosis of *Staphylococcus aureus* by monocytes. *American Journal of Physiology-Lung Cellular and Molecular Physiology*. 267 (5), L578–L584.

Geertz-Hansen, H.M., Blom, N., Feist, A.M., Brunak, S., *et al.*, 2014. Cofactory: Sequence-based prediction of cofactor specificity of Rossmann folds. *Proteins: Structure, Function, and Bioinformatics*. 82 (9), 1819–1828.

Geisinger, E., Chen, J. & Novick, R.P., 2012. Allele-Dependent Differences in Quorum-Sensing Dynamics Result in Variant Expression of Virulence Genes in *Staphylococcus aureus*. *Journal of Bacteriology*. 194 (11), 2854–2864.

Genovese, K.J., He, H., Swaggerty, C.L. & Kogut, M.H., 2013. The avian heterophil. *Developmental & Comparative Immunology*. 41 (3), 334–340.

Gerlach, D., Guo, Y., De Castro, C., Kim, S.-H., *et al.*, 2018. Methicillin-resistant *Staphylococcus aureus* alters cell wall glycosylation to evade immunity. *Nature*. 563(7733), 705.

Giese, B., Glowinski, F., Paprotka, K., Dittmann, S., *et al.*, 2011. Expression of δ-toxin by *Staphylococcus aureus* mediates escape from phago-endosomes of human epithelial and endothelial cells in the presence of β-toxin. *Cellular Microbiology*. 13(2), 316-329

Gill, S.R., Fouts, D.E., Archer, G.L., Mongodin, E.F., *et al.*, 2005. nsights on evolution of virulence and resistance from the complete genome analysis of an early methicillin-resistant *Staphylococcus aureus* strain and a biofilm-producing methicillin-resistant Staphylococcus epidermidis strain. *Journal of bacteriology*. 187 (7), 2426–2438.

Gillet, Y., Issartel, B., Vanhems, P., Fournet, J.-C., *et al.*, 2002. Association between *Staphylococcus aureus* strains carrying gene for Panton-Valentine leukocidin and highly lethal necrotising pneumonia in young immunocompetent patients. *The Lancet*. 359 (9308), 753–759.

Gladysheva, I.P., Turner, R.B., Sazonova, I.Y., Liu, L., *et al.*, 2003. Coevolutionary patterns in plasminogen activation. *Proceedings of the National Academy of Sciences of the United States of America*. 100 (16), 9168–9172.

Goerke, C., Köller, J. and Wolz, C., 2006. Ciprofloxacin and trimethoprim cause phage induction and virulence modulation in *Staphylococcus aureus*. *Antimicrobial agents and chemotherapy*. 50(1), 171-177.

Goerke, C., Matias y Papenberg, S., Dasbach, S., Dietz, K., *et al.* (2004) Increased Frequency of Genomic Alterations in *Staphylococcus aureus* during Chronic Infection Is in Part Due to Phage Mobilization . *The Journal of Infectious Diseases*. 189 (4), 724–734.

Goerke, C., Pantucek, R., Holtfreter, S., Schulte, B., *et al.* (2009) Diversity of prophages in dominant *Staphylococcus aureus* clonal lineages. *Journal of Bacteriology*. 50(1), 171-177.

Goerke, C. & Wolz, C., 2004. Regulatory and genomic plasticity of *Staphylococcus aureus* during persistent colonization and infection. *International Journal of Medical Microbiology*. 294 (2–3), 195–202.

Goethe, R. and Loc, P.V., 1994. The far upstream chicken lysozyme enhancer at-6.1

kilobase, by interacting with NF-M, mediates lipopolysaccharide-induced expression of the chicken lysozyme gene in chicken myelomonocytic cells. Journal of Biological Chemistry, 269(49), 31302-31309.

González-Juarbe, N., Gilley, R.P., Hinojosa, C.A., Bradley, K.M., *et al.*, 2015. Pore-Forming Toxins Induce Macrophage Necroptosis during Acute Bacterial Pneumonia Andreas Peschel (ed.). *PLOS Pathogens*. 11 (12), e1005337.

Goodman, J.L., Wang, S., Alam, S., Ruzicka, F.J., *et al.*, 2004. Ornithine cyclodeaminase: Structure, mechanism of action, and implications for the μ-crystallin family. *Biochemistry*. 43 (44), 13883–13891.

Gordon, S., 2003. Alternative activation of macrophages. *Nature Reviews Immunology*. 3 (1), 23–35.

Gorwitz, R.J., Kruszon- Moran, D., McAllister, S.K., McQuillan, G., *et al.*, 2008. Changes in the Prevalence of Nasal Colonization with *Staphylococcus aureus* in the United States, 2001–2004. *The Journal of Infectious Diseases*. 197 (9), 1226–1234.

Grayczyk, J.P. and Alonzo, F., 2019. *Staphylococcus aureus* lipoic acid synthesis limits macrophage reactive oxygen and nitrogen species production to promote survival during infection. *Infection and immunity*, IAI-00344.

Grayczyk, J.P., Harvey, C.J., Laczkovich, I. and Alonzo III, F., 2017. A lipoylated metabolic protein released by *Staphylococcus aureus* suppresses macrophage activation. *Cell host & microbe*, *22*(5), 678-687.

Grosser, M.R., Weiss, A., Shaw, L.N. and Richardson, A.R., 2016. Regulatory requirements for *Staphylococcus aureus* nitric oxide resistance. *Journal of bacteriology*, *198*(15), 2043-2055.

Grosz, M., Kolter, J., Paprotka, K., Winkler, A.C., Schäfer, D., Chatterjee, S.S., Geiger, T., Wolz, C., Ohlsen, K., Otto, M. and Rudel, T., 2014. Cytoplasmic replication of *Staphylococcus aureus* upon phagosomal escape triggered by phenol- soluble modulin α. *Cellular microbiology*, *16*(4), 451-465.

Guinane, C.M., Ben Zakour, N.L., Tormo-Mas, M.A., Weinert, L.A., *et al.*, 2010. Evolutionary Genomics of *Staphylococcus aureus* Reveals Insights into the Origin and Molecular Basis of Ruminant Host Adaptation. *Genome Biology and Evolution*. 2, 454–466.

de Haas, C.J.C., Veldkamp, K.E., Peschel, A., Weerkamp, F., *et al.*, 2004. Chemotaxis inhibitory protein of *Staphylococcus aureus*, a bacterial antiinflammatory agent. *The Journal of experimental medicine*. 199 (5), 687–695.

De Haas, C.J.C., Weeterings, C., Vughs, M.M., De Groot, P.G., Van Strijp, J.A. and Lisman, T., 2009. Staphylococcal superantigen- like 5 activates platelets and supports platelet adhesion under flow conditions, which involves glycoprotein Ibα and αIIbβ3. *Journal of Thrombosis and Haemostasis*, *7*(11), 1867-1874.

Haley, K.P. & Skaar, E.P., 2012. A battle for iron: host sequestration and

Staphylococcus aureus acquisition. *Microbes and infection*. 14 (3), 217–227.

Hall, R.J. & Erickson, C.A., 2003. ADAM 10: an active metalloprotease expressed during avian epithelial morphogenesis. *Developmental Biology*. 256 (1), 147–160.

Halsey, C.R., Lei, S., Wax, J.K., Lehman, M.K., *et al.*, 2017. Amino acid catabolism in *Staphylococcus aureus* and the function of carbon catabolite repression. *mBio*. 8 (1).

Hamza, T. and Li, B., 2014. Differential responses of osteoblasts and macrophages upon *Staphylococcus aureus* infection. *BMC microbiology*, *14*(1), 207.

Hanzelmann, D., Joo, H.-S., Franz-Wachtel, M., Hertlein, T., *et al.*, 2016. Toll-like receptor 2 activation depends on lipopeptide shedding by bacterial surfactants. *Nature Communications*. 7 (1), 12304.

Hayashi, T., Watanabe, C., Suzuki, Y., Tanikawa, T., *et al.*, 2014. Chicken MDA5 Senses Short Double-Stranded RNA with Implications for Antiviral Response against Avian Influenza Viruses in Chicken. *Journal of Innate Immunity*. 6 (1), 58–71.

He, H. & Kogut, M.H., 2003. CpG-ODN-induced nitric oxide production is mediated through clathrin-dependent endocytosis, endosomal maturation, and activation of PKC, MEK1/2 and p38 MAPK, and NF-κB pathways in avian macrophage cells (HD11). *Cellular Signalling*. 15 (10), 911–917.

He, H., Lowry, V.K., Swaggerty, C.L., Ferro, P.J., *et al.*, 2005. In vitro activation of chicken leukocytes and in vivo protection against *Salmonella enteritidis* organ invasion and peritoneal *S. enteritidis* infection-induced mortality in neonatal chickens by immunostimulatory CpG oligodeoxynucleotide. *FEMS Immunology & Medical Microbiology*. 43 (1), 81–89.

Hendrix, R.W., 2003. Bacteriophage genomics. *Current Opinion in Microbiology*. 6 (5), 506–511.

Hermans, S.J., Baker, H.M., Sequeira, R.P., Langley, R.J., *et al.*, 2012. Structural and functional properties of staphylococcal superantigen-like protein 4. *Infection and immunity*. 80 (11), 4004–4013.

Herrera, A., Kulhankova, K., Sonkar, V.K., Dayal, S., *et al.*, 2017. Staphylococcal β-toxin modulates human aortic endothelial cell and platelet function through sphingomyelinase and biofilm ligase activities. *mBio*. *8*(2), e00273-17.

Herrera, A., Vu, B.G., Stach, C.S., Merriman, J.A., Horswill, A.R., Salgado-Pabón, W. and Schlievert, P.M., 2016. *Staphylococcus aureus* β-toxin mutants are defective in biofilm ligase and sphingomyelinase activity, and causation of infective endocarditis and sepsis. *Biochemistry*, *55*(17), 2510-2517.

Herron-Olson, L., Fitzgerald, J.R., Musser, J.M. & Kapur, V. (2007a) Molecular Correlates of Host Specialization in *Staphylococcus aureus*. *PLoS ONE*. 2 (10), 1120.

Higgs, R., Cormican, P., Cahalane, S., Allan, B., *et al.*, 2006. Induction of a novel

chicken Toll-like receptor following Salmonella enterica serovar Typhimurium infection. *Infection and immunity*. 74 (3), 1692–1698.

Higuchi, M., Matsuo, A., Shingai, M., Shida, K., *et al.*, 2008. Combinational recognition of bacterial lipoproteins and peptidoglycan by chicken Toll-like receptor 2 subfamily. *Developmental & Comparative Immunology*. 32 (2), 147–155.

Hildebrand, A., Pohl, M. & Bhakdi, S., 1991. *Staphylococcus aureus* beta-toxin: Dual mechanism of binding to target cells. *Journal of Biological Chemistry*. 266 (26), 17195–17200.

Holzinger, D., Gieldon, L., Mysore, V., Nippe, N., *et al.*, 2012. *Staphylococcus aureus* Panton-Valentine leukocidin induces an inflammatory response in human phagocytes via the NLRP3 inflammasome. *Journal of Leukocyte Biology*. 92 (5), 1069–1081.

Hong, Y.H., Song, W., Lee, S.H. & Lillehoj, H.S., 2012. Differential gene expression profiles of -defensins in the crop, intestine, and spleen using a necrotic enteritis model in 2 commercial broiler chicken lines. *Poultry Science*. 91 (5), 1081–1088.

Hruz, P., Zinkernagel, A.S., Jenikova, G., Botwin, G.J., *et al.*, 2009. NOD2 contributes to cutaneous defense against *Staphylococcus aureus* through alpha-toxin-dependent innate immune activation. *Proceedings of the National Academy of Sciences of the United States of America*. 106 (31), 12873–12878.

Hughes, S., Poh, T.-Y., Bumstead, N. & Kaiser, P., 2007. Re-evaluation of the chicken MIP family of chemokines and their receptors suggests that CCL5 is the prototypic MIP family chemokine, and that different species have developed different repertoires of both the CC chemokines and their receptors. *Developmental & Comparative Immunology*. 31 (1), 72–86.

Hume, D.A., Underhill, D.M., Sweet, M.J., Ozinsky, A.O., *et al.*, 2001. Macrophages exposed continuously to lipopolysaccharide and other agonists that act via toll-like receptors exhibit a sustained and additive activation state. *BMC Immunology*. 2(1), 11.

Huseby, M., Shi, K., Brown, C.K., Digre, J., *et al.*, 2007. Structure and biological activities of beta toxin from *Staphylococcus aureus*. *Journal of bacteriology*. 189 (23), 8719–8726.

Huseby, M.J., Kruse, A.C., Digre, J., Kohler, P.L., Vocke, J.A., Mann, E.E., Bayles, K.W., Bohach, G.A., Schlievert, P.M., Ohlendorf, D.H. and Earhart, C.A., 2010. Beta toxin catalyzes formation of nucleoprotein matrix in staphylococcal biofilms. *Proceedings of the National Academy of Sciences*, *107*(32), 14407-14412.

Inoshima, I., Inoshima, N., Wilke, G.A., Powers, M.E., *et al.*, 2011. A *Staphylococcus aureus* pore-forming toxin subverts the activity of ADAM10 to cause lethal infection in mice. *Nature Medicine*. 17 (10), 1310–1314.

Inoue, N., Fukui, A., Nomura, M., Matsumoto, M., *et al.*, 2001. A novel chicken

membrane-associated complement regulatory protein: molecular cloning and functional characterization. *Journal of immunology*. 166 (1), 424–431.

Iqbal, M., Philbin, V.J., Withanage, G.S.K., Wigley, P., *et al.*, 2005. Identification and functional characterization of chicken toll-like receptor 5 reveals a fundamental role in the biology of infection with Salmonella enterica serovar typhimurium. *Infection and immunity*. 73 (4), 2344–2350.

Islam, D., Bandholtz, L., Nilsson, J., Wigzell, H., *et al.*, 2001. Downregulation of bactericidal peptides in enteric infections: A novel immune escape mechanism with bacterial DNA as a potential regulator. *Nature Medicine*. 7 (2), 180–185.

Itoh, S., Hamada, E., Kamoshida, G., Takeshita, K., *et al.*, 2010a. Staphylococcal superantigen-like protein 5 inhibits matrix metalloproteinase 9 from human neutrophils. *Infection and immunity*. 78 (7), 3298–3305.

Itoh, S., Hamada, E., Kamoshida, G., Yokoyama, R., *et al.*, 2010b. Staphylococcal superantigen-like protein 10 (SSL10) binds to human immunoglobulin G (IgG) and inhibits complement activation via the classical pathway. *Molecular Immunology*. 47 (4), 932–938.

Itoh, S., Yamaoka, N., Kamoshida, G., Takii, T., *et al.*, 2013a. Staphylococcal superantigen-like protein 8 (SSL8) binds to tenascin C and inhibits tenascin C–fibronectin interaction and cell motility of keratinocytes. *Biochemical and Biophysical Research Communications*. 433 (1), 127–132.

Itoh, S., Yokoyama, R., Kamoshida, G., Fujiwara, T., *et al.*, 2013b. Staphylococcal superantigen-like protein 10 (SSL10) inhibits blood coagulation by binding to prothrombin and factor Xa via their γ-carboxyglutamic acid (Gla) domain. *The Journal of biological chemistry*. 288 (30), 21569–21580.

Jacobsson, K., Ljungh, Å., Flock, J.-I., Bjerketorp, J., *et al.*, 2002. A novel von Willebrand factor binding protein expressed by *Staphylococcus aureus* a. *Microbiology*. 148 (7), 2037–2044.

Jevons, M.P. (1961) resistant Staphylococci. *BMJ*. 1 (5219), 124–125.

Jin, T., Bokarewa, M., Foster, T., Mitchell, J., *et al.*, 2004. *Staphylococcus aureus* Resists Human Defensins by Production of Staphylokinase, a Novel Bacterial Evasion Mechanism. *The Journal of Immunology*. 172 (2), 1169–1176.

Jin, T., Bokarewa, M. & Tarkowski, A., 2005. The role of urokinase in innate immunity against *Staphylococcus aureus*. *Microbes and Infection*. 7 (9–10), 1170–1175.

Joiner, K.S., Hoerr, F.J., van Santen, E. & Ewald, S.J., 2005. The Avian Major Histocompatibility Complex Influences Bacterial Skeletal Disease in Broiler Breeder Chickens. *Veterinary Pathology*. 42 (3), 275–281.

Jones, P., Binns, D., Chang, H.-Y., Fraser, M., *et al.*, 2014. InterProScan 5: genome-scale protein function classification. *Bioinformatics*. 30 (9), 1236–1240.

De Jong, N.W., Ramyar, K.X., Guerra, F.E., Nijland, R., Fevre, C., Voyich, J.M., McCarthy, A.J., Garcia, B.L., Van Kessel, K.P., Van Strijp, J.A. and Geisbrecht,

B.V., 2017. Immune evasion by a staphylococcal inhibitor of myeloperoxidase. *Proceedings of the National Academy of Sciences*. 114(35), 9439-9444.

De Jong, N.W., Vrieling, M., Garcia, B.L., Koop, G., Brettmann, M., Aerts, P.C., Ruyken, M., Van Strijp, J.A., Holmes, M., Harrison, E.M. and Geisbrecht, B.V., 2018. Identification of a staphylococcal complement inhibitor with broad host specificity in equid Staphylococcus aureus strains. *Journal of Biological Chemistry*. 293(12), 4468-4477.

Jongerius, I., Köhl, J., Pandey, M.K., Ruyken, M., van Kessel, K.P., van Strijp, J.A. and Rooijakkers, S.H., 2007. Staphylococcal complement evasion by various convertase-blocking molecules. *Journal of Experimental Medicine*. 204(10), 2461-2471.

Juan Hernandez-Doria, A.D. & Sperandio Correspondence, V., 2018. Bacteriophage Transcription Factor Cro Regulates Virulence Gene Expression in Enterohemorrhagic Escherichia coli. *Cell Host and Microbe*. 23, 607-617.e6.

Jubrail, J., Morris, P., Bewley, M.A., Stoneham, S., Johnston, S.A., Foster, S.J., Peden, A.A., Read, R.C., Marriott, H.M. and Dockrell, D.H., 2016. Inability to sustain intraphagolysosomal killing of Staphylococcus aureus predisposes to bacterial persistence in macrophages. *Cellular microbiology*, *18*(1), 80-96.

Juhala, R.J., Ford, M.E., Duda, R.L., Youlton, A., *et al.*, 2000. Genomic sequences of bacteriophages HK97 and HK022: pervasive genetic mosaicism in the lambdoid bacteriophages. *Journal of Molecular Biology*. 299 (1), 27–51.

Juul-Madsen, H., Munch, M., Handberg, K., Sorensen, P., *et al.*, 2003. Serum levels of mannan-binding lectin in chickens prior to and during experimental infection with avian infectious bronchitis virus. *Poultry Science*. 82 (2), 235–241.

Kahánková, J., Pantůček, R., Goerke, C., Růžičková, V., *et al.*, 2010. Multilocus PCR typing strategy for differentiation of *Staphylococcus aureus* siphoviruses reflecting their modular genome structure. *Environmental Microbiology*. 12 (9), 2527–2538.

Kaiser, P., 2010. Advances in avian immunology—prospects for disease control: a review. *Avian Pathology*, *39*(5), 309-324.

Kaiser, P., Poh, T.Y., Rothwell, L., Avery, S., *et al.*, 2005. A Genomic Analysis of Chicken Cytokines and Chemokines. *Journal of Interferon & Cytokine Research*. 25 (8), 467–484.

Kaiser, P. and Stäheli, P., 2014. Avian cytokines and chemokines. *Avian immunology*. 189-204.

Kaneko, J., Kimura, T., Narita, S., Tomita, T., *et al.*, 1998. Complete nucleotide sequence and molecular characterization of the temperate staphylococcal bacteriophage φPVL carrying Panton–Valentine leukocidin genes. *Gene*. 215 (1), 57–67.

Kang, M., Ko, Y.-P., Liang, X., Ross, C.L., *et al.*, 2013. Collagen-binding microbial

surface components recognizing adhesive matrix molecule (MSCRAMM) of Gram-positive bacteria inhibit complement activation via the classical pathway. *The Journal of biological chemistry*. 288 (28), 20520–20531.

Kannaki, T.R., Reddy, M.R., Shanmugam, M., Verma, P.C. and Sharma, R.P., 2010. Chicken toll-like receptors and their role in immunity. *World's poultry science journal*, *66*(4), 727-738.

Kannan, L., Rath, N.C., Liyanage, R. & Lay, J.O., 2009.Direct screening identifies mature beta-defensin 2 in avian heterophils. *Poultry Science*. 88 (2), 372–379.

Kapetanovic, R., Fairbairn, L., Beraldi, D., Sester, D.P., *et al.*, 2012. Pig Bone Marrow-Derived Macrophages Resemble Human Macrophages in Their Response to Bacterial Lipopolysaccharide. *The Journal of Immunology*. 188 (7), 3382–3394.

Karavolos, M.H., Horsburgh, M.J., Ingham, E. & Foster, S.J., 2003. Role and regulation of the superoxide dismutases of *Staphylococcus aureus*. *Microbiology*. 149 (10), 2749–2758.

Karray, A., Ali, Y. Ben, Gargouri, Y. & Bezzine, S., 2011. Antibacterial properties of chicken intestinal phospholipase A2. *Lipids in health and disease*. 10, 4.

Kaspers, B. and Kaiser, P., 2014. Avian antigen-presenting cells. In *Avian immunology* (pp. 169-188). Academic Press.

Katayama, Y., Baba, T., Sekine, M., Fukuda, M. and Hiramatsu, K., 2013. Beta-hemolysin promotes skin colonization by Staphylococcus aureus. *Journal of bacteriology*. 195(6), 1194-1203.

Kawai, T. & Akira, S., 2010. The role of pattern-recognition receptors in innate immunity: update on Toll-like receptors. *Nature Immunology*. 11 (5), 373–384.

Kebaier, C., Chamberland, R.R., Allen, I.C., Gao, X., Broglie, P.M., Hall, J.D., Jania, C., Doerschuk, C.M., Tilley, S.L. and Duncan, J.A., 2012. *Staphylococcus aureus* α-hemolysin mediates virulence in a murine model of severe pneumonia through activation of the NLRP3 inflammasome. *Journal of Infectious Diseases*. 205(5), 807-817.

Keestra, A.M., de Zoete, M.R., Bouwman, L.I. & van Putten, J.P.M., 2010. Chicken TLR21 is an innate CpG DNA receptor distinct from mammalian TLR9. *Journal of immunology*. 185 (1), 460–467.

Keestra, A.M., de Zoete, M.R., Bouwman, L.I., Vaezirad, M.M. and van Putten, J.P., 2013. Unique features of chicken Toll-like receptors. *Developmental & Comparative Immunology*, *41*(3), 316-323.

van Kessel, K.P.M., Bestebroer, J. & van Strijp, J.A.G., 2014. Neutrophil-Mediated Phagocytosis of *Staphylococcus aureus*. *Frontiers in Immunology*. 5, 467.

Kim, N.J., Ahn, K.B., Jeon, J.H., Yun, C.-H., *et al.*, 2015. Lipoprotein in the cell wall of *Staphylococcus aureus* is a major inducer of nitric oxide production in murine macrophages. *Molecular Immunology*. 65 (1), 17–24.

Kim, R.Y., Gassert, R. & Wistow, G.J., 1992. u-Crystallin is a mammalian homologue of Agrobacterium ornithine cyclodeaminase and is expressed in human retina. *Evolution*. 89, 9292–92.

Kim, S., Miska, K.B., Jenkins, M.C., Fetterer, R.H., *et al.*, 2010. Molecular cloning and functional characterization of the avian macrophage migration inhibitory factor (MIF). *Developmental & Comparative Immunology*. 34 (9), 1021–1032.

Kim, Y.B., Seo, K.W., Jeon, H.Y., Lim, S.-K., *et al.*, 2018. Characteristics of the antimicrobial resistance of *Staphylococcus aureus* isolated from chicken meat produced by different integrated broiler operations in Korea. *Poultry Science*. 97 (3), 962–969.

Kirby, W.M., 1944. Extraction of a highly potent penicillin inactivator from penicillin resistant staphylococci. *Science*. 99(2579), 452-453.

Kitur, K., Wachtel, S., Brown, A., Wickersham, M., Paulino, F., Peñaloza, H.F., Soong, G., Bueno, S., Parker, D. and Prince, A., 2016. Necroptosis promotes *Staphylococcus aureus* clearance by inhibiting excessive inflammatory signaling. *Cell reports*, *16*(8), 2219-2230.

Kjalke, M., Welinder, K.G. & Koch, C., 1993. Structural analysis of chicken factor B-like protease and comparison with mammalian complement proteins factor B and C2. *Journal of immunology*. 151 (8), 4147–4152.

Kneidl, J., Löffler, B., Erat, M.C., Kalinka, J., *et al.*, 2012. Soluble CD163 promotes recognition, phagocytosis and killing of *Staphylococcus aureus* via binding of specific fibronectin peptides. *Cellular Microbiology*. 14 (6), 914–936.

Knuefermann, P., Sakata, Y., Baker, J.S., Huang, C.-H., *et al.*, 2004. Toll-like receptor 2 mediates *Staphylococcus aureus*-induced myocardial dysfunction and cytokine production in the heart. *Circulation*. 110 (24), 3693–3698.

Ko, Y.-P., Kuipers, A., Freitag, C.M., Jongerius, I., *et al.*, 2013. Phagocytosis Escape by a *Staphylococcus aureus* Protein That Connects Complement and Coagulation Proteins at the Bacterial Surface Eric P. Skaar (ed.). *PLoS Pathogens*. 9 (12), e1003816.

Kogut, M.H., McGruder, E.D., Hargis, B.M., Corner, D.E. and DeLoach, J.R., 1995. In vivo activation of heterophil function in chickens following injection with Salmonella enteritidis- immune lymphokines. *Journal of Leukocyte Biology*, *57*(1), 56-62.

Kogut, M.H., Iqbal, M., He, H., Philbin, V., Kaiser, P. and Smith, A., 2005. Expression and function of Toll-like receptors in chicken heterophils. *Developmental & Comparative Immunology*, *29*(9), 791-807.

Kobylarz, M.J., Grigg, J.C., Takayama, S.J., Rai, D.K., *et al.*, 2014. Synthesis of L-2,3-Diaminopropionic Acid, a Siderophore and Antibiotic Precursor. *Chemistry & Biology*. 21 (3), 379–388.

Kodigepalli, K.M. & Nanjundan, M., 2015. Induction of PLSCR1 in a STING/IRF3-Dependent Manner upon Vector Transfection in Ovarian Epithelial Cells Tony

Wang. *PLOS ONE*. 10 (2), e0117464.

Kolar, S.L., Antonio Ibarra, J., Rivera, F.E., Mootz, J.M., *et al.*, 2013. Extracellular proteases are key mediators of *Staphylococcus aureus* virulence via the global modulation of virulence-determinant stability. *MicrobiologyOpen*. 2 (1), 18–34.

Koop, G., Vrieling, M., Storisteanu, D.M., Lok, L.S., Monie, T., Van Wigcheren, G., Raisen, C., Ba, X., Gleadall, N., Hadjirin, N. and Timmerman, A.J., 2017. Identification of LukPQ, a novel, equid-adapted leukocidin of S*taphylococcus aureus*. *Scientific reports*, *7*, 40660.

Koymans, K., Bisschop, A., Vughs, M., van Kessel, K., de Haas, C. and van Strijp, J., 2016. Staphylococcal superantigen-like protein 1 and 5 (SSL1 & SSL5) limit neutrophil chemotaxis and migration through MMP-inhibition. *International journal of molecular sciences*, *17*(7), 1072.

Koymans, K.J., Feitsma, L.J., Bisschop, A., Huizinga, E.G., van Strijp, J.A., de Haas, C.J. and McCarthy, A.J., 2018. Molecular basis determining species specificity for TLR2 inhibition by staphylococcal superantigen-like protein 3 (SSL3). *Veterinary research*, *49*(1), 115.

Koymans, K.J., Goldmann, O., Karlsson, C.A., Sital, W., Thänert, R., Bisschop, A., Vrieling, M., Malmström, J., van Kessel, K.P., De Haas, C.J. and Van Strijp, J.A., 2017. The TLR2 antagonist staphylococcal superantigen-like protein 3 acts as a virulence factor to promote bacterial pathogenicity in vivo. *Journal of innate immunity*, *9*(6), 561-573.

Koziel, J., Chmiest, D., Bryzek, D., Kmiecik, K., Mizgalska, D., Maciag-Gudowska, A., Shaw, L.N. and Potempa, J., 2015. The Janus Face of a-Toxin: A Potent Mediator of Cytoprotection in Staphylococci-Infected Macrophages. *Journal of innate immunity*, *7*(2), 187-198.

Krogh, A., Larsson, B., von Heijne, G. & Sonnhammer, E.L.., 2001. Predicting transmembrane protein topology with a hidden markov model: application to complete genomes. *Journal of Molecular Biology*. 305 (3), 567–580.

Krute, C.N., Carroll, R.K., Rivera, F.E., Weiss, A., *et al.*, 2015. The disruption of prenylation leads to pleiotropic rearrangements in cellular behavior in *S taphylococcus aureus*. *Molecular Microbiology*. 95 (5), 819–832.

Kubica, M., Guzik, K., Koziel, J., Zarebski, M., Richter, W., Gajkowska, B., Golda, A., Maciag-Gudowska, A., Brix, K., Shaw, L. and Foster, T., 2008. A potential new pathway for Staphylococcus aureus dissemination: the silent survival of *S. aureus* phagocytosed by human monocyte-derived macrophages. *PloS one*, *3*(1), e1409.

Kuroda, M., Ohta, T., Uchiyama, I., Baba, T., *et al.*, 2001. Whole genome sequencing of meticillin-resistant *Staphylococcus aureus*. *Lancet*. 357 (9264), 1225–1240.

Kwan, T., Liu, J., DuBow, M., Gros, P., *et al.*, 2005. The complete genomes and proteomes of 27 *Staphylococcus aureus* bacteriophages. *Proceedings of the National Academy of Sciences of the United States of America*. 102 (14), 5174–

5179.

Laarman, A.J., Mijnheer, G., Mootz, J.M., Rooijen, W.J.M. van, *et al.*, 2012. *Staphylococcus aureus* Staphopain A inhibits CXCR2-dependent neutrophil activation and chemotaxis. *The EMBO Journal*. 31 (17), 3607.

Laarman, A.J., Ruyken, M., Malone, C.L., van Strijp, J.A.G., *et al.*, 2011a. *Staphylococcus aureus* metalloprotease aureolysin cleaves complement C3 to mediate immune evasion. *Journal of immunology (Baltimore, Md. : 1950)*. 186 (11), 6445–6453.

Langley, R., Wines, B., Willoughby, N., Basu, I., *et al.*, 2005. The Staphylococcal Superantigen-Like Protein 7 Binds IgA and Complement C5 and Inhibits IgA-FcαRI Binding and Serum Killing of Bacteria. *The Journal of Immunology*. 174 (5), 2926–2933.

Laursen, I. & Koch, C., 1989. Purification of chicken C3 and a structural and functional characterization. *Scandinavian journal of immunology*. 30 (5), 529–538.

Laursen, N.S., Gordon, N., Hermans, S., Lorenz, N., *et al.*, 2010.Structural basis for inhibition of complement C5 by the SSL7 protein from *Staphylococcus aureus*. *Proceedings of the National Academy of Sciences of the United States of America*. 107 (8), 3681–3686.

Lawrence, D.W. & Kornbluth, J., 2018. Reduced inflammation and cytokine production in NKLAM deficient mice during Streptococcus pneumoniae infection. *PLoS ONE*. 13 (3).

Ledala, N., Zhang, B., Seravalli, J., Powers, R. and Somerville, G.A., 2014. Influence of iron and aeration on *Staphylococcus aureus* growth, metabolism, and transcription. *Journal of bacteriology*, *196*(12), 2178-2189.

Lee, C.Y. & Buranen, S.L., 1989. Extent of the DNA sequence required in integration of staphylococcal bacteriophage L54a. *Journal of bacteriology*. 171 (3), 1652–1657.

Lee, P.K., Kreiswirth, B.N., Deringer, J.R., Projan, S.J., *et al.*, 1992. Nucleotide Sequences and Biologic Properties of Toxic Shock Syndrome Toxin 1 from Ovine- and Bovine-Associated *Staphylococcus aureus*. *Journal of Infectious Diseases*. 165 (6), 1056–1063.

Lee, S.Y., Cho, J.Y., Lee, H.J., Kim, Y.H. and Min, J., 2010. Enhancement of ornithine production in proline-supplemented Corynebacterium glutamicum by ornithine cyclodeaminase. *Journal of microbiology and biotechnology*, *20*(1), 127-131.

Letunic, I. and Bork, P., 2019. Interactive Tree Of Life (iTOL) v4: recent updates and new developments. *Nucleic acids research*.

Leveque, G., Forgetta, V., Morroll, S., Smith, A.L., *et al.*, 2003. Allelic variation in TLR4 is linked to susceptibility to *Salmonella enterica* serovar Typhimurium infection in chickens. *Infection and immunity*. 71 (3), 1116–1124.

Lewandowska-Sabat, A.M., Boman, G.M., Downing, A., Talbot, R., *et al.*, 2013. The early phase transcriptome of bovine monocyte-derived macrophages infected with *Staphylococcus aureus* in vitro. *BMC Genomics*. 14(1), 891.

Li, H., Handsaker, B., Wysoker, A., Fennell, T., *et al.*, 2009. The Sequence Alignment/Map format and SAMtools. *Bioinformatics*. 25 (16), 2078–2079.

Li, X., Swaggerty, C.L., Kogut, M.H., Chiang, H.I., *et al.*, 2012. Systemic response to *Campylobacter jejuni* infection by profiling gene transcription in the spleens of two genetic lines of chickens. *Immunogenetics*. 64 (1), 59–69.

Lian, L., Ciraci, C., Chang, G., Hu, J., *et al.*, 2012. NLRC5 knockdown in chicken macrophages alters response to LPS and poly (I:C) stimulation. *BMC veterinary research*. 8, 23.

Liao, Y., Smyth, G.K. & Shi, W., 2014. featureCounts: an efficient general purpose program for assigning sequence reads to genomic features. *Bioinformatics*. 30 (7), 923–930.

Lin, A.W., Chang, C.C. and McCormick, C.C., 1996. Molecular cloning and expression of an avian macrophage nitric-oxide synthase cDNA and the analysis of the genomic 5′-flanking region. *Journal of Biological Chemistry*. 271(20), 11911-11919.

Lindsay, J.A. & Holden, M.T.G., 2004. *Staphylococcus aureus*: superbug, super genome? *Trends in Microbiology*. 12 (8), 378–385.

Lindsay, J.A. & Holden, M.T.G., 2006. Understanding the rise of the superbug: investigation of the evolution and genomic variation of *Staphylococcus aureus*. *Functional & Integrative Genomics*. 6 (3), 186–201.

Lindsay, J.A., 2014. *Staphylococcus aureus* genomics and the impact of horizontal gene transfer. *International Journal of Medical Microbiology*, *304*(2), pp.103-109.

Liu, P.T., Stenger, S., Li, H., Wenzel, L., *et al.*, 2006. Toll-like receptor triggering of a vitamin D-mediated human antimicrobial response. *Science*. 311 (5768), 1770–1773.

Lizak, M. & Yarovinsky, T.O., 2012. Phospholipid Scramblase 1 Mediates Type I Interferon-Induced Protection against Staphylococcal α-Toxin. *Cell Host & Microbe*. 11 (1), 70–80.

Lou, J., Li, X., Huang, W., Liang, J., *et al.*, 2017. SNX10 promotes phagosome maturation in macrophages and protects mice against *Listeria monocytogenes* infection. *Oncotarget*. 8 (33).

Lowder, B. V, Guinane, C.M., Ben Zakour, N.L., Weinert, L.A., *et al.*, 2009. Recent human-to-poultry host jump, adaptation, and pandemic spread of *Staphylococcus aureus*. *Proceedings of the National Academy of Sciences of the United States of America*. 106 (46), 19545–19550.

Lowy, F.D., 1998. *Staphylococcus aureus* Infections. *New England Journal of Medicine*. 339 (8), 520–532.

Luberto, C., Yoo, D.S., Suidan, H.S., Bartoli, G.M. and Hannun, Y.A., 2000. Differential effects of sphingomyelin hydrolysis and resynthesis on the activation of NF-κB in normal and SV40-transformed human fibroblasts. *Journal of Biological Chemistry*, 275(19), 14760-14766.

Lynch, N.J., Khan, S.-H., Stover, C.M., Sandrini, S.M., *et al.*, 2005. Composition of the Lectin Pathway of Complement in Gallus gallus: Absence of Mannan-Binding Lectin-Associated Serine Protease-1 in Birds. *The Journal of Immunology*. 174 (8), 4998–5006.

Lynn, D.J., Higgs, R., Gaines, S., Tierney, J., *et al.*, 2004. Bioinformatic discovery and initial characterisation of nine novel antimicrobial peptide genes in the chicken. *Immunogenetics*. 56 (3), 170–177.

De Jong, N.W., Ploscariu, N.T., Ramyar, K.X., Garcia, B.L., Herrera, A.I., Prakash, O., Katz, B.B., Leidal, K.G., Nauseef, W.M., Van Kessel, K.P. and Van Strijp, J.A., 2018. A structurally dynamic N-terminal region drives function of the staphylococcal peroxidase inhibitor (SPIN). *Journal of Biological Chemistry*, *293*(7), 2260-2271.

Ma, Y.G., Cho, M.Y., Zhao, M., Park, J.W., *et al.*, 2004. Human mannose-binding lectin and L-ficolin function as specific pattern recognition proteins in the lectin activation pathway of complement. *The Journal of biological chemistry*. 279 (24), 25307–25312.

Malachowa, N. & DeLeo, F.R., 2010. Mobile genetic elements of *Staphylococcus aureus*. *Cellular and molecular life sciences : CMLS*. 67 (18), 3057–3071.

Mao, X., Cai, T., Olyarchuk, J.G. and Wei, L., 2005. Automated genome annotation and pathway identification using the KEGG Orthology (KO) as a controlled vocabulary. *Bioinformatics*, *21*(19), 3787-3793.

Marchler-Bauer, A. & Bryant, S.H., 2004. CD-Search: protein domain annotations on the fly. *Nucleic Acids Research*. 32 (Web Server), W327–W331.

Marroquin, S., Gimza, B., Tomlinson, B., Stein, M., Frey, A., Keogh, R.A., Zapf, R., Todd, D.A., Cech, N.B., Carroll, R.K. and Shaw, L.N., 2019. MroQ is a Novel Abi-domain Protein That Influences Virulence Gene Expression in *Staphylococcus aureus* via Modulation of Agr Activity. *Infection and immunity*, *87*(5), e00002-19.

Martin, F.J., Gomez, M.I., Wetzel, D.M., Memmi, G., *et al.*, 2009. *Staphylococcus aureus* activates type I IFN signaling in mice and humans through the Xr repeated sequences of protein A. *The Journal of clinical investigation*. 119 (7), 1931–1939.

Mavroidis, M., Sunyer, J.O. & Lambris, J.D., 1995. Isolation, primary structure, and evolution of the third component of chicken complement and evidence for a new member of the alpha 2-macroglobulin family. *Journal of immunology*. 154 (5), 2164–2174.

McCarthy, A.J. and Lindsay, J.A., 2013. *Staphylococcus aureus* innate immune evasion is lineage-specific: a bioinfomatics study. *Infection, Genetics and*

Evolution, *19*, 7-14.

McNamee, P.T. & Smyth, J.A., 2000. Bacterial chondronecrosis with osteomyelitis ('femoral head necrosis') of broiler chickens: A review. *Avian Pathology*. 29 (5), 477–495.

Meade, K.G., Narciandi, F., Cahalane, S., Reiman, C., *et al.*, 2009. Comparative in vivo infection models yield insights on early host immune response to *Campylobacter* in chickens. *Immunogenetics*. 61 (2), 101–110.

Melehani, J.H. and Duncan, J.A., 2016. Inflammasome activation can mediate tissue-specific pathogenesis or protection in *Staphylococcus aureus* infection. In Inflammasome Signaling and Bacterial Infections (pp. 257-282). Springer, Cham.

Melehani, J.H., James, D.B., DuMont, A.L., Torres, V.J. and Duncan, J.A., 2015. *Staphylococcus aureus* leukocidin A/B (LukAB) kills human monocytes via host NLRP3 and ASC when extracellular, but not intracellular. *PLoS pathogens*, 11(6), e1004970.

Merle, N.S., Church, S.E., Fremeaux-Bacchi, V. & Roumenina, L.T., 2015. Complement System Part I Molecular Mechanisms of Activation and Regulation. *Frontiers in Immunology*. 6, 262.

Miettinen, T.P. & Björklund, M., 2015. Mevalonate Pathway Regulates Cell Size Homeostasis and Proteostasis through Autophagy. *Cell Reports*. 13 (11), 2610–2620.

Miyauchi, J., Sasadaira, H., Watanabe, K. & Watanabe, Y., 1985. Ultrastructural immunocytochemical localization of lysozyme in human monocytes and macrophages. *Cell and Tissue Research*. 242 (2), 269–277.

Mkize, N., Zishiri, O.T. & Mukaratirwa, S., 2017. Genetic characterisation of antimicrobial resistance and virulence genes in *Staphylococcus aureus* isolated from commercial broiler chickens in the Durban metropolitan area, South Africa. *Journal of the South African Veterinary Association*. 88 (0), e1–e7.

Mnich, M.E., van Dalen, R., Gerlach, D., Hendriks, A., *et al.*, 2019. The C-Type Lectin Receptor MGL senses *N* -acetylgalactosamine on the unique *Staphylococcus aureus* ST395 Wall Teichoic Acid. *Cellular Microbiology*. e13072.

Mölne, L. & Tarkowski, A., 2000. An experimental model of cutaneous infection induced by superantigen- producing *Staphylococcus aureus*. *Journal of Investigative Dermatology*. 114 (6), 1120–1125.

Monecke, S., Ruppelt, A., Wendlandt, S., Schwarz, S., *et al.*, 2013. Genotyping of *Staphylococcus aureus* isolates from diseased poultry. *Veterinary Microbiology*. 162 (2–4), 806–812.

Moon, B.Y., Park, J.Y., Hwang, S.Y., Robinson, D.A., *et al.*, 2015. Phage-mediated horizontal transfer of a *Staphylococcus aureus* virulence-associated genomic island. *Scientific Reports*. 5 (1), 9784.

Morita, C., Okada, T., Izawa, H. & Soekawa, M., 1976. Agarose Droplet Method of Macrophage Migration-Inhibition Test for Newcastle Disease Virus in Chickens. *Avian Diseases*. 20 (2), 230.

Müller, S., Faulhaber, A., Sieber, C., Pfeifer, D., Hochberg, T., Gansz, M., Deshmukh, S.D., Dauth, S., Brix, K., Saftig, P. and Peters, C., 2014. The endolysosomal cysteine cathepsins L and K are involved in macrophage-mediated clearance of Staphylococcus aureus and the concomitant cytokine induction. *The FASEB Journal*. 28(1), 162-175.

Münzenmayer, L., Geiger, T., Daiber, E., Schulte, B., *et al.*, 2016. Influence of Sae-regulated and Agr-regulated factors on the escape of *Staphylococcus aureus* from human macrophages. *Cellular Microbiology*. 18 (8), 1172–1183.

Murray, S., Pascoe, B., Meric, G., Mageiros, L., Yahara, K., Hitchings, M.D., Friedmann, Y., Wilkinson, T.S., Gormley, F.J., Mack, D. and Bray, J.E., 2017. Recombination-mediated host adaptation by avian *Staphylococcus aureus*. *Genome biology and evolution*. 9(4), 830-842.

Nairn, M.E. and Watson, A.R.A., 1972. Leg weakness of poultry—A clinical and pathological characterisation. *Australian Veterinary Journal*, 48(12), 645-656.

Nagase, N., Sasaki, A., Yamashita, K., Shimizu, A., *et al.*, 2002. Isolation and Species Distribution of Staphylococci from Animal and Human Skin. *J. Vet. Med. Sci*. 64 (3).

Nandi, A., Dey, S., Biswas, J., Jaiswal, P., Naaz, S., Yasmin, T. and Bishayi, B., 2015. Differential induction of inflammatory cytokines and reactive oxygen species in murine peritoneal macrophages and resident fresh bone marrow cells by acute *Staphylococcus aureus* infection: contribution of toll-like receptor 2 (TLR2). *Inflammation*. 38(1), pp.224-244.

Naumann, M., 2000. Nuclear factor-κB activation and innate immune response in microbial pathogen infection. *Biochemical Pharmacology*. 60 (8), 1109–1114.

Nemeghaire, S., Roelandt, S., Argudín, M.A., Haesebrouck, F., *et al.*, 2013. Characterization of methicillin-resistant *Staphylococcus aureus* from healthy carrier chickens. *Avian Pathology*. 42 (4), 342–346.

Nguyen, L.T. & Vogel, H.J., 2016. Staphylokinase has distinct modes of interaction with antimicrobial peptides, modulating its plasminogen-activation properties. *Scientific Reports*. 6 (1), 31817.

Novick, R.P., 2003. Mobile genetic elements and bacterial toxinoses: the superantigen-encoding pathogenicity islands of *Staphylococcus aureus*. *Plasmid*. 49 (2), 93–105.

Novick, R.P. and Subedi, A., 2007. The SaPIs: mobile pathogenicity islands of Staphylococcus. In *Superantigens and Superallergens* (Vol. 93, pp. 42-57). Karger Publishers.

Nygaard, T.K., Pallister, K.B., DuMont, A.L., DeWald, M., *et al.*, 2012. Alpha-Toxin Induces Programmed Cell Death of Human T cells, B cells, and

Monocytes during USA300 Infection. *PLoS ONE*. 7 (5), e36532.

Ohta, H., Yoshikawa, Y., Kai, C., Yamanouchi, K., *et al.*, 1984. Lysis of horse red blood cells mediated by antibody-independent activation of the alternative pathway of chicken complement. *Immunology*. 52 (3), 437–444.

Oppenheim, A.B., Kobiler, O., Stavans, J., Court, D.L. and Adhya, S., 2005. Switches in bacteriophage lambda development. *Annu. Rev. Genet.*. 39, 409-429.

Osmundson, J., Montero-Diez, C., Westblade, L.F., Hochschild, A., *et al.*, 2012. Promoter-Specific Transcription Inhibition in *Staphylococcus aureus* by a Phage Protein. *Cell*. 151 (5), 1005–1016.

Otter, J.A. & French, G.L., 2010. Molecular epidemiology of community-associated meticillin-resistant *Staphylococcus aureus* in Europe. *The Lancet Infectious Diseases*. 10 (4), 227–239.

Parker, A. & Kaufman, J., 2017. What chickens might tell us about the MHC class II system. *Current Opinion in Immunology*. 46, 23–29.

Parker, D. & Prince, A., 2012. *Staphylococcus aureus* induces type I IFN signaling in dendritic cells via TLR9. *Journal of immunology*. 189 (8), 4040–4046.

Patel, D., Wines, B.D., Langley, R.J. & Fraser, J.D., 2010. Specificity of staphylococcal superantigen-like protein 10 toward the human IgG1 Fc domain. *Journal of immunology*. 184 (11), 6283–6292.

Pei, J. & Grishin, N. V, 2001. Type II CAAX prenyl endopeptidases belong to a novel superfamily of putative membrane-bound metalloproteases. *Trends in Biochemical Sciences*. 26 (5), 275–277.

Pelz, A., Wieland, K.-P., Putzbach, K., Hentschel, P., *et al.*, 2005. Structure and biosynthesis of staphyloxanthin from *Staphylococcus aureus*. *The Journal of biological chemistry*. 280 (37), 32493–32498.

Penadés, J.R., Chen, J., Quiles-Puchalt, N., Carpena, N., *et al.*, 2015. Bacteriophage-mediated spread of bacterial virulence genes. *Current Opinion in Microbiology*. 23, 171–178.

Penniall, R. & Spitznagel, J.K., 1975. Chicken neutrophils: oxidative metabolism in phagocytic cells devoid of myeloperoxidase. *Proceedings of the National Academy of Sciences of the United States of America*. 72 (12), 5012–5015.

Pernet, E., Brunet, J., Guillemot, L., Chignard, M., *et al.*, 2015. *Staphylococcus aureus* Adenosine Inhibits sPLA2-IIA–Mediated Host Killing in the Airways. *The Journal of Immunology*. 194 (11), 5312–5319.

Peschel, A., Jack, R.W., Otto, M., Collins, L. V, *et al.*, 2001.*Staphylococcus aureus* resistance to human defensins and evasion of neutrophil killing via the novel virulence factor MprF is based on modification of membrane lipids with l-lysine. *The Journal of experimental medicine*. 193 (9), 1067–1076.

Peschel, A., Otto, M., Jack, R.W., Kalbacher, H., *et al.*, 1999. Inactivation of the dlt

operon in *Staphylococcus aureus* confers sensitivity to defensins, protegrins, and other antimicrobial peptides. *The Journal of biological chemistry*. 274 (13), 8405–8410.

Peschel, A. & Sahl, H.-G., 2006. The co-evolution of host cationic antimicrobial peptides and microbial resistance. *Nature Reviews Microbiology*. 4 (7), 529–536.

Petersen, T.N., Brunak, S., von Heijne, G. & Nielsen, H., 2011. SignalP 4.0: discriminating signal peptides from transmembrane regions. *Nature Methods*. 8 (10), 785–786.

Peton, V. & Le Loir, Y., 2014. *Staphylococcus aureus* in veterinary medicine. *Infection, Genetics and Evolution*. 21, 602–615.

Philbin, V.J., Iqbal, M., Boyd, Y., Goodchild, M.J., *et al.*, 2005. Identification and characterization of a functional, alternatively spliced Toll-like receptor 7 (TLR7) and genomic disruption of TLR8 in chickens. *Immunology*. 114 (4), 507–521.

Ploscariu, N.T., de Jong, N.W.M., van Kessel, K.P.M., van Strijp, J.A.G., *et al.*, 2018. Identification and structural characterization of a novel myeloperoxidase inhibitor from Staphylococcus delphini. *Archives of Biochemistry and Biophysics*. 645, 1–11.

Pollitt, E.J., Szkuta, P.T., Burns, N. and Foster, S.J., 2018. *Staphylococcus aureus* infection dynamics. PLoS pathogens, 14(6), p.e1007112.

Poupel, O., Proux, C., Jagla, B., Msadek, T. and Dubrac, S., 2018. SpdC, a novel virulence factor, controls histidine kinase activity in *Staphylococcus aureus.* PLoS pathogens, 14(3), e1006917.

Powers, J.-P.S. & Hancock, R.E.., 2003. The relationship between peptide structure and antibacterial activity. *Peptides*. 24 (11), 1681–1691.

Price, L.B., Stegger, M., Hasman, H., Aziz, M., *et al.*, 2012b. *Staphylococcus aureus* CC398: Host Adaptation and Emergence of Methicillin Resistance in Livestock. *mBio*. 3 (1), e00305-11.

Provan, H.M., 2011. Molecular pathogenesis of avian *Staphylococcus aureus* infection.

Rabinovich, L., Sigal, N., Borovok, I., Nir-Paz, R. and Herskovits, A.A., 2012. Prophage excision activates Listeria competence genes that promote phagosomal escape and virulence. *Cell*, 150(4), 792-802.

Rahman, O., Cummings, S.P., Harrington, D.J. & Sutcliffe, I.C., 2008. Methods for the bioinformatic identification of bacterial lipoproteins encoded in the genomes of Gram-positive bacteria. *World Journal of Microbiology and Biotechnology*. 24 (11), 2377–2382.

Ratcliffe, M.J. and Härtle, S., 2014. B cells, the bursa of Fabricius and the generation of antibody repertoires. *Avian immunology*, 65-89.

Resch, G., François, P., Morisset, D., Stojanov, M., Bonetti, E.J., Schrenzel, J., Sakwinska, O. and Moreillon, P., 2013. Human-to-bovine jump of *Staphylococcus aureus* CC8 is associated with the loss of a β-hemolysin converting prophage and the acquisition of a new staphylococcal cassette chromosome. PLoS One, 8(3), e58187.

Reyes-Robles, T., Alonzo, F., Kozhaya, L., Lacy, D.B., *et al.*, 2013. *Staphylococcus aureus* Leukotoxin ED Targets the Chemokine Receptors CXCR1 and CXCR2 to Kill Leukocytes and Promote Infection. *Cell Host & Microbe*. 14 (4), 453–459.

Ribeiro, C.M., Stefani, L.M., Lucheis, S.B., Okano, W., Cruz, J.C.M., Souza, G.V., Casagrande, T.A., Bastos, P.A.S., Pinheiro, R.R., Arruda, M.M. and Afreixo, V., 2018. Methicillin-Resistant *Staphylococcus aureus* in Poultry and Poultry Meat: A Meta-Analysis. *Journal of food protection*. 81(7), 1055-1062.

Richardson, A.R., Dunman, P.M. and Fang, F.C., 2006. The nitrosative stress response of *Staphylococcus aureus* is required for resistance to innate immunity. *Molecular microbiology*. 61(4), 927-939.

Richardson, A.R., Libby, S.J. & Fang, F.C., 2008a. A Nitric Oxide-Inducible Lactate Dehydrogenase Enables *Staphylococcus aureus* to Resist Innate Immunity. *Science*. 319 (5870), 1672–1676.

Richardson, A.R., Libby, S.J. & Fang, F.C., 2008b. DNA deaminating ability and genotoxicity of nitric oxide and its progenitors. *Science*. 254 (5034), 1001–1003.

Richardson, E.J., Bacigalupe, R., Harrison, E.M., Weinert, L.A., *et al.*, 2018. Gene exchange drives the ecological success of a multi-host bacterial pathogen. *Nature Ecology and Evolution*. 2 (9), 1468–1478.

Roach, J.C., Glusman, G., Rowen, L., Kaur, A., *et al.*, 2005. The evolution of vertebrate Toll-like receptors. *Proceedings of the National Academy of Sciences of the United States of America*. 102 (27), 9577–9582.

Robinson, M.D., McCarthy, D.J. & Smyth, G.K., 2010. edgeR: a Bioconductor package for differential expression analysis of digital gene expression data. *Bioinformatics*. 26 (1), 139–140.

Rodgers, J.D., McCullagh, J.J., McNamee, P.T., Bell, C., *et al.*, 2003. Recovery of pathogenic *Staphylococcus aureus* from broiler hatchery air samples. *The Veterinary record*. 153 (21), 656–657.

Rohmer, L., Fong, C., Abmayr, S., Wasnick, M., *et al.*, 2007. Comparison of *Francisella tularensis* genomes reveals evolutionary events associated with the emergence of human pathogenic strains. *Genome Biology*. 8 (6), R102.

Rooijakkers, S.H.M., Ruyken, M., Roos, A., Daha, M.R., *et al.*, 2005. Immune evasion by a staphylococcal complement inhibitor that acts on C3 convertases. *Nature Immunology*. 6 (9), 920–927.

Sadovskaya, I., Vinogradov, E., Flahaut, S., Kogan, G., *et al.*, 2005. Extracellular

carbohydrate-containing polymers of a model biofilm-producing strain, *Staphylococcus epidermidis* RP62A. *Infection and immunity*. 73 (5), 3007–3017.

Salgado-Pabón, W., Herrera, A., Vu, B.G., Stach, C.S., Merriman, J.A., Spaulding, A.R. and Schlievert, P.M., 2014. *Staphylococcus aureus* β-toxin production is common in strains with the β-toxin gene inactivated by bacteriophage. *The Journal of infectious diseases*, 210(5), 84-792.

Schauber, J., Modlin, R.L., Gallo, R.L., Dorschner, R.A., *et al.*, 2007. Injury enhances TLR2 function and antimicrobial peptide expression through a vitamin D-dependent mechanism. *The Journal of Clinical Investigation*. 117 (3).

Scherr, T.D., Hanke, M.L., Huang, O., James, D.B., Horswill, A.R., Bayles, K.W., Fey, P.D., Torres, V.J. and Kielian, T., 2015. *Staphylococcus aureus* biofilms induce macrophage dysfunction through leukocidin AB and alpha-toxin. *MBio*, 6(4), e01021-15.

Scherr, T.D., Roux, C.M., Hanke, M.L., Angle, A., Dunman, P.M. and Kielian, T., 2013. Global transcriptome analysis of *Staphylococcus aureus* biofilms in response to innate immune cells. *Infection and immunity*. 81(12), 4363-4376.

Schnaith, A., Kashkar, H., Leggio, S.A., Addicks, K., *et al.*, 2007. *Staphylococcus aureus* subvert autophagy for induction of caspase-independent host cell death. *The Journal of biological chemistry*. 282 (4), 2695–2706.

Schneemann, M. & Schoeden, G., 2007. Macrophage biology and immunology: man is not a mouse. *Journal of Leukocyte Biology*. 81 (3), 579–579.

Schneider, V.A.F., Coorens, M., Tjeerdsma-van Bokhoven, J.L.M., Posthuma, G., *et al.*, 2017. Imaging the Antistaphylococcal Activity of CATH-2: Mechanism of Attack and Regulation of Inflammatory Response. *mSphere*. 2 (6), e00370-17.

Schreiner, J., Kretschmer, D., Klenk, J., Otto, M., *et al.*, 2013. *Staphylococcus aureus* PSM peptides modulate dendritic cell functions and increase in vitro priming of regulatory T cells 1. *J Immunol*. 190 (7), 3417–3426.

Schroder, K., Irvine, K.M., Taylor, M.S., Bokil, N.J., *et al.*, 2012. Conservation and divergence in Toll-like receptor 4-regulated gene expression in primary human versus mouse macrophages. *Proceedings of the National Academy of Sciences*. 109 (16), E944–E953.

Schröder, N.W.J., Morath, S., Alexander, C., Hamann, L., *et al.*, 2003a. Lipoteichoic acid (LTA) of *Streptococcus pneumoniae* and *Staphylococcus aureus* activates immune cells via Toll-like receptor (TLR)-2, lipopolysaccharide-binding protein (LBP), and CD14, whereas TLR-4 and MD-2 are not involved. *The Journal of biological chemistry*. 278 (18), 15587–15594.

Schuster, C. and Bertram, R., 2016. Toxin-antitoxin systems of *Staphylococcus aureus*. Toxins, 8(5), 140.

Schuster, C.F., Mechler, L., Nolle, N., Krismer, B., Zelder, M.E., Götz, F. and Bertram, R., 2015. The MazEF toxin-antitoxin system alters the β-lactam

susceptibility of *Staphylococcus aureus*. *PLoS One*, 10(5), e0126118.

Schwarz, H., Schneider, K., Ohnemus, A., Lavric, M., *et al.*, 2007. Chicken Toll-like Receptor 3 Recognizes Its Cognate Ligand When Ectopically Expressed in Human Cells. *Journal of Interferon & Cytokine Research*. 27 (2), 97–102.

Scumpia, P.O., Botten, G.A., Norman, J.S., Kelly-Scumpia, K.M., Spreafico, R., Ruccia, A.R., Purbey, P.K., Thomas, B.J., Modlin, R.L. and Smale, S.T., 2017. Opposing roles of Toll-like receptor and cytosolic DNA-STING signaling pathways for *Staphylococcus aureus* cutaneous host defense. *PLoS pathogens*, 13(7), e1006496.

Sedlyarov, V., Eichner, R., Girardi, E., Essletzbichler, P., *et al.*, 2018. The Bicarbonate Transporter SLC4A7 Plays a Key Role in Macrophage Phagosome Acidification. *Cell Host & Microbe*. 23 (6), 766-774.e5.

Seidl, K., Goerke, C., Wolz, C., Mack, D., *et al.*, 2008. *Staphylococcus aureus* CcpA affects biofilm formation. *Infection and immunity*. 76 (5), 2044–2050.

Sharp, J.A., Echague, C.G., Hair, P.S., Ward, M.D., *et al.*, 2012. *Staphylococcus aureus* Surface Protein SdrE Binds Complement Regulator Factor H as an Immune Evasion Tactic Brian Stevenson (ed.). *PLoS ONE*. 7 (5), e38407.

Sheppard, S.K., Guttman, D.S. and Fitzgerald, J.R., 2018. Population genomics of bacterial host adaptation. *Nature Reviews Genetics*, 19(9), 549.

Shore, A.C. & Coleman, D.C., 2013. Staphylococcal cassette chromosome mec: Recent advances and new insights. *International Journal of Medical Microbiology*. 303 (6–7), 350–359.

Sinha, B., Francois, P., Que, Y.A., Hussain, M., *et al.*, 2000. Heterologously expressed *Staphylococcus aureus* fibronectin-binding proteins are sufficient for invasion of host cells. *Infection and immunity*. 68 (12), 6871–6878.

Soman, S.S., Arathy, D.S. & Sreekumar, E., 2009. Discovery of Anas platyrhynchos avian β-defensin 2 (Apl_AvBD2) with antibacterial and chemotactic functions. *Molecular Immunology*. 46 (10), 2029–2038.

Van Sorge, N.M., Beasley, F.C., Gusarov, I., Gonzalez, D.J., von Köckritz-Blickwede, M., Anik, S., Borkowski, A.W., Dorrestein, P.C., Nudler, E. and Nizet, V., 2013. Methicillin-resistant *Staphylococcus aureus* bacterial nitric-oxide synthase affects antibiotic sensitivity and skin abscess development. Journal of Biological Chemistry, 288(9), 6417-6426.

Spaan, A.N., Henry, T., van Rooijen, W.J.M., Perret, M., *et al.*, 2013a) The Staphylococcal Toxin Panton-Valentine Leukocidin Targets Human C5a Receptors. *Cell Host & Microbe*. 13 (5), 584–594.

Spaan, A.N., Surewaard, B.G., Nijland, R. and van Strijp, J.A., 2013. Neutrophils versus *Staphylococcus aureus*: a biological tug of war. *Annual review of microbiology*, 67, 629-650.

Spaan, A.N., Vrieling, M., Wallet, P., Badiou, C., Reyes-Robles, T., Ohneck, E.A., Benito, Y., De Haas, C.J., Day, C.J., Jennings, M.P. and Lina, G., 2014. The

staphylococcal toxins γ-haemolysin AB and CB differentially target phagocytes by employing specific chemokine receptors. *Nature communications*, 5, 5438.

Spoor, L.E., McAdam, P.R., Weinert, L.A., Rambaut, A., *et al.*, 2013. Livestock origin for a human pandemic clone of community-associated methicillin-resistant *Staphylococcus aureus*. *mBio*. 4 (4), e00356-13.

Spoor, L.E., Richardson, E., Richards, A.C., Wilson, G.J., *et al.*, 2015. Recombination-mediated remodelling of host-pathogen interactions during *Staphylococcus aureus* niche adaptation. *Microbial genomics*. 1 (4), e000036.

Sprouffske, K. & Wagner, A., 2016. Growthcurver: an R package for obtaining interpretable metrics from microbial growth curves. *BMC Bioinformatics*. 17 (1), 172.

Staines, K., Hunt, L.G., Young, J.R. & Butter, C., 2014. Evolution of an expanded mannose receptor gene family. *PloS one*. 9 (11), e110330.

Stapels, D.A., Woehl, J.L., Milder, F.J., Tromp, A.T., van Batenburg, A.A., de Graaf, W.C., Broll, S.C., White, N.M., Rooijakkers, S.H. and Geisbrecht, B.V., 2018. Evidence for multiple modes of neutrophil serine protease recognition by the EAP family of Staphylococcal innate immune evasion proteins. *Protein Science*, 27(2), 509-522.

Stenz, L., Francois, P., Whiteson, K., Wolz, C., *et al.*, 2011. The CodY pleiotropic repressor controls virulence in gram-positive pathogens. *FEMS Immunology & Medical Microbiology*. 62 (2), 123–139.

Stryjewski, M.E. and Corey, G.R., 2014. Methicillin-resistant *Staphylococcus aureus*: an evolving pathogen. *Clinical Infectious Diseases*. 58(suppl_1), S10-S19.

Stuart, L.M., Deng, J., Silver, J.M., Takahashi, K., *et al.*, 2005. Response to *Staphylococcus aureus* requires CD36-mediated phagocytosis triggered by the COOH-terminal cytoplasmic domain. *The Journal of cell biology*. 170 (3), 477–485.

Sullivan, M.J., Petty, N.K. & Beatson, S.A. 2011. Easyfig: a genome comparison visualizer. *Bioinformatics*. 27 (7), 1009–1010.

Sumby, P. and Waldor, M.K., 2003. Transcription of the toxin genes present within the staphylococcal phage φSa3ms is intimately linked with the phage's life cycle. *Journal of bacteriology*, 185(23), 6841-6851.

Sun, A., Zhang, H., Pang, F., Niu, G., *et al.*, 2018. Essential genes of the macrophage response to *Staphylococcus aureus* exposure. *Cellular and Molecular Biology Letters*. 23 (1).

Sung, J.M.-L., Lloyd, D.H. & Lindsay, J.A. 2008. *Staphylococcus aureus* host specificity: comparative genomics of human versus animal isolates by multi-strain microarray. *Microbiology*. 154 (7), 1949–1959.

Sung, Y.-J., Hotchkiss, J.H., Austic, R.E. & Dietert, R.R. 1991. L-Arginine-Dependent Production of a Reactive Nitrogen Intermediate by Macrophages of

a Uricotelic Species. *Journal of Leukocyte Biology*. 50 (1), 49–56.

Surewaard, B.G.J., de Haas, C.J.C., Vervoort, F., Rigby, K.M., *et al.*, 2013. Staphylococcal alpha-phenol soluble modulins contribute to neutrophil lysis after phagocytosis. *Cellular Microbiology*. 15 (8), 1427–1437.

Surewaard, B.G.J., Nijland, R., Spaan, A.N., Kruijtzer, J.A.W., *et al.*, 2012. Inactivation of Staphylococcal Phenol Soluble Modulins by Serum Lipoprotein Particles Michael. *PLoS Pathogens*. 8 (3), e1002606.

Swaggerty, C.L., Pevzner, I.Y., Ferro, P.J., Crippen, T.L., *et al.*, 2003. Association between *in vitro* heterophil function and the feathering gene in commercial broiler chickens. *Avian Pathology*. 32 (5), 483–488.

Swaggerty, C.L., Pevzner, I.Y., He, H., Genovese, K.J., *et al.*. 2009. Selection of Broilers with Improved Innate Immune Responsiveness to Reduce On-Farm Infection by Foodborne Pathogens. *Foodborne Pathogens and Disease*. 6 (7), 777–783.

Tajima, A., Iwase, T., Shinji, H., Seki, K. and Mizunoe, Y., 2009. Inhibition of endothelial interleukin-8 production and neutrophil transmigration by *Staphylococcus aureus* beta-hemolysin. *Infection and immunity*, 77(1), 327-334.

Takeuchi, F., Watanabe, S., Baba, T., Yuzawa, H., *et al.* 2005. Whole-Genome Sequencing of *Staphylococcus haemolyticus* Uncovers the Extreme Plasticity of Its Genome and the Evolution of Human-Colonizing Staphylococcal Species. *Journal of Bacteriology*. 187 (21), 7292–7308.

Takeuchi, O., Hoshino, K. & Akira, S. 2000. Cutting Edge: TLR2-Deficient and MyD88-Deficient Mice Are Highly Susceptible to *Staphylococcus aureus* Infection. *The Journal of Immunology*. 165 (10), 5392–5396.

Takeuchi, O., Kawai, T., Mühlradt, P.F., Morr, M., *et al.*, 2001. Discrimination of bacterial lipoproteins by Toll-like receptor 6. *International Immunology*. 13 (7), 933–940.

Takeuchi, O., Sato, S., Horiuchi, T., Hoshino, K., *et al.*, 2002a, Cutting Edge: Role of Toll-Like Receptor 1 in Mediating Immune Response to Microbial Lipoproteins. *The Journal of Immunology*. 169 (1), 10–14.

Takeuchi, S., Kinoshita, T., Kaidoh, T. & Hashizume, N. 1999. Purification and characterization of protease produced by *Staphylococcus aureus* isolated from a diseased chicken. *Veterinary Microbiology*. 67 (3), 195–202.

Takeuchi, S., Matsunaga, K., Inubushi, S., Higuchi, H., *et al.*, 2002b. Structural gene and strain specificity of a novel cysteine protease produced by *Staphylococcus aureus* isolated from a diseased chicken. *Veterinary Microbiology*. 89 (2–3), 201–210.

Temperley, N.D., Berlin, S., Paton, I.R., Griffin, D.K., *et al.* 2008. Evolution of the chicken Toll-like receptor gene family: A story of gene gain and gene loss. *BMC Genomics*. 9.

Thakker, M., Park, J.S., Carey, V. & Lee, J.C. 1998. *Staphylococcus aureus* serotype

5 capsular polysaccharide is antiphagocytic and enhances bacterial virulence in a murine bacteremia model. *Infection and immunity*. 66 (11), 5183–5189.

Thänert, R., Goldmann, O., Beineke, A. and Medina, E., 2017. Host-inherent variability influences the transcriptional response of *Staphylococcus aureus* during in vivo infection. *Nature communications*. 8, 14268.

Thurlow, L.R., Hanke, M.L., Fritz, T., Angle, A., *et al.*, 2011. *Staphylococcus aureus* Biofilms Prevent Macrophage Phagocytosis and Attenuate Inflammation In Vivo . *The Journal of Immunology*. 186 (11), 6585–6596.

Tran, P.M., Feiss, M., Kinney, K.J. and Salgado-Pabón, W., 2019. ϕSa3mw Prophage as a Molecular Regulatory Switch of *Staphylococcus aureus* β-Toxin Production. *Journal of bacteriology*, 201(14), e00766-18.

Tranchemontagne, Z.R., Camire, R.B., O'Donnell, V.J., Baugh, J. and Burkholder, K.M., 2016. *Staphylococcus aureus strain* USA300 perturbs acquisition of lysosomal enzymes and requires phagosomal acidification for survival inside macrophages. *Infection and immunity*, 84(1), 241-253.

Treangen, T.J., Ondov, B.D., Koren, S. & Phillippy, A.M. 2014. The Harvest suite for rapid core-genome alignment and visualization of thousands of intraspecific microbial genomes. *Genome Biology*. 15 (11), 524.

Tuchscherr, L., Medina, E., Hussain, M., Völker, W., *et al.*, 2011. *Staphylococcus aureus* phenotype switching: An effective bacterial strategy to escape host immune response and establish a chronic infection. *EMBO Molecular Medicine*. 3 (3), 129–141.

Tuffs, S.W., James, D.B., Bestebroer, J., Richards, A.C., Goncheva, M.I., O'Shea, M., Wee, B.A., Seo, K.S., Schlievert, P.M., Lengeling, A. and van Strijp, J.A., 2017. The *Staphylococcus aureus* superantigen SElX is a bifunctional toxin that inhibits neutrophil function. *PLoS pathogens*, 13(9), e1006461.

Ulrich-Lynge, S.L., Dalgaard, T.S., Norup, L.R., Song, X., *et al.*, 2015. Chicken mannose-binding lectin function in relation to antibacterial activity towards *Salmonella enterica*. *Immunobiology*. 220 (5), 555–563.

Verbrugh, H.A., Van Dijk, W.C., Peters, R., Van Der Tol, M.E., *et al.*, 1979. *Staphylococcus aureus* opsonization mediated via the classical and alternative complement pathways. A kinetic study using MgEGTA chelated serum and human sera deficient in IgG and complement factors C1s and C2. *Immunology*. 36 (3), 391–397.

Verkaik, N.J., Benard, M., Boelens, H.A., de Vogel, C.P., *et al.*, 2011. Immune evasion cluster-positive bacteriophages are highly prevalent among human *Staphylococcus aureus* strains, but they are not essential in the first stages of nasal colonization. *Clinical Microbiology and Infection*. 17 (3), 343–348.

Viana, D., Blanco, J., Tormo-Más, M.A., Selva, L., *et al.*, 2010. Adaptation of *Staphylococcus aureus* to ruminant and equine hosts involves SaPI-carried variants of von Willebrand factor-binding protein. *Molecular microbiology*. 77 (6), 1583–1594.

Viana, D., Comos, M., McAdam, P.R., Ward, M.J., Selva, L., Guinane, C.M., González-Muñoz, B.M., Tristan, A., Foster, S.J., Fitzgerald, J.R. and Penadés, J.R., 2015. A single natural nucleotide mutation alters bacterial pathogen host tropism. *Nature genetics*, 47(4), 361.

Volz, T., Nega, M., Buschmann, J., Kaesler, S., *et al.*, 2010. Natural *Staphylococcus aureus*-derived peptidoglycan fragments activate NOD2 and act as potent costimulators of the innate immune system exclusively in the presence of TLR signals. *The FASEB Journal*. 24 (10), 4089–4102.

Vrieling, F., Wilson, L., Rensen, P.C., Walzl, G., Ottenhoff, T.H. and Joosten, S.A., 2019. Oxidized low-density lipoprotein (oxLDL) supports *Mycobacterium tuberculosis* survival in macrophages by inducing lysosomal dysfunction. *PLoS pathogens*. 15(4), e1007724.

Vrieling, M., Boerhout, E.M., Van Wigcheren, G.F., Koymans, K.J., Mols-Vorstermans, T.G., De Haas, C.J., Aerts, P.C., Daemen, I.J., Van Kessel, K.P., Koets, A.P. and Rutten, V.P., 2016. LukMF′ is the major secreted leukocidin of bovine *Staphylococcus aureus* and is produced *in vivo* during bovine mastitis. *Scientific reports*. 6, 37759.

Vrieling, M., Koymans, K.J., Heesterbeek, D.A.C., Aerts, P.C., *et al.*, 2015. Bovine *Staphylococcus aureus* Secretes the Leukocidin LukMF' To Kill Migrating Neutrophils through CCR1. *mBio*. 6 (3), e00335.

Wagner, P.L. & Waldor, M.K. 2002. Bacteriophage control of bacterial virulence. *Infection and immunity*. 70 (8), 3985–3993.

Walenkamp, A.M.E., Bestebroer, J., Boer, I.G.J., Kruizinga, R., *et al.*, 2010. Staphylococcal SSL5 binding to human leukemia cells inhibits cell adhesion to endothelial cells and platelets. *Analytical Cellular Pathology*. 32 (1–2), 1–10.

Walev, I., Weller, U., Strauch, S., Foster, T., *et al.*, 1996. Selective Killing of Human Monocytes and Cytokine Release Provoked by Sphingomyelinase (β-Toxin) of *Staphylococcus aureus*. *Infection and Immunity*. 64 (8), 2974–2979.

van Wamel, W.J., Rooijakkers, S.H., Ruyken, M., van Kessel, K.P. and van Strijp, J.A., 2006. The innate immune modulators staphylococcal complement inhibitor and chemotaxis inhibitory protein of *Staphylococcus aureus* are located on β-hemolysin-converting bacteriophages. *Journal of bacteriology*.188(4), 1310-1315.

Wang, J.H., Zhou, Y.J. & He, P. 2010a. *Staphylococcus aureus* induces apoptosis of human monocytic U937 cells via NF-κB signaling pathways. *Microbial Pathogenesis*. 49 (5), 252–259.

Wang, J.H., Zhou, Y.J. & He, P. 2010b. *Staphylococcus aureus* induces apoptosis of human monocytic U937 cells via NF-κB signaling pathways. *Microbial Pathogenesis*. 49 (5), 252–259.

Wang, R., Braughton, K.R., Kretschmer, D., Bach, T.-H.L., *et al.* 2007. Identification of novel cytolytic peptides as key virulence determinants for community-associated MRSA. *Nature Medicine*. 13 (12), 1510–1514.

Wang, Z., Gerstein, M. & Snyder, M. 2009. RNA-Seq: a revolutionary tool for transcriptomics. *Nature Reviews Genetics*. 10 (1), 57–63.

Wanke, I., Steffen, H., Christ, C., Krismer, B., *et al.* 2011. Skin Commensals Amplify the Innate Immune Response to Pathogens by Activation of Distinct Signaling Pathways. *Journal of Investigative Dermatology*. 131 (2), 382–390.

Ward, M.J., Gibbons, C.L., McAdam, P.R., Van Bunnik, B.A.D., Girvan, E.K., Edwards, G.F., Fitzgerald, J.R. and Woolhouse, M.E.J., 2014. Time-scaled evolutionary analysis of the transmission and antibiotic resistance dynamics of *Staphylococcus aureus* clonal complex 398. *Appl. Environ. Microbiol.*, 80(23), 7275-7282.

Watanabe, I., Ichiki, M., Shiratsuchi, A. & Nakanishi, Y. 2007. TLR2-Mediated Survival of *Staphylococcus aureus* in Macrophages: A Novel Bacterial Strategy against Host Innate Immunity. *The Journal of Immunology*. 178(8), 4917-4925.

Wathen, L.K., LeBlanc, D., Warner, C.M., Lamont, S.J., *et al.* 1987. A chicken sex-limited protein that crossreacts with the fourth component of complement. *Poultry science*. 66 (1), 162–165.

Weiler, H. and Von Bülow, V., 1987. Detection of different macrophage- activating factor and interferon activities in supernatants of chicken lymphocyte cultures. *Avian Pathology*, 16(3), 439-452.

Weinert, L.A., Welch, J.J., Suchard, M.A., Lemey, P., *et al.*, 2012. Molecular dating of human-to-bovid host jumps by *Staphylococcus aureus* reveals an association with the spread of domestication. *Biology Letters*. 8 (5), 829–832.

Weihrauch, J.L. and Son, Y.S., 1983. Phospholipid content of foods. *Journal of the American Oil Chemists' Society*, 60(12), 1971-1978.

Wellman-Labadie, O., Picman, J. & Hincke, M.T. 2008. Antimicrobial activity of cuticle and outer eggshell protein extracts from three species of domestic birds. *British Poultry Science*. 49 (2), 133–143.

Wells, L.L., Lowry, V.K., DeLoach, J.R. & Kogut, M.H. 1998. Age-dependent phagocytosis and bactericidal activities of the chicken heterophil. *Developmental and Comparative Immunology*. 22 (1), 103–109.

Wendlandt, S., Kadlec, K., Fessler, A.T., Monecke, S., *et al.*, 2013. Resistance phenotypes and genotypes of methicillin-resistant *Staphylococcus aureus* isolates from broiler chickens at slaughter and abattoir workers. *Journal of Antimicrobial Chemotherapy*. 68 (11), 2458–2463.

Wigley, P., 2014. *Salmonella enterica* in the chicken: how it has helped our understanding of immunology in a non-biomedical model species. *Frontiers in immunology*, 5, 482.

Wigley, P., Berchieri A., J., Page, K.L., Smith, A.L., *et al.*, 2001. *Salmonella enterica* serovar pullorum persists in splenic macrophages and in the reproductive tract during persistent, disease-free carriage in chickens. *Infection and Immunity*. 69 (12), 7873–7879.

Wigley, P., Hulme, S., Rothwell, L., Bumstead, N., *et al.*, 2006. Macrophages isolated from chickens genetically resistant or susceptible to systemic salmonellosis show magnitudinal and temporal differential expression of cytokines and chemokines following *Salmonella enterica* challenge. *Infection and immunity*. 74 (2), 1425–1430.

Wilke, G.A. and Wardenburg, J.B., 2010. Role of a disintegrin and metalloprotease 10 in *Staphylococcus aureus* α-hemolysin–mediated cellular injury. *Proceedings of the National Academy of Sciences*, 107(30), 13473-13478.

Wilson, G.J., Seo, K.S., Cartwright, R.A., Connelley, T., Chuang-Smith, O.N., Merriman, J.A., Guinane, C.M., Park, J.Y., Bohach, G.A., Schlievert, P.M. and Morrison, W.I., 2011. A novel core genome-encoded superantigen contributes to lethality of community-associated MRSA necrotizing pneumonia. *PLoS pathogens*, 7(10), e1002271.

Winstel, V., Missiakas, D. & Schneewind, O., 2018. *Staphylococcus aureus* targets the purine salvage pathway to kill phagocytes. *Proceedings of the National Academy of Sciences of the United States of America*. 115 (26), 6846–6851.

Wolf, A.J., Arruda, A., Reyes, C.N., Kaplan, A.T., *et al.*, 2011. Phagosomal degradation increases TLR access to bacterial ligands and enhances macrophage sensitivity to bacteria. *Journal of immunology*. 187 (11), 6002–6010.

Wu, Y., Raymond, B., Goossens, P.L., Njamkepo, E., *et al.*, 2010. Type-IIA secreted phospholipase A2 is an endogenous antibiotic-like protein of the host. *Biochimie*. 92 (6), 583–587.

Wu, Z., Hu, T., Rothwell, L., Vervelde, L., *et al.*, 2016. Analysis of the function of IL-10 in chickens using specific neutralising antibodies and a sensitive capture ELISA. *Developmental and Comparative Immunology*. 63, 206-212.

Xia, G. and Wolz, C., 2014. Phages of *Staphylococcus aureus* and their impact on host evolution. *Infection, Genetics and Evolution*, 21, 593-601.

Xiao, Y., Hughes, A.L., Ando, J., Matsuda, Y., Cheng, J.F., Skinner-Noble, D. and Zhang, G., 2004. A genome-wide screen identifies a single β-defensin gene cluster in the chicken: implications for the origin and evolution of mammalian defensins. *BMC genomics*, 5(1), 56.

Xie, Y., Wei, Y., Shen, Y., Li, X., *et al.* 2018. TADB 2.0: an updated database of bacterial type II toxin–antitoxin loci. *Nucleic Acids Research*. 46 (D1), D749–D753.

Yamaguchi, T., Hayashi, T., Takami, H., Ohnishi, M., *et al.* 2001. Complete Nucleotide Sequence of a *Staphylococcus aureus* Exfoliative Toxin B Plasmid and Identification of a Novel ADP-Ribosyltransferase. *Infection and Immunity*. 69 (12), 7760–7771.

Yarwood, J.M., Bartels, D.J., Volper, E.M. & Greenberg, E.P., 2004. Quorum sensing in *Staphylococcus aureus* biofilms. *Journal of bacteriology*. 186 (6), 1838–1850.

Yarwood, J.M., McCormick, J.K., Paustian, M.L., Orwin, P.M., *et al.* 2002. Characterization and expression analysis of *Staphylococcus aureus* pathogenicity island 3. Implications for the evolution of staphylococcal pathogenicity islands. *The Journal of biological chemistry*. 277 (15), 13138–13147.

Yokoyama, R., Itoh, S., Kamoshida, G., Takii, T., *et al.* 2012. Staphylococcal Superantigen-Like Protein 3 Binds to the Toll-Like Receptor 2 Extracellular Domain and Inhibits Cytokine Production Induced by *Staphylococcus aureus*, Cell Wall Component, or Lipopeptides in Murine Macrophages A. J. Bäumler. *Infection and Immunity*. 80 (8), 2816–2825.

Yonemasu, K. & Sasaki, T. 1986. Purification, identification and characterization of chicken C1q, a subcomponent of the first component of complement. *Journal of Immunological Methods*. 88 (2), 245–253.

Young, R., Bush, S.J., Lefevre, L., Mcculloch, M.E.B., *et al.*, 2018.Species-Specific Transcriptional Regulation of Genes Involved in Nitric Oxide Production and Arginine Metabolism in Macrophages. *Europe PMC Funders Group*. 2 (1), 27–37.

Pang, Y.Y., Schwartz, J., Thoendel, M., Ackermann, L.W., Horswill, A.R. and Nauseef, W.M., 2010. agr-Dependent interactions of *Staphylococcus aureus* USA300 with human polymorphonuclear neutrophils. *Journal of innate immunity*, 2(6), 546-559.

Zhang, F., Tao, Y., Zhang, Z., Guo, X., *et al.*, 2012. Metalloreductase Steap3 coordinates the regulation of iron homeostasis and inflammatory responses. *Haematologica*. 97 (12), 1826–1835.

Zhang, G.-W., Li, D.-B., Lai, S.-J., Chen, S.-Y., *et al.* 2011. Effects of Dietary Vitamin D3 Supplementation on AvBD-1 and chCATH-1 Genes Expression in Chicken. *The Journal of Poultry Science*. 48 (4), 254–258.

Zhang, L., Lu, L., Li, S., Zhang, G., Ouyang, L., Robinson, K., Tang, Y., Zhu, Q., Li, D., Hu, Y. and Liu, Y., 2016. 1, 25-Dihydroxyvitamin-D3 induces avian β-defensin gene expression in chickens. *PloS ONE*, 11(5), e0154546.

Zhao, C., Nguyen, T., Liu, L., Sacco, R.E., *et al.*, 2001.Gallinacin-3, an inducible epithelial beta-defensin in the chicken. *Infection and immunity*. 69 (4), 2684–2691.

Zhao, Y.L., Tian, P.X., Han, F., Zheng, J., Xia, X.X., Xue, W.J., Ding, X.M. and Ding, C.G., 2017. Comparison of the characteristics of macrophages derived from murine spleen, peritoneal cavity, and bone marrow. *Journal of Zhejiang University*, 18(12), 1055-1063.

Zhao, Y., van Kessel, K.P.M., de Haas, C.J.C., Rogers, M.R.C., *et al.* 2018. Staphylococcal superantigen-like protein 13 activates neutrophils via formyl peptide receptor 2. *Cellular Microbiology*. 20 (11), e12941.

Zhou, Z., Wang, Z., Cao, L., Hu, S., *et al.* 2013. Upregulation of chicken TLR4, TLR15 and MyD88 in heterophils and monocyte-derived macrophages

stimulated with *Eimeria tenella* in vitro. *Experimental Parasitology*. 133 (4), 427–433.

Zhu, F., Yue, W. & Wang, Y. 2014.The nuclear factor kappa B (NF-κB) activation is required for phagocytosis of *Staphylococcus aureus* by RAW 264.7 cells. *Experimental Cell Research*. 327 (2), 256–263.

Zhu, X.Y., Wu, C.C. and Hester, P.Y., 1999. Induction of the delayed footpad and wattle reaction to killed *Staphylococcus aureus* in chickens. *Poultry science*, 78(3), 346-352.

Zhu, X.Y., Wu, C.C. and Hester, P.Y., 2001. Systemic distribution of *Staphylococcus aureus* following intradermal footpad challenge of broilers. *Poultry science*, 80(2), 145-150.

Zingarelli, B., Piraino, G., Hake, P.W., O'Connor, M., *et al.*, 2010. Peroxisome Proliferator-Activated Receptor δ Regulates Inflammation via NF-κB Signaling in Polymicrobial Sepsis. *The American Journal of Pathology*. 177 (4), 1834–1847.

De Zoete, M.R., Bouwman, L.I., Keestra, A.M. & Van Putten, J.P.M. 2011. Cleavage and activation of a Toll-like receptor by microbial proteases. *Proceedings of the National Academy of Sciences of the United States of America*. 108 (12), 4968–4973.

Zou, J., Chang, M., Nie, P. & Secombes, C.J. 2009. Origin and evolution of the RIG-I like RNA helicase gene family. *BMC Evolutionary Biology*. 9 (1), 85.